STUDY OF APPLICATIONS OF RETRODIRECTIVE AND SELF-ADAPTIVE ELECTROMAGNETIC WAVE PHASE CONTROLS TO A MARS PROBE

By A. T. Villeneuve
J. E. Howard
N. J. Bershad

Final Report - Part II

Prepared under Contract No. NAS 2-3297 by
Antenna Department, Aerospace Group
HUGHES AIRCRAFT COMPANY
Culver City, California
(HAC Report No. P68-70, Ref. A8076)

for

NATIONAL AERONAUTICS AND SPACE ADMINISTRATION

Distribution of this report is provided in the interest of information exchange. Responsibility for the contents resides in the author or organization that prepared it.

(Hughes Report No. P68-70, HAC Ref. A8076)

CONTENTS

		Page
INTRODUCTION		1
DISCUSSION		4
1.0	Multipath Model	4
2.0	Phase-Locked-Loop Operation in a Multipath Environment	6
2.1	Phase-Locked-Loop Model	6
2.2	Loop Performance Criteria	11
2.3	Statistical Description of Loop Errors	18
2.4	Multipath and Phase-Locked-Loop Models for Fast Fading Signals	27
2.5	Statistical Description of Loop Error for Fast-Fading Signals	28
2.6	Comparison of Loop Performance for Slow Fading and Fast Fading	33
2.7	First-Order Phase-Locked Loop with Arbitrary Fading Spectrum	45
2.8	Mathematical Analysis of First-Order Loop	48
2.9	Lock-On and Loss-Of-Lock Probabilities for Slow Fading	62
3.0	Convergence to Gaussian Statistics	64
4.0	Effect of Multipath on Detection	72
4.1	Multipath Environment and Modulation	72
4.2	Error Probability	73
4.3	Effect of Doppler Shifts on Demodulation Errors	85
4.4	Optimum Weighting of Phase-Locked-Loop Outputs	86
4.5	Effect of Multipath Signals on Operation of Systems That Use Phase Inversion by Mixing	95
4.6	Effective Radiation Patterns of Self-Steering Arrays with Phase-Locked Loops	104
5.0	Scattering By a Rough Surface	106
6.0	Use of Millimeter Waves to Overcome Blackout	130
7.0	Evaluation of Systems at Different Frequencies	135
CONCLUSION		145
Analysis of Results		145
Recommendations		147
APPENDICES		
Appendix A	Probability Density Function of Steady-State Phase Errors in Phase-Locked Loops	149
Appendix B	Probability Density Functions of Phase Errors in Multi-Element Arrays	165
Appendix C	Average Error Probabilities of Coherent Phase Shift Key Modulation in a Multipath Environment	171
Appendix D	Average Error Probabilities of Differentially Coherent Phase Shift Key Modulation in a Multipath Environment	174

		Page
Appendix E	Average Error Probabilities of Coherent Frequency Shift Key Modulation in a Multipath Environment	176
Appendix F	Average Error Probabilities of Incoherent Frequency Shift Key Modulation in a Multipath Environment	184
Appendix G	Average Error Probabilities of Coherent Amplitude Shift Key Modulation in a Multipath Environment	187
Appendix H	Average Error Probabilities of Incoherent Amplitude Shift Key Modulation in a Multipath Environment	191
Appendix I	Evaluation of Expectations	197
Appendix J	Interaction of Electromagnetic Waves With Plasmas	198
REFERENCES		200

ILLUSTRATIONS

		Page
Figure 1.	Relative positions of bus, lander, and planet	1
Figure 2.	Multipath model	4
Figure 3.	Phase-locked loop models	7
Figure 4.	Exact mathematical model of phase-lock-loop	9
Figure 5.	Phase-locked loop with bandpass limiter	11
Figure 6.	Filter for second-order loop	12
Figure 7.	First-order loop locus	18
Figure 8.	Phase error probability density functions ($p[\phi]$) for four loop signal-to-noise ratios (a) with various doppler change rate multipliers (b) and statistical parameters (μ_3 and σ_3).	24
Figure 9.	Phase errors of phase-locked loops with a signal-to-noise ratio of 3 in a multipath fading environment	35
Figure 10.	Phase errors of phase-locked loops with a signal-to-noise ratio of 10 in a multipath fading environment	38
Figure 11.	Phase errors of phase-locked loops with a signal-to-noise ratio of 30 in a multipath fading environment	42
Figure 12.	First-order loop with random gain and phase	46
Figure 13.	Equivalent phase-locked loop with only white gaussian inputs	49
Figure 14.	Comparison between the gaussian reference function and the phase error probability density functions for small arrays	68
Figure 15.	Multipath error probability	82
Figure 16.	Adaptive array receiver	86
Figure 17.	Portion of self-steering array that illustrates signal and noise performance of the system	96
Figure 18.	Equivalent radiation patterns of self-steering arrays with phase-locked loops	107
Figure 19.	Coordinates for scattering problem	116
Figure 20.	Illustration of plasma sheath about entry vehicle	131
Figure 21.	Assumed shape of entry vehicle	132
Figure 22.	Typical entry profiles for non-survivable probe	133
Figure 23.	Attenuation versus time for entry profiles	134
Figure 24.	Possible self-steering array configurations	136

TABLES

Table I.	Variance of errors in single phase-locked loops	67
Table II.	Estimated weights and power requirements of self-steering arrays	140
Table III.	Summary of characteristics of representative self-steering systems for fixed prime power	144

STUDY OF APPLICATIONS OF RETRODIRECTIVE AND SELF-ADAPTIVE ELECTROMAGNETIC WAVE PHASE CONTROLS TO A MARS PROBE

FINAL REPORT – PART II

By A. T. Villeneuve, J. E. Howard, and N. J. Bershad
Hughes Aircraft Company

SUMMARY

The report presents the results of the second phase of a study of the applicability of self-steering and adaptive arrays to planetary probe missions. Analyses were performed of arrays that obtain self-steering by the use of either phase-locked loops or phase inversion by mixing. The performance of these systems was studied during their assumed reception of multipath signals with various digital modulations. Probabilities of error in reception of these signals were computed.

The problem of determining the character of a multipath signal that is scattered by a rough spherical scatterer was also attacked. A vector formulation was used, and integral expressions were obtained for the scattered signal autocorrelation function.

The possibility of using millimeter waves to overcome entry blackout was also considered for several Mars entry profiles. Results indicate that for these profiles, signals in the 100-GHz region may not be significantly attenuated.

Several self-steering configurations were considered at microwave and millimeter-wave frequencies. Estimates were made of expected effective radiated powers and weights of these systems. The results are presented in tabular form.

INTRODUCTION

This report is Part II of the Final Report on Contract NAS 2-3297 and covers work performed from 26 January 1967 to 31 December 1967 (refs. 1-3). Work performed from 8 November 1965 to 8 October 1966 is reported in Quarterly Reports 1 through 4 and in Part I of the Final Report (refs. 4-8). The problem under consideration is the applicability of retrodirective and self-adaptive electromagnetic wave phase controls to a Mars Probe.

The situation of interest is illustrated in figure 1. A lander vehicle is ejected from a fly-by or orbiting bus in the vicinity of the planet. During its descent, the lander communicates with the bus which, in turn, communicates with the earth. In an alternative mode of operation, the lander may communicate directly with the earth. The lander may be spinning and may undergo unpredictable motion during its descent. If it is desired to use high-gain antennas to communicate, the relative motion of bus and lander makes beam steering necessary. Because of the unpredictable nature of the motion, self-steering techniques look very desirable for this application. A number of theoretical and experimental studies dealing with the general properties of self-steering antenna arrays have been reported in the literature (refs. 9-19); none of that work has been concerned with the specific problems under consideration in the present study.

The subject of prime interest in the phase of the study reported here has been the performance capabilities of two general types of self-steering arrays when they are applied to planetary probes as communication antennas.

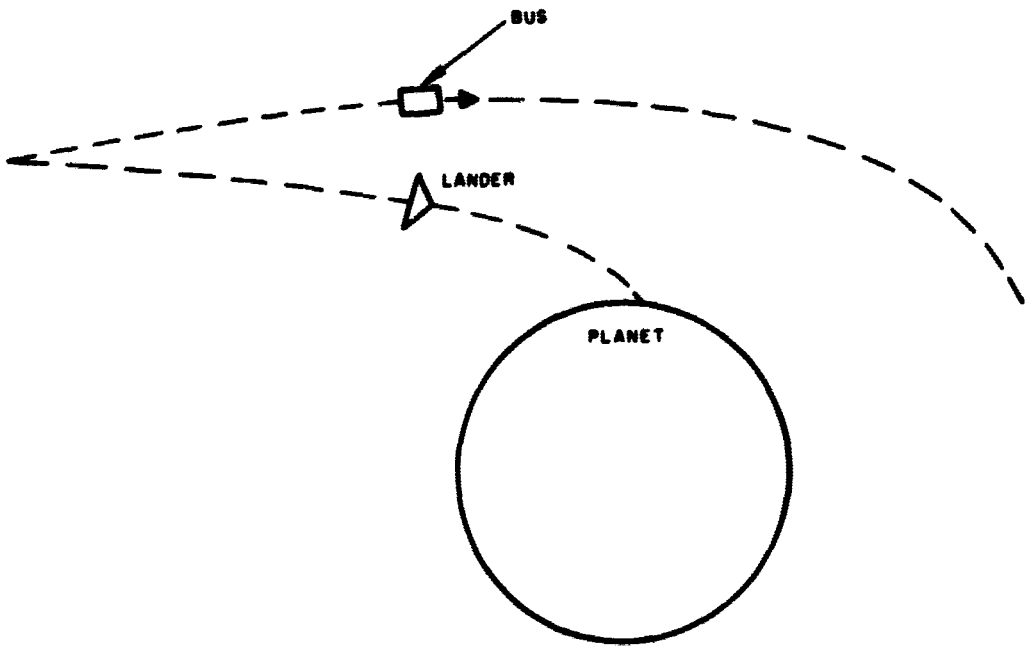

Figure 1. Relative positions of bus, lander, and planet.

The types of arrays investigated utilize either phase-locked loops or phase inversion by mixing to obtain self-steering. Their operating principles are described in general terms in the First Quarterly Report on this contract and in Part I of the Final Report.

During this portion of the study several topics were considered. The first of these topics was the effect of input noise and simple multipath structures on the probability density function of phase errors in self-steering circuits. This study included an analysis of the effects of various signal-to-noise ratios and multipath models on the phase-locked-loop output. Both slow fading and fast fading signals due to the multipath environment were considered, and numerical values were computed of the probability density functions of the resulting loop phase errors. A study was also made of intermediate fading signals and their effect on the probability density functions of the phase errors in first-order, phase-locked loops..

The second topic studied was loop lock-on stability, tracking, and acquisition in a multipath environment. Such factors as lock-on probabilities and the probability of loss-of-lock were considered.

The third topic was the shape of the probability density function of the phase errors that result in a signal consisting of the sum of the outputs of two and three phase-locked loops. While the density functions of the phase errors of single loops are not gaussian, the density functions of phase errors of the sum signals should tend toward gaussian as a large number of outputs are combined. The rate of convergence of the density function toward a gaussian density function is considered.

The effects of simple multipath models on the probabilities of error in detection of digitally coded signals were also considered. The effects of time delay on the error probabilities was included in the study.

The effect of multipath signals on the operation of self-steering arrays that use phase inversion by mixing was also considered. Expressions were derived for the outputs of correlation detections when the signals are digitally modulated. These correlator outputs can be employed to determine error probabilities in signal detection.

The multipath model that was used in the probability of error studies was a simple one. However, since the secondary path signal arises from reflection by a rough scatterer, the actual signal may be quite complex and its spectrum is not easily calculated. The problem of determining the spectrum of the reflected signal was attacked using a vector formulation, and integrals were obtained for the autocorrelation function of the reflected signal.

When a lander enters the Martian atmosphere, it will be surrounded by a plasma sheath during a portion of its descent. This plasma may interfere seriously with the propagation of radio waves unless the frequency of the

waves is sufficiently high. The attenuation versus time for several frequencies is presented for two entry paths. It is shown that at 94 GHz blackout may be avoided.

Finally, several configurations of possible self-steering systems are presented, and estimates are given of weights and effective radiated powers of systems implemented at 8 GHz and 94 GHz for the constraint of a fixed available prime power.

The conclusions drawn from the research results are presented at the end of the technical discussion along with recommendations for further work. The details of the several analyses are given in the appendices.

The authors wish to thank Dr. G. O. Young for valuable discussions during the course of the study, R. A. Birgenheier for supplying material for power and weight estimates, and Marjorie Delzell for her very diligent editorial assistance in the preparation of the reports.

DISCUSSION

1.0 Multipath Model

The most significant multipath problem in a communications link among Earth, Mars, and a bus orbiting about Mars (figure 1) or among an orbiting bus, a lander, and Mars is the dual path in which Mars acts as a major reflector. The phases of the two signals will differ as a result of different path lengths as well as the random multipath fluctuations arising from fluctuations in the external media. The modulation in each signal will also differ because of a time delay τ.

If the original signal sent is of the form

$$s(t) = \hat{a}(t) \sin (\omega_0 t + m(t)) \tag{1a}$$

then a signal received along the primary path may be characterized as

$$s_p(t) = a_p(t) \sin (\omega_0 t + m(t) + \theta_p(t)) \tag{1b}$$

(excluding the additive noise for the moment), and a signal received along the secondary path will be

$$s_s(t) = a_s(t) \sin (\omega_0 t + m(t + \tau) + \theta_s(t) \tag{1c}$$

Then the composite signal as received by a noisy receiver is

$$s(t) = a_p(t) \left\{1 + 2\Omega \cos [\Delta\theta + \Delta m] + \Omega^2\right\}^{1/2} \sin \left\{\omega_0 t + m(t) + \theta_p(t) + \sin^{-1} \left[\frac{\Omega \sin (\Delta\theta + \Delta m)}{\left(1 + 2\Omega \cos [\Delta\theta + \Delta m] + \Omega^2\right)^{1/2}}\right]\right\} + \hat{n}(t) \tag{1d}$$

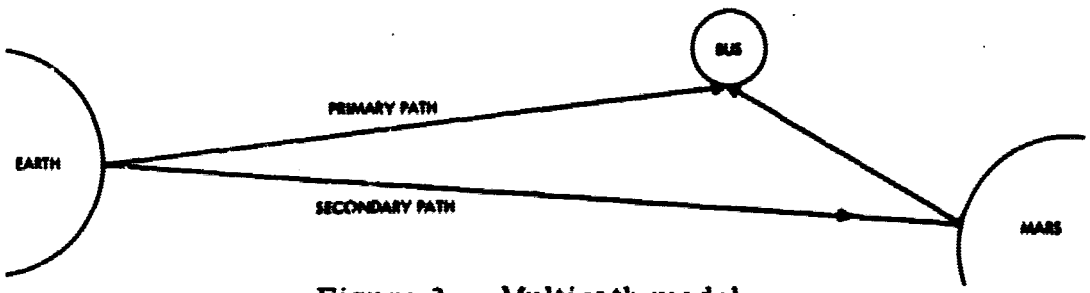

Figure 2. Multipath model.

where

$$\Omega = a_s(t)/a_p(t)$$

$$\Delta\theta = \theta_s(t) - \theta_p(t)$$

$$\Delta m = m(t + \tau) - m(t)$$

The modulation is inherently restricted to frequency or phase modulation since bandpass limiters will be used. Amplitude modulation is thus ruled out.

As described in more detail later, the first operation of the receiver will be to limit the received signal so that the signal seen by the loop will have constant amplitude. Furthermore, the modulation rate is assumed much greater than the rate of change of phase errors so that the phase or frequency tracking loop does not see the modulation because of its low pass characteristics. Consequently, the signal input to the phase-locked loop is of the form

$$s(t) = \sqrt{2}\, A \sin\left\{\omega_0 t + \theta_p(t) + \sin^{-1}\left[\frac{\Omega \sin(\Delta\theta)}{\left(1 + 2\Omega\cos(\Delta\theta) + \Omega^2\right)^{1/2}}\right]\right\} + n(t) \qquad (2)$$

where A is constant and n(t) is gaussian white noise with a one-sided spectral density N_0. The output of the loop to be demodulated will then be

$$s(t) = \sqrt{2}\, A \sin\left\{\omega_0 t + \phi_{ss} + m_p(t) + m(t, \tau)\right\}$$

where ϕ_{ss} is the steady-state phase error random variable arising from equation (2) after passing through the loop, and $m(t, \tau)$ is the modulation perturbation caused by a time delay τ between the two major paths.

In this section of the report the emphasis is on the solution for ϕ_{ss} and its effect on phase-locked loop operation. In a succeeding section, the accuracy of demodulation of the term $\phi_{ss} + m_p(t) + m(t, \tau)$ will be explored. In the first year of this study, the problem of demodulating $\phi_{ss} + m_p(t)$ was considered in the absence of multipath effects where ϕ_{ss} was gaussian. (It may be noted that ϕ_{ss} is the composite of phase errors of all loops, assuming demodulation after summing, and so is approximately gaussian by the Central Limit Theorem.)

2.0 Phase-Locked-Loop Operation in a Multipath Environment

2.1 Phase-Locked-Loop Model

To analyze the operation of a phase-locked loop, a basic component of an adaptive array, the loop model to be used must first be defined (see figure 3). The most general phase-locked loop consists of a phase detector, a filter, and a voltage-controlled oscillator (VCO) as shown in figure 3a. Since the VCO frequency is linearly controlled by the feedback voltage e(t), the ideal operation for the phase detector is linear. That is, if s(t) and $s_v(t)$ are separated by ϕ radians in phase, then $g(\phi) = \phi$ is the preferred output of the phase detector.

The analysis for such a loop is particularly simple; however, the mechanization of the proper phase detector is difficult. A phase detector with a linear phase response (modulo 2π) is possible by the use of flip-flops synchronized with the carrier.[20] However the flip-flops require a very high input signal-to-noise ratio for reliable triggering. In space communications applications, in which the signal-to-noise ratio (SNR) is typically low, such an ideal phase detector is not possible. A reasonable approximation can be achieved by a "tanlock" phase detector[21, 22] but greater circuit complexity results.

The most common phase detector (figure 3b) acts like a multiplier so that in the noiseless case

$$f(\phi) = s(t) \times s_v(t) \propto \sin\left[\theta(t) - \theta_v(t)\right]$$

Instead of a linear phase characteristic, the detector has a sinusoidal nonlinearity. To be precise A and $\theta(t)$ are defined:

$$\begin{cases} \sqrt{2}\,A = a(t)\left[1 + 2\,\Omega\cos\left(\theta_s(t) - \theta_p(t)\right) + \Omega^2\right]^{1/2} \\ \theta(t) = \omega_0 t + \theta_p(t) + \sin^{-1}\left[\dfrac{\Omega\sin(\Delta\theta)}{(1 + 2\,\Omega\cos(\Delta\theta) + \Omega^2)^{1/2}}\right] \end{cases} \tag{3}$$

Then equation (2) may be written

$$s(t) = \sqrt{2}\,A \sin\theta(t) + n(t) \tag{4}$$

If the filter in the loop is a linear filter with transfer function F(s) and impulse response f(t), then an output voltage e(t) is related to an input voltage x(t) by

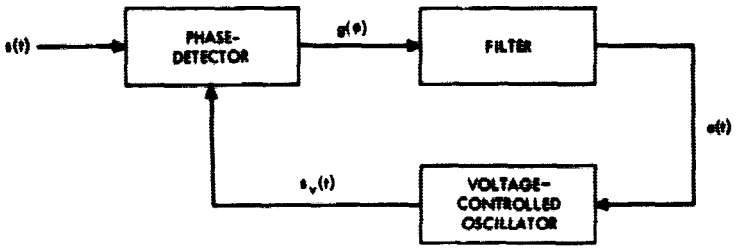

a. General model

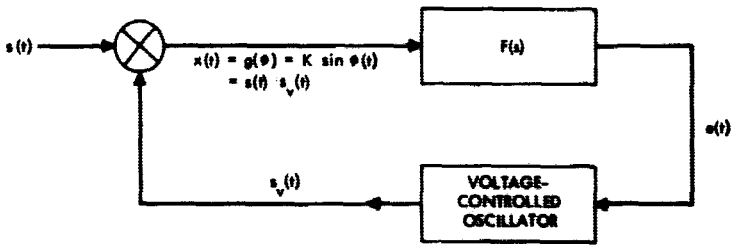

b. Common model

Figure 3. Phase-locked loop models.

$$\begin{cases} e(t) = x(t) * f(t) \\ E(s) = X(s)\,F(s) \end{cases} \tag{5}$$

where E(s) and X(s) are, respectively, the transforms of e(t) and x(t) and * denotes a convolution. If the output rms amplitude of the VCO is K_1, then

$$s_v(t) = \sqrt{2}\,K_1 \cos \theta_v(t)$$

and the phase detector output is

$$x(t) = AK_1 \left\{ \sin \left[\theta(t) - \theta_v(t)\right] + \sin \left[\theta(t) + \theta_v(t)\right] \right\} + \sqrt{2}\,K_1\, n(t) \cos \theta_v(t)$$

If the quiescent frequency of the VCO is ω_0, then $\theta(t) - \theta_v(t)$ is a low frequency term but $\theta(t) + \theta_v(t)$ is centered at $2\omega_0$ rad/sec. However the VCO cannot respond to such a high frequency signal and so it has no effect on the loop operation. Similarly, the high frequency noise components do not affect the loop. After the noise has been filtered, it can be represented as a narrow-band gaussian process,

$$n(t) = \sqrt{2}\, n_1(t) \sin \omega_0 t + \sqrt{2}\, n_2(t) \cos \omega_0 t$$

then the phase detector output is effectively

$$x(t) = AK_1 \sin \phi(t) + K_1 \hat{n}(t) \tag{6}$$

where

$$\phi(t) = \theta(t) - \theta_v(t)$$

$$\hat{n}(t) = -n_1(t) \sin (\theta_v(t) - \omega_0 t) + n_2(t) \cos (\theta_v(t) - \omega_0 t)$$

thus, $\hat{n}(t)$ has a low-pass spectrum, and the random coefficients are independent and gaussian. If the VCO has a proportionality constant of K_2 rad/sec/volt, then

$$\frac{d\theta_v(t)}{dt} = \omega_0 + K_2\, e(t) \tag{7}$$

Equations (5) through (7) completely describe the phase-locked loop operation. In fact they may be combined to yield the operating integrodifferential equation of the loop. After $\theta(t) = \omega_0 t + \theta_1(t)$ has been defined, then

$$\frac{d\phi(t)}{dt} = \frac{d\theta_1(t)}{dt} - K_1 K_2 \int_0^t \left[A \sin \phi(\sigma) + \hat{n}(\sigma)\right] f(t-\sigma)\, d\sigma \tag{8}$$

where the variables are

$$\begin{cases} A = \frac{1}{\sqrt{2}}\, a(t) \left[1 + 2\,\Omega \cos \left(\theta_s(t) - \theta_p(t) + \Omega^2\right)\right]^{1/2} \\ \theta_1(t) = \theta_p(t) + \sin^{-1} \left[\dfrac{\Omega \sin (\theta_s - \theta_p)}{\left(1 + 2\,\Omega \cos (\theta_s - \theta_p) + \Omega^2\right)^{1/2}}\right] \end{cases}$$

and the loop parameters are K_1 K_2, f(t). The velocity constant of the loop (the d-c loop gain) is $AK_1 K_2 F(s = 0)$.

Equation (8) has a graphical representation that is very convenient for demonstrating the operation of this phase-locked loop (figure 4). This representation is the exact model that is used for the exact analyses that are necessary for determination of acquisition and unlock thresholds. For low error tracking, sin $\phi(t)$ is approximated by $\phi(t)$; this modification linearizes the loop for simple analyses.

If frequency or phase modulation but not amplitude modulation is used to carry the transmitted information, a bandpass limiter is beneficial. It provides a constant power input to the phase-locked loop that permits consistent, well defined action. Furthermore, the noise bandwidth of the loop will automatically decrease as input SNR decreases; the resulting adaptive loop bandwidth will improve the loop SNR. The analysis of this improvement follows.

A bandpass limiter consists of an ideal limiter and a bandpass filter. A signal input is limited to a constant peak voltage output ±L, and then filtered to produce the desired bandpass limited signal. If $(SNR)_i$ is the signal-to-additive-noise ratio of the received signal, then the peak output power from the bandpass limiter is

$$P_o = P_s + P_n$$

The signal power is[20]

$$P_s \approx \frac{2L^2}{\pi} \left[\frac{\frac{4}{\pi}(SNR)_i}{\frac{4}{\pi} + (SNR)_i} \right] \tag{9}$$

and the noise power is

$$P_n \approx \frac{2L^2}{\pi} \left[\frac{4/\pi}{1 + 2(SNR)_i} \right] \tag{10}$$

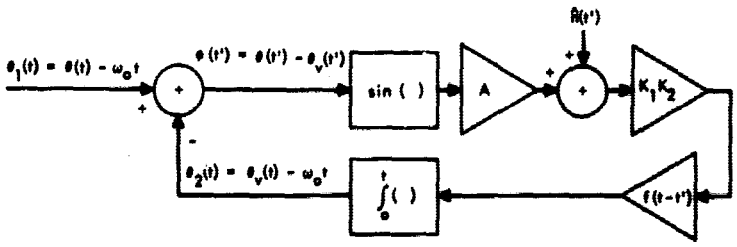

Figure 4. Exact mathematical model of phase-lock-loop.

Again, the total output power is

$$P_o = P_s + P_n \approx \frac{8L^2}{\pi}\left[\frac{(SNR)_i^2 + (SNR)_i + 2/\pi}{(SNR)_i^2 + \left(\frac{4}{\pi}+\frac{1}{2}\right)(SNR)_i + 2/\pi}\right] \tag{11}$$

From equation (11) it is seen that the bandpass limiter output is $8L^2/\pi$ within $\pm 1/2$ db for all input signal and noise levels (above the threshold required for limiting voltage to reach L). The output signal-to-noise ratio is also approximately constant:

$$(SNR)_o = \frac{P_s}{P_n} \approx 2\,(SNR)_i \left[\frac{(SNR)_i + 1/2}{(SNR)_i + 4/\pi}\right] \tag{12}$$

In fact $(SNR)_o > (SNR)_i$ for $(SNR)_i > 0.27$ (-5.7 db). The bandpass limiter thus achieves up to a 3 db improvement in SNR to the phase-locked loop. The new complete phase-locked-loop model is then as shown in figure 5.

As set earlier, the input is $s(t) = \sqrt{2}\hat{A} \sin \theta(t) + \hat{n}(t)$. After the signal has passed through the bandpass limiter the portion reaching the phase-locked loop is defined as

$$\tilde{s}(t) = \sqrt{2}\,\hat{A} \sin \theta(t) + \tilde{n}(t)$$

where

$$\hat{A} = (P_s/2)^{1/2} = \frac{2L}{\pi}\sqrt{\frac{(SNR)_i}{4/\pi + (SNR)_i}} \tag{13}$$

$$\sigma_{\tilde{n}} = \sqrt{\overline{\tilde{n}^2(t)}} = (P_n/2)^{1/2} = \frac{2L}{\pi}\sqrt{\frac{1}{1 + 2(SNR)_i}}$$

Hereafter, $\hat{A}$ and $\sigma_{\tilde{n}}$ take the place of A and σ_n in equations (4) through (8).

The "limiter signal suppression factor" of equation (9) may be redefined as

$$\alpha = \frac{\hat{A}}{\hat{A} \text{ at } (SNR)_i \to \infty} = \sqrt{\frac{1}{1 + \frac{4}{\pi(SNR)_i}}} \tag{14}$$

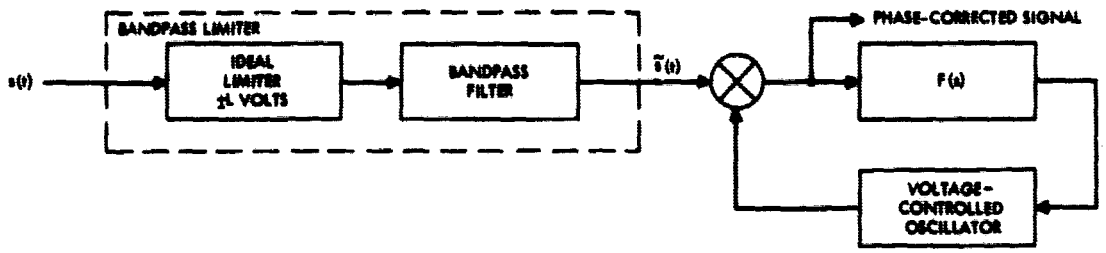

Figure 5. Phase-locked look with bandpass limiter.

This expression describes the effective decrease in loop gain when $(SNR)_i$ decreases. This decreased loop gain then implies decreased loop bandwidth, which in turn reduces the noise power seen by the phase-locked loop. Therefore, $\hat{A}$ may be rewritten as

$$\hat{A} = \alpha \tilde{A}$$

where

$$\tilde{A} = \frac{2L}{\pi} = \text{constant} \tag{15}$$

2.2 Loop Performance Criteria

Before the statistics of loop phase errors are determined, the criteria used to describe loop performance for deterministic perturbations will be demonstrated. The fluctuation limits on $\Delta\theta$ for the noiseless deterministic case will be calculated. These calculations will demonstrate the guidelines necessary in the calculation of lock-on and lock-loss probabilities in the noisy random case.

Loop fundamentals. – The most common phase-locked loop is a second-order loop. The perfect second-order loop uses a filter transfer function:

$$F(s) = C_0 + C_1/s \tag{16}$$

Then the closed-loop transfer function of the phase-locked loop is

$$H(s) = \frac{\hat{A} K_1 K_2 F(s)}{s + \hat{A} K_1 K_2 F(s)} = \frac{\hat{A} K_1 K_2 (C_0 s + C_1)}{s^2 + C_0 \hat{A} K_1 K_2 s + C_1 \hat{A} K_1 K_2} \tag{17}$$

The denominator of H(s) is of the form

$$s^2 + 2\omega_n \zeta s + \omega_n^2$$

The loop acts like a low pass filter with natural frequency,

$$\omega_n = \sqrt{C_1 \hat{A} K_1 K_2} \tag{18a}$$

and damping factor,

$$\zeta = \frac{C_0}{2} \sqrt{\frac{\hat{A} K_1 K_2}{C_1}} \tag{18b}$$

The rate of cutoff of the loop may then be partially described by the 3-db bandwidth of the effective filter:

$$\omega_{3db} = \omega_n \sqrt{2\zeta^2 + 1 + \sqrt{(2\zeta^2 + 1)^2 + 1}}$$

The linear filter in the second-order loop is mechanized by the operational amplifier circuit shown in figure 6. If the operational amplifier does not have infinite gain, the resulting loop will not be perfectly second-order.† In other words, under the conditions of an imperfect second-order loop, the new filter transfer function will be

$$F(s) = \frac{C_0 s + C_1}{s + \epsilon} \tag{19}$$

where $0 < \epsilon \ll C_1/C_0$. The closed-loop transfer function is

$$H(s) = \frac{\hat{A} K_1 K_2 (C_0 s + C_1)}{s^2 + s(\hat{A} K_1 K_2 C_0 + \epsilon) + \hat{A} K_1 K_2 C_1} \tag{20}$$

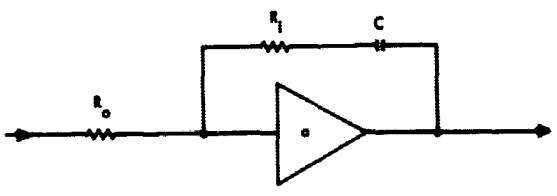

Figure 6. Filter for second-order loop.

†The second-order loops described here use filters of the proportional plus integral control (or Wiener) type.

and the loop response is described by

$$\omega_n = \sqrt{C_1 \hat{A} K_1 K_2}$$

$$\zeta = \frac{C_0}{2} \sqrt{\frac{\hat{A} K_1 K_2}{C_1}} + \frac{\epsilon}{2\sqrt{C_1 \hat{A} K_1 K_2}} \tag{21}$$

Lock loss and acquisition — noiseless case. — The bandpass limited signal can be considered to be

$$\tilde{S}(t) = \alpha \tilde{A} \sin(\omega_0 t + m(t) + \tilde{\theta}(t)) \tag{22a}$$

where

$$\tilde{\theta}(t) = \theta_p(t) + \sin^{-1}\left[\frac{\Omega \sin\left(\theta_s(t) - \theta_p(t)\right)}{\left(1 + 2\Omega \cos\left(\theta_s(t) - \theta_p(t)\right) + \Omega^2\right)^{1/2}}\right] \tag{22b}$$

The only assumption inherent in equations (22) is zero additive noise. It is next assumed that the composite phase $\tilde{\theta}(t)$ may be written in a quadratic form,

$$\tilde{\theta}(t) = (\delta\tilde{\theta}) + (\delta\dot{\tilde{\theta}})\, t + \frac{1}{2}(\delta\ddot{\tilde{\theta}})\, t^2 \tag{22c}$$

which neglects any nonlinearities in $\tilde{\theta}(t)$ higher than second degree in t.

For the noiseless case, the phase-locked loop equation for a bandpass limited signal is, from equation (8),

$$\frac{d\phi(t)}{dt} = \frac{d\tilde{\theta}(t)}{dt} - \alpha \tilde{A} K_1 K_2 \int_0^t \sin\phi(\sigma)\, f(t-\sigma)\, d\sigma \tag{23}$$

In the Laplace transform s-plane, this expression becomes

$$s\Phi(s) = s\tilde{\Theta}(s) - \alpha \tilde{A} K_1 K_2 F(s)\, L[\sin\phi(t)] \tag{24}$$

When the expression is solved for sin $\phi(t)$,

$$L[\sin \phi(t)] = \frac{s \tilde{\Theta}(s) - s \Phi(s)}{\alpha \tilde{A} K_1 K_2 F(s)} \tag{25}$$

By the final value theorem, the steady-state value is

$$\sin \phi_{ss} = \lim_{t \to \infty} [\sin \phi(t)] = \lim_{s \to 0} s L[\sin \phi(t)]$$

$$\sin \phi_{ss} = \lim_{s \to 0} \frac{s^2 \tilde{\Theta}(s)}{\alpha \tilde{A} K_1 K_2 F(s)} - \lim_{s \to 0} \frac{s^2 \Phi(s)}{\alpha \tilde{A} K_1 K_2 F(s)} \tag{26}$$

But if ϕ_{ss} is bounded, then

$$|\phi_{ss}| = \left|\lim_{s \to 0} s \Phi(s)\right| < \infty$$

so that

$$\left[\lim_{s \to 0} s^2 \Phi(s) = 0\right]$$

But

$$F(s) = \frac{s + C}{C_0 s + C_1}$$

so that

$$\left[\lim_{s \to 0} s^2 \Phi(s)/F(s) = 0\right]$$

Then equation (26) becomes

$$\sin \phi_{ss} = \lim_{s \to 0} \frac{s^2 \tilde{\Theta}(s)}{\alpha \tilde{A} K_1 K_2 F(s)} \tag{27}$$

In the application of equation (27), care must be taken to satisfy the condition of the final value theorem. For an application of the theorem to f(t),

$$\lim_{t \to \infty} f(t) = \lim_{s \to 0} s F(s)$$

the hypotheses of the theorem are[23]

(1) f(t) is L-transformable.

(2) f'(t) is L-transformable.

(3) If $F(s) = L[f(t)]$, then $s F(s)$ must be analytic on the imaginary axis and the right-half plane.

Condition (3) automatically rules out the use of nondecaying periodic functions of t for f(t).

When the quadratic form for $\tilde{\theta}(t)$ given in equation (22c) is used, equation (27) becomes

$$\sin \phi_{ss} = \lim_{s \to 0} \frac{s (\delta\tilde{\theta} + \delta\dot{\tilde{\theta}}/s + \delta\ddot{\tilde{\theta}}/s^2)}{\alpha \tilde{A} K_1 K_2 F(s)} \tag{28}$$

For the perfect second-order loop, $F(s) = C_0 + C_1/s$, and equation (28) yields

$$\sin \phi_{ss} = \delta\ddot{\tilde{\theta}} / (C_1 \alpha \tilde{A} K_1 K_2)$$

To prevent loss of lock, the requirement must be met that $|\sin \phi_{ss}| < 1$. The maximum linear rate of frequency change allowable in a perfect second-order loop is

$$|\delta\ddot{\tilde{\theta}}|_{\text{unlock}} = C_1 \alpha \tilde{A} K_1 K_2 = \omega_n^2 \tag{29}$$

For the imperfect second-order loop,

$$F(s) = \frac{C_0 s + C_1}{s + \epsilon}$$

Then if $\delta\ddot{\theta} = 0$ (required for finite steady-state phase error), the maximum frequency shift allowable is

$$|\delta\dot{\tilde{\theta}}|_{unlock} = C_1 \alpha \tilde{A} K_1 K_2/\epsilon = \omega_n^2/\epsilon \qquad (30)$$

The above requirements insure proper steady-state values for $\phi(t)$ with the assumption of no cross-over into the $|\sin \phi(t)| \geq 1$ region for $t < \infty$. However, a transient of frequency shift in $\dot{\tilde{\theta}}(t)$ may well cause an overshoot of $\sin \phi(t)$ before $t \to \infty$. For this reason the maximum allowable transient frequency shift is considerably smaller than the maximum allowable static frequency shift, or as can be shown from empirical data of a high-gain second-order loop,[20]

$$\begin{aligned} |\delta\dot{\tilde{\theta}}|_{max\ trans} &\approx 1.8\, \omega_n (\zeta + 1) \\ &\approx 0.9\, C_0 \alpha \tilde{A} K_1 K_2 + 1.8 \sqrt{C_1 \alpha \tilde{A} K_1 K_2} + 0.9\epsilon \qquad (31) \\ &\ll |\delta\dot{\tilde{\theta}}|_{max} = C_1 \alpha \tilde{A} K_1 K_2/\epsilon \end{aligned}$$

In the analysis thus far, the limits for loss-of-lock have been considered from the standpoint that the loop is initially locked-on. The limits for achievement of lock (acquisition) when no lock has yet been achieved are now estimated. Generally, the acquisition limits will be much narrower than the loss-of-lock limits, as will be shown.

It is constructive to analyze first the acquisition problem for the first-order loop. It will be shown later that the result is also applicable to the second-order loop. For the first-order loop ($F(s) = C_0$, $f(t) = C_0\, \delta(t)$), equation (23) becomes

$$\frac{d\,\phi(t)}{dt} = \frac{d\,\tilde{\theta}(t)}{dt} - C_0 \alpha \tilde{A} K_1 K_2 \sin \phi(t) \qquad (32)$$

This equation exhibits the stability of lock-on in a first-order loop. If $\tilde{\theta}(t) = (\delta\tilde{\theta})\,t$, that is, frequency shift only, then equation (32) becomes

$$\frac{d\,\phi(t)}{dt} = \delta\dot{\tilde{\theta}} - C_0\,\alpha\,\tilde{A}\,K_1\,K_2 \sin\,\phi(t)$$

A plot of this equation is shown as the phase plane plot of figure 7; it demonstrates that as long as the locus crosses the $d\,\phi(t)/dt = 0$ axis, lock-on is immediate since the only stable point is $\phi_0 = \sin^{-1} \delta\tilde{\theta}/C_0\,\alpha\,A\,K_1\,K_2$ (modulo 2π), and this point is reached in less than one cycle of ϕ, provided ϕ_0 exists. For the first-order loop, the condition for acquisition is the same as the condition for no loss-of-lock. That is, $|\sin\,\phi(t)| < 1$ is required for the solution to equation (32) at $d\,\phi(t)/dt = 0$. Therefore, the maximum frequency difference between the received carrier and the VCO that will ensure acquisition without cycle slipping is

$$|\delta\dot{\tilde{\theta}}|_{acq} = C_0\,\alpha\,\tilde{A}\,K_1\,K_2 \qquad (33)$$

The first-order loop has a linear filter with transfer function $F(s) = C_0$. The second-order loop has a linear filter with transfer function $F(s) = C_0 + C_1/s$. However, for high frequencies ($|s| = |j\omega| = \omega$ high), there exists $F(s) \approx C_0$. As long as $|C_0| \gg |C_1/s|$, or

$$\omega \gg |C_1/C_0|,$$

it may be assumed that the second-order loop acts like the first-order loop. The acquisition frequency will be expected to be at such a high frequency[20] for a phase-locked loop with high loop gain ($\alpha\,\tilde{A}\,K_1\,K_2$), so that equation (33) is valid for the second-order loop as well as for the first-order loop. It describes the frequency shift limit for immediate lock-on, that is, with no cycle slipping. The acquisition time[20] is about $1/\omega_n$ sec.

The second-order loop is actually capable of eventually locking a signal with deviation greater than $|\delta\tilde{\theta}|$. However, cycle slipping may occur for some time before the lock-on is achieved. The more liberal frequency deviation allowance will be called the pull-in frequency, $|\delta\tilde{\theta}|_{pull}$. For a second-order loop with a high gain operational amplifier[20]

$$|\delta\dot{\tilde{\theta}}|_{pull} \approx 2\sqrt{\zeta\omega_n C_1/\epsilon} = \sqrt{\frac{C_0\,C_1\,\alpha\,\tilde{A}\,K_1\,K_2}{2\epsilon} + \frac{C_1}{2}} \qquad (34)$$

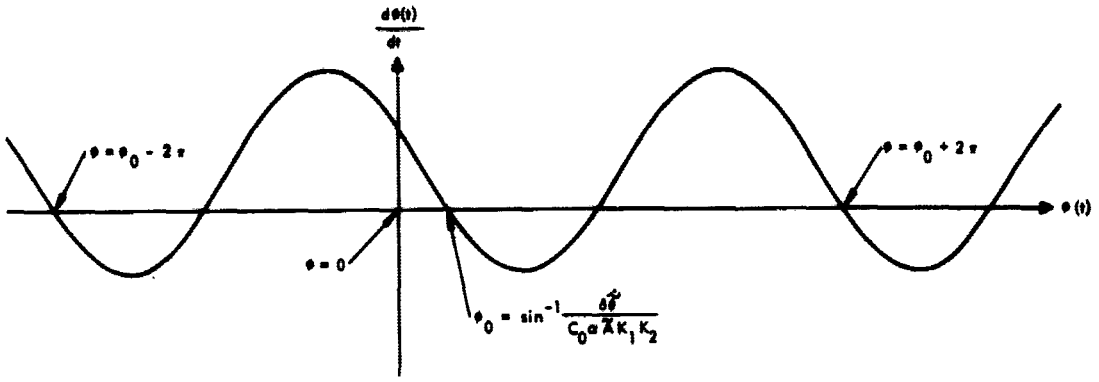

Figure 7. First-order loop locus.

For the perfect second-order loop ($\epsilon = 0$), pull-in is possible from any frequency. However pull-in time may be prohibitive; for example, if $|\delta\dot{\tilde{\theta}}|_{acq} << |\tilde{\omega}| << |\delta\dot{\tilde{\theta}}|_{pull}$, pull-in time is[20]

$$T_{pull} \approx \frac{1}{2\zeta\omega_n}\left(\frac{\dot{\tilde{\omega}}}{\omega_n}\right)^2 = \frac{(\tilde{\omega})^2}{C_1 \alpha \tilde{A} K_1 K_2 \left(C_0 \alpha \tilde{A} K_1 K_2 + \epsilon\right)} \approx \frac{C_1}{C_0}\frac{\tilde{\omega}^2}{\omega_n^4} \qquad (35)$$

The perfect second-order loop may acquire a signal with linearly varying frequency, as well as constant frequency shift. From Viterbi's phase plane plots of the phase-locked loop equations,[24] it can be seen that the maximum allowable frequency change rate for which acquisition is always ensured is

$$|\delta\ddot{\tilde{\theta}}|_{acq} = \frac{1}{2} C_1 \alpha \tilde{A} K_1 K_2 = \frac{1}{2}\omega_n^2 \qquad (36)$$

2.3 Statistical Description of Loop Errors

The above results described the allowable limits on $\tilde{\theta}(t)$ for perfect loop performance in a noiseless environment. In reality, noise will exist. For the present analysis, the noise is separated into two parts; one will be the additive gaussian white noise $n(t)$ discussed previously, while the other will be the statistical behavior of $\tilde{\theta}(t)$ (assumed deterministic above). Either of these noises will make perfect loop operation impossible. The quality of loop operation may be described statistically with assumed independent probability distributions for the coefficients of $\tilde{\theta}(t)$ and $n(t)$.

The quality of loop operation is described by such parameters as lock-on and lock-loss probabilities. Any such probabilities are found by integrating

the probability density function (p.d.f.) of loop errors over the appropriate limits, which were described in the previous section. In general, a "loop quality probability" will be of the form

$$p = \int_{\Lambda} p(\phi)\, d\phi \tag{37}$$

where Λ is the appropriate "perfect operation" region for ϕ and $p(\phi)$ is the probability density function of loop phase errors.

The probability density function of loop phase errors depends on the probability density functions of the coefficients of $\delta\tilde{\theta}(t)$ and $n(t)$:

$$p(\phi) = \int_{-\infty}^{\infty}\int_{-\infty}^{\infty}\int_{-\infty}^{\infty}\int_{-\infty}^{\infty} p(\delta\tilde{\theta}, \delta\dot{\tilde{\theta}}, \delta\ddot{\tilde{\theta}}, n)\, p(\phi \,|\, \delta\tilde{\theta}, \delta\dot{\tilde{\theta}}, \delta\ddot{\tilde{\theta}}, n)\, d(\delta\tilde{\theta})\, d(\delta\dot{\tilde{\theta}})\, d(\delta\ddot{\tilde{\theta}})\, dn$$

All coefficients are assumed to be independent gaussian random variables so that

$$p(\delta\tilde{\theta}, \delta\dot{\tilde{\theta}}, \delta\ddot{\tilde{\theta}}, n) = p(\delta\tilde{\theta})\, p(\delta\dot{\tilde{\theta}})\, p(\delta\ddot{\tilde{\theta}})\, p(n)$$

From these relationships the expression may be written

$$p(\phi) = \int_{-\infty}^{\infty}\int_{-\infty}^{\infty}\int_{-\infty}^{\infty} p(\delta\tilde{\theta})\, p(\delta\dot{\tilde{\theta}})\, p(\delta\ddot{\tilde{\theta}})\, p(\phi \,|\, \delta\tilde{\theta}, \delta\dot{\tilde{\theta}}, \delta\ddot{\tilde{\theta}})\, d(\delta\tilde{\theta})\, d(\delta\dot{\tilde{\theta}})\, d(\delta\ddot{\tilde{\theta}}) \tag{38}$$

where

$$p(\phi \,|\, \delta\tilde{\theta}, \delta\dot{\tilde{\theta}}, \delta\ddot{\tilde{\theta}}) = \int_{-\infty}^{\infty} p(n)\, p(\phi \,|\, \delta\tilde{\theta}, \delta\dot{\tilde{\theta}}, \delta\ddot{\tilde{\theta}}, n)\, dn\,.$$

The parameter $p(\phi \,|\, \delta\tilde{\theta}, \delta\dot{\tilde{\theta}}, \delta\ddot{\tilde{\theta}})$ will be found first from a knowledge of the statistical character of the additive noise. (Viterbi[24] does this calculation for a somewhat simpler case than that which is treated here.) Then, from a knowledge of the statistical character of $\delta\tilde{\theta}$, $\delta\dot{\tilde{\theta}}$, $\delta\ddot{\tilde{\theta}}$, $p(\phi)$ will be found as shown above.

Because of the presence of gaussian white noise, the phase error ϕ, given $\delta\tilde{\theta}$, $\delta\dot{\tilde{\theta}}$, $\delta\ddot{\tilde{\theta}}$, satisfies the Fokker-Planck equation.[24] For the first-order loop with $\delta\ddot{\tilde{\theta}} = 0$, this equation reduces to

$$0 = \frac{d}{d\phi}\left[\frac{4\alpha\tilde{A}}{K_1 K_2 N_0}\left(\sin\phi - \frac{\delta\dot{\tilde{\theta}}}{C_0 \alpha \tilde{A} K_1 K_2}\right) p\left(\phi \,\middle|\, \delta\tilde{\theta},\ \delta\dot{\tilde{\theta}} = 0\right) + \frac{d\, p\left(\phi \,\middle|\, \delta\tilde{\theta},\ \delta\dot{\tilde{\theta}} = 0\right)}{d\phi}\right]$$

The general solution to the conditional probability density function is then

$$p\left(\phi \,\middle|\, \delta\tilde{\theta}, \delta\dot{\tilde{\theta}} = 0\right) = C \exp\left(\frac{4\alpha\tilde{A}}{K_1 K_2 N_0}\cos\phi + \frac{4\delta\dot{\tilde{\theta}}}{C_0 (K_1 K_2)^2 N_0}\phi\right)$$

$$\left[1 + D\int_{-\pi}^{\phi} \exp\left(-\frac{4\alpha\tilde{A}}{K_1 K_2 N_0}\cos x - \frac{4\delta\dot{\tilde{\theta}}}{C_0 (K_1 K_2)^2 N_0}x\right) dx\right] (\text{modulo } 2\pi) \tag{39}$$

$$D = \frac{\exp\left(\dfrac{-8\delta\dot{\tilde{\theta}}\pi}{C_0 (K_1 K_2)^2 N_0}\right) - 1}{\displaystyle\int_{-\pi}^{\pi} \exp\left(-\frac{4\alpha\tilde{A}}{K_1 K_2 N_0}\cos x - \frac{4\delta\dot{\tilde{\theta}}}{C_0 (K_1 K_2)^2 N_0}x\right) dx}$$

$$C = 1 \Big/ \int_{-\pi}^{\pi} \frac{1}{C}\, p\left(\phi \,\middle|\, \delta\dot{\tilde{\theta}},\ \delta\ddot{\tilde{\theta}} = 0\right) d\phi$$

as shown by Viterbi.[24]

The perfect second-order loop case is much more difficult. Viterbi solved it for $\delta\ddot{\tilde{\theta}} = 0$; however in this report, the more general case in which $\delta\ddot{\tilde{\theta}} \neq 0$ is considered. The details of the analysis are included in Appendix A. The results are given here. For high signal-to-noise ratios the probability density function of the steady-state phase error is

$$p(\phi|\delta\ddot{\tilde{\theta}}) = C \exp\left\{\frac{4(\alpha\tilde{A})^2/N_0}{\alpha\tilde{A}K_1K_2 + \frac{C_1}{C_0^2}}(\cos\phi) + \frac{4\delta\ddot{\tilde{\theta}}\,\phi}{C_1N_0(K_1K_2)^2}\right\}$$

$$\cdot\left[1 + D\int_{-\pi}^{\varphi}\exp\left\{-\frac{4(\alpha\tilde{A})^2\cos x}{(\alpha\tilde{A}K_1K_2 + C_1/C_0^2)N_0} - \frac{4\delta\ddot{\tilde{\theta}}\,x}{C_1N_0(K_1K_2)^2}\right\}dx\right] -\pi\le\phi<\pi \tag{40}$$

where

$$D = \frac{\exp\left(-2\pi\, 4\delta\ddot{\tilde{\theta}}/C_1N_0(K_1K_2)^2\right) - 1}{\int_{-\pi}^{\pi}\exp\left\{-\frac{4(\alpha\tilde{A})^2\cos x}{N_0(\alpha\tilde{A}K_1K_2 + C_1/C_0^2} - \frac{4\delta\ddot{\tilde{\theta}}\,x}{C_1N_0(K_1K_2)^2}\right\}dx}$$

and C is chosen to make

$$\int_{-\pi}^{\pi} p(\phi|\delta\ddot{\tilde{\theta}})\,d\phi = 1$$

A second approximation valid for $0 < C_1 \ll C_0\,\alpha\,\tilde{A}K_1K_2$ is given by

$$p(\phi|\delta\ddot{\tilde{\theta}}) \approx C\exp\left\{\frac{4\alpha\tilde{A}}{K_1K_2N_o}\left(\cos\phi + \frac{\delta\ddot{\tilde{\theta}}}{C_1\alpha\tilde{A}K_1K_2}\phi\right)\right\}$$

$$\left[1 + D\int_{-\pi}^{\phi}\exp\left\{-\frac{4\alpha\tilde{A}}{K_1K_2N_o}\left(\cos x + \frac{\delta\ddot{\tilde{\theta}}}{C_1\alpha\tilde{A}K_1K_2}x\right)\right\}dx\right] -\pi\le\phi<\pi \tag{41}$$

where

$$D = \frac{\exp\left(-2\pi\frac{4\delta\ddot{\tilde{\theta}}}{C_1(K_1K_2)^2N_o}\right) - 1}{\int_{-\pi}^{\pi}\exp\left\{-\frac{4\alpha\tilde{A}}{K_1K_2N_o}\left(\cos x + \frac{\delta\ddot{\tilde{\theta}}}{C_1\alpha\tilde{A}K_1K_2}x\right)\right\}dx}$$

There are now two approximate solutions to $p(\phi|\delta\ddot{\tilde{\theta}})$ for the second-order-loop, equations (40) and (41). For $\delta\ddot{\tilde{\theta}} = 0$, these solutions reduce to Viterbi's results. In addition, if $\delta\ddot{\tilde{\theta}}$ is not random, these solutions are the same as those for $p(\phi)$ and may be used in equation (37) to calculate the "loop quality probabilities." However, if $\delta\ddot{\tilde{\theta}}$ is random, the integration indicated in equation (38) must be performed first:

$$p(\phi) = \int_{-\infty}^{\infty} p(\delta\ddot{\tilde{\theta}})\, p(\phi|\delta\ddot{\tilde{\theta}})\, d(\delta\ddot{\tilde{\theta}}) \tag{42}$$

Assuming $\delta\ddot{\tilde{\theta}}$ is a gaussian random variable with mean μ_3 and variance σ_3^2, then $p(\phi)$ is of the form

$$p(\phi) = I_1 + I_2 \tag{43}$$

where

$$I_1 = \int_{-\infty}^{\infty} \frac{\exp\left[-(\delta\ddot{\tilde{\theta}} - \mu_3)^2/2\sigma_3^2\right]}{\sqrt{2\pi\sigma_3^2}}\, C\, \exp\left|a\cos\phi + b(\delta\ddot{\tilde{\theta}})\phi\right| d(\delta\ddot{\tilde{\theta}})$$

$$I_2 = \int_{-\infty}^{\infty} \frac{\exp\left[-(\delta\ddot{\tilde{\theta}} - \mu_3)^2/2\sigma_3^2\right]}{\sqrt{2\pi\sigma_3^2}}\, C\, \exp\left|a\cos\phi + b(\delta\ddot{\tilde{\theta}})\phi\right| D$$

$$\int_{-\pi}^{\phi} \exp\left\{-a\cos x - b(\delta\ddot{\tilde{\theta}})x\right\} dx$$

$$D = \frac{\exp\left\{-2\pi b\,\delta\ddot{\tilde{\theta}}\right\} - 1}{\int_{-\pi}^{\pi} \exp\left\{-a\cos x - b\delta\ddot{\tilde{\theta}}x\right\} dx}$$

The values of a and b are implied by either equations (40) or (41), depending on the pertinent approximation, and C is chosen so that

$$\int_{-\pi}^{\pi} p(\phi)\, d\phi = 1$$

The integral I_1 may be evaluated exactly by completing the square of the functions of $\delta\ddot{\theta}$ in the exponent. Performing this function results in

$$I_1 = C \exp\left| a \cos\phi + b\mu_3 \phi + b^2\phi^2 \sigma_3^2/2 \right| \tag{44}$$

For $|\mu|_3 + \sigma_3$ small, D is small since $\exp\{-2\pi b \delta\ddot{\theta}\} \approx 1$. Then $I_2 \approx 0$, and equation (44) is a good approximation to $p(\phi)$. However, for $|\mu|_3 + \sigma_3$ significant, I_2 must be calculated numerically since it provides an important contribution to $p(\phi)$.

Equation (44) was evaluated through a numerical integration of C by a computer. The resulting density functions were plotted for various loop signal-to-noise ratios, a, and doppler change rate multipliers, b, in figures 8a through 8d. The statistical parameters of the doppler change rate, μ_3 and σ_3, are used as parameters. The a and b terms from equation (44) correspond to the following loop and noise parameters.

1. For $C_1 \ll C_0 \alpha \tilde{A} K_1 K_2$, any signal-to-noise ratio:

$$\left.\begin{aligned} a &\approx \frac{4\alpha\tilde{A}}{K_1 K_2 N_0} \\ b &\approx \frac{1}{C_1 \alpha \tilde{A} K_1 K_2} \end{aligned}\right\} \tag{45}$$

2. For high signal-to-noise ratios, any C_1:

$$\left.\begin{aligned} a &\approx \frac{4(\alpha\tilde{A})^2/N_0}{\alpha\tilde{A}K_1K_2 + C_1/C_0^2} \\ b &\approx \frac{4}{C_1 N_0 (K_1 K_2)^2} \end{aligned}\right\} \tag{46}$$

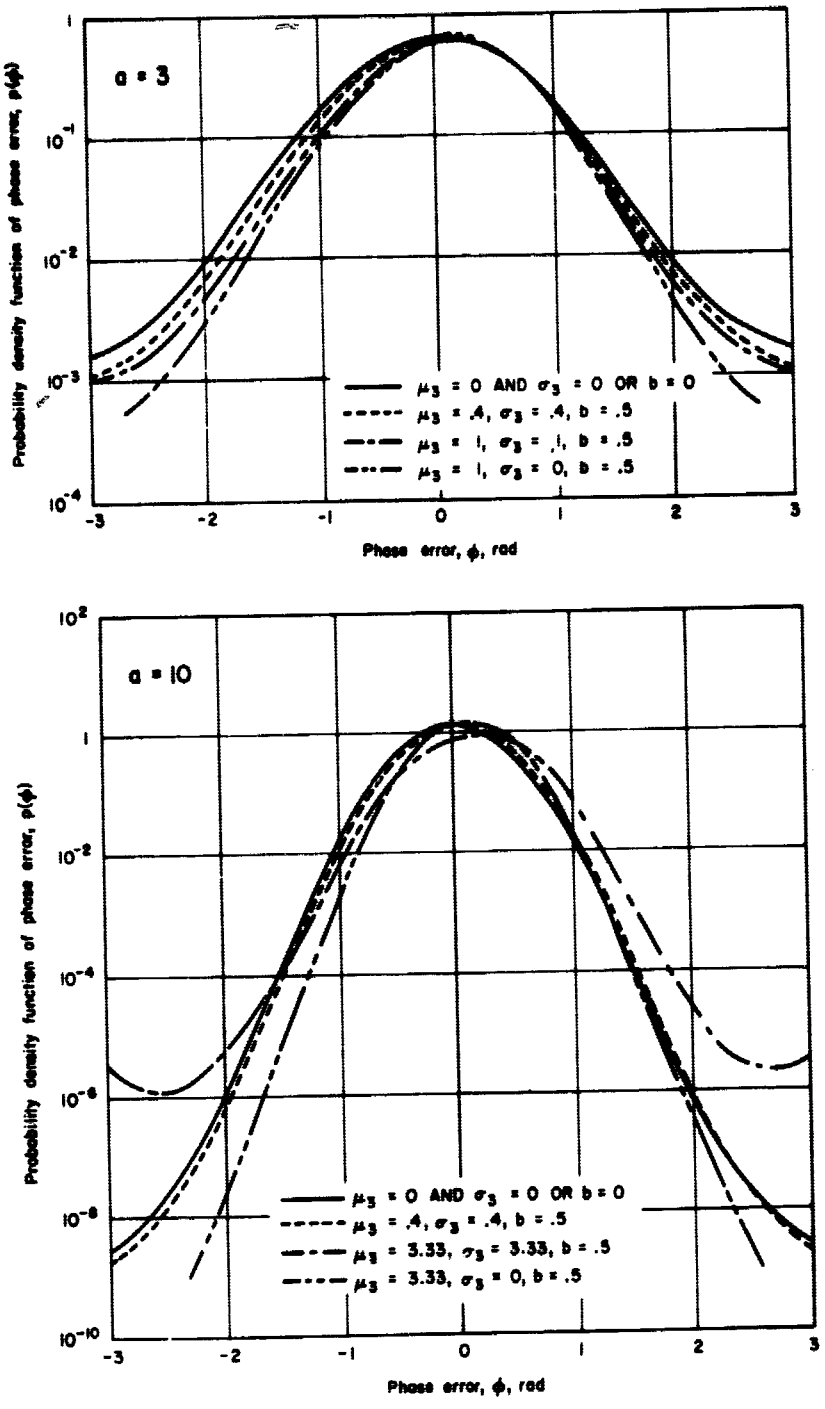

Figure 8. Phase error probability density functions ($p[\phi]$) for four loop signal-to-noise ratios (a) with various doppler change rate multipliers (b) and statistical parameters (μ_3 and σ_3).

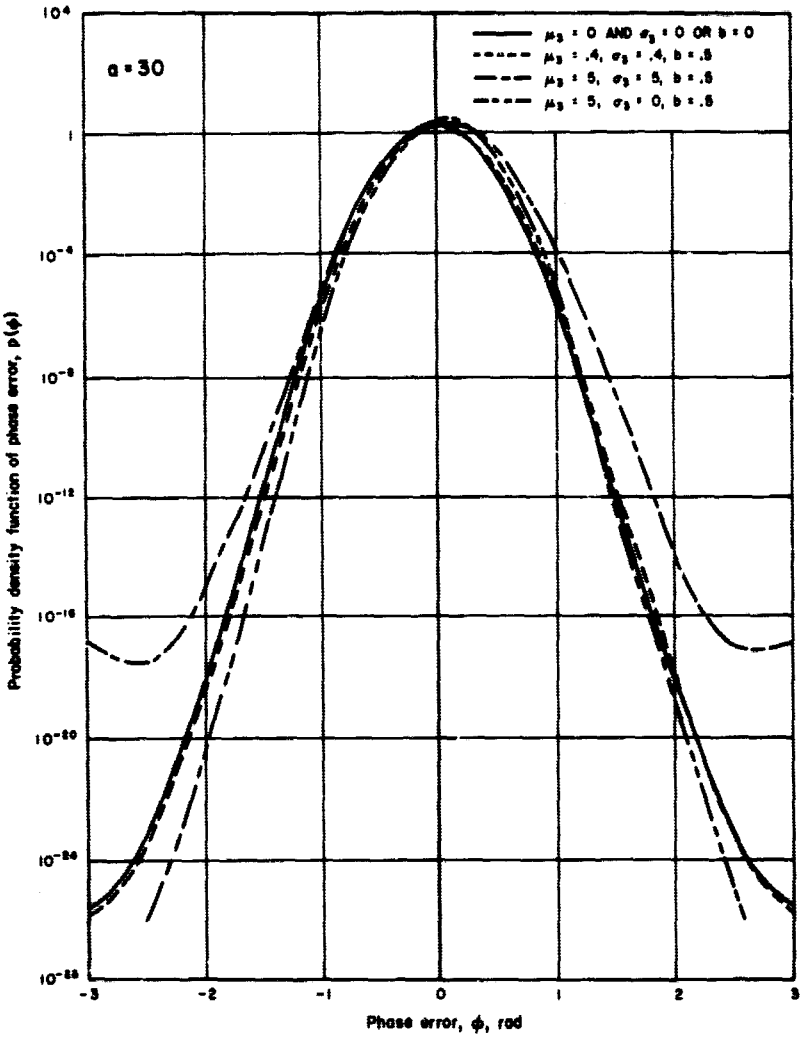

Figure 8. – Continued.

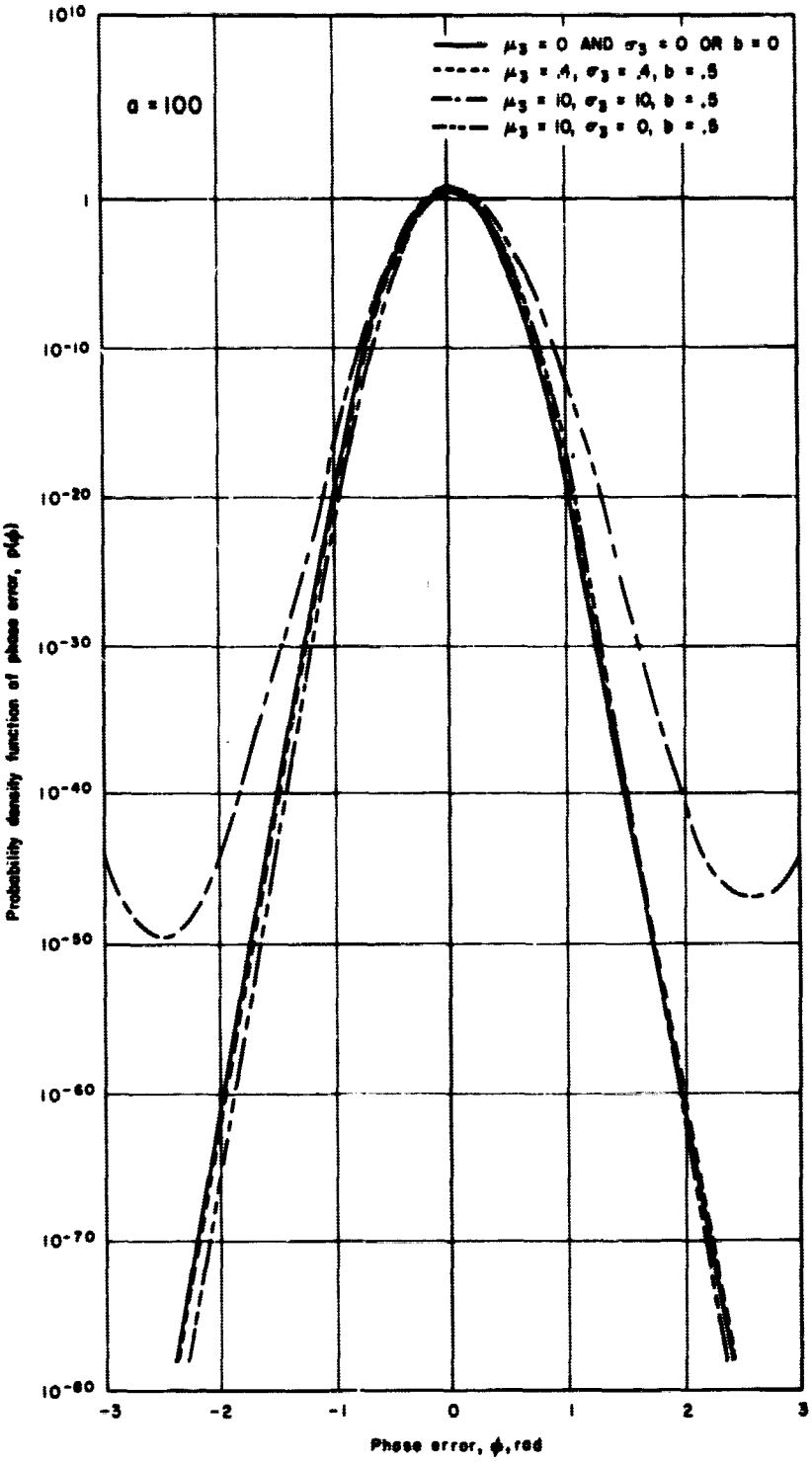

Figure 8. – Concluded.

For small $\underline{b}$, equation (44) yields a good approximation to $p(\phi)$ for all $-\pi < \phi \leq \pi$. For larger $\underline{b}$, the expression becomes inaccurate as $\phi \to \pi$. In fact, it can be seen with reference to equation (43) that I_2 vanishes at $\phi = \pi$ and progressively subtracts from $p(\phi)$ (for $\mu_3 > 0$) as ϕ increases. Essentially the term I_2 insures that

$$\lim_{\phi \to -\pi} p(\phi) = \lim_{\phi \to +\pi} p(\phi) \tag{46}$$

but does not significantly change any other characteristics of the density function. Consequently, equation (44) is plotted in the graphs of figure 8 with an estimated correction due to I_2.

A few major conclusions may be based on these figures. First, for a given parameter $\underline{b}$, the effect of $\delta\tilde{\theta}$ on $p(\phi)$ becomes negligible for high signal-to-noise ratios ($\underline{a} \to \infty$). The mean of $\delta\tilde{\theta}$, μ_3, shifts the peak of $p(\phi)$ away from $\phi = 0$. On the other hand, because σ_3^2, the variance of $\delta\tilde{\theta}$ does not vanish, the tails of $p(\phi)$ are raised significantly and the peak is lowered. Thus, the nonvanishing variance in $\delta\tilde{\theta}$ results in the expected equivalent degradation of the signal-to-noise ratio.

2.4 Multipath and Phase-Locked-Loop Models for Fast Fading Signals

The tracking behavior of phase-locked loops for a very slowly fading signal was discussed in the preceding section. The amplitude and phase fading rates were assumed small in comparison with the response rates of the phase-locked loop so that the signal amplitude and phase could be described by random variables. Derivations were then carried out for fixed amplitude and phase, and these results were averaged over their respective probability density functions.

The tracking behavior of phase-locked loops for a very rapidly fading signal was the subject of the present investigation. In this case the amplitude and phase fading rates were assumed large in comparison with the response rates of the phase-locked loop so that the signal amplitude and phase could be described by white random processes. The Fokker-Planck diffusion equation was then used to describe completely the phase error process, $\phi(t)$.

The multipath model from which the fading arises was the same as that used for the slowly fading case. The modulation was assumed to be phase or frequency modulation, since rapid fading degrades any information contained in an amplitude-modulated carrier. The transmitted signal may be written

$$s(t) = \hat{a}(t) \sin[\omega_0 t + m(t)] \tag{47a}$$

The received signal in a rapidly fading environment may be written

$$s(t) = \sqrt{2}\, A(t) \sin[\omega_0 t + m(t) + \hat{\theta}(t)] + n(t) \tag{47b}$$

The phase error term $\hat{\theta}(t)$ in equation (47b) includes intersymbol interference arising from the secondary transmission paths. However, the present analysis will be concerned only with phase-locking capabilities. The spectrum of m(t) and the intersymbol interference part of $\hat{\theta}(t)$ are assumed to be outside the passband of the phase-locked loop. Consequently, the signal effectively seen by the loop is

$$s(t) = \sqrt{2}\, A(t) \sin[\omega_0 t + \theta(t)] + n(t) \tag{47c}$$

where n(t), $\theta(t)$, and A(t) are random processes.

The additive noise, n(t), arises mainly from noise in the receiver and is therefore independent of the channel multipath noise, A(t) and $\theta(t)$. It is assumed white since it appears white to the narrowband phase-locked loop. Since the multipath signal results from contributions from a large number of randomly located and oriented scatterers, the quadrature components approach independent gaussian random processes. The fluctuation of these components results from motions of the signal source and receiver relative to the scattering surfaces, and for large relative velocities, the fluctuations will be rapid compared with fluctuations within the phase-locked loop. Consequently, in the ensuing analysis, the fading signal is considered white, and the associated fading is rapid.

The multipath signal is a perturbation of the transmitted signal so that the total received signal has quadrature components with nonzero means. Written in terms of amplitude and phase, the amplitude of the received signal forms a Rician random process, while the phase forms a dependent nonuniform random process.

2.5 Statistical Description of Loop Error for Fast-Fading Signals

In a multipath environment, the received signal may be assumed to consist of a stationary signal (i.e., the nonfading mean) $s_1(t)$, a Rayleigh fading signal $s_2(t)$, and additive noise. The resulting signal, $s_1(t) + s_2(t)$, is a Rician fading signal and

$$\left.\begin{aligned} s(t) &= s_1(t) + s_2(t) + n(t) \\ &= \sqrt{2}\, A \sin(\theta_1 + \omega_0 t) + \sqrt{2}\, B(t) \sin[\theta_2(t) + \omega_0 t] + n(t) \\ &= \sqrt{2}\, A \sin(\theta_1 + \omega_0 t) + n_F(t) + n(t) \end{aligned}\right\} \tag{48}$$

where $n_F(t)$ and n(t) may be represented as narrowband gaussian processes (compared with ω_0):

$$n_F(t) = \sqrt{2}\, B_1(t) \sin \omega_0 t + \sqrt{2}\, B_2(t) \cos \omega_0 t$$

$$n(t) = \sqrt{2}\, n_1(t) \sin \omega_0 t + \sqrt{2}\, n_2(t) \cos \omega_0 t$$

where

$$B_1(t) = B(t) \cos \theta_2(t)$$

$$B_2(t) = B(t) \sin \theta_2(t)$$

$n_1(t)$ and $n_2(t)$ = independent gaussian processes

The phase detector output is then

$$\left.\begin{aligned} x(t) &= s(t)\sqrt{2}\, K_1 \cos \theta_v(t) \\ &= AK_1 \left\{ \sin[\theta_1 + \omega_0 t - \theta_v(t)] + \sin[\theta_1 + \omega_0 t + \theta_v(t)] \right\} \\ &\quad + \sqrt{2}\, K_1 [n_F(t) + n(t)] \cos \theta_v(t) \\ &= AK_1 \sin[\theta_1 + \omega_0 t - \theta_v(t)] + AK_1 \sin[\theta_1 + \omega_0 t + \theta_v(t)] \\ &\quad + K_1 \left\{ -[n_1(t) + B_1(t)] \sin[\theta_v(t) - \omega_0 t] \right. \\ &\qquad \left. + [n_2(t) + B_2(t)] \cos[\theta_v(t) - \omega_0 t] \right\} \end{aligned}\right\} \quad (49)$$

where θ_v is the total instantaneous phase of the signal from the voltage-controlled oscillator.

If higher frequency terms ($\approx 2\omega_0$) are neglected (because of low pass filtering), the phase detector output may be written

$$x(t) = AK_1 \sin \varphi(t) + K_1 \hat{n}(t) \quad (50)$$

where

$$\varphi(t) = \theta_1 + \omega_0 t - \theta_v(t)$$

$$\hat{n}(t) = -[n_1(t) + B_1(t)] \sin[\theta_v(t) - \omega_0 t] + [n_2(t) + B_2(t)] \cos[\theta_v(t) - \omega_0 t]$$

The phase-locked loop equation is

$$\frac{d\phi(t)}{dt} = \frac{d\theta_1}{dt} - K_1K_2\int_0^t [A \sin \phi(\sigma) + \hat{n}(\sigma)]\, f(t-\sigma)\, d\sigma \tag{51}$$

As shown previously, the steady-state probability function for ϕ is the steady-state solution to the Fokker-Planck equation:[24]

$$\begin{aligned} 0 = &-\frac{\partial}{\partial y_0}\left[A_0(\underline{y})p(\underline{y})\right] - \frac{\partial}{\partial y_1}\left[A_1(\underline{y})p(\underline{y})\right] \\ &+ \frac{1}{2}\frac{\partial^2}{\partial y_0^2}\left[A_{00}(\underline{y})p(\underline{y})\right] + \frac{1}{2}\frac{\partial^2}{\partial y_0 \partial y_1}\left[A_{01}(\underline{y})p(\underline{y})\right] \\ &+ \frac{1}{2}\frac{\partial^2}{\partial y_1 \partial y_0}\left[A_{10}(\underline{y})p(\underline{y})\right] + \frac{1}{2}\frac{\partial^2}{\partial y_1^2}\left[A_{11}(\underline{y})p(\underline{y})\right] \end{aligned} \tag{52}$$

in which

$$A_k(\underline{y}) \equiv \lim_{\Delta t \to 0} \frac{E(\Delta y_k \mid \underline{y})}{\Delta t}$$

$$A_{k\ell}(\underline{y}) \equiv \lim_{\Delta t \to 0} \frac{E(\Delta y_k \Delta y_\ell \mid \underline{y})}{\Delta t}$$

But $\phi(t) = C_1 y_0(t) + C_0 y_1(t)$ where $dy_0/dt = y_1$ The increments in y for use in the Fokker-Planck coefficients are

$$\begin{aligned} \Delta y_0 &= y_1(t)\Delta t \\ \Delta y_1 &= -[K_1K_2\alpha\tilde{A} \sin(C_1y_0 + C_0y_1) - \frac{1}{C_1}(\delta\ddot{\theta})]\,\Delta t \\ &\quad - K_1K_2\int_t^{t+\Delta t} \hat{n}(u)\, du \end{aligned} \tag{53}$$

Consequently, the coefficients are

$$A_0(\underline{y}) = \lim_{\Delta t \to 0} \frac{E[y_1(t)\Delta t]}{\Delta t} = y_1(t)$$

and

$$A_1(\underline{y}) = \lim_{\Delta t \to 0} \frac{E\left\{-\left[K_1 K_2 \alpha \tilde{A} \sin(C_1 y_0 + C_0 y_1) - \frac{1}{C_1}(\delta\dot{\theta})\right]\Delta t - K_1 K_2 \int_t^{t+\Delta t} \hat{n}(u)\, du\right\}}{\Delta t}$$

$$= -K_1 K_2 \alpha \tilde{A} \sin(C_1 y_0 + C_0 y_1) - \frac{1}{C_1}(\delta\dot{\theta}) \qquad \text{(zero mean noise assumed)}$$

$$A_{00}(\underline{y}) = A_{01}(\underline{y}) = A_{10}(\underline{y}) = 0 \text{ since numerators are } 0(\Delta t)^2.$$

$$A_{11}(\underline{y}) = \lim_{\Delta t \to 0} \frac{E\left\{\left[K_1 K_2 \int_t^{t+\Delta t} \hat{n}(u)\, du\right]^2\right\}}{\Delta t}$$

$$= (K_1 K_2)^2 \lim_{\Delta t \to 0} \frac{1}{\Delta t} E\left[\int_{u=t}^{t+\Delta t} \int_{v=t}^{t+\Delta t} \hat{n}(v)\, \hat{n}(u)\, dv\, du\right]$$

$$= (K_1 K_2)^2 \lim_{\Delta t \to 0} \frac{1}{\Delta t} \int_{u=t}^{t+\Delta t} \int_{v=t}^{t+\Delta t} E[\hat{n}(v)\, \hat{n}(u)]\, dv\, du$$

$$A_{11}(\underline{y}) = (K_1 K_2)^2 \lim_{\Delta t \to 0} \frac{1}{\Delta t} \int_{u=t}^{t+\Delta t} \int_{v=t}^{t+\Delta t} R_{\hat{n}}(u, v)\, dv\, du \tag{54}$$

where $R_{\hat{n}}(u, v) = E[\hat{n}(u)\, \hat{n}(v)]$ is the noise covariance function (which describes the additive combination of the receiver noise and the fading noise). If the Rician fading noise has a white noise spectrum with one-sided spectral density, N_F, and if the additive noise has a white noise spectrum with one-sided spectral density N_0, then

$$\left.\begin{aligned} R_{\hat{n}}(u, v) &= R_n(u, v) + R_{n_F}(u, v) \\ &= \tfrac{1}{2} N_0\, \delta(u - v) + \tfrac{1}{2} N_F\, \delta(u - v) \end{aligned}\right\} \tag{55}$$

Then

$$A_{11}(\underline{\gamma}) = \frac{1}{2}(K_1K_2)^2(N_0+N_F)\lim_{\Delta t\to 0}\frac{1}{\Delta t}\int_t^{t+\Delta t}\int_t^{t+\Delta t}\delta(u-v)\,dv\,du$$

$$= \frac{1}{2}(K_1K_2)^2(N_0+N_F)\lim_{\Delta t\to 0}\frac{1}{\Delta t}\int_t^{t+\Delta t} 1\,du$$

$$A_{11}(\underline{\gamma}) = \frac{1}{2}(K_1K_2)^2(N_0+N_F) \tag{56}$$

The only difference between the equations for rapidly fading signals and those derived previously for nonfading signals is in the coefficient $A_{11}(\underline{\gamma})$. In effect, the fast Rician fading only raises the noise level from N_0 to $N_0 + N_F$, without changing any other part of the phase error calculation. This fact leaves intact the analysis of the signal-to-noise ratio for bandpass limiting that was performed previously. The implication is that bandpass limiting is beneficial to fast-fading systems as well as to nonfading systems.

The spectral density, N_F, of the fading signal is determined by the intensity and rapidity of fluctuation of the multipath signal. The relationships among these quantities will be discussed in a later section of the report. A preliminary estimate of the relations may be obtained, however, if it is assumed that the actual fading spectral density is uniform and band-limited to a bandwidth B_F. The bandwidth B_F is much greater than the bandwidth of the loop noise, B_L, so that the assumption that the fading is white is still valid as far as the loop is concerned. With these assumptions, the spectral density is given by

$$N_F = \frac{\Gamma A^2}{B_F} \qquad B_F >> B_L \tag{57}$$

where Γ is defined as the ratio between the rms value of the fading portion of the signal and the nonfading portion of the signal, i.e., the ratio of the power in the indirect path signal to the power in the direct path signal, A^2.

2.6 Comparison of Loop Performance for Slow Fading and Fast Fading

In the previous sections, analyses were carried out for the probability density function of phase errors in phase-locked loops for the two extremes of very rapid fading and very slow fading. In both analyses the received signal was assumed to be a constant phasor plus a Rayleigh phasor. The results of the analyses are presented in this section.

If the amplitude of the constant phasor is A_0 and the variance of the quadrature components of the Rayleigh random phasor is σ^2, then A, the received signal amplitude process, has a Rician density function[25] which is given by

$$p(A) = \frac{A}{\sigma^2} \exp\left[-\frac{1}{2\sigma^2}\left(A^2 + A_0^2\right)\right] I_0\left(\frac{AA_0}{\sigma^2}\right) \quad 0 \leq A < \infty \tag{58}$$

where $I_0(x)$ is the modified Bessel function of the first kind and of order zero.

The associated phase process is distributed as

$$p(\theta) = \left\{\frac{1}{2\pi} + \frac{1}{\sqrt{2\pi}}\left(A_{0x}\cos\theta + A_{0y}\sin\theta\right)\left[1 - \operatorname{erfc}\left(\frac{A_{0x}\cos\theta + A_{0y}\sin\theta}{\sigma}\right)\right]\right\}$$

$$\cdot \exp\left[-\frac{1}{2\sigma^2}\left(A_{0x}\sin\theta + A_{0y}\cos\theta\right)^2\right] \quad -\pi \leq \theta < \pi \tag{59}$$

In a fast fading environment the randomly fading signal appears to have a white spectral density function if the fading bandwidth, B_F, is much greater than the phase-locked loop bandwidth, B_L. Then the fading noise looks like additive white noise to the loop.[7] If this additive fading noise is assumed to have a one-sided spectral density N_F watts/hertz and is band-limited to B_F hertz, then $\sigma^2 = N_F B_F$. Similarly, if the non-fading noise is "white" gaussian with spectral density N_0 watts/hertz and is band-limited to B_0 hertz, then the non-fading noise variance is $N_0 B_0$. At any rate, the loop sees only the noise variance, $(N_0 + N_F)B_L$. Consequently, the fading effectively raises the overall noise power by a factor $1 + N_F/N_0$.

In a slowly fading environment, the fading bandwidth, B_F, is much smaller than the loop bandwidth, B_L. If it is assumed the time

derivative of the random phase, W, is band-limited to

$$W << \omega_n = \sqrt{C_1 A K}$$

then all phase and frequency fluctuations due to the fading are completely tracked by the phase-locked loop. In the expression above, the loop parameters are

ω_n = the natural frequency of the loop filter

C_1 = the second-order-loop filter constant, defined on pages 15 and 16

A = the rms amplitude of the signal input

$K = K_1K_2$ (where K_1 is the rms amplitude of the voltage-controlled oscillator and K is a proportionality constant of the voltage-controlled oscillator)

As a result the phase error probability density function conditioned on the amplitude and phase of the noiseless fading input is

$$p(\phi|A,\theta) = \exp\left(\frac{4A}{KN_0}\cos\phi\right)\Big/2\pi I_0\left(\frac{4A}{KN_0}\right) \qquad (60)$$

the unconditional phase error probability density function is available from equations (1) and (2) as

$$p(\phi) = \int_0^\infty p(\phi|A,\theta)\, p(A)\, dA \qquad (61)$$

The fading signal is statistically described by A_0 and $\sigma^2 (= N_F B_F)$. However, the mean and variance of the amplitude of the signal are only approximated by A_0 and $2\sigma^2$ for $\sigma/A_0 << 1$. In fact, for the Rician distribution, the mean amplitude is always greater than A_0 and the amplitude variance is always less than $2\sigma^2$.

The probability density functions of phase errors in phase-locked loops with various signal-to-noise ratios in multipath fading environments are plotted in figures 9 through 11 for fast fading, slowly fading, and non-fading signals. These curves again show that fast fading just raises the effective system noise level. The curves also display the fact that slow fading improves performance if the performance criterion is based on $p(\phi)$ for $|\phi| << \pi/2$. It is especially obvious at low loop signal-to-noise ratios ($a = A_0^2/B_L N_0$) that phase error variance is reduced by the presence of a slowly fading signal. However, average error probability calculations depend most critically on $p(\phi)$ for $|\phi| > \pi/2$. On this basis a no-fade performance is usually

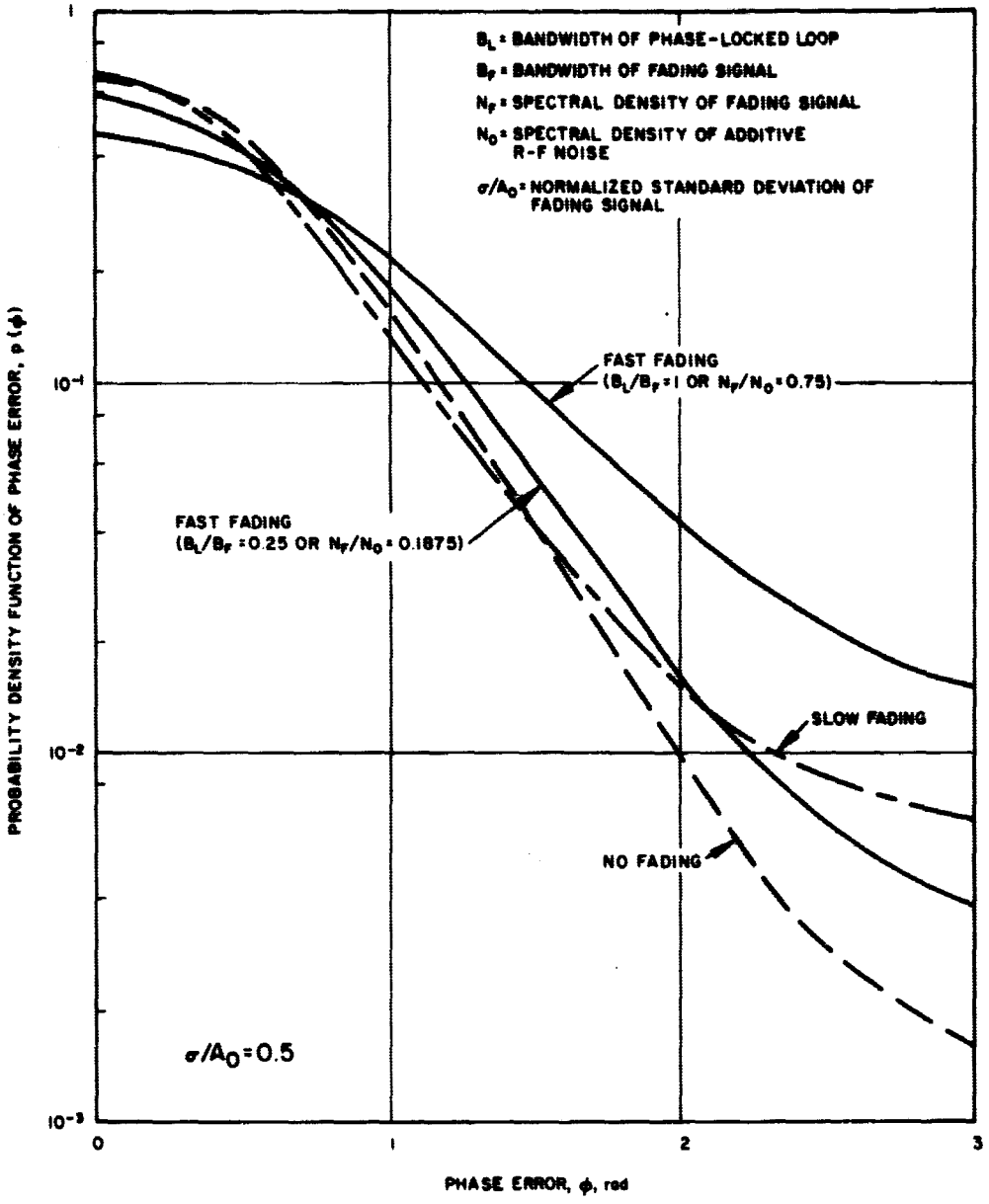

Figure 9. Phase errors of phase-locked loops with a signal-to-noise ratio of 3 in a multipath fading environment.

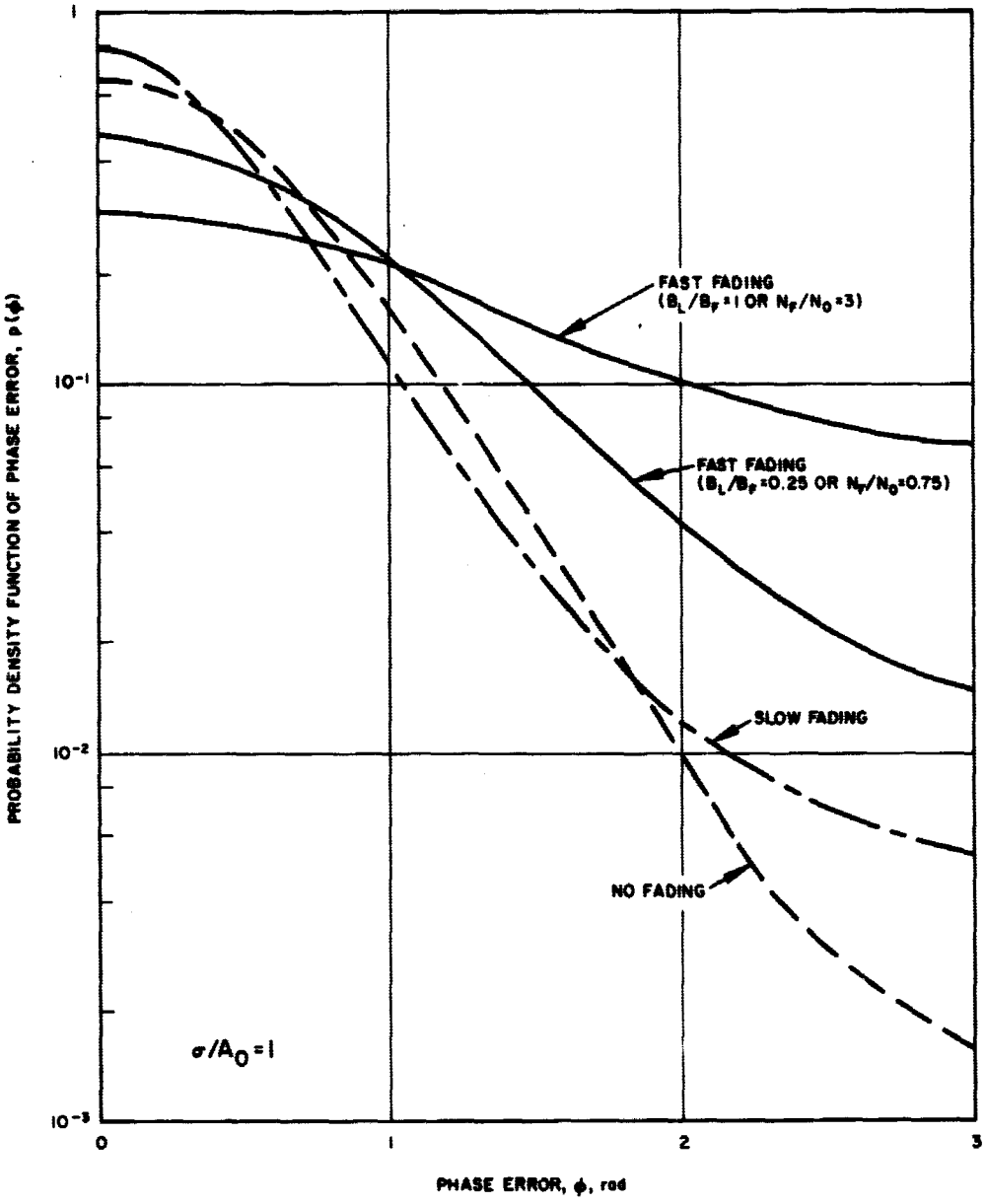

Figure 9. - Continued.

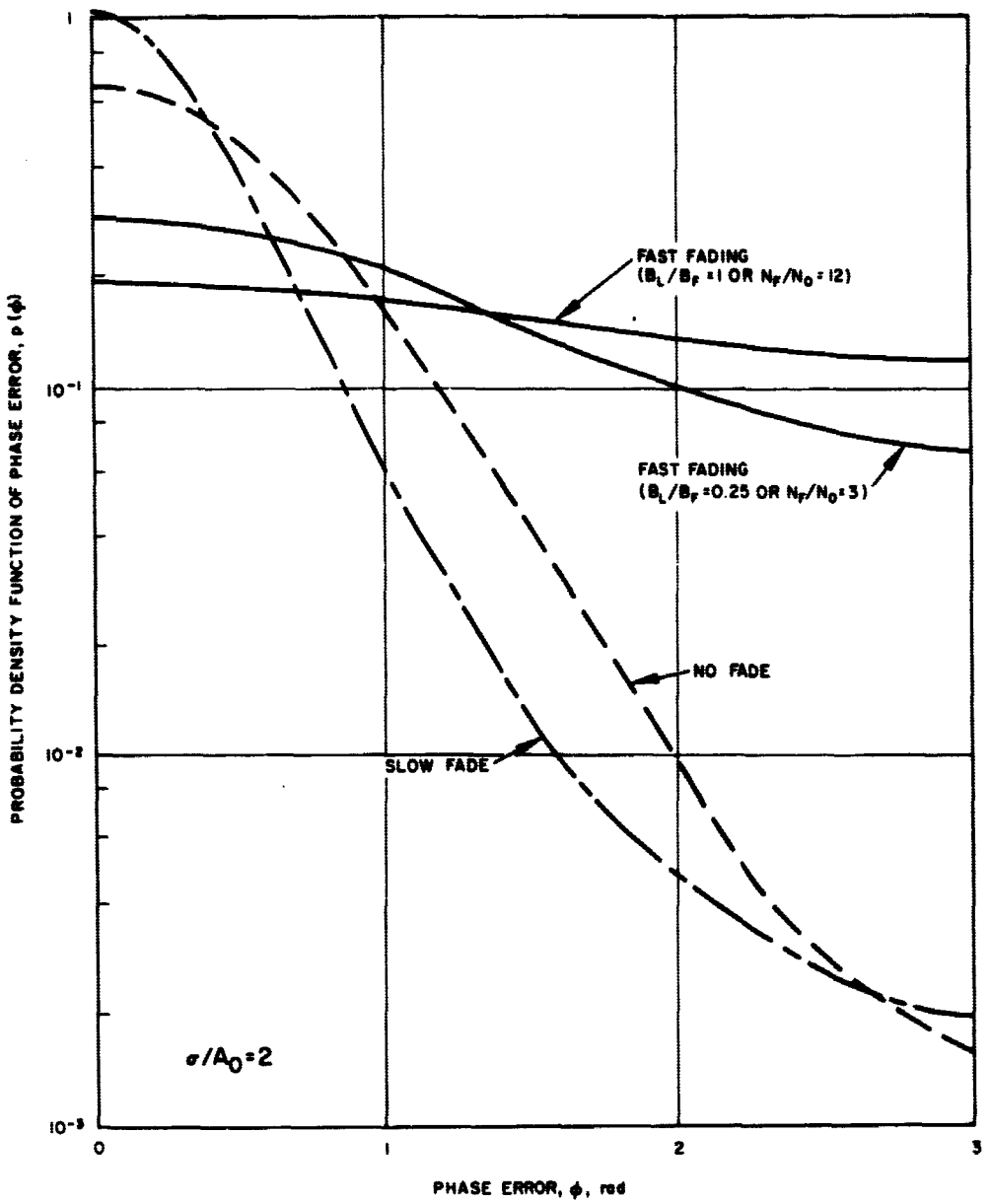

Figure 9. - Concluded.

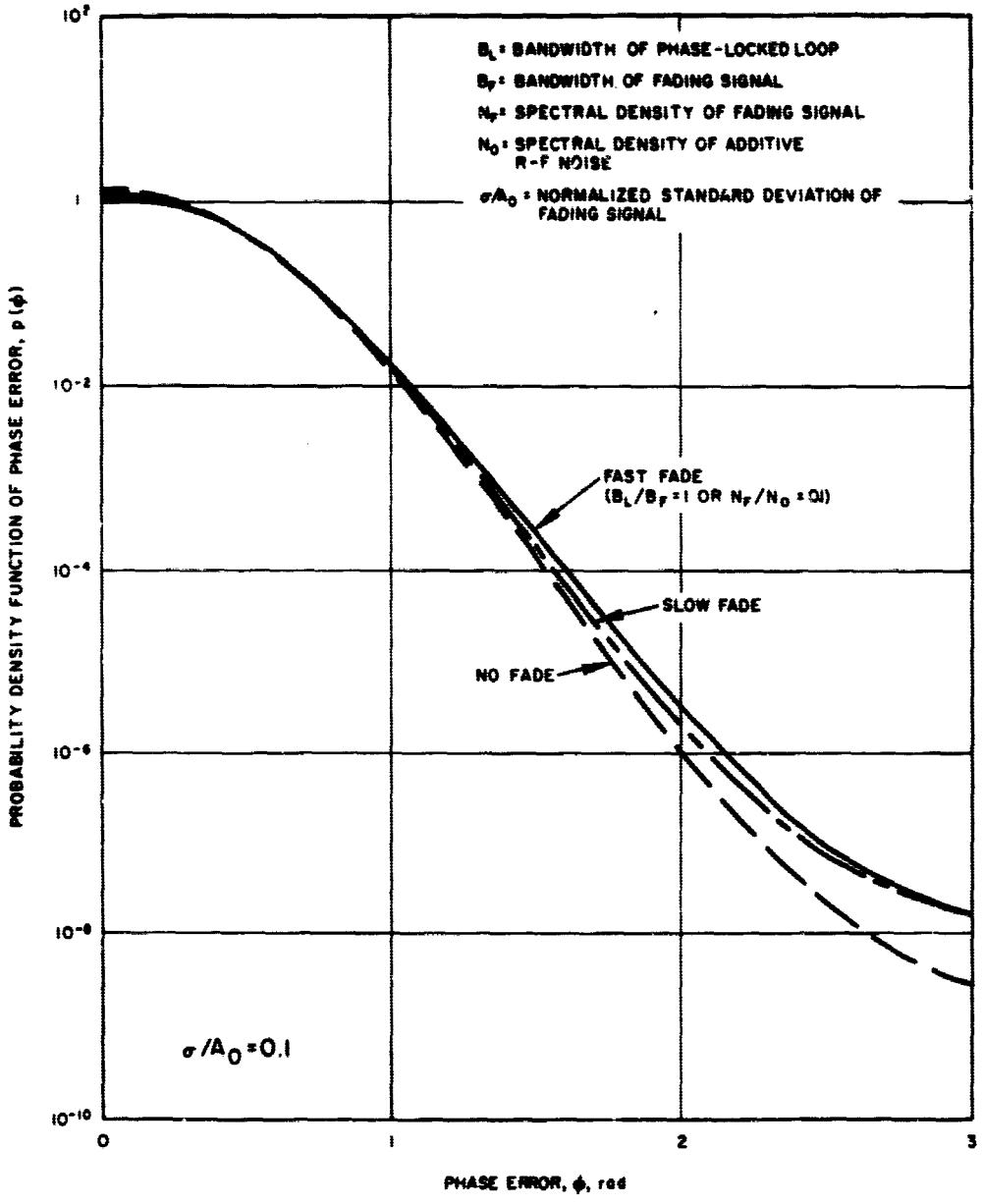

Figure 10. Phase errors of phase-locked loops with a signal-to-noise ratio of 10 in a multipath fading environment.

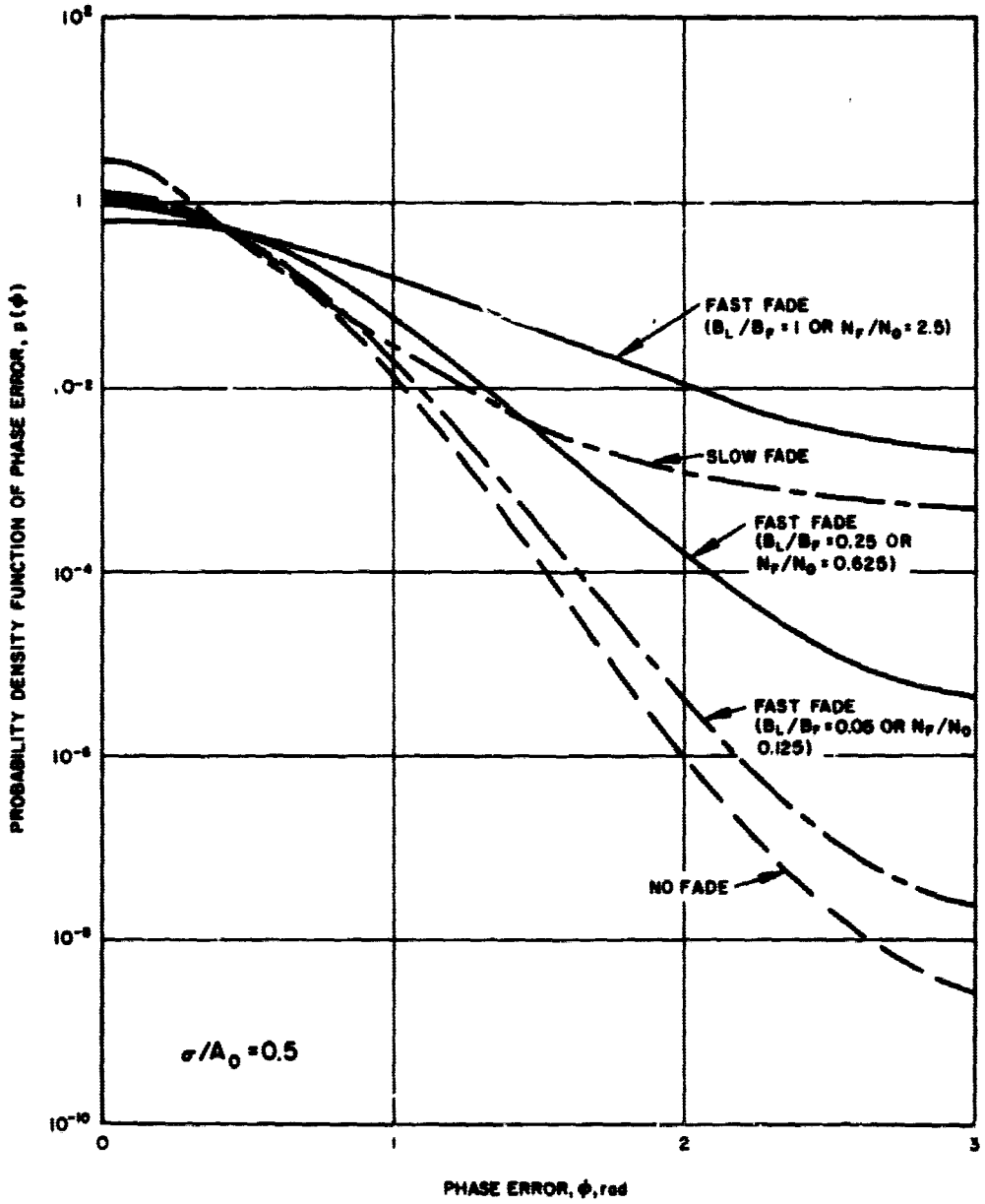

Figure 10. - Continued.

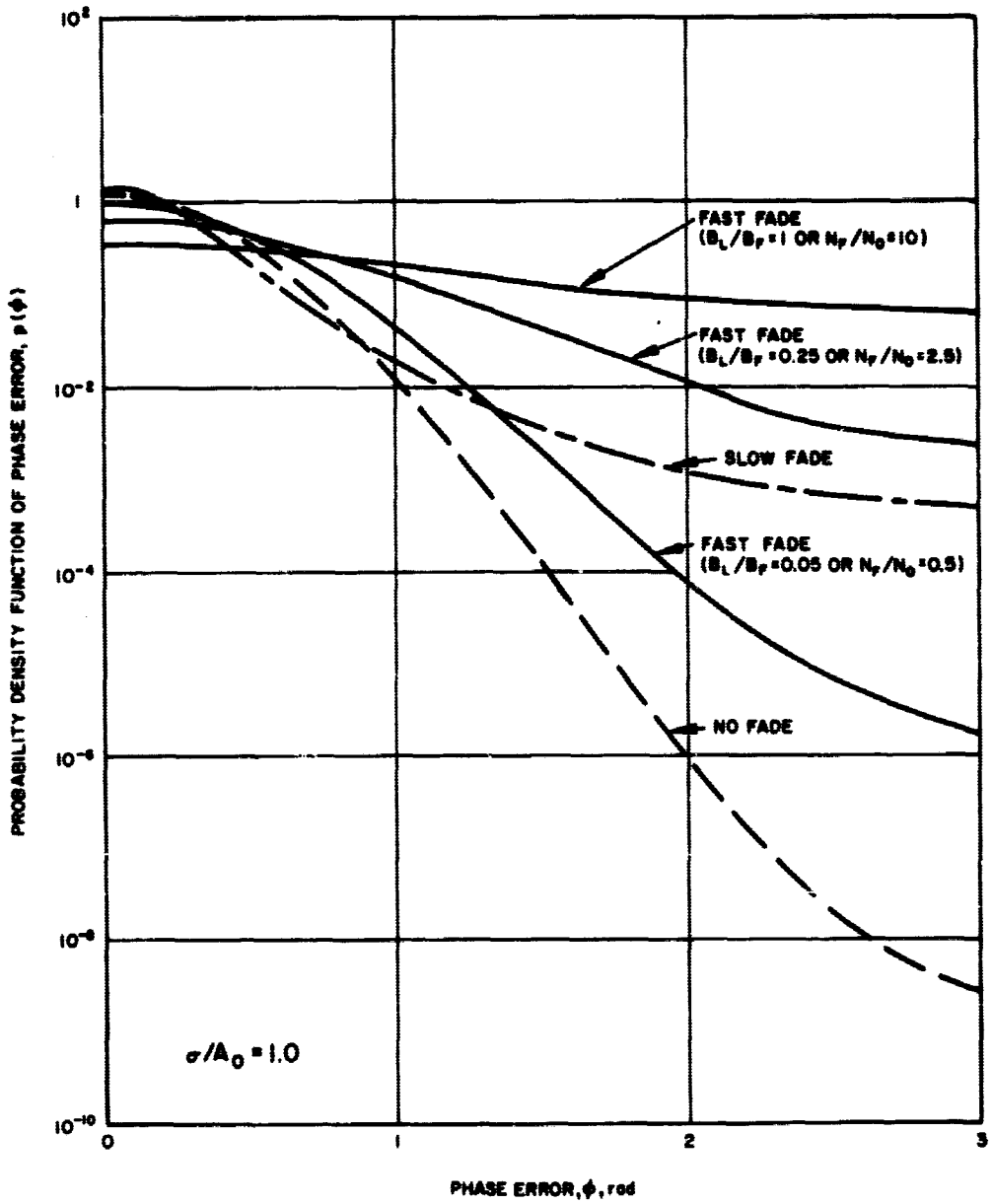

Figure 10. - Continued.

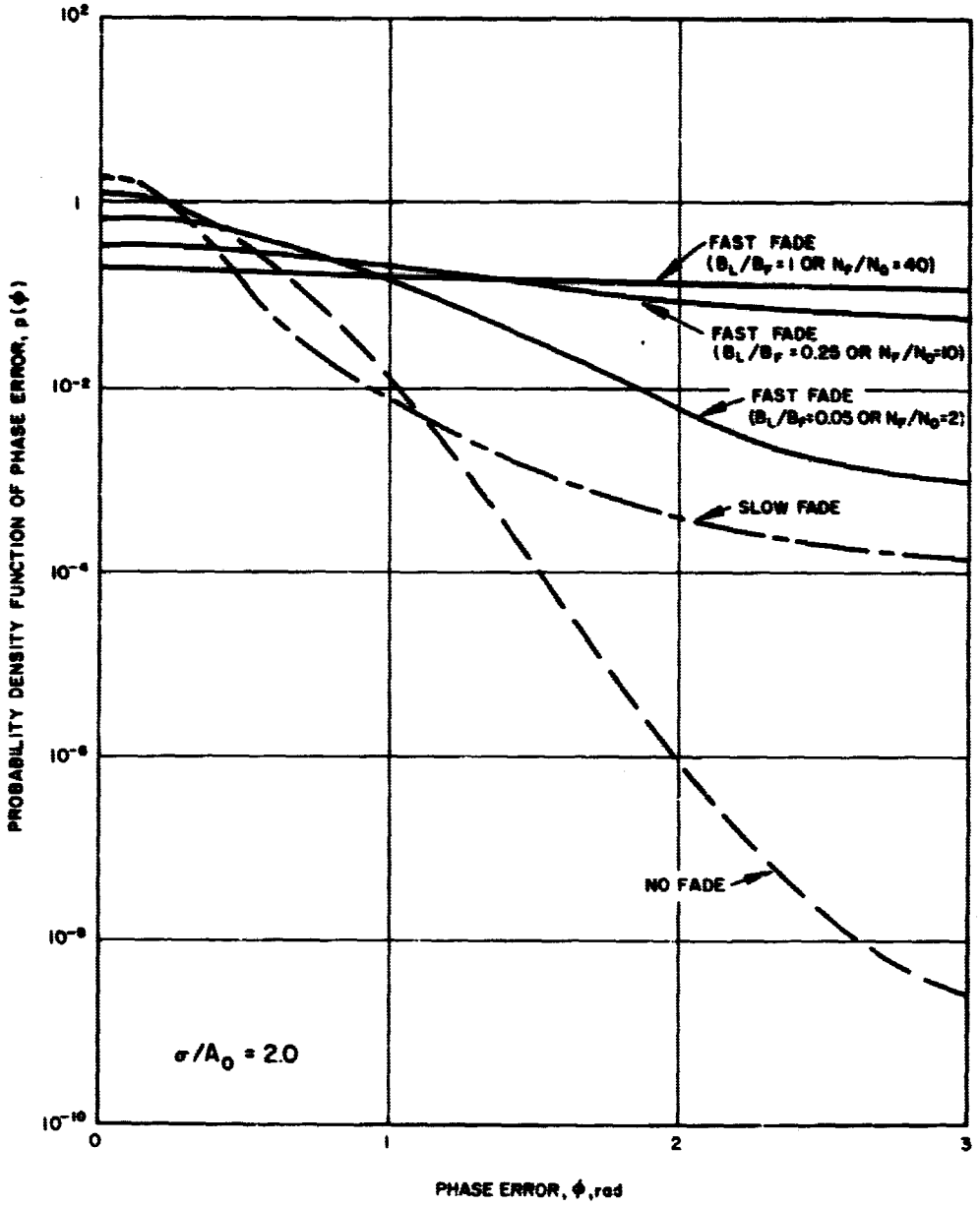

Figure 10. - Concluded.

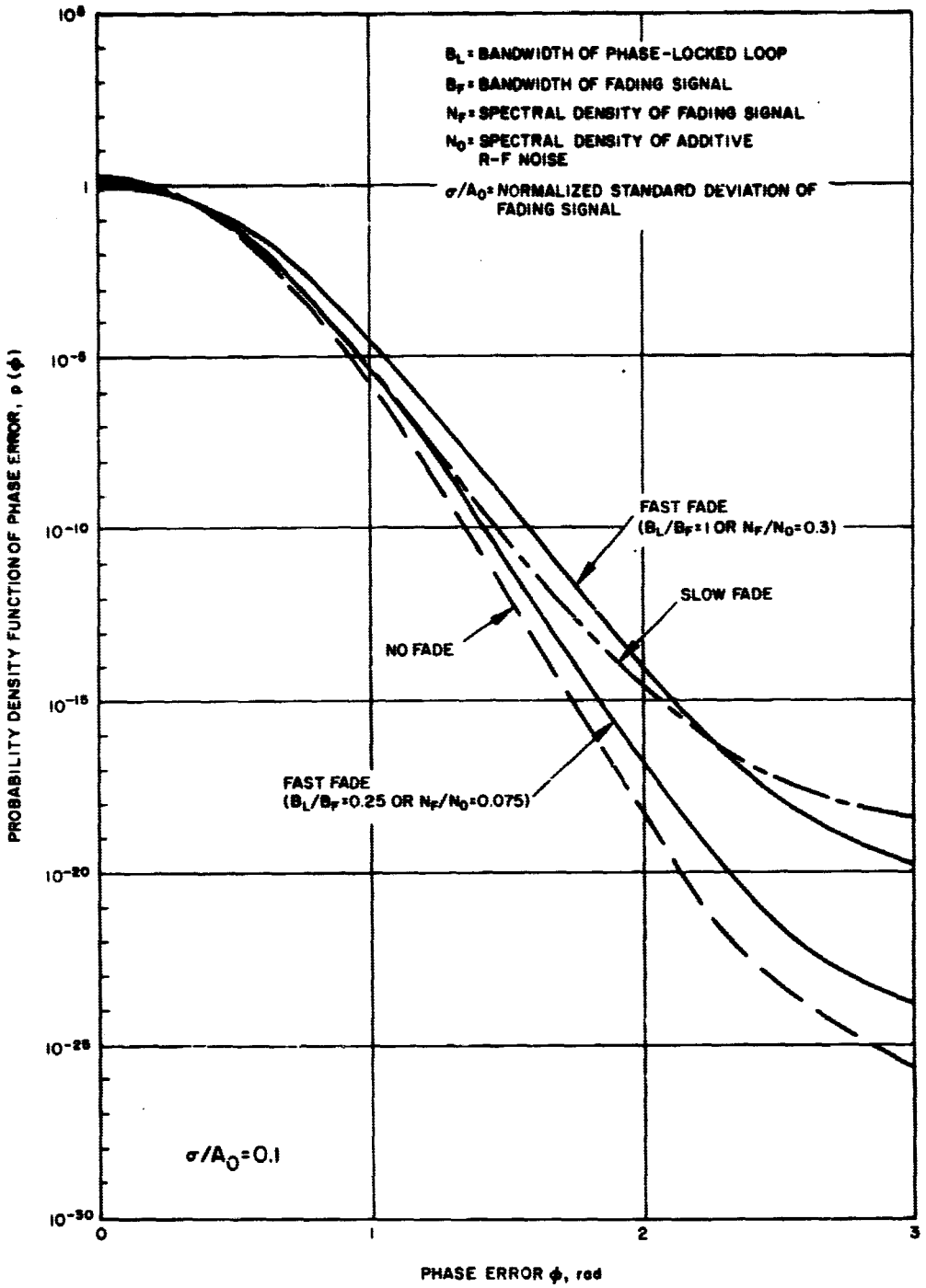

Figure 11. Phase errors of phase-locked loops with a signal-to-noise ratio of 30 in a multipath fading environment.

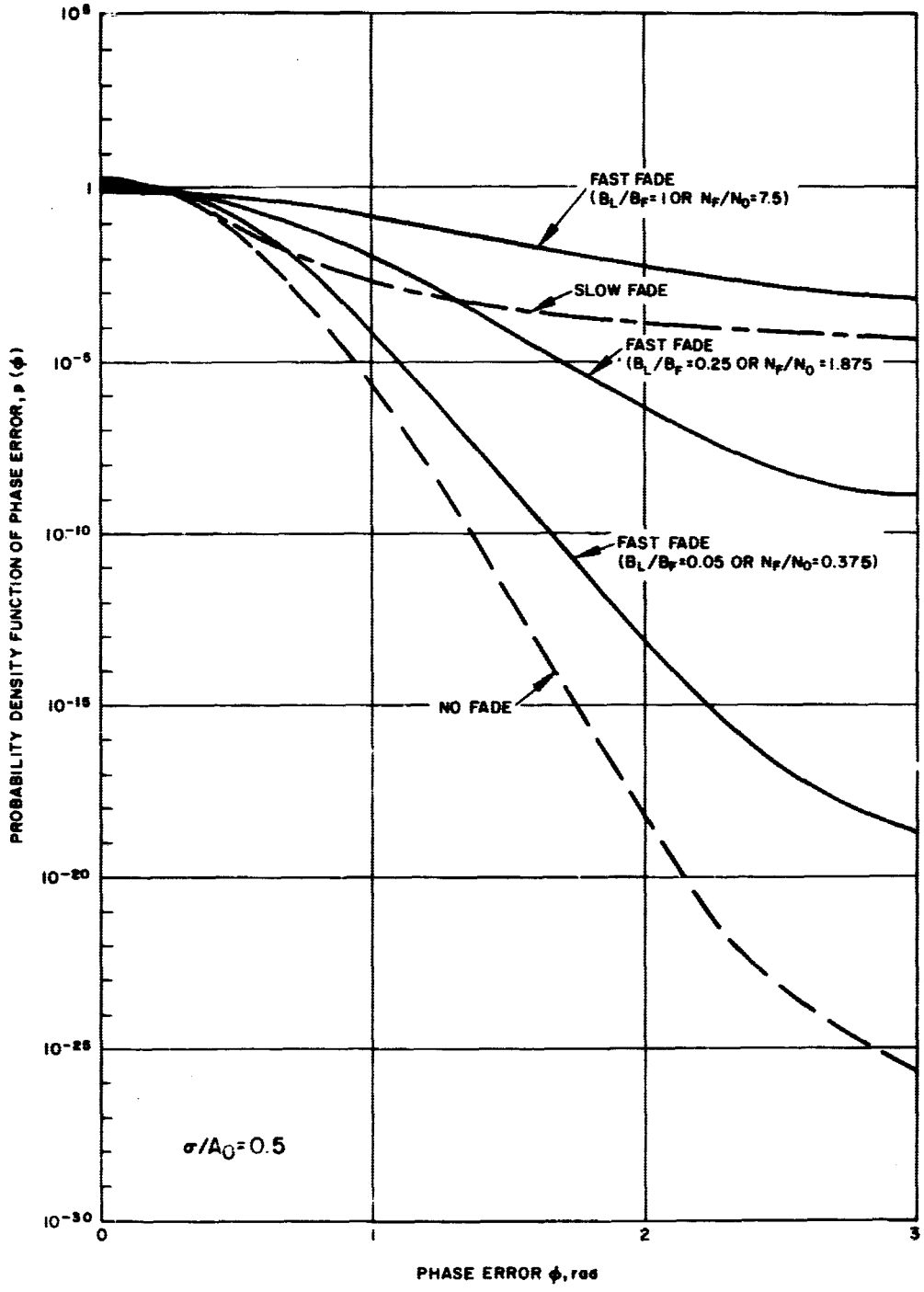

Figure 11. - Continued.

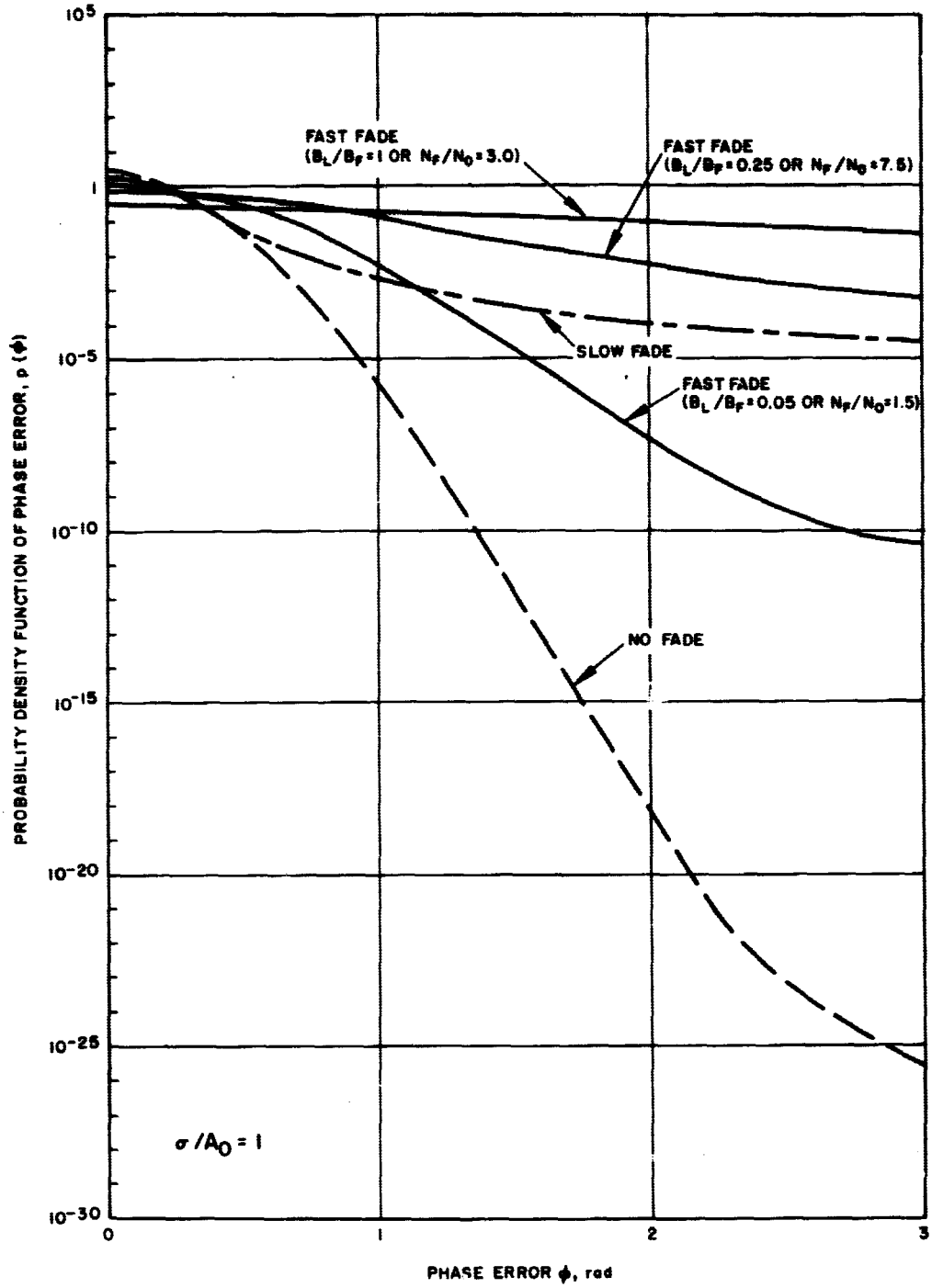

Figure 11. - Concluded.

better than a slowly fading performance, with an exception for low a and high σ/A_0 (see $\sigma/A_0 = 2$ in figure 9).

The improvements due to slow fading are unrealistic in the present system, however. For the communications channel considered here, it is highly unlikely that the rms value of the random phasor fluctuations will exceed the constant phasor amplitude, since selective focusing of the fading signal is unrealistic. Consequently, the variance of the random fluctuations will be small, or $\sigma^2 < A_0^2$. For these cases the slowly fading signal is normally inferior to the non-fading signal.

Performance for fast fading signals is improved by decreasing the loop bandwidth, while the performance for slowly fading signals is independent of loop bandwidth. The reason for these properties is that, for fast fading, $B_F >> B_L$ so that the loop sees only the fading noise variance $N_F B_L$, while for slow fading, $B_F << B_L$ so that the loop sees $N_F B_F$ irrespective of B_L. For fast fading, the extreme case of $B_F = B_L$ is plotted as a lower limit to fast fading performance, although it should be recalled that $B_F >> B_L$ is required for quantitative accuracy of the fast fade calculations.

2.7 First-Order Phase-Locked Loop with Arbitrary Fading Spectrum

In this section of the report the problem of determining the probability density function of phase errors is considered in a first-order phase-locked loop in the presence of a non-white multipath signal.

It is assumed that the loop is initially in lock on the primary signal and that the increase in the multipath signal as the planet surface is approached tends to disturb the system and to cause it to lose lock. Expressions are derived here for the probability of loss of lock as a function of the relative received powers of the primary and secondary paths, of the power spectrum of the secondary fluctuating path, and of the receiver noise power.

The receiver is assumed to be approximated by a first-order phase-locked loop as shown in figure 12. This model differs from conventional loop models since the gain of the loop A(t) (proportional to the received signal amplitude) and the input reference phase $\theta(t)$, in addition to the additive noise $n'(t)$, are random processes.

It is assumed that, for the primary path signal, doppler shift is automatically compensated and variations in A due to increasing range are relatively slow, so that the primary path signal can be written

$$s_p(t) = \sqrt{2}\, A \sin\left(\omega_0 t + \beta_p(t)\right) \tag{62}$$

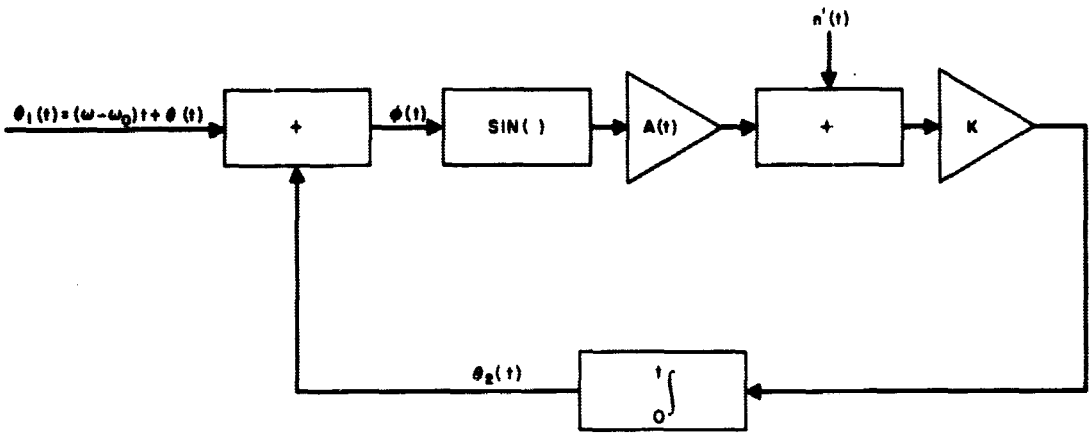

Figure 12. First-order loop with random gain and phase.

where

ω_0 = carrier frequency

β_p = the phase of the primary path signal

The secondary path signal $s_s(t)$ is given by

$$s_s(t) = \sqrt{2}\, V(t) \sin\left(\omega_0 t + \beta_s(t)\right) \tag{63}$$

where

β_s = phase of secondary path signal

$V(t)$ = amplitude of secondary path signal

It is also assumed that $V(t)$ and $\beta_s(t)$ vary slowly enough in comparison with the reciprocal of the carrier frequency so that equation (63) can be written as

$$s_s(t) = \sqrt{2}\, V_s(t) \sin\, \omega_0 t + \sqrt{2}\, V_c(t) \cos\, \omega_0 t \tag{64}$$

where $V_c(t)$ and $V_s(t)$ are the in-phase and quadrature components of $s_s(t)$. Hence, the total input signal is

$$s(t) = \sqrt{2}\left[A \cos \beta_p(t) + V_s(t)\right] \sin \omega_0 t + \sqrt{2}\left[A \sin \beta_p(t) + V_c(t)\right] \cos \omega_0 t \tag{65}$$

$$= \sqrt{2\left(A^2 + 2A\left[\cos\, \beta_p(t)\, V_s(t) + \sin \beta_s(t)\, V_c(t)\right] + V_s^2(t) + V_c^2(t)\right)}$$

$$\cdot \sin\left[\omega_0 t + \Phi(t)\right] \tag{66}$$

where

$$\tan \Phi(t) = \frac{A \sin \beta_p(t) + V_c(t)}{A \cos \beta_p(t) + V_s(t)} \tag{67}$$

If it is assumed that the indirect signal power is much smaller than the direct signal power, that is that $A^2 >> V_s^2(t) + V_c^2(t)$, then equation (66) becomes approximately

$$s(t) \approx \sqrt{2}\left[A + V_s(t) \cos \beta_p(t) + V_c(t) \sin \beta_p(t)\right] \sin\left[\omega_0 t + \Phi(t)\right] \tag{68}$$

When the loop is initially locked onto the primary signal, it can be assumed, without loss of generality, that $\beta_p(t) = 0$. Thus,

$$\tan \phi(t) = \frac{V_c(t)}{A + V_s(t)} \approx \frac{V_c(t)}{A} \tag{69}$$

so that s(t) can finally be written approximately as

$$s(t) = \sqrt{2}\left[A + V_s(t)\right] \sin\left[\omega_0 t + \frac{V_c(t)}{A}\right] \tag{70}$$

Association of equation (70) with figure 12 indicates that

$$\theta(t) = \frac{V_c(t)}{A}$$

$$A(t) = A + V_s(t) \tag{71}$$

It is now assumed that

1) $V_c(t)$ and $V_s(t)$ are zero mean stationary gaussian processes with correlation matrix[25]

$$\Lambda' = \begin{bmatrix} \sigma_c^2 & R_c(\tau) & 0 & R_{cs}(\tau) \\ R_c(\tau) & \sigma_c^2 & -R_{cs}(\tau) & 0 \\ 0 & -R_{cs}(\tau) & \sigma_c^2 & R_c(\tau) \\ R_{cs}(\tau) & 0 & R_c(\tau) & \sigma_c^2 \end{bmatrix} \tag{72}$$

where σ_c^2 = the variance of V_c and R_{cs}, the autocorrelation function of V_c, and $R_{cs}(\tau)$, the cross-correlation function of V_c and V_s, are represented by

$$R_c(\tau) = E\left[V_c(t)\, V_c(t-\tau)\right] = \frac{1}{\pi} \int_0^\infty S_v(\omega) \cos\left(\omega - \omega_c\right)\tau \, d\omega \qquad (73)$$

$$R_{cs}(\tau) = E\left[V_c(t)\, V_s(t-\tau)\right] = \frac{1}{\pi} \int_0^\infty S_v(\omega) \sin\left(\omega - \omega_c\right)\tau \, d\omega \qquad (74)$$

where $S_v(\omega)$ is the narrow-band power spectrum of $s_s(t)$, centered about ω_0.

2) $n'(t)$ is a white gaussian noise process with two-sided spectral density $N_0/2$ which is independent of $V_c(t)$ and $V_s(t)$.

2.8 Mathematical Analysis of First-Order Loop

The mathematical analysis of the system in figure 12 proceeds in three parts:

1) The system is represented in a form such that Fokker-Planck diffusion techniques may be applied. A differential equation is derived that describes the probability density function of the phase error ϕ. The equation cannot immediately be solved directly for $p(\phi)$ since it involves the conditional moments $E\left[V_c' \mid \phi\right]$ and $E\left[V_s \mid \phi\right]$ where V_c' represents the time derivative of V_c. These moments are unknown.

2) The system is linearized so that a closed form solution for $\phi(t)$ can be obtained. By assuming that V_c', and V_s, and ϕ are jointly gaussion, calculation of Var ϕ, $E\left[V_c' \phi\right]$, and $E\left[V_s \phi\right]$ yields

$$E\left[V_c' \mid \phi\right] = \frac{E\left[V_c' \phi\right]\phi}{\text{Var } \phi} \approx \frac{E\left[V_c' \phi\right]}{\text{Var } \phi} \sin\phi$$

$$E\left[V_s \mid \phi\right] = \frac{E\left[V_s \phi\right]\phi}{\text{Var } \phi} \approx \frac{E\left[V_s \phi\right]}{\text{Var } \phi} \sin\phi$$

for small ϕ.

3) The results of part 2) are placed in part 1), and the differential equation is solved to obtain an expression for the probability density function of ϕ.

Fokker-Planck techniques. – To make use of the Fokker-Planck diffusion equation,[26] it is necessary to exhibit a set of system variables that are components of a first-order vector Markov process. This procedure requires generating $V_s(t)$ and $V_c(t)$ by passage of two stationary white gaussian processes, $n_s(t)$ and $n_c(t)$, through two identical fixed parametric filters as is shown in figure 13. (The in-phase and quadrature spectra of a narrowband process are identical.) The filters have a low-pass transfer function, $H(j\omega)$, whose square magnitude is the same shape as $S_v(\omega + \omega_0) + S_v(\omega - \omega_0)$ for $|\omega| << \omega_0$. From equation (74), it is seen that the random processes $V_c(t_1)$ and $V_s(t_2)$ are not independent unless $t_1 = t_2$. Therefore, $n_c(t)$ and $n_s(t)$ must have a cross-power spectral density $Sn_cn_s(\omega)$ that satisfies the equation

$$R_{cs}(\tau) = \int_{-\infty}^{\infty} |H(j\omega)|^2 \; S_{n_c n_s}(\omega) \exp[j\omega\tau] \, d\omega \tag{75a}$$

where

$$H(s) = \frac{1}{s^2 + a_1 s + a_2} \tag{75b}$$

Therefore, $S_{n_c n_s}(\omega)$ must be assumed an imaginary odd function of ω which is sufficient information to solve the present problem.

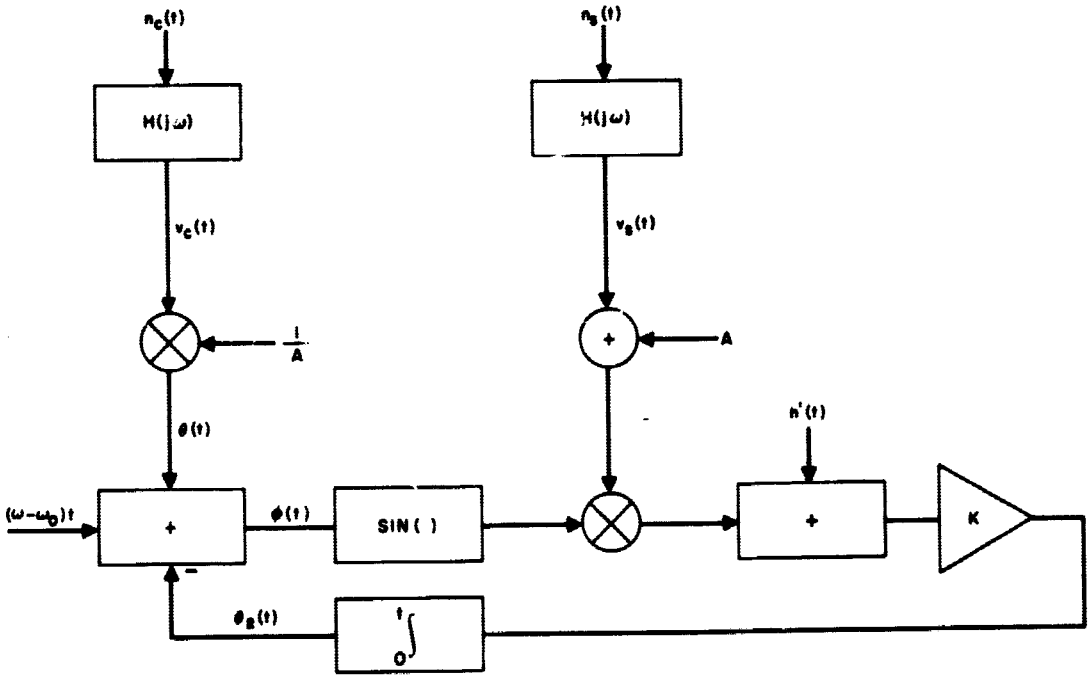

Figure 13. Equivalent phase-locked loop with only white gaussian inputs.

The differential equation describing the system in figure 12 is given by

$$\frac{d\phi}{dt} = (\omega - \omega_0) + \theta'(t) - K A(t) \sin \phi(t) - Kn'(t) \tag{76}$$

where K is the gain of the amplifier as illustrated in figure 13. Therefore, from (14), $V_c(t)$ must be a differentiable random process. Hence, $H(j\omega)$ must have a denominator polynomial in ω at least 2 degrees greater than the numerator polynomial. The simplest system that satisfies this criterion has a differential equation that is second order. Hence, choosing this simplest form for $H(j\omega)$ yields a set of first-order differential equations:

$$\frac{d\phi}{dt} = \omega - \omega_0 + \frac{x_2(t)}{A} - K (A + V_s(t)) \sin \phi(t) - Kn'(t) \tag{77}$$

$$\frac{dx_1(t)}{dt} = -a_1 x_1(t) - a_2 V_s(t) + n_c(t) \tag{78}$$

$$\frac{dV_s(t)}{dt} = x_1(t) \tag{79}$$

$$\frac{dx_2(t)}{dt} = -a_1 x_2(t) - a_2 V_c(t) + n_s(t) \tag{80}$$

$$\frac{dV_c(t)}{dt} = x_2(t) \tag{81}$$

with

$$E\left[n'(t)\, n'(t+\tau)\right] = \frac{N_0}{2} \delta(\tau) \tag{82}$$

$$E\left[n_c(t)\, n_c(t+\tau)\right] = \frac{N_1}{2} \delta(\tau) \tag{83}$$

$$E\left[n_s(t)\, n_s(t+\tau)\right] = \frac{N_1}{2} \delta(\tau) \tag{84}$$

$n'(t)$ independent of $n_c(t)$, $n_s(t)$

$S_{n_1 n_2}(\omega)$ an odd imaginary function of ω.

Now equations (77) - (84) constitute a set of differential equations that describe a five-dimensional, first-order vector Markov process as can be seen by noting that the rates of change (i. e. , hence the future values) of ϕ, x_1, x_2, V_s, and V_c depend only on the present values of ϕ, x_1, x_2, V_s, and V_c.

The multidimensional Kolmogorov diffusion equation for the joint density function of a vector Markov process is given by[26]

$$\frac{\partial p_1(z)}{dt} = \sum_{m+n+p+q+r>0} \frac{(-1)^{m+n+p+q+r}}{m!\, n!\, p!\, q!\, r!} \frac{\partial^{m+n+p+q+r}}{\partial \phi^m \partial V_s^n dx_1^p dV_c^q dx_2^r} \left[A_{m,n,p,q,r}(z) p_1(z) \right] \quad (85)$$

where $z = (\phi, V_s, x_1, V_c, x_2)$ and

$$A_{m,n,p,q,r}(\phi, V_s, x_1, V_c, x_2) = \lim_{\Delta t \to 0} \frac{1}{\Delta t} \cdot \left[(\Delta\phi)^m (\Delta V_s)^n (\Delta x_1)^p (\Delta V_c)^q (\Delta x_2)^r \,\middle|\, \phi, V_s, x_1, V_c, x_2 \right]$$

$$= A_{m,n,p,q,r}(z) \quad (86)$$

Formal integration of equations (77) - (81) over (t, t + Δt) yields

$$\Delta\phi = (\omega - \omega_0)\Delta t + \frac{1}{A}\int_t^{t+\Delta t} x_2(\tau)\,d\tau - K\,A\int_t^{t+\Delta t} \sin\phi(\tau)d\tau$$

$$- K\int_t^{t+\Delta t} V_s(\tau)\sin\phi(\tau)d\tau - K\int_t^{t+\Delta t} n'(\tau)\,d\tau \qquad (87)$$

$$\Delta x_1 = -a_1\int_t^{t+\Delta t} x_1(\tau)\,d\tau - a_2\int_t^{t+\Delta t} V_s(\tau)d\tau + \int_t^{t+\Delta t} n_c(\tau)d\tau \qquad (88)$$

$$\Delta V_s = \int_t^{t+\Delta t} x_1(\tau)\,d\tau \qquad (89)$$

$$\Delta x_2 = -a_1\int_t^{t+\Delta t} x_2(\tau)d\tau - a_2\int_t^{t+\Delta t} V_c(\tau)d\tau + \int_t^{t+\Delta t} n_s(\tau)d\tau \qquad (90)$$

$$\Delta V_c = \int_t^{t+\Delta t} x_2(\tau)\,d\tau \qquad (91)$$

Use of equations (87) - (91) in equation (86) yields

$$A_{1,0,0,0,0}(z) = \omega - \omega_0 + \frac{x_2}{A} - K\,A\sin\phi - K\,V_s\sin\phi \qquad (92a)$$

$$A_{0,1,0,0,0}(z) = x_1 \qquad (92b)$$

$$A_{0,0,1,0,0}(z) = -a_1 x_1 - a_2\,V_s \qquad (92c)$$

$$A_{0,0,0,1,0}(z) = x_2 \tag{92d}$$

$$A_{0,0,0,0,1}(z) = -a_1 x_2 - a_2 V_c \tag{92e}$$

$$A_{2,0,0,0,0}(z) = \frac{K^2 N_0}{2} \tag{92f}$$

$$A_{0,2,0,0,0}(z) = A_{0,0,0,2,0}(z) = 0 \tag{92g}$$

$$A_{0,0,2,0,0}(z) = A_{0,0,0,0,2}(z) = \frac{N_1}{2} \tag{92h}$$

All other combinations of subscripts yield zero, including

$$A_{0,0,1,0,1} = \lim_{\Delta t \to 0} E\left[\Delta x_1 \Delta x_2 \middle| z\right] = \lim_{\Delta t \to 0} \frac{1}{\Delta t} \int_t^{t+\Delta t} \int_t^{t+\Delta t} E\left[n_s(\tau_1)\, n_c(\tau_2)\right] d\tau_1\, d\tau_2 = 0 \tag{92i}$$

since $R_{cs}(\tau)$ is an odd function of τ.

Therefore on using equation (92) in equation (85) and requiring only the steady-state density

$$p_2(z) = \lim_{t \to \infty} p_1(z)$$

The following equation results:

$$0 = \frac{\partial}{\partial\phi}\left[\left|\omega - \omega_0 + \frac{x_2}{A} - KA\sin\phi - KV_s\sin\phi\right| p_2(z)\right]$$

$$- \frac{\partial}{\partial V_s}\left[x_1 p_2(z)\right] + \frac{\partial}{\partial x_1}\left[\left|a_1 x_1 + a_2 V_s\right| p_2(z)\right]$$

$$- \frac{\partial}{\partial V_c}\left[x_2 p_2(z)\right] + \frac{\partial}{\partial x_2}\left[\left|a_1 x_2 + a_2 V_c\right| p_2(z)\right]$$

$$+ \frac{K^2 N_0}{4}\frac{\partial^2}{\partial\phi^2} p_2(z) + \frac{N_1}{4}\frac{\partial^2}{\partial x_1^2} p_2(z) + \frac{N_1}{4}\frac{\partial^2}{\partial x_2^2} p_2(z) \qquad (93)$$

The solution to (93) is extremely difficult to obtain. However, if the equation is integrated over x_1, x_2, V_s, and V_c, there results

$$0 = \frac{-\partial}{\partial\phi}\left[\left|\omega - \omega_0 + \frac{E\left[x_2 \mid \phi\right]}{A} - KA\sin\phi - KE\left[V_s \mid \phi\right]\sin\phi\right| p_3(\phi)\right]$$

$$+ \frac{K^2 N_0}{4}\frac{\partial^2}{\partial\phi^2} p_3(\phi) \qquad (94)$$

where $p_3(\phi)$ is the desired probability density function of the phase error. Equation (94) would be relatively easy to solve if $E\left[x_2 \mid \phi\right]$ and $E\left[V_s \mid \phi\right]$ were known. However, they are only obtainable exactly from the solution to equation (93). Therefore, at this point, a linearized version of the system will be considered to obtain an approximate evaluation of the unknown conditional expectations.

Linearized Analysis of System. — In the preceding analysis, a differential equation for the density function of the phase error was obtained, but it was not easily solvable. In this part, an easily solved differential equation for the phase error process itself is obtained, and from the solution for the phase error process various moments are calculated for use in equation (94).

On replacing sin $\phi(t)$ by $\phi(t)$ and letting $\omega = \omega_0$ (frequency lock is initially achieved) in equation (77), the following equation results.

$$\frac{d\phi}{dt} + K\,(A + V_s(t))\,\phi(t) = \frac{V_c'(t)}{A} - K\,n'(t) \tag{95}$$

The solution to equation (95), subject to the initial conditions $\phi(t_0) = 0$, is

$$\phi(t) = \int_{t_0}^{t} n(\tau)\,\exp\left[-\int_{\tau}^{t} \mathcal{E}(x_1)\,dx_1\right] d\tau \tag{96}$$

where

$$n(t) = \frac{V_c'(t)}{A} - Kn'(t)$$

$$\mathcal{E}(t) = K\,(A + V_s(t)) \tag{97}$$

$$E\left[\phi(t)\right] = E\left[\int_{t_0}^{t} n(\tau)\,\exp\left[-\int_{\tau}^{t} \mathcal{E}(x_1)\,dx_1\right] d\tau\right] \tag{98}$$

$$E\left[\phi^2(t)\right] = E\left[\int_{t_0}^{t}\int_{t_0}^{t} n(t_1)n(t_2)\,\exp\left[-\int_{t_1}^{t} \mathcal{E}(x_1)dx_1 - \int_{t_2}^{t} \mathcal{E}(x_1)dx_1\right] dt_1\,dt_2\right] \tag{99}$$

$$E\left[\phi(t)\ V_s(t)\right] = E\left[\int_{t_0}^{t} r(\tau)\ V_s(\tau)\ \exp\left[-\int_{\tau}^{t} \mathcal{E}(x_1)dx_1\right] d\tau\right] \qquad (100)$$

$$E\left[\phi(t)\ V_c'(t)\right] = E\left[\int_{t_0}^{t} n(\tau)\ V_c'(\tau)\ \exp\left[-\int_{\tau}^{t} \mathcal{E}(x_1)dx_1\right] d\tau\right] \qquad (101)$$

By using the techniques described in reference 27, equations (98) - (101) can be evaluated to yield the steady-state results:

$$\lim_{t\to\infty} \text{Var}\ \phi(t) = \frac{1}{4\pi}\int_{-\infty}^{\infty} \frac{\left[N_1 \frac{\omega^2}{A^2} \left|H(j\omega)\right|^2 + K^2 N_0\right]}{C^2 + \omega^2} d\omega$$

$$+ \left[\frac{K}{A} S_{12}(0)\right]^2 \left[\exp\left[K^2 E\left[V_s^2(t)\right]\right] - \frac{1}{4}\right] \qquad (102)$$

$$\lim_{t\to\infty} E\left[\phi(t)\ V_s(t)\right] = \frac{K}{A}\left[\frac{S_{12}(B)}{2} - \frac{S_{12}(0)}{2}\left(1 + \frac{A}{B}\right)\right] \qquad (103)$$

$$\lim_{t\to\infty} E\left[\phi(t)\ V_c'(t)\right] = \frac{N_1}{2A} \frac{C}{2a_1\left(C^2 + a_1 C + a_2\right)}$$

$$+ \frac{K^2 S_{12}(0)}{2AB} \omega\left|H(j\omega)\right|^2\Big|_{\omega=0} \qquad (104)$$

where

$$B = K\left[A - \frac{KN_1\left|H(0)\right|^2}{4}\right] \qquad (105a)$$

$$C = K\left[A - \frac{KN_1\left|H(0)\right|^2}{2}\right] > 0 \qquad (105b)$$

and

$$S_{12}(x) = 2\int_0^\infty R'_{cs}(\tau)\exp(-x\tau)\,d\tau \qquad x>0 \qquad (106)$$

If it is assumed that ϕ, V_s, and V_c' are jointly gaussian,[+] then

$$KE\left[V_s(t)\middle|\phi(t)\right] \approx K\frac{E\left[\phi(t)\,V_s(t)\right]}{\text{Var }\phi(t)}\,\phi = R_1\,\phi \approx R_1 \sin\phi(t) \qquad (107)$$

$$E\left[V_c'(t)\middle|\phi(t)\right] = \frac{E\left[V_c'(t)\,\phi(t)\right]}{A\ \text{Var }\phi(t)}\,\phi = R_2\phi \approx R_2 \sin\phi(t) \qquad (108)$$

for small ϕ.

If ϕ, V_s, and V_c' are not exactly jointly gaussian, then they are at least approximately so. From the form of (96), $\phi(t)$ is the sum of a large number of dependent random variables, each with a density function of a random variable which is the product of gaussian and log-normal random variables. Application of the central limit theorem would indicate that $\phi(t)$ is approximately gaussian, and thus, ϕ, V_s, and V_c are approximately jointly gaussian.

Results of linear model. — The quantity of interest is the determination of the probability of loss of lock as a vehicle approaches Mars. Hence, the loop is initially in phase-lock so that the density function of the phase error is concentrated about zero, and for relatively high signal-to-noise ratios and negligible secondary path returns $p(\phi)$ is very close to a gaussian shape.[24] Therefore, the results of the linear

[+] It is assumed that the system described by (95) is stable in the mean square so that $A > K N_1 |H(0)|^2/2$.

model are very good approximations to the actual conditional moments of the first-order phase-locked loop.†

Use of (107) and (108) in (94) yields

$$0 = \frac{-\partial}{\partial\phi}\left[\left|\omega - \omega_0 + R_2 \sin\phi - KA \sin\phi - R_1 \sin^2\phi\right| p_3(\phi)\right]$$

$$+ \frac{K^2 N_0}{4} \frac{\partial}{\partial\phi^2} p_3(\phi) \tag{109}$$

If it is assumed that $\omega = \omega_0$ and equation (109) is integrated twice, then

$$p_3(\phi) = \exp\left[-\int^{\phi} A(\phi')d\phi'\right] \int_{-\pi}^{\phi} CD \exp\left[\int^{t} A(\tau)d\tau\right] dt$$

$$+ C \exp\left[-\int^{\phi} A(t)\, dt\right] \tag{110}$$

where

$$\int^{\phi} A(\phi)d\phi = -\alpha \cos\phi + \beta\left(\frac{\phi}{2} - \frac{\sin 2\phi}{4}\right)$$

$$\alpha = \frac{4}{K^2 N_0}(KA - R_2) \quad , \quad \beta = \frac{4R_1}{K^2 N_0}$$

Equation (110) is subject to two conditions:

$$p_3(\pi) = p_3(-\pi)$$

$$\int_{-\pi}^{\pi} p_3(\phi)\, d\phi = 1$$

†Actually it is only necessary that the conditioned density functions of V_s and V_c' in the linear and non-linear model be close to each other for the high probability portions of their density functions.

The terms R_1 and R_2 can now be evaluated from equations (105) and (106). Integration of (106) by parts yields

$$S_{12}(x) = 2 R_{cs}(0) - 2x \int_0^\infty R_{cs}(\tau) \exp(-x\tau)\, d\tau \qquad (111)$$

Substitution of the spectral representation of $R_{cs}(\tau)$ (equation (74)), interchange of the order of integration, and integration on τ yield

$$S_{12}(x) = \frac{2x}{\pi} \int_0^\infty \frac{S_v(\omega)(\omega - \omega_c)}{(\omega - \omega_c)^2 + x^2}\, d\omega \qquad (112)$$

It may be noted that $R_{cs}(0) = 0$. When the narrowband signal spectrum $S_v(\omega)$, which is symmetric about ω_c, is used, equation (112) becomes

$$S_{12}(x) \approx \frac{2x}{\pi} \int_0^\infty \frac{\omega |H(j\omega)|^2}{\omega^2 + x^2}\, d\omega \approx 0 \qquad (113)$$

Since $S_v(\omega)$ is the spectrum of a narrowband process, the fold-over term that has been ignored in going from (112) to (113) is negligible.

When equation (113) is used in equations (102), (103), and (104), there results

$$\lim_{t\to\infty} \mathrm{Var}\, \phi(t) = \frac{N_1}{4\pi A^2} \int_{-\infty}^\infty \frac{\omega^2 |H(j\omega)|^2}{C^2 + \omega^2}\, d\omega + \frac{K^2 N_0}{4\pi} \int_{-\infty}^\infty \frac{d\omega}{C^2 + \omega^2}$$

$$= \frac{N_1}{2A^2} \frac{1}{2a_1(C^2 + a_1 C + a_2)} + \frac{K^2 N_0}{4C} \qquad (114)$$

$$\lim_{t\to\infty} E\left[\phi(t)\, v_s(\quad)\right] = 0 \qquad (115)$$

$$\lim_{t\to\infty} \quad E\left[\phi(t)\, v_c'(t)\right] = \frac{N_1}{2A}\,\frac{C}{2a_1(C^2 + a_1 C + a_2)} \tag{116}$$

Evaluation of R_1 and R_2 results in

$$R_1 = 0 \tag{117}$$

$$R_2 = \frac{C^2}{C + (KA)^2 \frac{N_0}{N_1} a_1 (C^2 + a_1 C + a_2)} \tag{118}$$

With $R_1 = 0$, $\beta = 0$ so that use of the above in equation (110) yields the well-known result[24] for the phase error probability density function:

$$p_3(\phi) = \frac{\exp(\alpha \cos\phi)}{2\pi I_0(\alpha)} \qquad -\pi < \phi < \pi \tag{119}$$

As a check on the validity of the various assumptions that led up to equation (118), Var $\phi(t)$ can be calculated from equation (118) and compared with Var $\phi(t)$ in equation (114). For small α, from equation (118),

$$\text{Var}\,\phi(t) = \frac{1}{\alpha} = \frac{K^2 N_0}{4(KA - R_2)} \tag{120}$$

Using equation (108) in equation (120) yields

$$\text{Var}\,\phi(t) = \frac{K N_0}{4A}\left\{\frac{1 + \frac{C}{(KA)^2}\frac{N_1}{N_0}\frac{1}{a_1(C^2 + a_1 C + a_2)}}{1 + \frac{1 - C/KA}{\frac{(KA)^2}{C}\frac{N_0}{N_1} a_1(C^2 + a_1 C + a_2)}}\right\} \tag{121}$$

In the region in which $C \approx KA$ (small multipath fluctuations in comparison to loop damping)

$$\text{Var } \phi(t) \approx \frac{KN_0}{4A} + \frac{C^2}{4A^2(KA)^2} \frac{N_1}{a_1(C^2 + a_1 C + a_2)} \qquad (122)$$

which is in first-order agreement with equation (114). As C decreases away from KA, equations (122) and (114) will diverge. Thus, in the region in which $C \approx KA$, equation (120) is a valid representation of $1/\alpha$. Therefore, α may be used in the equations derived in ref. 24 to obtain such results as first passage time and frequency of slipping cycles.

The results in (114) and (116) are precisely the results that would be obtained from the linear fixed parameter system governed by the differential equation

$$\frac{d\phi(t)}{dt} + C\,\phi(t) = \frac{V_c'(t)}{A} - K n'(t) \qquad (123)$$

Comparison of equation (123) with equation (95) yields the following conclusions:

1) The portions of the secondary path signal fluctuations that are out-of-phase with the primary path signal act as a random additive noise input to the phase-locked loop. The power spectrum of the noise is proportional to the power spectrum of the derivative of the envelope of the secondary signal.

2) The portions of the secondary path signal fluctuations that are in-phase with the primary signal act as a modulation on the loop time constant. The effect of the modulation is to broaden the loop bandwidth and increase the loop sensitivity to noise.

Comments (1) and (2) above are valid over the region of phase errors ϕ in which $\sin\phi \approx \phi$.

3) In the nonlinear region of phase-locked loop operation, the results of equation (121) are more appropriate.

In summary, it has been shown that for small multipath disturbances, the linearized model of the phase-locked loop yields results that are in agreement with the nonlinear results obtained from an analysis of small multipath disturbances using Fokker-Planck techniques.

2.9 Lock-On and Loss-Of-Lock Probabilities for Slow Fading

The "loop quality probabilities" will be calculated exactly for the case of no additive noise (i.e., SNR $\to\infty$) but with the slow fading multipath phase inputs described by the random coefficients $\delta\theta$, $\delta\dot{\theta}$, $\delta\ddot{\theta}$. These qualities will then be discussed for the more general case including gaussian white additive noise.

Noiseless case. – In the case of no additive noise, the steady-state loop phase error, given $\delta\theta$, $\delta\dot{\theta}$, $\delta\ddot{\theta}$, is given by equation (28). The solution was actually for $\sin\phi$ rather than ϕ because of the nonlinearity of the phase detector. In that form $\sin\phi$ was a linear function of $\delta\theta$, $\delta\dot{\theta}$, and $\delta\ddot{\theta}$. So $\sin\phi$ is a gaussian random variable since $\delta\theta$, $\delta\dot{\theta}$, and $\delta\ddot{\theta}$ are gaussian.† Since, as shown previously, the acquisition and loss-of-lock limits can be described as limits on $|\sin\phi|$, the "loop quality probabilities" may be written precisely in terms of error functions.

It may be recalled that for prevention of loss-of-lock, $|\sin\phi| \leq 1$ is required or, from equation (29), for a perfect second-order-loop, $|\delta\ddot{\theta}| < C_1 \triangleq \tilde{A}K_1K_2 = \omega_n^2$ is required. The probability of loss-of-lock is just

$$P_{unlock} = Pr\left(|\delta\ddot{\theta}| \geq \omega_n^2\right) = 1 - Pr\left(|\delta\ddot{\theta}| < \omega_n^2\right)$$

$$= 1 - \int_{-\omega_n^2}^{\omega_n^2} \frac{\exp\left[-(\delta\ddot{\theta} - \mu_3)^2/2\sigma_3^2\right]}{\sqrt{2\pi\sigma_3^2}}\, d(\delta\ddot{\theta}) = 1 - \int_{\frac{-\omega_n^2 - \mu_3}{\sigma_3}}^{\frac{\omega_n^2 - \mu_3}{\sigma_3}} \frac{\exp\left[-x^2/2\right]}{\sqrt{2a}}\, dx$$

$$= 1 - \text{erfc}\left(\frac{-\omega_n^2 - \mu_3}{\sigma_3}\right) + \text{erfc}\left(\frac{\omega_n^2 - \mu_3}{\sigma_3}\right)$$

$$P_{unlock} = \text{erfc}\left(\frac{\omega_n^2 + \mu_3}{\sigma_3}\right) + \text{erfc}\left(\frac{\omega_n^2 - \mu_3}{\sigma_3}\right) \qquad (124)$$

† $\delta\theta$, $\delta\dot{\theta}$, $\delta\ddot{\theta}$ are gaussian with respective means μ_1, μ_2, μ_3 and variances σ_1^2, σ_2^2, σ_3^2.

where

$$\operatorname{erfc}(a) = \int_a^\infty \frac{\exp\left[-x^2/2\right]}{\sqrt{2\pi}}\,dx$$

Similarly, from equation (30), for the imperfect second-order loop with $\delta\ddot{\tilde{\theta}} \equiv 0$,

$$P_{unlock} = \operatorname{erfc}\left(\frac{\omega_n^{\,2}/\epsilon + \mu_2}{\sigma_2}\right) + \operatorname{erfc}\left(\frac{\omega_n^{\,2}/\epsilon - \mu_2}{\sigma_2}\right) \tag{125}$$

The limits on $\delta\tilde{\theta}$, $\delta\dot{\tilde{\theta}}$, $\delta\ddot{\tilde{\theta}}$ for acquisition of lock are given by equations (33) and (36). For either a first- or second-order loop, the probability of lock-on with $\delta\ddot{\tilde{\theta}} \equiv 0$ is

$$P_{acq.} > \Pr\left(|\delta\dot{\tilde{\theta}}| < C_0\,\alpha\,\tilde{A}K_1\,K_2\right)$$

$$P_{acq.} > 1 - \operatorname{erfc}\left(\frac{C_0\,\alpha\,\tilde{A}K_1\,K_2 + \mu_2}{\sigma_2}\right) - \operatorname{erfc}\left(\frac{C_0\,\alpha\,AK_1\,K_2 - \mu_2}{\sigma_2}\right) \tag{126}$$

For the perfect second-order loop with $\delta\dddot{\tilde{\theta}} \neq 0$, from equation (36), there results

$$P_{acq.} > 1 - \operatorname{erfc}\left(\frac{\omega_n^{\,2}/2 + \mu_3}{\sigma_3}\right) - \operatorname{erfc}\left(\frac{\omega_n^{\,2}/2 - \mu_3}{\sigma_3}\right) - \operatorname{erfc}\left(\frac{C_0\,\alpha\,\hat{A}K_1\,K_2 + \mu_2}{\sigma_2}\right) - \operatorname{erfc}\left(\frac{C_0\,\alpha\,\tilde{A}K_1K_2 - \mu_2}{\sigma_2}\right) \tag{127}$$

These results are directly applicable whenever the signal-to-noise ratio is so high that the random phase fluctuations in $\tilde{\theta}(t)$ override the additive noise. Otherwise, the situation is more involved, as is discussed in the next section.

Noisy case. — When additive noise is significant, equation (124) still gives the probability of permanent loss-of-lock. However, the presence of additive random noise permits a temporary loss-of-lock in the form of cycle slipping. Therefore, a complete description of the tracking capabilities of a phase-locked loop includes the probability of cycle slipping, or the mean

cycle slipping rates, as well as the probability of permanent loss-of-lock previously calculated.

The derivation of the acquisition probability is greatly complicated by the presence of the additive noise. A steady-state solution of the Fokker-Planck equation no longer exists. In fact, the phase fluctuations are solutions to a nonstationary Fokker-Planck equation. If the signal-to-noise ratio of the signal is very high, then equation (127) gives a sufficiently accurate estimate of acquisition probability.

3.0 Convergence to Gaussian Statistics

In the adaptive antenna array, the outputs of the N antenna elements are added approximately in phase. The phase error in the resultant signal is

$$\gamma = \theta + \xi = \tan^{-1}\left[\frac{\sum_{k=1}^{N} A_k \sin \beta_k}{\sum_{k=1}^{N} A_k \cos \beta_k}\right] + \theta \qquad (128)$$

where β_k is the phase error in the k^{th} phase-locked loop (associated with the k^{th} antenna element); A_k is the amplitude weighting of the signal summer; and θ is a phase error common to all loops. If θ is assumed to be equal to zero or if θ is largely removed by a phase reference return, then $\gamma = \xi$. In the Third Quarterly Report,[6] it was assumed that γ was a gaussian random variable, an assumption justified by the central limit theorem for very large N (i.e., a multi-element array). However, under significant multipath fading, many of the coefficients A_k may be very small so that only a remaining few large coefficients contribute to γ. For this reason, it is important to know the accuracy of the gaussian distribution as an approximation to $p_\gamma(\gamma)$ for small N.

The probability density functions derived here for a single-element antenna are reduced to modulo 2π. Consequently, for a direct comparison of probability density functions, the gaussian distribution must also be reduced to modulo 2π. The gaussian distribution is

$$p_\phi(\phi) = \frac{1}{\sqrt{2\pi\sigma^2}} \exp\left[-\phi^2/2\sigma^2\right] \qquad -\infty < \phi < \infty \qquad (129)$$

The polar variable into which ϕ is transformed is

$$\gamma = \phi - 2\pi n \qquad -\pi + 2\pi n < \phi \leq \pi + 2\pi n$$

The Jacobian of this transformation is unity ($d\gamma/d\phi = 1$) so that the density function of γ is just

$$p_\gamma(\gamma) = \sum_{n=-\infty}^{\infty} p_\phi(\gamma + 2\pi n) \qquad -\pi < \gamma \leq \pi \tag{130}$$

Consequently, from equations (129) and (130), p_θ, the gaussian reference function, becomes

$$p_0(\gamma) = \frac{\exp[-\gamma^2/2\sigma^2]}{\sqrt{2\pi\sigma^2}}\left[1 + \sum_{n=1}^{\infty} \exp[-2(\pi n/\sigma)^2]\ 2\cosh\left(\frac{2\pi n\gamma}{\sigma^2}\right)\right] \qquad -\pi < \gamma \leq \pi \tag{131}$$

For low variance, σ^2, the infinite series is negligible and equation (131) becomes essentially a truncated gaussian density function. This function is the one that was assumed for the error probability calculations contained in the third Quarterly Report.[4] It is precisely the density function of an infinite array.

The density function of phase errors in a single-element array with no doppler offset is given by equation (44) with b = 0:

$$p_1(\gamma) = \frac{1}{2\pi I_0(a)} \exp(a\cos\gamma) \qquad -\pi < \gamma \leq \pi \tag{132}$$

where $I_0(a)$ is the modified Bessel function of the first kind and order zero.

The density function of phase errors in a two-element array may be derived from equations (128) and (132) through the use of probability theory characteristic functions. It is assumed that $A_1 = A_2 \neq 0$, $A_k = 0$, $k \neq 1, 2$. Then equation (128) yields

$$\tan\gamma = \frac{\sin\beta_1 + \sin\beta_2}{\cos\beta_1 + \cos\beta_2}$$

whose exact solution is

$$\gamma = \tfrac{1}{2}(\beta_1 + \beta_2) \tag{133}$$

The density function of β_1 or β_2 is given by equation (132). The resultant density function of γ, derived in Appendix B, is

$$p_2(\gamma) = \frac{1}{\pi^2 I_0^2(a)} \int_0^{\pi - |\gamma|} \exp[2a \cos\gamma \cos\phi]\, d\phi \qquad -\pi < \gamma \leq \pi \tag{134}$$

The density function of phase errors in a three-element array may be similarly derived from equations (128) and (132). For multi-element arrays, however, the assumption of small errors must be added so that

$$\gamma \approx \frac{\sum_{k=1}^{3} \sin\beta_k}{\sum_{k=1}^{3} \cos\beta_k} \approx \frac{1}{3}(\beta_1 + \beta_2 + \beta_3) \tag{135}$$

The linearization permits the convenient use of characteristic functions as before, and the density function of γ for a three-element array (Appendix B) results:

$$p_3(\gamma) = \begin{cases} \dfrac{3}{[2\pi I_0(a)]^3} \displaystyle\int_{|3\gamma|-2\pi}^{\pi} dx \int_{|3\gamma|-x-\pi}^{\pi} dy \exp\left[a\cos x + a\cos y + a\cos(|3\gamma| - x - y)\right] \\ \qquad\qquad \text{for } \frac{\pi}{3} < |\gamma| < \pi \\ \dfrac{3}{[2\pi I_0(a)]^3} \left\{ \displaystyle\int_{-|3\gamma|}^{\pi} dx \int_{|3\gamma|+x-\pi}^{\pi} dy \left[\exp a\cos x + a\cos y + a\cos(|3\gamma| + x - y)\right] \right. \\ \qquad \left. + \displaystyle\int_{+|3\gamma|}^{\pi} dx \int_{-|3\gamma|+x-\pi}^{\pi} dy \exp\left[a\cos x + a\cos y + a\cos(-|3\gamma| + x - y)\right] \right\} \\ \qquad\qquad \text{for } |\gamma| < \frac{\pi}{3} \end{cases} \tag{136}$$

The distributions $p_0(\gamma)$, $p_1(\gamma)$, $p_2(\gamma)$, and $p_3(\gamma)$ were evaluated by a computer with the results shown in figure 14. For a meaningful comparison of the distributions, the four cases shown were plotted for equal variances of their distributions, rather than with a as a parameter. The variance of $p_0(\gamma)$ is approximately the parameter σ^2 (to a very high accuracy for $\sigma < 1$). The variance of $p_1(\gamma)$ was calculated by numerical integration as

$$\sigma_1^2 = \frac{1}{2\pi I(a)} \int_{-\pi}^{\pi} \gamma^2 \exp(a \cos \gamma)\, d\gamma \tag{137}$$

The computed results of this integration are shown in Table I.

TABLE I. - VARIANCE OF ERRORS IN SINGLE PHASE-LOCKED LOOPS

Loop signal-to-noise ratio	Variance (σ_1^2)
6	.1885
10	.1071
30	.0341
60	.0168

The variances of $p_2(\gamma)$ and $p_3(\gamma)$ for a given $\underline{a}$ are just $\sigma_2^2 = \sigma_1^2/2$ and $\sigma_3^2 = \sigma_1^2/3$, respectively, since these distributions arise from the sum of independent random variables with variances σ_1^2.

From the graphs of figure 14 it can be seen that the small array error distributions (p_1, p_2, p_3) differ from the large array error distribution (p_0) most significantly for $\gamma > \pi/2$. The effect of this deviation on the error probabilities calculated for the Third Quarterly Report[6] is to greatly increase P_e for high signal-to-noise ratios ($E/2N_0$), since at high signal-to-noise ratios the principal contribution to the error integrals comes from phase errors $\gamma > \pi/2$, at least for the binary cases. On the other hand, at low signal-to-noise ratios or for m-ary codes with $m > 4$, contributions to the error integrals for $\gamma < \pi/2$ are the most significant. In these cases, P_e is increased only slightly by the use of the small array density functions instead of the gaussian density functions.

The convergence of the density functions to gaussian for a large number of elements is portrayed by the graphs. It is seen that the p_3 curve simulates the shape of p_0 better than p_2 and, especially, p_1. However, the tails of the distribution, although of semigaussian shape, would come from a gaussian distribution with higher variance than that of p_3. It appears that arrays larger than five elements could utilize the previous error calculations directly, but for arrays of between five and ten elements, the equivalent phase error variance must be raised.

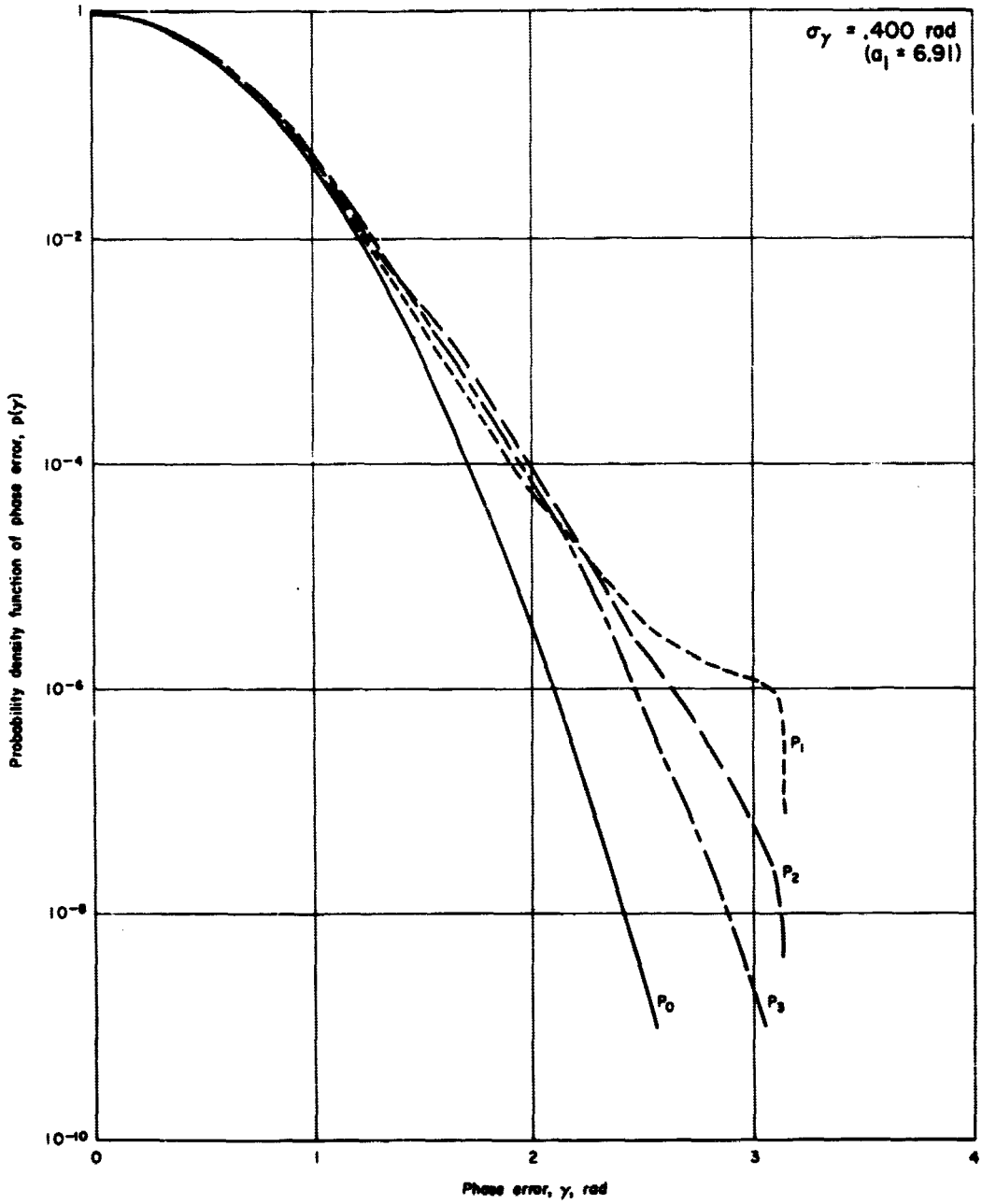

Figure 14. Comparison between the gaussian reference function and the phase error probability density functions for small arrays.

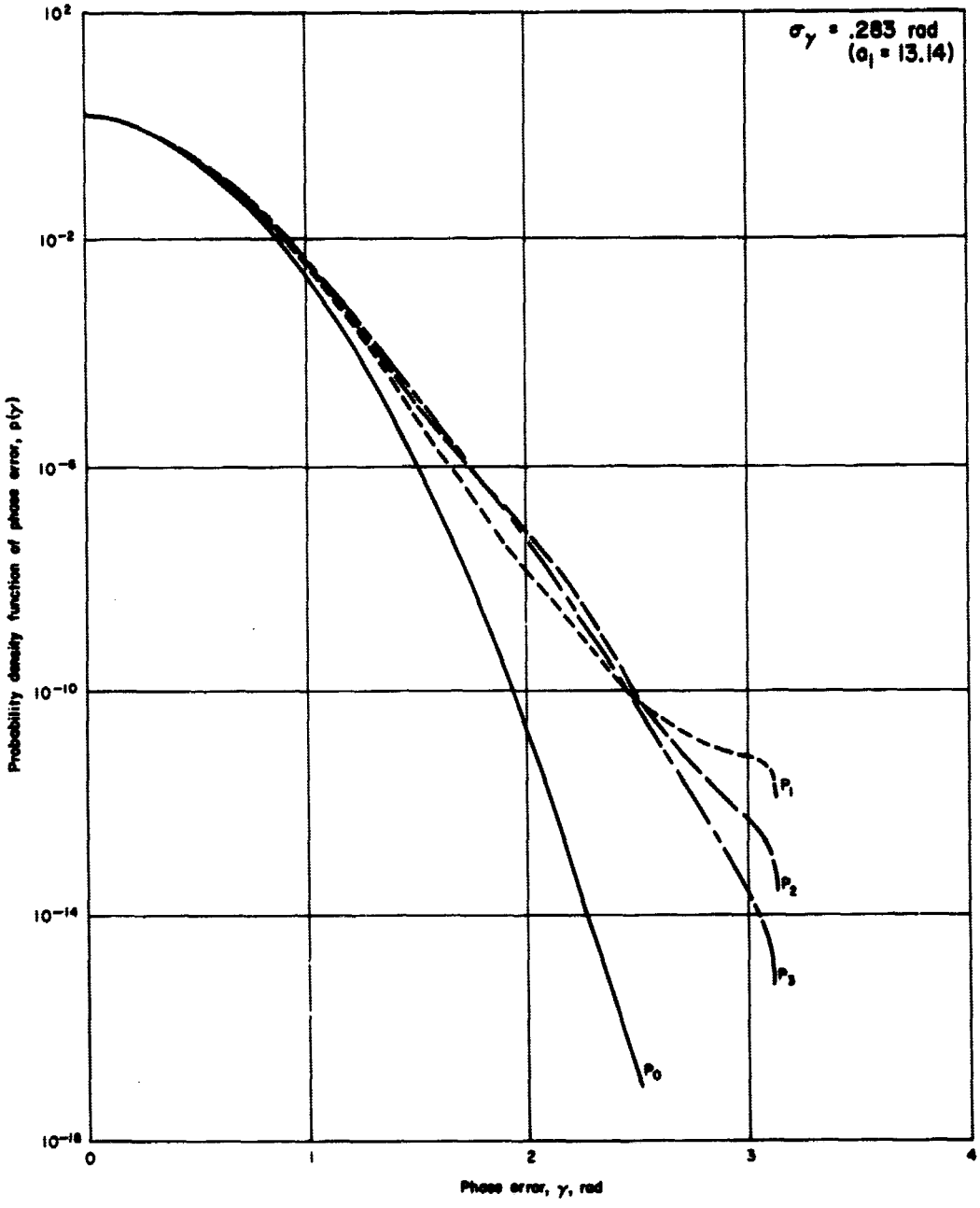

Figure 14. – Continued.

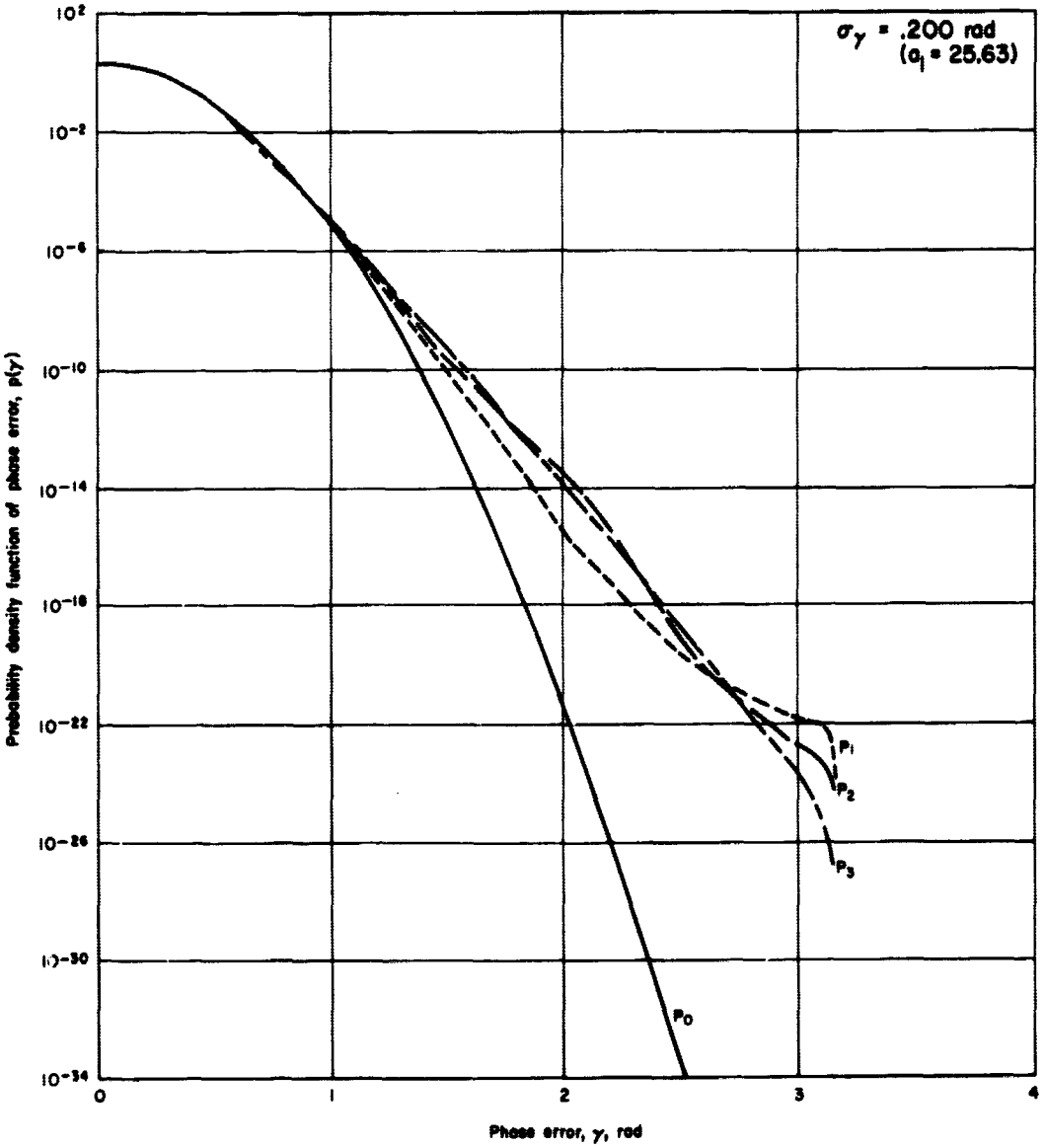

Figure 14. — Continued.

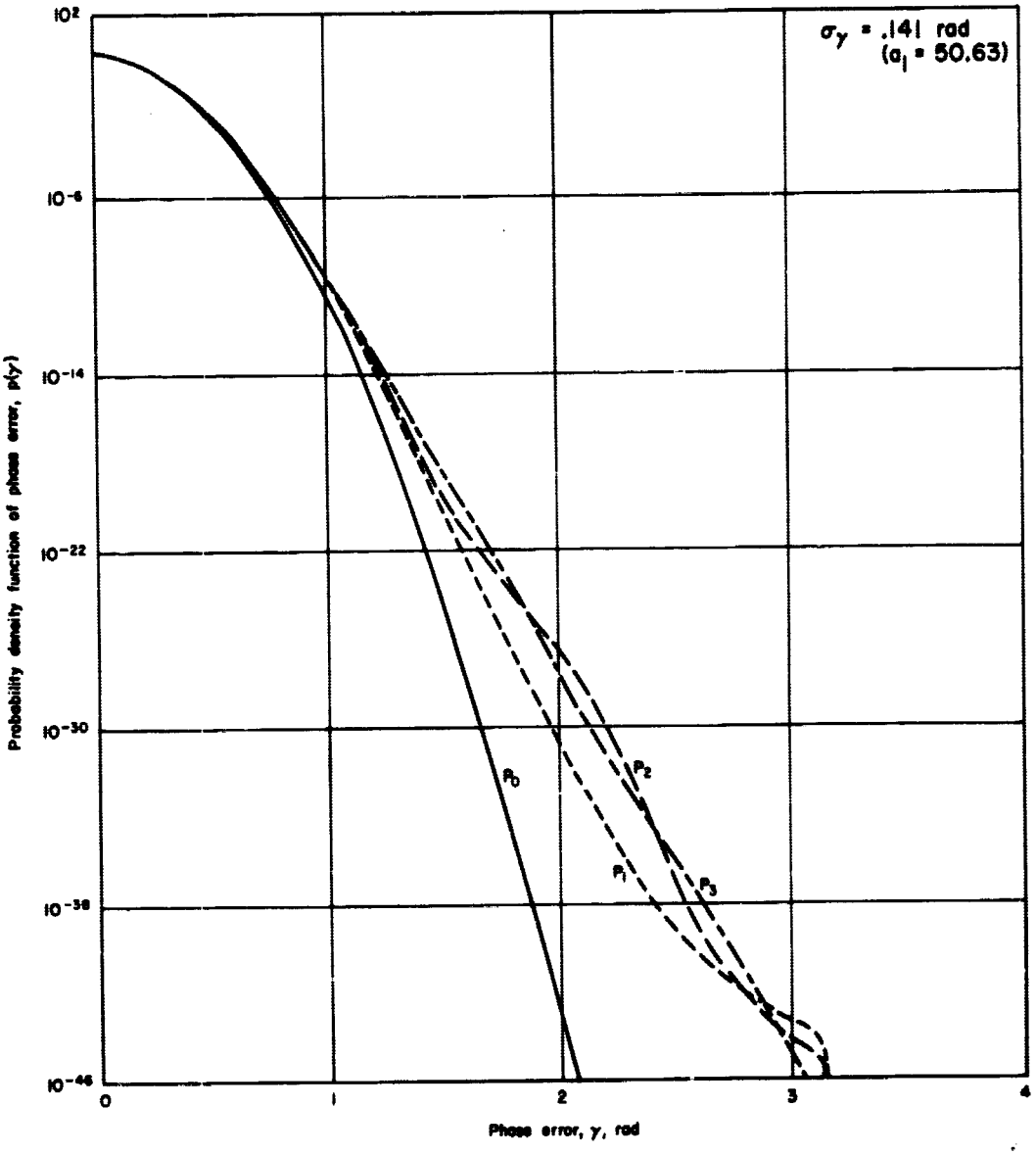

Figure 14. – Concluded.

4.0 Effect of Multipath on Detection

4.1 Multipath Environment and Modulation

The multipath environment in a Mars probe mission presents some special demodulation problems to the retrodirective array since the secondary path signals contain time-delayed modulation. Calculations of the error probabilities in the demodulation of the received signals are presented here. A dual-path model is assumed, although the later results may be generalized to include many paths by the replacement of the secondary path signal parameters with random variables and averaging.

The primary path signal is of the form

$$s_p(t) = \sqrt{\frac{2E_p}{T}} \cos(\omega_p t + \zeta_p) \tag{138a}$$

and the secondary path signal is

$$s_s(t) = \Omega\sqrt{\frac{2E_s}{T}} \cos\left[\omega_s (t + \tau) + \zeta_s\right] \tag{138b}$$

where Ω is the relative amplitude of the multipath signal.

The composite received signal is

$$s(t) = s_p(t) + s_s(t) + n(t) \tag{138c}$$

where n(t) is white gaussian noise with one-sided spectral density N_0, the subscripts p, s = 1,2,....,m denote the m-ary modulation symbols, and τ is the time delay of the secondary signal referenced to the primary signal.

The modulation codes are selected as optimum codes and are therefore pseudo-random codes to make full use of the available transmission energy. As long as $\tau > T$, where T is the duration of a single m-ary symbol, the modulation received from the secondary signal is independent of the modulation received from the primary signal so that s is independent of p. For maximum utilization of available energy, any p = 1,2,....,m must be equally likely to occur. Consequently, p and s have uniform discrete probability density functions. These properties permit the computation of average error probability in terms of error probability conditioned on p and s:

$$P_e = \frac{1}{m} \sum_{s=1}^{m} \frac{1}{m} \sum_{p=1}^{m} P_e(p,s) \tag{139}$$

In the ensuing sections, the average error probabilities in multipath environments are calculated, following the methods used in the no-multipath environment described in the appendices of the Final Report - Part I of this contract.[8]

4.2 Error Probability

Error probabilities were calculated for various m-ary coding schemes. It was assumed that the demodulators were those that are optimum for no multipath. It was also assumed that the demodulator was synchronized to the primary signal, an assumption which is quite reasonable for small Ω (secondary path amplitude ratio) but which reduces error probability for Ω near unity.

The demodulators depend on correlators for their operation. They correlate the orthonormal bases of the transmitted signal with the received signal. Allowing for a random phase uncertainty in the phase-locked loops, θ, the orthonormal functions are generally

$$\begin{cases} \phi_{1k} = \sqrt{\frac{2}{T}} \cos(\omega_k t - \theta_k) \\ \phi_{2k} = \sqrt{\frac{2}{T}} \sin(\omega_k t - \theta_k) \end{cases} \tag{140}$$

Then the correlator outputs are

$$x_k = \int_0^T s(t)\,\phi_{1k}(t)\,dt$$

$$= \sqrt{E_p}\,\frac{2}{T}\int_0^T \cos(\omega_k t + \phi_p)\cos(\omega_k t - \theta_k)\,dt$$

$$+ \Omega\sqrt{E_s}\,\frac{2}{T}\int_0^T \cos\left[\omega_s(t+\tau) + \phi_s\right]\cos(\omega_k t - \theta_k)\,dt$$

$$+ n_{1k}$$

$$y_k = \int_0^T s(t)\,\phi_{2k}(t)\,dt$$

$$= \sqrt{E_p}\,\frac{2}{T}\int_0^T \cos(\omega_p t + \phi_p)\sin(\omega_k t - \theta_k)\,dt$$

$$+ \Omega\sqrt{E_s}\,\frac{2}{T}\int_0^T \cos\left[\omega_s(t+\tau) + \phi_s\right]\sin(\omega_k t - \theta_k)\,dt$$

$$+ n_{2k} \qquad (141)$$

Coherent receivers use x_k only for decisions, while incoherent receivers must use $z_k^2 \equiv x_k^2$. The major difference among various demodulating schemes is in the values of the correlation integrals. From these bases, the average error probabilities are derived in Appendices C through H.

The conclusions are discussed here.

All error probabilities below are given conditioned on the phase and amplitude of the summand of the adaptive array and the time delay between the secondary path and the primary path. The overall average error probabilities and associated probability percentiles are then available directly from a knowledge of the probability density functions of the amplitudes $\sqrt{E}$ (which are Rician distributed for gaussian quadrature fading), the phase-locked loop composite phase error θ and the time delay τ (which depends on the environmental conditions).

To compare these results conveniently with the probabilities calculated under no-multipath conditions, the general expressions for error probability are specialized to binary coding and zero phase error. The latter assumes ideal phase-locked loop operation as well as in-phase addition of primary and secondary signals. The latter is the worst possible case since phase information cannot be used to discriminate between primary and secondary signals.

As derived in Appendix C, the error probability for coherent phase shift key (PSK) systems is

$$P_e(\theta,\tau) = 1 - \int_0^{\infty} dx \int_{x\tan\left(-\frac{2\pi i}{m}-\frac{\pi}{m}\right)}^{-x\tan\left(-\frac{2\pi i}{m}+\frac{\pi}{m}\right)} dy \frac{1}{m}\sum_{s=1}^{m} p\,(x,y|i,s,\theta,\tau) \tag{142}$$

where

$$p(x,y|i,s,\theta,\tau) = \frac{1}{2\pi N_0} \exp\left\{\frac{1}{2N_0}\left[\left(x - \sqrt{E}\left[\cos\left(\theta - \frac{2\pi i}{m}\right) + \Omega\cos\left(\theta - \frac{2\pi s}{m} - \omega\tau\right)\right]\right)^2 + \left(y - \sqrt{E}\left[\sin\left(\theta - \frac{2\pi i}{m}\right) + \Omega\sin\left(\theta - \frac{2\pi s}{m} - \omega\tau\right)\right]\right)^2\right\}$$

For perfectly coherent reception and binary coding this expression reduces to

$$P_e(\tau) = \frac{1}{2}\Phi\left[-\sqrt{\frac{E}{N_0}}\left(1 - \Omega|\cos\omega\tau|\right)\right] + \frac{1}{2}\Phi\left[-\sqrt{\frac{E}{N_0}}\left(1 + \Omega|\cos\omega\tau|\right)\right] \tag{143}$$

It can be seen that the multipath signal modulation has no effect on the error probability when it is 90 degrees out-of-phase with the primary signal modulation.

As derived in Appendix E the error probability for coherent frequency shift key (FSK) systems is

$$P_e\left(|\theta_i|, \tau\right) = \frac{1}{m^2} \sum_{p=1}^{m} \left\{ 1 - \frac{1}{(2\pi N_0)^{m/2}} \int_{-\infty}^{\infty} dx \right.$$

$$\cdot \exp\left[- \frac{1}{2N_0} \left[x - \sqrt{E} \left(\cos\theta_p + \Omega \cos(\theta_p + \omega_p \tau) \right) \right]^2 \right\}$$

$$\cdot \left[\int_{-\infty}^{x} \exp\left(\frac{-y^2}{2N_0} \right) dy \right]^{m-1} \Bigg\}$$

$$+ \frac{1}{m^2} \underbrace{\sum_{p=1}^{m} \sum_{s=1}^{m}}_{p \neq s} \left\{ 1 - \frac{1}{(2\pi N_0)^{m/2}} \int_{-\infty}^{\infty} dx \right. \qquad (144)$$

$$\cdot \exp\left[- \frac{1}{2N_0} \left(x - \sqrt{E} \cos\theta_p \right)^2 \right]$$

$$\cdot \int_{-\infty}^{x} dy \exp\left[- \frac{1}{2N_0} \left(y - \sqrt{E} \Omega \cos(\theta_s + \omega_s \tau) \right)^2 \right]$$

$$\cdot \left[\int_{-\infty}^{x} \exp\left(\frac{-z^2}{2N_0} \right) dz \right]^{m-2} \Bigg\}$$

For perfectly coherent reception and binary coding this expression reduces to

$$P_e(\tau) = 1 - \int_{-\infty}^{\infty} dx \frac{e^{-x^2/2}}{\sqrt{2\pi}} \left\{ \frac{1}{4} \sum_{\beta=1}^{2} \sum_{\ell=1}^{2} \Phi \left[x + \sqrt{\frac{E}{N_0}} \cdot \left(1 + \Omega (-1)^k \cos \omega_\ell \tau \right) \right] \right\}$$

$$= \frac{1}{4} \sum_{k=1}^{2} \sum_{\ell=1}^{2} \Phi \left[- \sqrt{\frac{E}{2N_0}} \left(1 + \Omega (-1)^k \cos \omega_\ell \tau \right) \right] \qquad (145)$$

$$= \frac{1}{2} \sum_{\ell=1}^{2} \left\{ \frac{1}{2} \Phi \left[- \sqrt{\frac{E}{2N_0}} \left(1 - \Omega |\cos \omega_\ell \tau| \right) \right] \right.$$

$$\left. + \frac{1}{2} \Phi \left[- \sqrt{\frac{E}{2N_0}} \left(1 + \Omega |\cos \omega_\ell \tau| \right) \right] \right\}$$

The results are similar to the those obtained for coherent PSK with the exception that, since two frequencies exist here, the multi-path signal will always degrade performance since $\omega_1 \tau = n\pi/2$ does not imply $\omega_2 \tau = n\pi/2$, n odd.

As derived in Appendix F the error probability for incoherent frequency shift key (FSK) systems is

$$P_e(\tau) = 1 - \frac{1}{m^2} \sum_{s=1}^{m} \sum_{p=1}^{m} \int_0^{\infty} d\nu_p \, p\left(\nu_p | p,s\right) \prod_{\substack{k=1 \\ k\neq p}}^{m} \int_0^{\nu_p} d\nu_k p\left(\nu_p | p,s\right) \tag{146}$$

where

$$p\left(\nu_k | p, s\right) = \nu_k I_0\left(\nu_k C_{psk} \sqrt{\frac{E}{N_0}}\right) \exp\left[-\frac{1}{2}\left(\nu_k^2 + \frac{E}{N_0} C_{psk}^2\right)\right]$$

$$C_{psk}^2 = \begin{cases} 1 + \Omega^2 + 2\Omega \cos \omega\tau \,, & p = k = s \\ 1 \,, & p = k \neq s \\ \Omega^2 \,, & p \neq k = s \\ 0 \,, & p \neq k \neq s \end{cases}$$

For binary coding, this equation reduces to

$$P_e(\tau) = 1 - \frac{1}{4} \sum_{i=1}^{2} \int_0^{\infty} d\nu \; \nu I_0\left[\nu \sqrt{\frac{E}{N_0}} \left(1 + \Omega^2 + 2\Omega \cos \omega_i \tau\right)^{1/2}\right]$$

$$\cdot \exp\left[-\frac{1}{2}\left(\nu^2 + \frac{E}{N_0}\left[1 + \Omega^2 + 2\Omega \cos \omega_i \tau\right]\right)\right]$$

$$\cdot \int_0^{\nu} d\omega \, \omega \exp\left[-\omega^2/2\right] - \frac{1}{2} \int_0^{\infty} d\nu \; \nu I_0\left(\nu \sqrt{\frac{E}{N_0}}\right)$$

$$\cdot \exp\left[-\frac{1}{2}\left(\nu^2 + \frac{E}{N_0}\right)\right] \int_0^{\nu} d\omega \, \omega I_0\left(\omega \Omega \sqrt{\frac{E}{N_0}}\right) \exp\left[-\frac{1}{2}\left(\omega^2 + \Omega^2 \frac{E}{N_0}\right)\right] \tag{147}$$

As derived in Appendix G the error probability for coherent amplitude shift key (ASK) systems is

$$P_e(\theta,\tau) = \frac{1}{m^2}\sum_{v=0}^{m-1}\Phi\left\{-\frac{\Delta}{2\sqrt{N_0}}\left[1 - 2\Omega v\cos(\theta+\omega\tau)\right]\right\} + \frac{m-2}{m}$$

$$- \frac{1}{m^2}\sum_{v=0}^{m-1}\sum_{u=1}^{m-2}\Phi\left\{\frac{u\Delta}{\sqrt{N_0}}\left[1 + \frac{1}{2u} - \cos\theta - \Omega\frac{v}{u}\cos(\theta+\omega\tau)\right]\right\}$$

$$+ \frac{1}{m^2}\sum_{v=0}^{m-1}\sum_{u=1}^{m-1}\Phi\left\{\frac{u\Delta}{\sqrt{N_0}}\left[1 - \frac{1}{2u} - \cos\theta - \Omega\frac{v}{u}\cos(\theta+\omega\tau)\right]\right\} \quad (148)$$

For perfectly coherent reception and binary coding this equation reduces to

$$P_e(\tau) = \frac{1}{2}\,\Phi\left(-\frac{\Delta}{2\sqrt{N_0}}\right) + \frac{1}{4}\,\Phi\left[-\frac{\Delta}{2\sqrt{N_0}}\left(1 - 2\Omega\left|\cos\omega\tau\right|\right)\right]$$

$$+ \frac{1}{4}\,\Phi\left[-\frac{\Delta}{2\sqrt{N_0}}\left(1 + 2\Omega\left|\cos\omega\tau\right|\right)\right] \quad (149)$$

As can be seen from a comparison of equations (143) and (149), the performance degradation in coherent ASK systems due to multipath time delays is similar to that of coherent PSK systems.

As derived in Appendix H the error probability for incoherent amplitude shift key (ASK) systems is

$$P_e(\tau) = \frac{m-1}{m} + \frac{1}{m}\sum_{v=0}^{m-1}\left\{\frac{1}{m}\int_{\Delta/2\sqrt{N_0}}^{\infty} I_0\left(\frac{\nu\Omega v\Delta}{\sqrt{N_0}}\right)\exp\left[-\frac{1}{2}\left(\nu^2+\frac{\Omega^2v^2\Delta^2}{N_0}\right)\right]d\nu\right.$$

$$-\frac{1}{m}\sum_{u=1}^{m-1}\int_{\left(u-\frac{1}{2}\right)\frac{\Delta}{\sqrt{N_0}}}^{\nu} I_0\left\{\frac{\nu\Delta}{\sqrt{N_0}}\left[u^2+\Omega^2v^2+2\Omega uv\cos\ \omega\tau\right]^{1/2}\right\}$$

$$\left.\cdot\exp\left\{-\frac{1}{2}\left[\nu^2+\frac{\Delta^2}{N_0}\left(u^2+\Omega^2v^2+2\Omega uv\cos\ \omega\tau\right)\right]\right\}d\nu\right. \qquad (150)$$

$$+\frac{1}{m}\sum_{u=1}^{m-2}\int_{\left(u+\frac{1}{2}\right)\frac{\Delta}{\sqrt{N_0}}}^{\infty}\nu\ I_0\left\{\frac{\nu\Delta}{\sqrt{N_0}}\left[u^2+\Omega^2v^2+2\Omega uv\cos\ \omega\tau\right]^{1/2}\right\}$$

$$\cdot\exp\left\{-\frac{1}{2}\left[\nu^2+\frac{\Delta^2}{N_0}\left(u^2+\Omega^2v^2+2\Omega uv\cos\ \omega\tau\right)\right]\right\}d\nu$$

For binary coding, this equation reduces to

$$P_e(\tau) = \frac{1}{2}\int_{\Delta/2\sqrt{N_0}}^{\infty}\nu\exp(-\nu^2/2)\left[\frac{1}{2}+\frac{1}{2}I_0\left(\frac{\nu\Delta\Omega}{\sqrt{N_0}}\right)\exp-\frac{\Delta^2\Omega^2}{2N_0}\right]d\nu$$

$$+\frac{1}{2}\left\{1-\int_{\Delta/2\sqrt{N_0}}^{\infty}\nu\exp-\frac{1}{2}\left(\nu^2+\frac{\Delta^2}{N_0}\right)\left[\frac{1}{2}I_0\left(\frac{\nu\Delta}{\sqrt{N_0}}\right)\right.\right. \qquad (151)$$

$$\left.\left.+\frac{1}{2}I_0\left(\frac{\nu\Delta}{\sqrt{N_0}}\sqrt{1+\Omega^2+2\Omega\cos\ \omega\tau}\right)\exp-\frac{\Delta^2\Omega}{2N_0}\left(\Omega+2\cos\ \omega\tau\right)\right]d\nu\right.$$

which displays a multipath modulation degradation for all time delays.

For a quantitative comparison of error probabilities, binary coherent PSK, FSK, and ASK modulations were evaluated numerically for a number of cases and plotted in figures 15a, b, c. Parameters of the graphs were the relative amplitude of the secondary signal, Ω (Ω=0 for no multipath, Ω=1 for maximum multipath), and time delay of the secondary signal, τ. Error probabilities are plotted for Ω=0, 0.1, 0.5, and for the time delays that provide maximum or minimum errors, $=\frac{(2n-1)\pi}{2\omega}$ and $n\pi/\omega$, where n=any integer.

A direct comparison of results for the three modulations shows that the coherent FSK system is always degraded 3 db with respect to the coherent PSK system. This relation is the same as that when there is no multipath environment. However, the coherent ASK system is degraded even further when multipath signals exist. For $\Omega = 0.1$ and $\tau = n\pi/\omega$ (maximum multipath interference), the presence of multipath signals degrades P_e by 0.6 db at high signal-to-noise ratios for coherent PSK and FSK systems. On the other hand, P_e is degraded by 1.2 db for coherent ASK systems under the same conditions. At larger values of Ω, the effect is even more drastic. It is especially evident for $0.5 \leq \Omega \leq 1$ since P_e has a lower bound of 0.125 for $\tau = n\pi/\omega$ in coherent ASK systems, while no lower bound exists for $\Omega<1$ in coherent PSK and FSK systems.

As a result, the coherent ASK system is automatically eliminated from consideration as an optimum code. The relative advantages distinguishing the PSK and FSK systems are the same as those when no multipath exists.

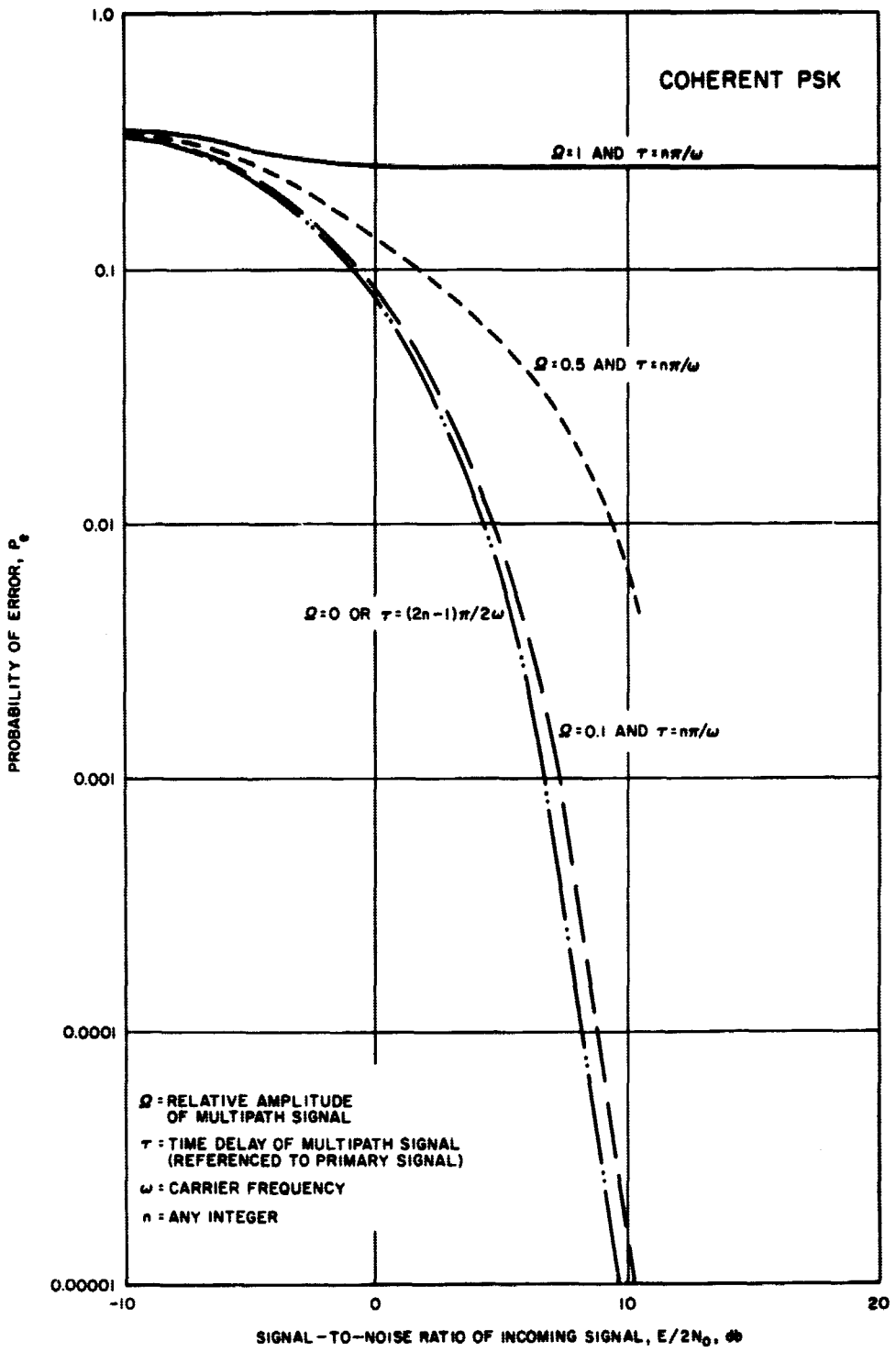

(a)

Figure 15. Multipath error probability.

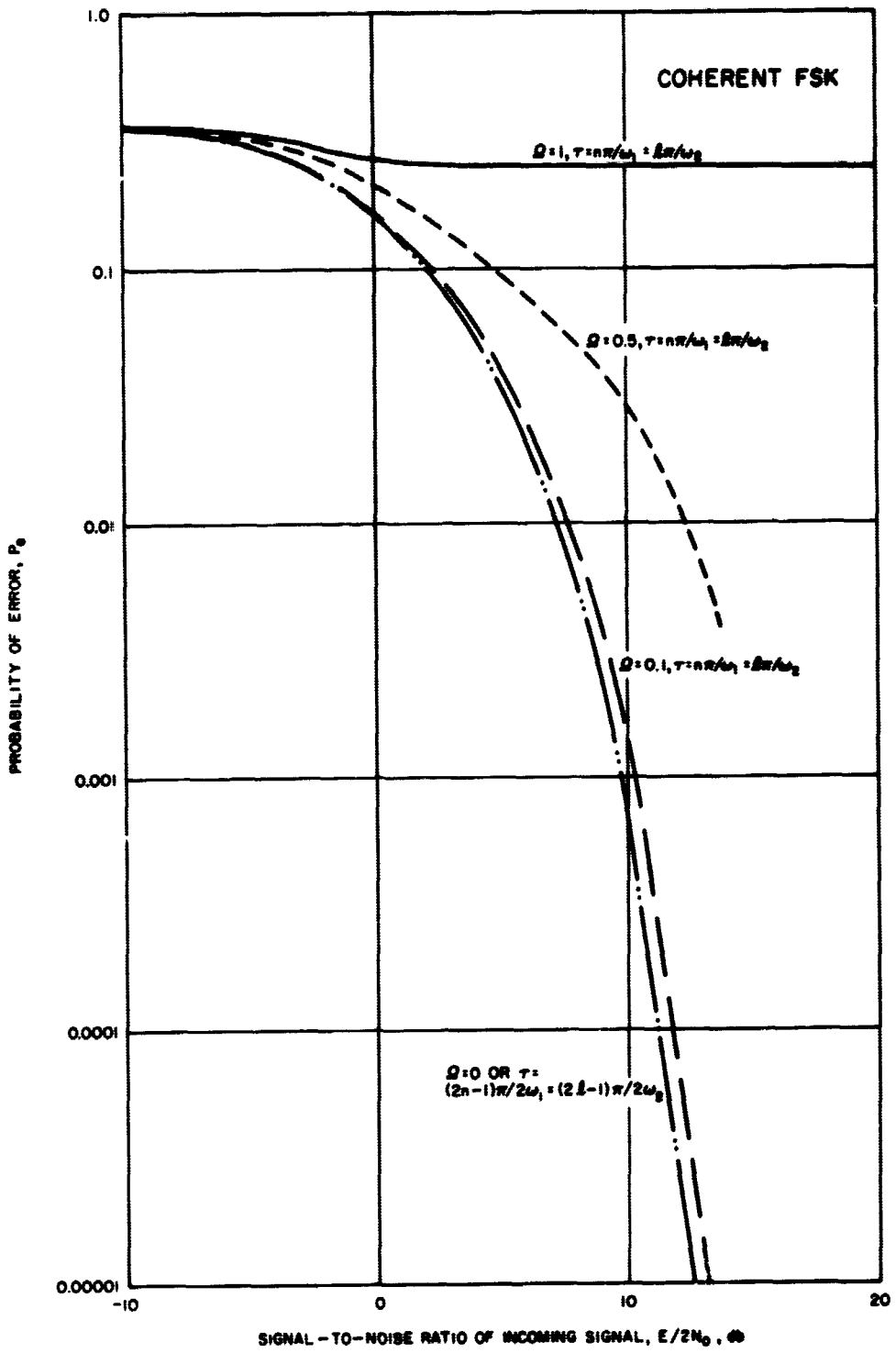

(b)

Figure 15. - Continued.

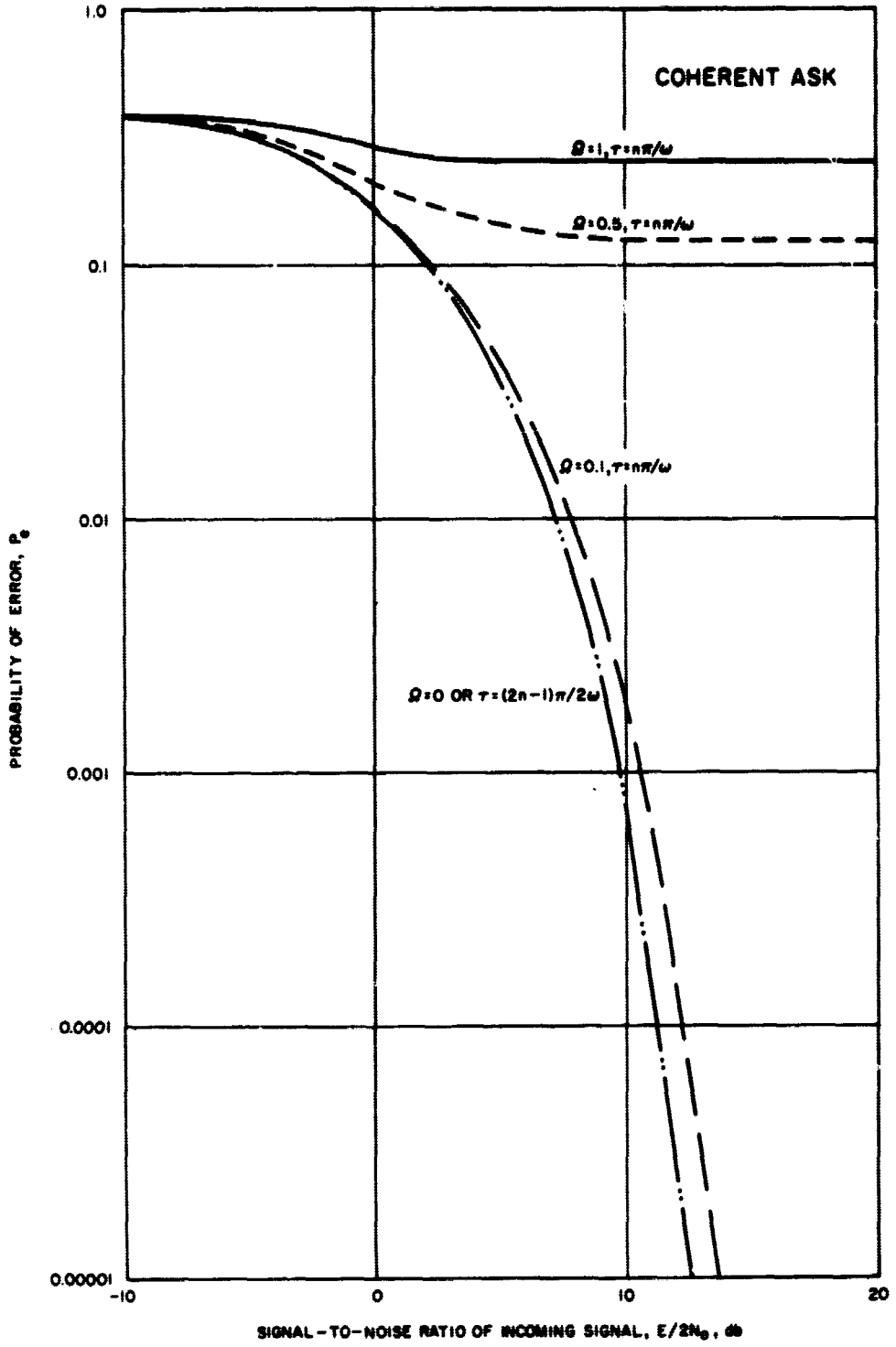

(c)

Figure 15. - Concluded.

4.3 Effect of Doppler Shifts on Demodulation Errors

The error probabilities calculated previously assume no difference in doppler shift between the primary and secondary signals. The effects of such a difference on demodulation accuracy is considered here.

If the reflector that generates the secondary signal is in motion with respect to the receiver, then the secondary signal will carry a doppler shift that is different from the shift of the primary signal. The demodulator is a correlation detector, so that optimal decoding requires a knowledge of the primary path doppler shift. If it is assumed that the primary path signal strength is much greater than the secondary path signal strength ($\Omega << 1$), the frequency of the primary signal may be found by selecting the frequency of greatest received power over the band, Δf, where Δf is the expected range of doppler shifts.

If the primary signal frequency, f_p, is found by this technique, then the demodulator uses correlators referenced to this frequency. (For FSK decoding, an $(m+1)^{th}$ carrier must be continuously transmitted and tracked: then the correct correlator frequencies may be obtained from this frequency.) Setting $\omega_k = \omega_p$ in equation (142) and $\omega_s \neq \omega_p$, then the correlator outputs contain the term

$$\Omega\sqrt{E_s}\ \frac{2}{T}\int_0^T \cos\left[\omega_s(t+\tau) + \phi_s\right] \cos\left(\omega_p t - \theta_p\right)dt \qquad (152)$$

instead of

$$\Omega\sqrt{E_s}\ \frac{2}{T}\int_0^T \cos\left[\omega_p(t+\tau) + \phi_s\right] \cos\left(\omega_p t - \theta_p\right)dt \qquad (153)$$

The integral in expression (152) is always less than the integral in expression (153), except for a small number of noise-generated errors, since the (153) contains perfect frequency correlation. As a result, the effect of $\omega_s \neq \omega_p$ is a reduction in the secondary correlator term or is the same as that of a lower secondary signal power (lower Ω). But the demodulators operate optimally for $\Omega \longrightarrow 0$, so that the secondary signal doppler shift (with respect to the primary signal) improves system performance by the proportionate amount.

The foregoing analysis leads to the important conclusion that the demodulation analyses contained in the preceding sections are actually worst case analyses with respect to doppler shift environments. That is, the case in which the secondary and primary signals carry the same doppler shift yields the highest error probability. The improved performance due

to doppler shifts is greatest when the moving reflector is moving parallel to the signal path lines. The resulting average and/or percentile error probabilities may then be calculated through a knowledge of mission trajectories.

4.4 Optimum Weighting of Phase-Locked-Loop Outputs

The weighting of the outputs of the individual elements of a retrodirective array may be adjusted so that the signal-to-noise ratio of the sum is maximized. It is known that if the elements are identical and the incident wave is plane, then the optimum weighting is uniform. However, situations may arise in which the above conditions are not met and uniform weighting is not optimum. One such situation is that in which the elements are identical but the signal arrives from a variety of directions (multipath signals) without significant delay or distortion of the modulation. A second situation is that in which the elements are not identically oriented. As the array position changes, the relative amplitudes of signals received by the various elements fluctuate. The weighting problem is considered here with specific reference to the first situation, but the results may be extended to the second situation as well.

The retrodirective array structure will be reviewed first. The array consists of N antenna elements, each with independent phase-locked loops. (See figure 16.) The signal at each element is independently amplified and tracked by a phase-locked loop. Then the phase corrected output of each phase-locked loop is weighted (that is, amplified or attenuated) in accordance with some optimization criterion, which will in general depend on the original uncorrected signal. These weighted phase-corrected signals are then linearly added and detected, in that order. A system could be conceived in which the signal at each antenna element is detected first with the detector outputs subsequently added in some optimum manner. However, the method of adding first and then detecting is not only less costly, since only one detector is required rather than N, but is also best in the mean-square-error sense.[28]

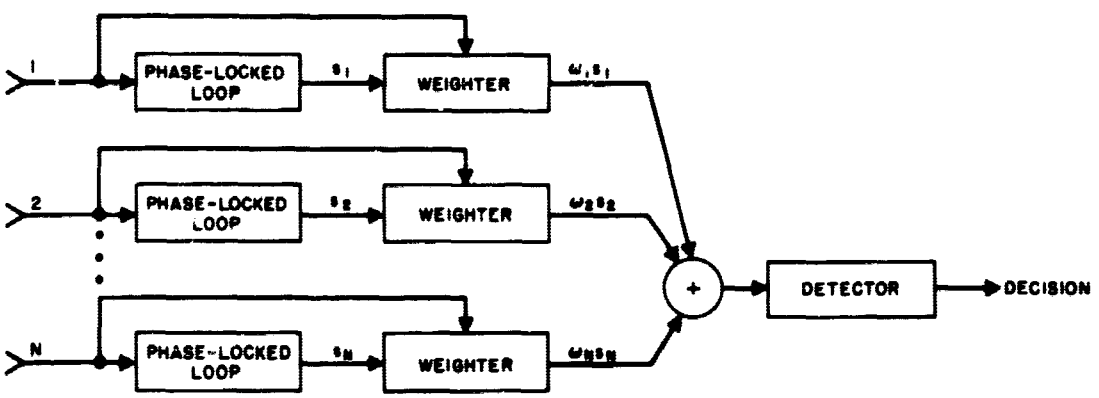

Figure 16. Adaptive array receiver.

The use of this system justifies the gaussian phase error assumption in the calculation of detector error probabilities; that is, although the phase error outputs of the phase-locked loops are not gaussian,[1] the sum of these independent errors, as seen by the detector, approaches gaussian by the Central Limit Theorem, provided the number of antenna elements is large. An exact analysis requires the use of error distributions derived elsewhere in this report. However, for the present, more qualitative analysis, a large number of elements will be assumed.

The optimum weighter will essentially weight most heavily those signals for which the primary and secondary (multipath) signals are most nearly in phase. The optimization criterion is to maximize the signal-to-noise ratio in the signal sum. The precise way in which this operation is accomplished is shown in the next section.

Optimum phase-locked-loop weighting. — A set of weighting coefficients $\{w_i\}$ is desired that can multiply phase-locked-loop outputs to maximize the signal-to-noise ratio in the output sum of a retrodirective array. If $s_i(t) + n_i(t)$ is the signal-plus-noise output of the i^{th} phase-locked loop, then the weighted sum of N loop outputs (associated with N antenna array elements) is

$$s(t) = \sum_{i=1}^{N} w_i \left[s_i(t) + n_i(t)\right] \tag{154}$$

and the signal-to-noise ratio of this sum, referenced to a single modulation period T, is

$$\mathrm{SNR} = \frac{\frac{1}{T}\int_0^T \left[\sum_{i=1}^{N} w_i s_i(t)\right]^2 dt}{E\left\{\frac{1}{T}\int_0^T \left[\sum_{i=1}^{N} w_i n_i\right]^2 dt\right\}} \tag{155}$$

This definition of signal-to-noise ratio uses signal power and noise power as quotients. However, the probability of error results presented in this report and in previous reports were given as functions of the quotient of signal energy and noise spectral density. The maximization of the former quotient is identical with the maximization of the latter quotient since the two differ only by constants; that is, the noise spectral density is N_0, whereas the average noise power is N_0B_0 ($B_0 \to \infty$ for white noise) in a single phase-locked-loop output. The signal energy is just the signal power times the signal duration T. Consequently the two quotients differ by a factor T/B_0.

The general problem of choosing w_i to maximize SNR is discussed first, for general forms of $s_i(t)$ and $n_i(t)$. Then the problem will be specialized to fast and slowly fading signals with white additive receiver noise.

General signal-to-noise ratio maximization. – To maximize the signal-to-noise ratio, equation (73) is differentiated† and set equal to zero, while the normalization $\sum_{i=1}^{N} w_i = 1$ is maintained.[30]

$$\frac{d(SNR)}{dw_j} = 0 = \frac{E\left[\frac{1}{T}\int_0^T \left(\sum w_i n_i\right)^2 dt\right]\left[\frac{1}{T}\int_0^T 2\sum w_i s_i s_j\, dt\right]}{\left\{E\left[\frac{1}{T}\int_0^T \left(\sum w_i n_i\right)^2 dt\right]\right\}^2} - \frac{\left[\frac{1}{T}\int_0^T \left(\sum w_i s_i\right)^2 dt\right] E\left[\frac{1}{T}\int_0^T 2\sum w_i n_i n_j\, dt\right]}{\left\{E\left[\frac{1}{T}\int_0^T \left(\sum w_i n_i\right)^2 dt\right]\right\}^2} \tag{156}$$

The w_j must satisfy

$$\frac{\sum_{i=1}^{N} w_i R_s(i,j)}{\sum_{i=1}^{N} w_i R_n(i,j)} = \frac{\sum_{\ell=1}^{N}\sum_{k=1}^{N} w_\ell w_k R_s(\ell,k)}{\sum_{\ell=1}^{N}\sum_{k=1}^{N} w_\ell w_k R_n(\ell,k)} \tag{157}$$

†The problem can also be formulated in matrix notation. It then becomes one of determining the largest eigenvalue and the corresponding eigenvector of a pencil of matrices, Cf. Ref. 29.

where the signal and noise correlation coefficients are defined as

$$R_s(i,j) = \frac{1}{T}\int_0^T s_i s_j^* \, dt$$
$$R_n(i,j) = E\left[n_i(t)\, n_j^*(t)\right] \tag{158}$$

The noise is assumed stationary.

More specific results arise from the specialization to fast or slowly fading signals. Specific forms for $R_s(i,j)$ and $R_n(i,j)$ become available. It is assumed that no limiters are used in phase-locked loops.

Slow fading. – For the dual-path model, the fading signal is of the form

$$s_i(t) = a_p\left(1 + 2\Omega\cos\Delta_i + \Omega^2\right)^{1/2} \cdot \sin\left\{\omega_0 t + m_p(t) + \theta_p(t) + \sin^{-1}\left[\frac{\Omega\sin\Delta_i}{\left(1 + 2\Omega\cos\Delta_i + \Omega^2\right)^{1/2}}\right]\right\} \tag{159}$$

where

$$\Delta_i = \theta_{s_i}(t) - \theta_p(t) + m(t+\tau_i) - m(t)$$

The signal power at the i^{th} loop is

$$R_s(i,i) = \frac{1}{T}\int_0^T |s_i|^2 \, dt = a_p^2\left(1 + 2\Omega\cos\Delta_i + \Omega^2\right)$$

where Δ_i is essentially constant over the period T. The correlation among signals at different antenna elements follows from equations (158) and (159):

$$R_s(i,j) = \frac{1}{2} a_p^2 \left(1 + 2\Omega\cos\Delta_i + \Omega^2\right)^{1/2} \left(1 + 2\Omega\cos\Delta_j + \Omega^2\right)^{1/2}$$

$$\cos\left[\sin^{-1}\frac{\Omega\sin\Delta_i}{\left(1+2\Omega\cos\Delta_i+\Omega^2\right)^{1/2}} - \sin^{-1}\frac{\Omega\sin\Delta_j}{\left(1+2\Omega\cos\Delta_j+\Omega^2\right)^{1/2}}\right] \tag{160}$$

$$R_s(i,j) = \frac{1}{2} a_p^2 \left[1 + \Omega\left(\cos\Delta_i + \cos\Delta_j\right) + \Omega^2\right]$$

The only noise present is white receiver noise, which is independent at each antenna element since independent RF amplifiers are used. The noise correlation is

$$R_n(i,j) = \delta_{ij} N_0 B_0$$

where N_0 is the noise spectral density, B_0 is the true noise bandwidth, $\delta_{ij} = 0$ for $i \neq j$, and $\delta_{ii} = 1$.

The set of equations for $|w_j|$ then simplifies to

$$|w_j| = \frac{\sum_\ell w_\ell^2}{\sum_\ell \sum_k w_\ell w_k R_s(\ell,k)} \sum_i w_i R_s(i,j)$$

Since the ratio on the right-hand side is independent of i and j, the set $|w_j|$ satisfies

$$\frac{w_j}{\sum_i w_i R_s(i,j)} = \frac{w_k}{\sum_i w_i R_s(i,k)} \qquad \text{all } j,k \tag{161}$$

The optimum choice of the set $|w_j|$ then requires an optimum estimate for the set $|R_s(i,j)|$. The estimation of $R_s(i,j)$ is complicated by the presence of the noise. This operation will be discussed later.

Fast fading. — For the fast fading case, the fading noise is assumed to fluctuate sufficiently, in a period T, to be considered white to the phase-locked loop. Then the loop output may be written as a signal-plus-noise where all the multipath fading is incorporated into the noise term.[2] Consequently, the signal correlation function is

$$R_s(i,j) = \frac{1}{T}\int_0^T s_i s_j^* \, dt = a_p^2/2 \qquad \text{for all } i, j$$

The noise correlation function is the sum of the receiver noise correlation function and the muitipath noise correlation function.

$$R_n(i,j) = R_n(i,j) + R_m(i,j)$$

$$= \delta_{ij} N_0 B_0 + R_m(i,j)$$

But the multipath noise at the i^{th} element is often just a time-delayed version of the multipath noise at the j^{th} element. Therefore, if the mutual time delays in the secondary path signals are large enough, the correlation function is that of white noise samples at different times. Then,

$$R_m(i,j) = \delta_{ij} N_i B_i$$

It must be remembered that this assumption is valid only when the multi-path signal source appears at a significantly different angular position than the primary signal source. Otherwise, all elements would see correlated time samples of the white fading noise at a given instant. This case is more complicated than the uncorrelated case and has not been considered in the present study.

Since the noise variance is the variable in this case, instead of the fading signal levels, the set $|w_j|$ must satisfy the set of equations

$$w_j(N_0 B_0 + N_j B_j) = w_i(N_0 B_0 + N_i B_i) \qquad \text{all } i, j. \tag{162}$$

This equation demonstrates that in the usual case, where $N_i B_i = N_j B_j$, all i, j, the optimum weighting is equal weighting. In other words, nothing can be done to improve performance if the fading is white. On the other hand, if the fading is directional (or if the fading is non-stationary across the array although appearing stationary at one element for a period T), then equation (162) will define the optimum weighters.

Physical realization. — The weighting coefficients for slow and fast fading are described by equations (161) and (162), respectively. The first requires a knowledge of the signal with fading. The second requires a knowledge of the receiver and fading noise variances. Since a knowledge of these quantities is generally difficult to obtain, the practical usefulness of the preceding analyses is greatly impaired. Reasonable estimates of these values can be made by judicious use of a knowledge of the process bandwidths. However, these techniques are useful only under extreme conditions on fading and noise bandwidths.

For slow fading the pertinent quantity is

$$R_s(i,j) = \frac{1}{T}\int_0^T s_i s_j^* \, dt$$

A gross estimate of $R_s(i,j)$ is available directly as[+]

$$\hat{R}_s(i,j) = \frac{1}{T}\int_0^T \left(s_i+n_i\right)\left(s_j+n_j\right)^* dt$$

$$= R_s(i,j) + \frac{1}{T}\int_0^T \left(s_i n_j^* + s_j^* n_i\right) dt + \frac{1}{T}\int_0^T n_i n_j^* \, dt \qquad (163)$$

$$\text{Then } \hat{R}_s(i,i) = R_s(i,i) + \frac{2}{T}\int_0^T s_i n_i \, dt + \frac{1}{T}\int_0^T |n_i|^2 \, dt$$

When receiver noise is low, $\hat{R}_s(i,j)$ approximates $R_s(i,j)$ well. However, when receiver noise is high, equation (163) will yield high variance random variables as estimates of $R_s(i,j)$. This situation may be improved if the modulation bandwidth is very much greater than the fading bandwidth. Then the estimator

$$\hat{R}_s(i,j) = R_s(i,j) + \frac{1}{mT}\int_0^{mT}\left(s_i n_j + s_j n_i\right) dt + \frac{1}{mT}\int_0^{mT} n_i n_j \, dt$$

may be used. This estimator is a great improvement over equation (163) since

$$\lim_{m\to\infty} \frac{1}{mT}\int_0^{mT}\left(s_i n_j + s_j n_i\right) dt = 0$$

$$\lim_{m\to\infty} \frac{1}{mT}\int_0^{mT} n_i n_j \, dt = E\left(n_i n_j\right) = \delta_{ij} N_0 B_0$$

Therefore as long as $B_F \ll \frac{1}{mT} \ll \frac{1}{T}$ and m is a large integer, the latter $\hat{R}_s(i,j)$ provides a good estimate of $R_s(i,j)$. Furthermore, if zero-signal testing is used, the noise variance $N_0 B_0$ may be estimated by

---

[+]Ordinarily the estimator is an ensemble average, not a time average. The time average is used here since it can be easily implemented. If the process is ergodic, the time average is the same as the ensemble average.

the same technique and subtracted from $\hat{R}_s(i, j)$. The final estimator is

$$\hat{R}_s(i,j) = \frac{1}{mT}\int_0^{mT}\left(s_i+n_i\right)\left(s_j+n_j\right)dt - \frac{1}{mT}\int_{nmT}^{(n+1)mT} n_i n_j\, dt$$

$$= \frac{1}{mT}\int_0^{mT} s_i s_j\, dt + \frac{1}{mT}\int_0^{mT}\left(s_i n_j + s_j n_i\right)dt \qquad (164)$$

$$+ \frac{1}{mT}\left\{\int_0^{mT} n_i n_j\, dt - \int_{nmT}^{(n+1)mT} n_i n_j\, dt\right\}$$

where, since separation of antenna elements is much less than $c/f_{\text{mod } n}$,

$$R_s(i,j) = \frac{1}{T}\int_0^{T} s_i s_j\, dt \cong \frac{1}{mT}\int_0^{mT} s_i s_j\, dt$$

and where, for stationary receiver noise,

$$\int_0^{mT} n_i n_j\, dt - \int_{nmT}^{(n+1)mT} n_i n_j\, dt \longrightarrow 0$$

and for zero mean white noise

$$\frac{1}{mT}\int_0^{mT}\left(s_i n_j + s_j n_i\right) dt \longrightarrow 0$$

For fast fading, the fading-plus-receiver-noise variance must be estimated. Since white noise (with respect to the modulation frequency) is assumed, $R_n(i, j) = 0$ for $i \neq j$. On the other hand, for fading that is stationary for a period $\gg mT$, use may be made of the estimator

$$\hat{R}_s(i,i) = \frac{1}{mT}\int_0^{mT} |s_i + n_i|^2\, dt$$

$$= \frac{1}{mT}\int_0^{mT} |s_i|^2\, dt + \frac{2}{mT}\int_0^{mT} s_i n_i\, dt + \frac{1}{mT}\int_0^{mT} |n_i|^2\, dt$$

$$\cong R_s(i,i) + \frac{2}{mT}\int_0^{mT} s_i n_i\, dt + R_n(i,i)$$

$$R_n(i,i) \cong \hat{R}_s(i,i) - R_s(i,i) - \frac{2}{mT}\int_0^{mT} s_i n_i\, dt$$

But

$$\frac{2}{mT}\int_0^{mT} s_i n_i\, dt \longrightarrow 0 \quad \text{as} \quad m \longrightarrow \infty$$

and

$$R_s(i,i) \equiv a_p^2/2 \ .$$

For a good estimate of $R_n(i,i)$, the non-fading signal amplitude must be known. If precise transmitting power, distance, and attenuation are available, then a_p may be calculated precisely. But if these factors are unknown, more sophisticated techniques are necessary. If the former is assumed, a reasonable estimate of the noise variance is

$$\hat{R}_n(i,i) = \hat{R}_s(i,i) - a_p^2/2 \tag{165}$$

Finally, with the above estimators, the equations for the weighting coefficients simplify to

Slow Fading:

$$\frac{w_j}{\sum_i w_i \hat{R}_s(i,j) - w_j \hat{R}_{n_0}(j,j)} \approx \frac{w_k}{\sum_i w_i \hat{R}_s(i,k) - w_k \hat{R}_{n_0}(k,k)} \tag{166}$$

Fast Fading:

$$w_j\left[\hat{R}_s(j,j) - \frac{a_p^2}{2}\right] \approx w_k\left[\hat{R}_s(k,k) - \frac{a_p^2}{2}\right], \quad \text{all } j,k \tag{167}$$

where

$$\hat{R}_s(i,j) \equiv \frac{1}{mT}\int_0^{mT} (s_i + n_i)(s_j + n_j)\, dt$$

$$\hat{R}_{n_0}(j,j) = \frac{1}{mT}\int_{nmT}^{(n+1)mT} |n_j|^2\, dt = \hat{R}_s(j,j) \quad s_j = 0$$

4.5 Effect of Multipath Signals on Operation of Systems That Use Phase Inversion by Mixing

The effect of multipath signals on the operation of self-steering systems that use phase inversion by mixing is considered in this section. The system to be analyzed is the same as that considered previously and described in the Final Report – Part 1.[8] The diagram is reproduced here in figure 17. The signal incident on the n^{th} element consists of the direct path signal plus the multipath signal scattered by the planet. The direct path signal consists of the information signal and the pilot signal and may be written as

$$v_s = K_c \sqrt{g_{en}}\, \lambda_c\, f(t) \cos\left[(\omega_c - \omega_1)t + \Phi_n + \Phi(t) - \zeta + \xi_n\right]$$

$$+ K_{c1} \sqrt{g_{en1}}\, \lambda_{c1}\, f_1(t) \cos\left[(\omega_{c1} - \omega_0)t + \Phi_{n1} + \Phi_1(t) - \zeta + \xi_{n1}\right]$$

$$+ n'_n(t) \cos\left[(\omega_c - \omega_0)t + \theta_{nc}(t)\right] \qquad (168)$$

where $f(t)$ denotes any amplitude modulations and $\Phi(t)$ represents phase modulation of the direct path signal and $f_1(t)$ and $\Phi_1(t)$ represent, respectively, amplitude and phase modulation on the secondary path signal. Both $f_1(t)$ and $\Phi_1(t)$ are delayed and distorted versions of $f(t)$ and $\Phi(t)$. K_c and K_{c1} represent, respectively, the system response to the direct path information signal at angular frequency ω_c and the secondary path information signal at ω_{c1}. The signal phase at the n^{th} element is Φ_n for the direct path carrier frequency and Φ_{n1} for the secondary path carrier frequency. The element field patterns in the directions of the direct and secondary paths are respectively $\sqrt{g_{en}}$ and $\sqrt{g_{en1}}$ with the phase angles ξ_n and ξ_{n1}. The signal has already been mixed with a local oscillator operating at an angular frequency ω_0 with phase ζ. The noise generated by the receiver at the n^{th} element is denoted by the term

$$n'_n(t) \cos\left[(\omega_c - \omega_0)\, t + \theta_{nc}(t)\right] = a'_n(t) \cos(\omega_c - \omega_0)\, t + b'_n(t) \sin(\omega_c - \omega_0)t \qquad (169)$$

where a'_n and b'_n are independent gaussian random processes with zero means and variance σ^2. The signal in the pilot channel is given by

$$v_p = K_p \sqrt{g_{en}}\, \lambda_p\, C \cos\left[(\omega_p - \omega_0)\, t + \Phi_{pn} - \zeta + \xi_n\right]$$

$$+ K_{p1} \sqrt{g_{en1}}\, \lambda_{p1}\, C_1(t) \cos\left[(\omega_{p1} - \omega_0)\, t + \Phi_{pn1} - \zeta + \xi_{n1}\right]$$

$$+ n''_n(t) \cos\left[(\omega_p - \omega_0)\, t + \theta_{np}(t)\right] \qquad (170)$$

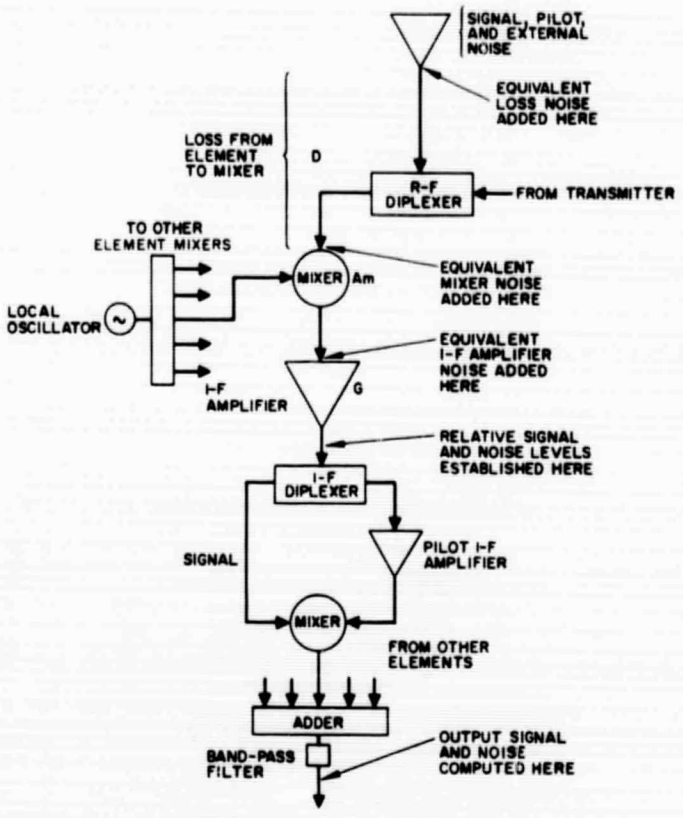

Figure 17. Portion of self-steering array that illustrates signal and noise performance of the system.

where C and $C_1(t)$ represent, respectively, the amplitudes of the direct path pilot signal and of the secondary path pilot signal. The $C_1(t)$ is shown as a function of time to illustrate possible distortions introduced by the reflecting surface as the source and receiver move. Other quantities are similar to those defined for the information signal except that the subscript p (for pilot) replaces the subscript c and the double prime is used on the noise term. The signal from the second mixer is combined with similar signals from the remaining elements in the array and may be written as

$$v_0(t) = \frac{1}{2} K_c K_p \lambda_c \lambda_p C f(t) \sum_n g_{en} \cos [(\omega_p - \omega_c)t + \phi_{pn} - \phi_n - \phi(t)]$$

$$+ \frac{1}{2} K_c \lambda_c f(t) \sum_n \sqrt{g_{en}} \left(a_n'' \cos [(\omega_p - \omega_c)t - \phi_n - \phi(t) + \zeta - \xi_n] \right.$$

$$\left. + b_n'' \sin [(\omega_p - \omega_c)t - \phi_n - \phi(t) + \zeta - \xi_n] \right)$$

$$+ \frac{1}{2} K_p \lambda_p C \sum_n \sqrt{g_{en}} \left(a_n' \cos [(\omega_p - \omega_c)t + \phi_{pn} - \zeta + \xi_n] \right.$$

$$\left. - b_n' \sin [(\omega_p - \omega_c)t + \phi_{pn} - \zeta + \xi_n] \right)$$

$$+ \frac{1}{2} \sum_n [(a_n'' a_n' + b_n'' b_n') \cos (\omega_p - \omega_c)t + (b_n'' a_n' - a_n'' b_n') \sin (\omega_p - \omega_c)t]$$

$$+ \frac{1}{2} K_p K_{c1} \lambda_p \lambda_{c1} C f_1(t) \sum_n \sqrt{g_{en} g_{en1}} \cos [(\omega_p - \omega_{c1})t + \phi_{pn} - \phi_{n1} - \phi_1(t)]$$

$$+ \frac{1}{2} K_c K_{p1} \lambda_{p1} \lambda_c C_1(t) f(t) \sum_n \sqrt{g_{en} g_{en1}} \cos [(\omega_{p1} - \omega_c)t + \phi_{pn1} - \phi_n - \phi(t)]$$

$$+ \frac{1}{2} K_{c1} K_{p1} \lambda_{c1} \lambda_{p1} C_1(t) f_1(t) \sum_n g_{en1} \cos [(\omega_{p1} - \omega_{c1})t + \phi_{pn1} - \phi_{n1} - \phi(t)]$$

$$+ \frac{1}{2} K_{c1} \lambda_{c1} f_1(t) \sum_n \sqrt{g_{en1}} \left(a_n'' \cos [(\omega_p - \omega_{c1})t - \phi_{n1} - \phi_1(t) + \zeta - \xi_{n1}] \right.$$

$$\left. + b_n'' \sin [(\omega_p - \omega_{c1})t - \phi_{n1} - \phi_1(t) + \zeta - \xi_{n1}] \right)$$

$$+ \frac{1}{2} K_{p1} \lambda_{p1} C_1(t) \sum_n \sqrt{g_{en1}} \left(a_n' \cos [(\omega_{p1} - \omega_c)t + \phi_{pn1} - \zeta + \xi_n] \right.$$

$$\left. - b_n' \sin [(\omega_{p1} - \omega_c)t + \phi_{pn1} - \zeta + \xi_n] \right)$$

(171)

The first summation in equation (171) represents the desired direct path signal received with full array gain since the ϕ_{pn} and ϕ_n nearly cancel.

The seventh summation represents the secondary path signal received with a gain that depends on the spectral characteristics of the reflected signal. For example, if the doppler shifts of the secondary path pilot signal do not move it out of the passband of the pilot amplifier and the spectrum is not spread significantly so that the secondary path information signal and pilot signal are still closely correlated, then the signal will be received with essentially full array gain. Any decorrelation between the reflected pilot and information signals introduced by the reflecting surface reduces the magnitude of this term. It should also be pointed out that, since the amplitude of this secondary path term is proportional to the product of the secondary path pilot amplitude and the secondary path information-signal amplitude, its amplitude relative to the direct path amplitude is Ω^2 where Ω is the ratio of secondary path signal amplitude to primary path signal amplitude. Therefore, if the secondary path signal were 10 db below the direct path signal, this term would be 20 db below the desired direct path signal in the first summation. This observation assumes that there is no limiting used in the system.

The fifth summation represents the secondary path signal arriving on a sidelobe of the pattern pointed toward the direct path signal. This term would be present in any system.

The sixth summation represents the direct path signal arriving on a sidelobe of the pattern pointed toward the secondary path signal. It is introduced specifically by the nature of the self-steering technique being used.

The third summation is the noise in the information channel and is the same as would exist in a conventionally steered system.

The remaining sums are noise-signal and noise-noise cross terms that arise from the type of self-steering system being considered.

The probabilities of error in the detection of coded signals are the quantities of interest. All the demodulators depend on correlators for their operation. They correlate the orthonormal bases of the transmitted signal with the received signal. Allowing for a random phase uncertainty in the orthonormal function generators, the orthonormal functions have the general representation,

$$\varphi_{1k} = \sqrt{\frac{2}{T}} \cos (\omega_k t - \theta_k) \tag{172a}$$

$$\varphi_{2k} = \sqrt{\frac{2}{T}} \sin (\omega_k t - \theta_k) \tag{172b}$$

The correlator outputs are

$$x_k = \int_0^T v_0(t)\, \varphi_{1k}(t)\, dt \tag{173a}$$

$$y_k = \int_0^T v_0(t)\, \varphi_{2k}(t)\, dt \tag{173b}$$

In digitally modulated signals, the amplitude, phase, or frequency may take on only quantized values $f_m(t)$, $\theta_m(t)$ or ω_m, depending on whether amplitude, phase, or frequency modulation is used. The outputs of the correlators may be written as

$$\begin{aligned}
x_k = {} & \tfrac{1}{4}\sqrt{\tfrac{2}{T}} K_c K_p \lambda_c \lambda_p C \sum_n \varepsilon_{en} \int_0^T f_m(t) \cos\left[(\omega_p - \omega_{cm} - \omega_k)t + \theta_{pn} - \theta_n - \theta_m(t) + \theta_k\right] dt \\
& + \tfrac{1}{4}\sqrt{\tfrac{2}{T}} K_c \lambda_c \sum_n \sqrt{\varepsilon_{en}} \int_0^T f_m(t)\, a_n'' \cos\left[(\omega_p - \omega_{cn} - \omega_k)t - \theta_n - \theta_m(t) + \zeta - \tau_n + \theta_k\right] dt \\
& + \tfrac{1}{4}\sqrt{\tfrac{2}{T}} K_c \lambda_c \sum_n \sqrt{\varepsilon_{en}} \int_0^T f_m(t)\, b_n'' \sin\left[(\omega_p - \omega_{cm} - \omega_k)t - \theta_n - \theta_m(t) + \zeta - \tau_n + \theta_k\right] dt \\
& + \tfrac{1}{4}\sqrt{\tfrac{2}{T}} K_p \lambda_p \sum_n \sqrt{\varepsilon_{en}}\, C \int_0^T a_n' \cos\left[(\omega_p - \omega_{cm} - \omega_k)t + \theta_{pn} - \zeta + \tau_n + \theta_k\right] dt \\
& - \tfrac{1}{4}\sqrt{\tfrac{2}{T}} K_p \lambda_p \sum_n \sqrt{\varepsilon_{en}}\, C \int_0^T b_n' \sin\left[(\omega_p - \omega_{cm} - \omega_k)t + \theta_{pn} - \zeta + \tau_n + \theta_k\right] dt \\
& + \tfrac{1}{4}\sqrt{\tfrac{2}{T}} \sum_n \int_0^T (a_n'' a_n' + b_n'' b_n') \cos\left[(\omega_p - \omega_{cm} - \omega_k)t + \theta_k\right] dt + \tfrac{1}{4}\sqrt{\tfrac{2}{T}} \sum_n \int_0^T (b_n'' a_n' - a_n'' b_n') \sin\left[(\omega_p - \omega_{cm} - \omega_k)t + \theta_k\right] dt \\
& + \tfrac{1}{4}\sqrt{\tfrac{2}{T}} K_p K_{c1} \lambda_p \lambda_{c1} C \sum_n \sqrt{\varepsilon_{en}\, \varepsilon_{en1}} \int_0^T f_{1m}(t) \cos\left[(\omega_p - \omega_{c1m} - \omega_k)t + \theta_{pn} - \theta_{n1} - \theta_{1m}(t) + \theta_k\right] dt \\
& + \tfrac{1}{4}\sqrt{\tfrac{2}{T}} K_c K_{p1} \lambda_{p1} \lambda_c \sum_n \sqrt{\varepsilon_{en}\, \varepsilon_{en1}} \int_0^T C_1(t)\, f_m(t) \cos\left[(\omega_{p1} - \omega_{cm} - \omega_k)t + \theta_{pn1} - \theta_n - \theta_m(t) + \theta_k\right] dt \\
& + \tfrac{1}{4}\sqrt{\tfrac{2}{T}} K_{c1} K_{p1} \lambda_{c1} \lambda_{p1} \sum_n \varepsilon_{en1} \int_0^T C_1(t)\, f_{1m}(t) \cos\left[(\omega_{p1} - \omega_{c1m} - \omega_k)t + \theta_{pn1} - \theta_{n1} - \theta_{1m}(t) + \theta_k\right] dt \\
& + \tfrac{1}{4}\sqrt{\tfrac{2}{T}} K_{c1} \lambda_{c1} \sum_n \sqrt{\varepsilon_{en1}} \int_0^T f_{1m}(t)\, a_n'' \cos\left[(\omega_p - \omega_{c1m} - \omega_k)t - \theta_{n1} - \theta_{1m}(t) + \zeta - \tau_{n1} + \theta_k\right] dt \\
& + \tfrac{1}{4}\sqrt{\tfrac{2}{T}} K_{c1} \lambda_{c1} \sum_n \sqrt{\varepsilon_{en1}} \int_0^T f_{1m}(t)\, b_n'' \sin\left[(\omega_p - \omega_{c1m} - \omega_k)t - \theta_{n1} - \theta_{1m}(t) + \zeta - \tau_{n1} + \theta_k\right] dt \\
& + \tfrac{1}{4}\sqrt{\tfrac{2}{T}} K_{p1} \lambda_{p1} \sum_n \sqrt{\varepsilon_{en1}} \int_0^T C_1(t)\, a_n' \cos\left[(\omega_{p1} - \omega_{cm} - \omega_k)t + \theta_{pn1} - \zeta + \tau_{n1} + \theta_k\right] dt \\
& - \tfrac{1}{4}\sqrt{\tfrac{2}{T}} K_{p1} \lambda_{p1} \sum_n \sqrt{\varepsilon_{en1}} \int_0^T C_1(t)\, b_n' \sin\left[(\omega_{p1} - \omega_{cm} - \omega_k)t + \theta_{pn1} - \zeta + \tau_{n1} + \theta_k\right] dt
\end{aligned} \tag{174a}$$

$$
\begin{aligned}
y_k = &-\frac{1}{4}\sqrt{\frac{2}{T}}\,K_c K_p \lambda_c \lambda_p\, C \sum_n g_{en} \int_0^T f_m(t)\,\sin\left[(\omega_p-\omega_{cm}-\omega_k)t+\phi_{pn}-\phi_n-\phi_m(t)+\theta_k\right]dt \\
&-\frac{1}{4}\sqrt{\frac{2}{T}}\,K_c\lambda_c \sum_n \sqrt{g_{en}} \int_0^T f_m(t)\,a_n''\,\sin\left[(\omega_p-\omega_{cm}-\omega_k)t-\phi_n-\phi_m(t)+\zeta-\xi_n+\theta_k\right]dt \\
&+\frac{1}{4}\sqrt{\frac{2}{T}}\,K_c\lambda_c \sum_n \sqrt{g_{en}} \int_0^T f_m(t)\,b_n''\,\cos\left[(\omega_p-\omega_{cm}-\omega_k)t-\phi_n-\phi_m(t)+\zeta-\xi_n+\theta_k\right]dt \\
&-\frac{1}{4}\sqrt{\frac{2}{T}}\,K_p\lambda_p \sum_n \sqrt{g_{en}}\,C \int_0^T a_n'\,\sin\left[(\omega_p-\omega_{cm}-\omega_k)t+\phi_{pn}-\zeta+\xi_n+\theta_k\right]dt \\
&-\frac{1}{4}\sqrt{\frac{2}{T}}\,K_p\lambda_p \sum_n \sqrt{g_{en}}\,C \int_0^T b_n'\,\cos\left[(\omega_p-\omega_{cm}-\omega_k)t+\phi_{pn}-\zeta+\xi_n+\theta_k\right]dt \\
&-\frac{1}{4}\sqrt{\frac{2}{T}} \sum_n \int_0^T (a_n''a_n'+b_n''b_n')\,\sin\left[(\omega_p-\omega_{cm}-\omega_k)t+\theta_k\right]dt \\
&+\frac{1}{4}\sqrt{\frac{2}{T}} \sum_n \int_0^T (b_n''a_n'-a_n''b_n')\,\cos\left[(\omega_p-\omega_{cm}-\omega_k)t+\theta_k\right]dt \\
&-\frac{1}{4}\sqrt{\frac{2}{T}}\,K_p K_{c1}\lambda_p\lambda_{c1}\,C \sum_n \sqrt{g_{en}\,g_{en1}} \int_0^T f_{1m}(t)\,\sin\left[(\omega_p-\omega_{c1m}-\omega_k)t+\phi_{pn}-\phi_{n1}-\phi_{1m}(t)+\theta_k\right]dt \\
&-\frac{1}{4}\sqrt{\frac{2}{T}}\,K_c K_{p1}\lambda_c\lambda_{p1} \sum_n \sqrt{g_{en}\,g_{en1}} \int_0^T C_1(t)\,f_m(t)\,\sin\left[(\omega_{p1}-\omega_{cm}-\omega_k)t+\phi_{pn1}-\phi_n-\phi_m(t)+\theta_k\right]dt \\
&-\frac{1}{4}\sqrt{\frac{2}{T}}\,K_{c1}K_{p1}\lambda_{c1}\lambda_{p1} \sum_n g_{en1} \int_0^T C_1(t)\,f_{1m}(t)\,\sin\left[(\omega_{p1}-\omega_{c1m}-\omega_k)t+\phi_{pn1}-\phi_{n1}-\phi_{1m}(t)+\theta_k\right]dt \\
&-\frac{1}{4}\sqrt{\frac{2}{T}}\,K_{c1}\lambda_{c1} \sum_n \sqrt{g_{en1}} \int_0^T f_{1m}(t)\,a_n''\,\sin\left[(\omega_p-\omega_{c1m}-\omega_k)t-\phi_{n1}-\phi_{1m}(t)+\zeta-\xi_{n1}+\theta_k\right]dt \\
&+\frac{1}{4}\sqrt{\frac{2}{T}}\,K_{c1}\lambda_{c1} \sum_n \sqrt{g_{en1}} \int_0^T f_{1m}(t)\,b_n''\,\cos\left[(\omega_p-\omega_{c1m}-\omega_k)t-\phi_{n1}-\phi_{1m}(t)+\zeta-\xi_{n1}+\theta_k\right]dt \\
&-\frac{1}{4}\sqrt{\frac{2}{T}}\,K_{p1}\lambda_{p1} \sum_n \sqrt{g_{en1}} \int_0^T C_1(t)\,a_n'\,\sin\left[(\omega_{p1}-\omega_{cm}-\omega_k)t+\phi_{pn1}-\zeta+\xi_{n1}+\theta_k\right]dt \\
&-\frac{1}{4}\sqrt{\frac{2}{T}}\,K_{p1}\lambda_{p1} \sum_n \sqrt{g_{en1}} \int_0^T C_1(t)\,b_n'\,\cos\left[(\omega_{p1}-\omega_{cm}-\omega_k)t+\phi_{pn1}-\zeta+\xi_{n1}+\theta_k\right]dt
\end{aligned}
$$

(174b)

The first seven terms are the terms that exist in the absence of multipath. These terms are discussed in Part I of the Final Report.[8] The last seven terms arise from the presence of the secondary path, and their effects on the probability of error are not easy to assess for several reasons. First, since the secondary path pilot and signal are both reflected from a rough surface, they each have in-phase and quadrature components that are independent, zero-mean, gaussian processes. Further, their spectra are distorted in an unknown manner by the reflecting surface so that an evaluation of their effects on the detection process is difficult to make. In addition, the secondary path signal modulation is delayed with respect to the direct path signal so that the secondary path modulation does not generally coincide with the synchronizing signal of the detector.

In spite of these difficulties, the conditional probabilities of error can be computed, conditioned on the transmitted signal, S_m, the time delay, τ, the correlator phase error, θ_k, and the multipath signal S_{1m}. This computation can be performed because when the noise-noise product terms are small, the conditional probability density functions of x_k and y_k are approximately gaussian. Once the conditional probability of error is computed, the unconditional probability can be computed, provided that the joint probability density function of the transmitted signal, the time delay, the correlator phase error, and the multipath signal are known.

As mentioned in the preceding paragraph, when the noise-noise terms are small, the correlator outputs, x_k and y_k, conditioned on S_m, S_{1m}, τ, and θ_k, are independent, gaussian, random variables. They have means $\mu_{1k}^{(m)}$ and $\mu_{2k}^{(m)}$, respectively, and equal variances, σ_k^2. These quantities are given by

$$\mu_{1k}^{(m)} = \frac{1}{4}\sqrt{2T}\,K_c K_p \lambda_c \lambda_p\, C\, f_m\, \delta_{mk} \sum_n g_{en} \cos\left[\phi_{pn} - \phi_n - \phi_m + \theta_k\right]$$

$$+ \frac{1}{4}\sqrt{\frac{2}{T}}\,K_p K_{c1} \lambda_p \lambda_{c1}\, C \sum_n \sqrt{g_{en} g_{en1}} \int_0^T f_{1m}(t) \cos\left[(\omega_p - \omega_{c1m} - \omega_k)\,t + \phi_{pn} - \phi_{n1} - \phi_{1m}(t) + \theta_k\right] dt$$

$$+ \frac{1}{4}\sqrt{\frac{2}{T}}\,K_c K_{p1} \lambda_c \lambda_{p1}\, f_m \sum_n \sqrt{g_{en} g_{en1}} \int_0^T C_1(t) \cos\left[(\omega_{p1} - \omega_{cm} - \omega_k)\,t + \phi_{pn1} - \phi_n - \phi_m + \theta_k\right] dt$$

$$+ \frac{1}{4}\sqrt{\frac{2}{T}}\,K_{c1} K_{p1} \lambda_{c1} \lambda_{p1} \sum_n g_{en1} \int_0^T C_1(t)\, f_{1m}(t) \sin\left[(\omega_{p1} - \omega_{c1m} - \omega_k)\,t + \phi_{pn1} - \phi_{n1} - \phi_{1m}(t) + \theta_k\right] dt \qquad (175)$$

$$\mu_{2k}^{(m)} = -\frac{1}{4}\sqrt{2T}\,K_c K_p \lambda_c \lambda_p C f_m \delta_{mk} \sum_n g_{en} \sin\left[\Phi_{pn} - \Phi_n - \Phi_m + \theta_k\right]$$

$$-\frac{1}{4}\sqrt{\frac{2}{T}}K_p K_{c1} \lambda_p \lambda_{c1} C \sum_n \sqrt{g_{en} g_{en1}} \int_0^T f_{1m}(t) \sin\left[(\omega_p - \omega_{c1m} - \omega_k)t\right.$$

$$\left. + \Phi_{pn} - \Phi_{n1} - \Phi_{1m}(t) + \theta_k\right] dt$$

$$-\frac{1}{4}\sqrt{\frac{2}{T}}\,K_c K_{p1} \lambda_c \lambda_{p1} f_m \sum_n \sqrt{g_{en} g_{en1}} \int_0^T C_1(t) \sin\left[(\omega_{p1} - \omega_{cm} - \omega_k)t\right.$$

$$\left. + \Phi_{pn1} - \Phi_n - \Phi_m + \theta_k\right] dt$$

$$-\frac{1}{4}\sqrt{\frac{2}{T}}K_{c1} K_{p1} \lambda_{c1} \lambda_{p1} \sum_n g_{en1} \int_0^T C_1(t) f_{1m}(t) \sin\left[(\omega_{p1} - \omega_{c1m} - \omega_k)t\right.$$

$$\left. + \Phi_{pm} - \Phi_{n1} - \Phi_{1m}(t) + \theta_k\right] dt \qquad (176)$$

$$\sigma^2 = \frac{1}{8T} K_c^2 \lambda_c^2 f_m^2 \sum_n g_{en} \int_0^T \int_{-t}^{T-t} R''(\tau) \cos\left[(\omega_p - \omega_{cm} - \omega_k)\tau\right] d\tau\, dt$$

$$+ \frac{1}{8T} K_p^2 \lambda_p^2 C^2 \sum_n g_{en} \int_0^T \int_{-t}^{T-t} R'(\tau) \cos\left[(\omega_p - \omega_{cm} - \omega_k)\tau\right] d\tau\, dt$$

$$+ \frac{1}{8T} K_{c1}^2 \lambda_{c1}^2 \sum_n g_{en1} \int_0^T \int_{-t}^{T-t} f_{1m}(t) f_{1m}(t+\tau) R''(\tau) \cos\left[(\omega_p - \omega_{c1m} - \omega_k)\tau\right] d\tau\, dt$$

$$+ \frac{1}{8T} K_{p1}^2 \lambda_{p1}^2 \sum_n g_{en1} \int_0^T \int_{-t}^{T-t} C_1(t) C_{1m}(t+\tau) R'(\tau) \cos\left[(\omega_{p1} - \omega_{cm} - \omega_k)\tau\right] d\tau\, dt$$

$$+ \frac{1}{4T} K_c K_{c1} \lambda_c \lambda_{c1} \sum_n \sqrt{g_{en} g_{en1}}\, f_m$$

$$\int_0^T \int_{-t}^{T-t} f_{1m}(t+\tau) R''(\tau) \cos\left[(\omega_{c1m} - \omega_{cm})t - (\omega_p - \omega_{c1m} - \omega_k)\tau - \phi_n + \phi_{n1} - \phi_m + \phi_{1m}(t+\tau) - \xi_n + \xi_{n1}\right] d\tau\, dt$$

$$+ \frac{1}{4T} K_p K_{p1} \lambda_p \lambda_{p1} \sum_n \sqrt{g_{en} g_{en1}}\, C$$

$$\int_0^T \int_{-t}^{T-t} C_1(t+\tau) R'(\tau) \cos\left[(\omega_p - \omega_{p1})t - (\omega_{p1} - \omega_{cm} - \omega_k)\tau + \phi_{pn} - \phi_{pn1} + \xi_n - \xi_{n1}\right] d\tau\, dt$$

$$+ \frac{M}{4T} \int_0^T \int_{-t}^{T-t} R'(\tau) R''(\tau) \cos\left[(\omega_p - \omega_{cm} - \omega_k)\tau\right] d\tau\, dt$$

(177)

The probability of error conditioned on θ_k, S_m, S_{1m}, and τ can then be obtained from the probability density functions of x_k and y_k by use of the relation

$$P_e(S_m, S_{1m}, \theta_k, \tau) = 1 - Pr(x, y \in R_m | S_m, S_{1m}, \theta_k, \tau) \quad (178)$$

where R_m represents the region in signal space corresponding to S_m.

4.6 Effective Radiation Patterns of Self-Steering Arrays with Phase-Locked Loops

The previous sections are concerned in part with analyses of detection error probabilities when multipath signals are present in communication systems that use self-steering arrays in which the phasing of the arrays is accomplished by the use of phase-locked loops. The communication theory approach that was used in the analyses masked the usual antenna concepts, specifically, pattern and gain. In this section, the effective patterns of this type of array are considered.

The signal received by the n^{th} element is represented by

$$s_n(t) = s_{pn}(t) + s_{sn}(t) \quad (179)$$

where s_{pn} and s_{sn} represent, respectively, the primary path signal and the secondary path signal.

$$s_{pn}(t) = a_{pn}(t) \sin(\omega_p t + \theta_{pn}) \quad (180a)$$

$$s_{sn}(t) = a_{sn}(t) \sin(\omega_s t + \theta_{sn}) \quad (180b)$$

The sum signal can be rewritten as

$$s_n(t) = |a_{pn}| \sqrt{1 + \Omega^2 + 2\Omega \cos[(\omega_s - \omega_p)t + \theta_{sn} - \theta_{pn}]} \cos(\omega_p t + \theta_{pn} + \psi_n) \quad (181)$$

where

$$\psi_n = \tan^{-1}\left[\frac{\Omega \sin\left[(\omega_s-\omega_p)\,t + \theta_{sn}-\theta_{pn}\right]}{1 + \Omega \cos\left[(\omega_s-\omega_p)\,t + \theta_{sn}-\theta_{pn}\right]}\right]$$

$$\Omega = \frac{a_{sn}}{a_{pn}} \text{ (assumed independent of n)}$$

The phase of the signal at the n^{th} element is therefore

$$\theta_n = \theta_{pn} + \tan^{-1}\left[\frac{\Omega \sin\left[(\omega_s-\omega_p)\,t + \theta_{sn}-\theta_{pn}\right]}{1 + \Omega \cos\left[(\omega_s-\omega_p)\,t + \theta_{sn}-\theta_{pn}\right]}\right] \qquad (182)$$

It is evident that both the amplitude and the phase of the total signal fluctuate periodically at a frequency equal to the difference in primary path and secondary path doppler frequencies. Several conditions are possible: first, the separation in frequency may be greater than the loop bandwidth; then, the secondary path signal will not get through the tracking loop and a conventional pattern will be steered in the direction of the primary path signal. Second, the difference in the primary path and secondary path doppler frequencies may be within the loop bandwidth; then the loop will track the combined signal so that the effective pattern will fluctuate periodically about the correct pattern. A limiting case is that in which ω_s and ω_p are equal. In this case there will be no fluctuation and the effective pattern will assume some shape distorted from the desired shape. Some special cases of this latter condition were computed for a linear array with a uniform aperture distribution. It was assumed for the computations that the amplitude of the composite tracking signal had been amplified and limited so that the effective pattern could be written as

$$E(\theta) = \frac{1}{(2N+1)} \sum_{-N}^{N} \exp j\,(n\,k\,d\,\sin\varphi - \theta_n) \qquad (183)$$

where, for this special case,

$$\theta_n = n\,k\,d\,\sin\varphi_p + \tan^{-1}\left[\frac{\Omega \sin\left[n\,k\,d\,(\sin\varphi_s - \sin\varphi_p)\right]}{1 + \Omega \cos\left[n\,k\,d\,(\sin\varphi_s - \sin\varphi_p)\right]}\right]$$

This equation, with $d = \lambda/2$, was programmed for the GE-265 Time-Sharing Computer system. The results are plotted in figures 18a through 18h for a range of Ω between 0 and 1. It was assumed that the primary path signal arrives along $\varphi_p = 0$. Two different values of φ_s were assumed, $\varphi_s = 25$ degrees and $\varphi_s = 70$ degrees. It should be noted that the curves give the effective pattern of the array and not the relative signal strengths of the primary path signal and secondary path signal at the combining point. That is to say, the primary path signal is given by

$$V_p = a_p E(0) \tag{184}$$

while the secondary path signal is

$$V_s = a_p \Omega E(\varphi_s) \tag{185}$$

Consequently, the relative powers are in the ratio

$$\left|\frac{V_s}{V_p}\right|^2 = \Omega^2 \frac{|E(\varphi_s)|^2}{|E(0)|^2} \tag{186}$$

5.0 Scattering By a Rough Surface

When a communication link exists between two vehicles in space and an object that scatters electromagnetic waves is "visible" to the antennas on both vehicles, then the waves scattered by the object will interfere with the waves that move along the line-of-sight path. To determine the effects that the scattered signal has on the reception of the direct path signal, it is necessary to ascertain the nature of the scattered signal.

If the scatterer is a rough object whose characteristics are known only statistically, then only the statistics of the scattered signal can be determined. The statistical quantities of interest are the probability density function of the scattered signal as it is received by an antenna on one of the vehicles and the autocorrelation function of the received signal as a function of the positions of the source and receiver. The spectrum of the scattered signal is then the Fourier transform of the autocorrelation function as the position of the source and the receiver change with time. In general, the spectrum will change with time since the signal statistics will vary as the positions of transmitter and receiver change. The spectral characteristics depend on the statistical properties of the surface and on the motion of the source and receiver.

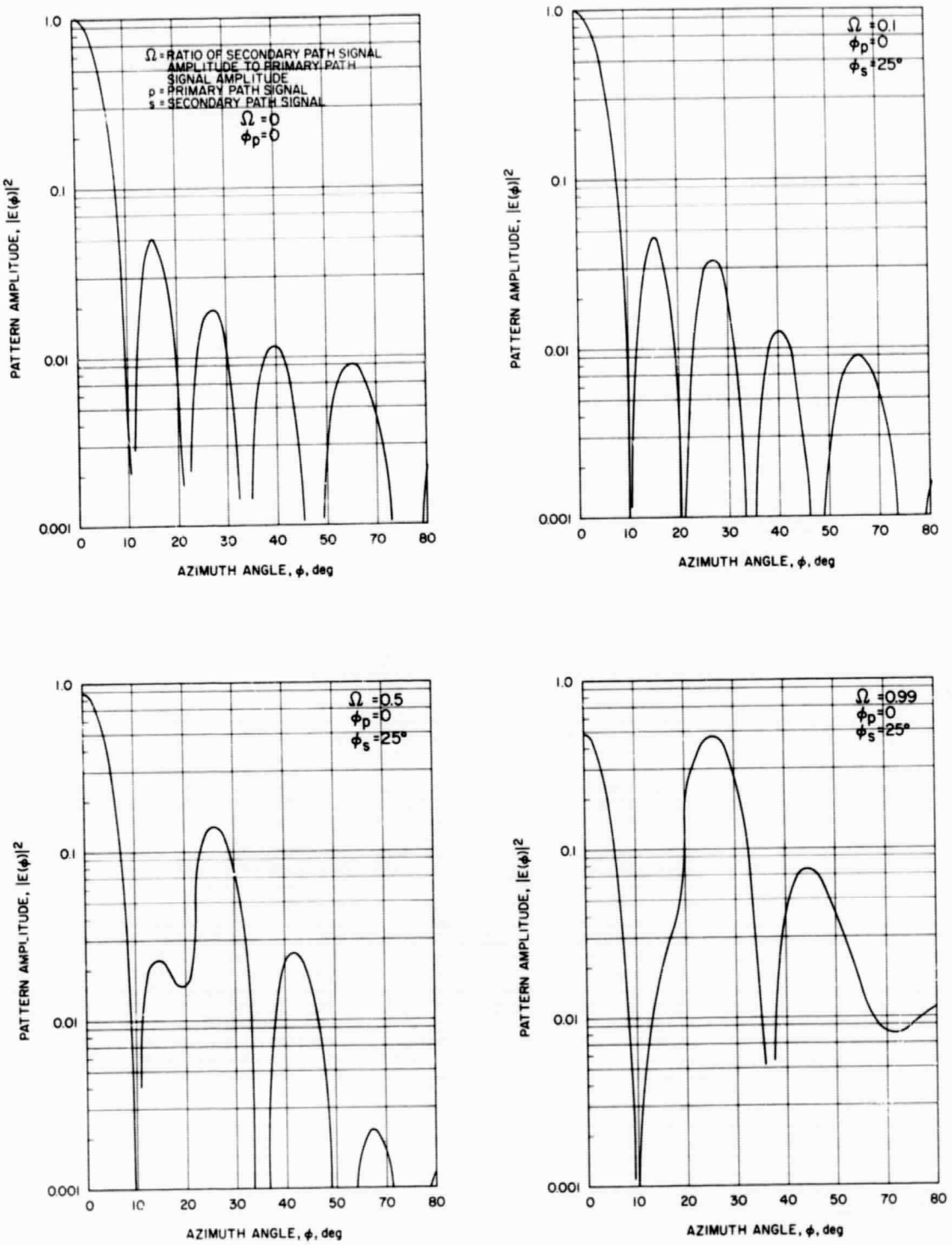

Figure 18. Equivalent radiation patterns of self-steering arrays with phase-locked loops.

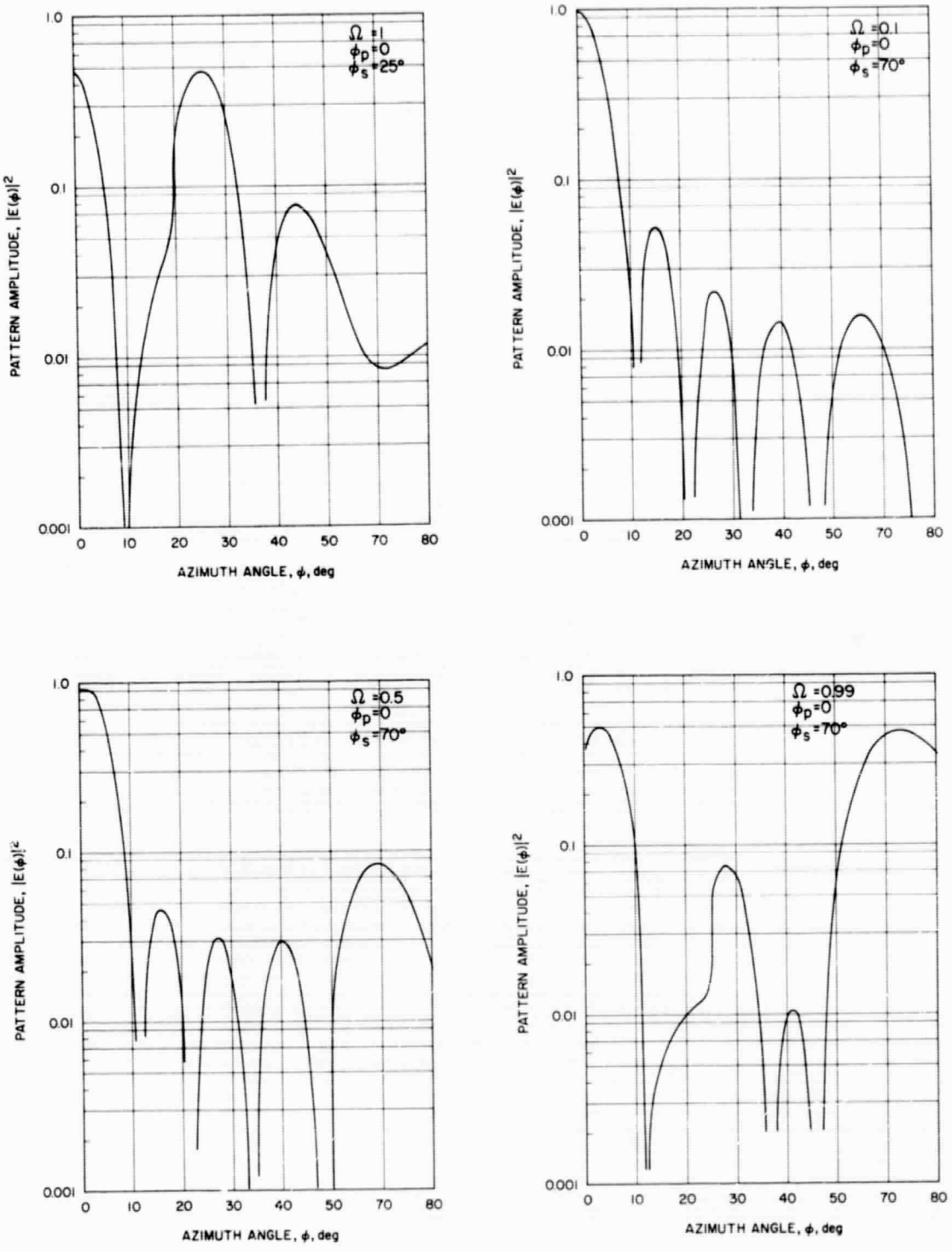

Figure 18. – Concluded.

Calculation of the spectrum is a complicated problem. A scalar approach has been employed by Staras[31] who applied the technique followed in Beckmann and Spizzichino[32] to obtain approximate expressions for the autocorrelation function. In addition to being a scalar theory, the analysis is restricted to surfaces whose mean value is a plane and only one of the terminals is allowed to move. A vector method of calculating the spectrum is outlined in this section. A vector study of scattering by rough planar surfaces has recently appeared.[33] However, the study does not consider the spectrum of the signal when source and receiver are in motion and is restricted to far zone scattering from planes of restricted size rather than to scattering from curved surfaces.

If the amplitude and polarization characteristics of the scattered electric field do not vary significantly over the region of the receiving antenna, then the signal received by the antenna can be expressed as some linear combination of the three orthogonal components of the electric field. Therefore, the received signal, V_r (in phasor notation) can be written as

$$V_r = \alpha E_1 + \beta E_2 + \gamma E_3 \tag{187}$$

where E_m (m=1, 2, 3) represents the three orthogonal spatial components of the electric field vector, $\bar{E}$, and α, β, and γ are complex constants characteristic of the receiving antenna and its orientation. The time signal is then given by

$$v_r(t) = \sqrt{2}|\alpha E_1| \cos\left(\omega_0 t + \psi_{10} + \psi_{11} + \psi_\alpha\right) + \sqrt{2}\,|\beta E_2| \cos\left(\omega_0 t + \psi_{20} + \psi_{21} + \psi_\beta\right) + \sqrt{2}|\gamma E_3| \cos\left(\omega_0 t + \psi_{30} + \psi_{31} + \psi_\gamma\right) \tag{188}$$

where ψ_{m0} represents a predictable component of the phase of E_m and ψ_{m1} represents the random component. The field components E_m are computed by an integration over the scattering surface. Since the surface height above some mean is a random process with a finite autocorrelation distance, the integral is essentially the sum of many independent integrals. Consequently, each spatial component, E_m, has quadrature components that approach independent gaussian random variables. Therefore, $v_r(t)$ may be written as

$$v_r(t) = v_0 \cos\left(\omega_0 t + \psi_0\right) + v_1 \sin\left(\omega_0 t + \psi_0\right) \tag{189a}$$

$$v_r(t) = v \cos\left(\omega_0 t + \psi_0 + \psi\right) \tag{189b}$$

where ψ_0 represents the predictable portion of the phase of $v_r(t)$. The components v_0 and v_1 are independent gaussian random variables of variance σ_v^2 so that v is Rayleigh distributed and ψ is uniformly

distributed from $-\pi$ to π. In the absence of motion of source and receiver, $v_r(t)$ varies cosinusoidally at angular frequency ω_0. When there is predictable motion of the source and/or receiver, then ψ_0 is time varying and the angular frequency is given by $\omega_0 + \dot{\psi}_0$. In addition, v_0 and v_1 become random processes so that the signal spectrum is spread about $\omega_0 + \dot{\psi}_0$. The spectrum of the resulting $v_r(t)$ may then be determined as the Fourier transform of the autocorrelation function $R_v(t, t+\tau)$ where

$$R_v(t, t+\tau) = E\left[v_r(t) v_r(t+\tau)\right] \tag{190}$$

The surface is assumed to be a random process of two independent variables ζ, ξ and is denoted by $g(\zeta, \xi)$; the E_m are given by integrals of the following forms,

$$E_m = \iint f_m \left[P_i, P_s, g(\zeta, \xi), g_\zeta(\zeta, \xi), g_\xi(\zeta, \xi)\right] d\zeta d\xi \tag{191a}$$

where

$$g_\zeta \equiv \frac{\partial g}{\partial \zeta} \tag{191b}$$

$$g_\xi \equiv \frac{\partial g}{\partial \xi} \tag{191c}$$

P_i represents the point of origin of the incident wave

P_s represents the receiver location

The correlations of the signals are then represented by

$$R_{mn}\left(P_{i1}, P_{s1}, P_{i2}, P_{s2}\right) = \iiiint E\Big(f_m\left[P_{i1}, P_{s1}, g(\zeta, \xi), g_\zeta(\zeta, \xi), g_\xi(\zeta, \xi)\right] f_n\left[P_{i2}, P_{s2}\, g(\zeta', \xi')\, g_\zeta(\zeta', \xi')\, g_\xi(\zeta', \xi')\right] d\xi d\zeta \; d\xi' d\zeta'\Big) \tag{192}$$

where E(f) denotes the expectation of f.

Consequently, the expectation of $f_m f_n$ must be evaluated and the resulting integrations performed. The expectation of $f_m f_n$ is given by

$$E(f_m f_n) = \iiiint f_m f_n p(g, g', g_\zeta, g_\zeta', g_\xi, g_\xi') \, dg dg' dg_\zeta dg_\zeta' dg_\xi dg_\xi' \tag{193}$$

where $p\left(g, g', g_\zeta, g_{\zeta'}, g_\xi, g_{\xi'}\right)$ is the joint probability density function of $g, g', g_\zeta, g_{\zeta'}, g_\xi, g_{\xi'}$. It may be readily determined when g is gaussian with autocorrelation function $R_{gg'}(\zeta, \xi, \zeta', \xi')$. The form of p is[25]

$$p\left(g, g', g_\zeta, g_{\zeta'}, g_\xi, g_{\xi'}\right) = \frac{\exp\left[\frac{1}{2|\Lambda|}\sum_{p=1}^{6}\sum_{q=1}^{6}|\Lambda_{pq}|x_p x_q\right]}{(2\pi)^3|\Lambda|^{1/2}} \tag{194}$$

where

$$\begin{aligned} x_1 &\equiv g & x_4 &\equiv g' \\ x_2 &\equiv g_\zeta & x_5 &\equiv g_{\zeta'} \\ x_3 &\equiv g_\xi & x_6 &\equiv g_{\xi'} \end{aligned} \tag{195}$$

and Λ is the covariance matrix of elements

$$\lambda_{pq} \equiv R_{pq}(\zeta, \xi, \zeta', \xi') = E\left(x_p x_q\right) \tag{196}$$

That is, Λ is given by

$$\Lambda = \begin{bmatrix} \lambda_{11} & \lambda_{12} \cdots & \lambda_{16} \\ \lambda_{21} & & \vdots \\ \vdots & & \vdots \\ \lambda_{61} & \cdots & \lambda_{66} \end{bmatrix} \tag{197}$$

The next task is to obtain expressions for the f_m to enable the averaging process to be carried out. If the averaging can be carried out then the four dimensional integrations over the sources on the surface must be carried out.

From Silver[34] the fields radiated by a surface distribution of electric and magnetic currents are given exactly by

$$\overline{E} = -\frac{j}{4\pi\omega\epsilon_0}\int_S \left[\left(\overline{J}_s \cdot \nabla\right)\nabla + k^2\overline{J}_s - j\omega\epsilon\overline{M}_s \times \nabla\right] \frac{\exp(-jkr)}{r}\, dS \tag{198}$$

$$\overline{H} = -\frac{j}{4\pi\omega\mu_0}\int_S \left[\left(\overline{M}_s \cdot \nabla\right)\nabla + k^2\overline{M}_s + j\omega\mu\overline{J}_s \times \nabla\right] \frac{\exp(-jkr)}{r}\, dS \tag{199}$$

where $\overline{J}_s$ and $\overline{M}_s$ are, respectively, surface densities of electric and magnetic currents distributed over S, and r is the distance from source point to field point. The propagation constant is denoted by k $\left(= \omega\sqrt{\mu_0\epsilon_0}\right)$. The operator ∇ operates on the source coordinates so that

$$\nabla\left(\frac{\exp[-jkr]}{r}\right) = \left(jk + \frac{1}{r}\right)\frac{\exp[-jkr]}{r}\,\overline{r}_1 \tag{200}$$

and

$$(\overline{J}\cdot\nabla)\left(\frac{\exp[-jkr]}{r}\right) = \left[-k^2(\overline{J}\cdot\overline{r}_1)\overline{r}_1 + \frac{3}{r}\left(jk + \frac{1}{r}\right)(J\cdot\overline{r}_1)\overline{r}_1 - \frac{\overline{J}}{r}\left(jk + \frac{1}{r}\right)\right]\frac{\exp[-jkr]}{r} \tag{201}$$

For $kr \gg 1$, which is the usual condition for the scattering problem of interest, equation (189) and (190) reduce to

$$\nabla\left(\frac{\exp\,[-jkr]}{r}\right) \approx jk\,\frac{\exp\,[-jkr]}{r}\;\bar{r}_1 \tag{202}$$

$$\left(\bar{J}\cdot\nabla\right)\;\nabla\;\left(\frac{\exp\,[-jkr]}{r}\right) \approx -\,k^2\left(\bar{J}\;\cdot\;\bar{r}_1\right)\bar{r}_1 \tag{203}$$

On using these approximations, equations (198) and (199) are reduced to

$$\bar{E} = \frac{-j}{4\pi\omega\epsilon_o}\int_S \left[k^2\bar{J}_s - k^2\left(\bar{J}_s\;\cdot\;\bar{r}_1\right)\bar{r}_1 + k\,\omega\,\epsilon_o\bar{M}_s\times\bar{r}_1\right]\frac{\exp\,[-jkr]}{r}\,dS \tag{204}$$

$$\bar{H} = \frac{-j}{4\pi\omega\mu_o}\int_S \left[k^2\bar{M}_s - k^2\left(\bar{M}_s\;\cdot\;\bar{r}_1\right)\bar{r}_1 - k\,\omega\,\mu_o\bar{J}_s\times\bar{r}_1\right]\frac{\exp\,[-jkr]}{r}\,dS \tag{205}$$

If $\bar{J}_s$ and $\bar{M}_s$ are known, then the fields in regions for which $kr \gg 1$ can be calculated exactly from equations (204) and (205). Ordinarily $\bar{J}_s$ and $\bar{M}_s$ are not known and must be approximated. An approximation can be used when the radius of curvature of the surface is everywhere much greater than λ, the wavelength. In this case the surface and fields are assumed to be locally plane. Plane wave reflection coefficients are then used to describe the fields at the surface. With the plane wave approximations, the following expressions result for the surface currents

$$\bar{J}_s = \left[\frac{\left(\hat{n}\cdot\bar{E}^i\right)\bar{k} - \left(\hat{n}\cdot\bar{k}\right)\bar{E}^i}{k\eta_0}\right]\left(1 - R^+\right) + \frac{\left(\hat{n}\times\bar{k}\right)\left(\bar{k}\;\cdot\;\hat{n}\right)\left[\left(\bar{k}\times\hat{n}\right)\;\cdot\;\bar{E}^i\right]}{k\eta_0\left|\bar{k}\times\hat{n}\right|^2}\left(R^+ - R^-\right) \tag{206}$$

$$\overline{M}_s = \overline{E}^i \times \hat{n} \left(1 + R^+\right) - \frac{\left[\left(\hat{n} \cdot \overline{k}\right)\hat{n} - \overline{k}\right]\left[\left(\overline{k} \times \hat{n}\right)\ \overline{E}^i\right]}{\left|\overline{k} \times \hat{n}\right|^2}\left(R^+ - R^-\right) \tag{207}$$

where

$\hat{n}$ is a unit normal vector out of the surface

$\overline{E}^i$ is the incident electric field intensity at the surface

$\overline{k}$ is a vector of magnitude k directed along the direction of incidence of $\overline{E}^i$

R^+ is the reflection coefficient of a plane wave polarized perpendicular to the plane of incidence

R^- is the reflection coefficient of a plane wave polarized in the plane of incidence

The two reflection coefficients are given by the following equations

$$R^+ = \frac{1 - \dfrac{\eta_0}{\eta_2}\dfrac{\cos\psi_i}{\sqrt{1 - \left(k/k_2\right)^2 \sin^2\psi_i}}}{1 + \dfrac{\eta_0}{\eta_2}\dfrac{\cos\psi_i}{\sqrt{1 - \left(k/k_2\right)^2 \sin^2\psi_i}}} \tag{207a}$$

$$R^- = \frac{1 - \dfrac{\eta_0}{\eta_2}\dfrac{\sqrt{1 - \left(k/k_2\right)^2 \sin^2\psi_i}}{\cos\psi_i}}{1 + \dfrac{\eta_0}{\eta_2}\dfrac{\sqrt{1 - \left(k/k_2\right)^2 \sin^2\psi_i}}{\cos\psi_i}} \tag{207b}$$

where ψ_i is the angle between $\hat{n}$ and $-\overline{k}$; η_0 and η_2 are, respectively, the intrinsic impedance of free space and of the planetary material; and the symbol k_2 is the propagation constant of the planetary material.

Implicit in the use of the plane wave approximations are several assumptions. It is assumed that the radius of curvature of the surface is much greater than the wavelength of incident radiation. In addition, any multiple scattering that might take place among the surface irregularities is ignored. The possibility of shadowing of portions of the surface is also

ignored. This latter condition is reasonable provided that the angle of incidence to the average surface is not near grazing and the actual surface slopes are not too large.

The planetary surface can be denoted by

$$r_p = R_0 + g(\theta, \phi) \tag{208}$$

where R_0 is the mean radius of a smooth spherical planet and $g(\theta, \phi)$ is a gaussian random process with zero mean and variance σ_g^2. Then the probability density function of g is

$$p_g(g) = \frac{1}{\sqrt{2\pi}\,\sigma_g} \exp\left(-g^2/2\,\sigma_g^2\right) \tag{209}$$

It is also assumed that g has a normalized autocorrelation function ρ given by

$$\rho = \exp\left(-\ell^2/L^2\right) \tag{210}$$

where ℓ is the distance between two points on the planet surface as measured on the mean surface and L is the correlation distance. The distance ℓ is given by

$$\ell = R_0 \cos^{-1}\left[\cos\theta\cos\theta' + \sin\theta\,\sin\theta'\cos\left(\phi'-\phi\right)\right] \tag{211}$$

where θ, ϕ and θ', ϕ' are respectively the coordinates of the two points on the surface.

In terms of the spherical coordinate system shown in figure 19, the vectors $\hat{n}$ and $\bar{k}$ on the planetary surface are given by

$$\begin{aligned}\hat{n} = \frac{1}{R}\Bigg\{ & \bar{u}_x \left[\left(R_0 + g\right)\sin\theta\cos\phi - \frac{\partial g}{\partial\theta}\cos\theta\cos\phi + \frac{\partial g}{\partial\phi}\frac{\sin\phi}{\sin\theta}\right] \\ & + \bar{u}_y \left[\left(R_0 + g\right)\sin\theta\sin\phi - \frac{\partial g}{\partial\phi}\cos\theta\sin\phi - \frac{\partial g}{\partial\phi}\frac{\cos\phi}{\sin\theta}\right] \\ & + \bar{u}_z \left[\left(R_0 + g\right)\cos\theta + \frac{\partial g}{\partial\theta}\sin\theta\right]\Bigg\}\end{aligned} \tag{212}$$

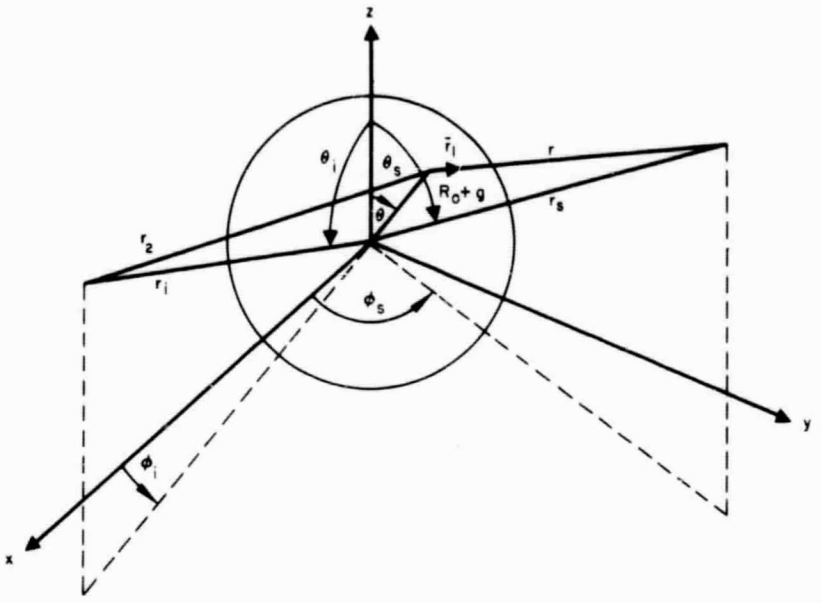

Figure 19. Coordinates for scattering problem.

$$\bar{k} = \frac{k}{r_2}\left\{\bar{u}_x\left[\left(R_0+g\right)\sin\theta\cos\phi - r_i\sin\theta_i\cos\phi_i\right]\right.$$
$$+\bar{u}_y\left[\left(R_0+g\right)\sin\theta\sin\phi - r_i\sin\theta_i\sin\phi_i\right] \qquad (213)$$
$$\left.+\bar{u}_z\left[\left(R_0+g\right)\cos\theta - r_i\cos\theta_i\right]\right\}$$

where

$$R \equiv \sqrt{\left(R_0+g\right)^2 + \left(\frac{\partial g}{\partial\theta}\right)^2 + \left(\frac{1}{\sin\theta}\frac{\partial g}{\partial\phi}\right)^2} \qquad (214)$$

$$r_2 \equiv \sqrt{\left(R_0+g\right)^2 + r_i^2 - 2\left(R_0+g\right)r_i\left[\sin\theta\sin\theta_i\cos(\phi-\phi_i) + \cos\theta\cos\theta_i\right]} \qquad (215)$$

In addition,

$$\cos\psi_i = \frac{\hat{n}\cdot\bar{k}}{k} = \frac{1}{Rr_2}\left\{\left(R_0+g\right)^2\right.$$
$$-r_i\left(R_0+g\right)\left[\sin\theta\sin\theta_i\cos\left(\phi_i-\phi\right) + \cos\theta\cos\theta_i\right]$$
$$+r_i\frac{\partial g}{\partial\theta}\left[\sin\theta_i\cos\theta\cos\left(\phi_i-\phi\right) - \cos\theta_i\sin\theta\right]$$
$$\left.+\frac{r_i}{\sin\theta}\frac{\partial g}{\partial\phi}\sin\theta_i\sin\left(\phi_i-\phi\right)\right\} \qquad (216)$$

The incident electric field is expressed in terms of its components in Cartesian coordinates as

$$\bar{E}^i = \bar{u}_x E_x + \bar{u}_y E_y + \bar{u}_z E_z \tag{217}$$

For the case of interest here it is assumed that the source and receiver move about the planetary surface in coplanar orbits. Without loss of generality, these orbits are assumed to lie in the plane $\theta_i = \theta_s = \frac{\pi}{2}$. In that case

$$r_2 = \sqrt{(R_0 + g)^2 + r_i^2 - 2(R_0 + g) r_i \sin\theta \cos(\phi - \phi_i)} \tag{218}$$

$$\begin{aligned} \bar{k} = \frac{k}{r_2} \Big\{ & \bar{u}_x \left[(R_0 + g) \sin\theta \cos\phi - r_i \cos\phi_i \right] \\ & + \bar{u}_y \left[(R_0 + g) \sin\theta \sin\phi - r_i \sin\phi_i \right] \\ & + \bar{u}_z (R_0 + g) \cos\theta \Big\} \end{aligned} \tag{219}$$

An arbitarily polarized incident wave may be expressed as a sum of two waves, one polarized perpendicular to the plane of incidence and one polarized in the plane of incidence. Each polarization can be treated separately. The case to be treated here is that for which the incident electric field is z polarized at $\theta = \pi/2$. If the source is sufficiently far from the planetary surface, the incident field will remain essentially z directed over the illuminated planetary surface. Then the incident field is given by

$$\bar{E}^i = \bar{u}_z E^i \tag{220}$$

In addition, over the scattering surface the vector $\bar{k}$ will lie nearly parallel to the x - y plane so that

$$\bar{k} \approx -k \left| \bar{u}_x \cos\phi_i + \bar{u}_y \sin\phi_i \right| \tag{221}$$

When these specializations and approximations are applied to the expressions for the surface currents that appear in the integrals for the scattered field, a tedious but straightforward procedure results in the following expressions.

$$J_{sx} = \frac{\left[(R_0+g)\cos\theta + \frac{\partial g}{\partial\theta}\sin\theta\right] E^i \left(-\cos\phi_i\right)}{\sqrt{(R_0+g)^2 + \left(\frac{\partial g}{\partial\theta}\right)^2 + \left(\frac{1}{\sin\theta}\frac{\partial g}{\partial\phi}\right)^2}\,\eta_0} \left(1-R^+\right)$$

(222a)

$$- \left(R^+-R^-\right) \frac{\sin\phi_i \left[\left(R_0+g\right)\cos\theta + \frac{\partial g}{\partial\theta}\sin\theta\right] \left[\left(R_0+g\right)\sin\theta\cos\left(\phi_i-\phi\right) - \frac{\partial g}{\partial\theta}\cos\theta\cos\left(\phi_i-\phi\right) - \frac{\partial g}{\partial\phi}\frac{\sin\left(\phi_i-\phi\right)}{\sin\theta}\right] \left[\left(\left(R_0+g\right)\sin\theta - \frac{\partial g}{\partial\theta}\cos\theta\right)\sin\left(\phi_i-\phi\right) + \frac{\partial g}{\partial\phi}\frac{\cos\left(\phi_i-\phi\right)}{\sin\theta}\right] E^i}{\eta_0\sqrt{(R_0+g)^2 + \left(\frac{\partial g}{\partial\theta}\right)^2 + \left(\frac{1}{\sin\theta}\frac{\partial g}{\partial\phi}\right)^2} \left[\left[(R_0+g)\cos\theta + \frac{\partial g}{\partial\theta}\sin\theta\right]^2 + \left[\left((R_0+g)\sin\theta\frac{\partial g}{\partial\theta}\cos\theta\right)\sin\left(\phi_i-\phi\right) + \frac{\partial g}{\partial\phi}\frac{\cos\left(\phi_i-\phi\right)}{\sin\theta}\right]^2\right]}$$

$$J_{sy} = \frac{-\left[\left(R_0+g\right)\cos\theta + \frac{\partial g}{\partial\theta}\sin\theta\right] E^i \sin\phi_i}{\sqrt{\left(R_0+g\right)^2 + \frac{\partial g}{\partial\theta}^2 + \frac{1}{\sin\theta}\frac{\partial g}{\partial\phi}^2}\,\eta_0} \left(1-R^+\right)$$

$$+ \left(R^+-R^-\right) \frac{\cos\phi_i \left[\left(R_0+g\right)\cos\theta + \frac{\partial g}{\partial\theta}\sin\theta\right] \left[\left(R_0+g\right)\sin\theta\cos\left(\phi_i-\phi\right) - \frac{\partial g}{\partial\theta}\cos\theta\cos\left(\phi_i-\phi\right) - \frac{\partial g}{\partial\phi}\frac{\sin\left(\phi_i-\phi\right)}{\sin\theta}\right] \left[\left(\left(R_0+g\right)\sin\theta - \frac{\partial g}{\partial\theta}\cos\theta\right)\sin\left(\phi_i-\phi\right) + \frac{\partial g}{\partial\phi}\frac{\cos\left(\phi_i-\phi\right)}{\sin\theta}\right] E^i}{\eta_0\sqrt{\left(R_0+g\right)^2 + \left(\frac{\partial g}{\partial\theta}\right)^2 + \left(\frac{1}{\sin\theta}\frac{\partial g}{\partial\phi}\right)^2} \left[\left[\left(R_0+g\right)\cos\theta + \frac{\partial g}{\partial\theta}\sin\theta\right]^2 + \left[\left(\left(R_0+g\right)\sin\theta - \frac{\partial g}{\partial\theta}\cos\theta\right)\sin\left(\phi_i-\phi\right) + \frac{\partial g}{\partial\phi}\frac{\cos\left(\phi_i-\phi\right)}{\sin\theta}\right]^2\right]}$$

(222b)

$$J_{sz} = \frac{-\left[\left(R_0+g\right)\sin\theta\cos\left(\phi_i-\phi\right) - \frac{\partial g}{\partial\theta}\cos\theta\cos\left(\phi_i-\phi\right) - \frac{\partial g}{\partial\phi}\frac{\sin\left(\phi_i-\phi\right)}{\sin\theta}\right] E^i}{\sqrt{\left(R_0+g\right)^2 + \left(\frac{\partial g}{\partial\theta}\right)^2 + \left(\frac{1}{\sin\theta}\frac{\partial g}{\partial\phi}\right)^2}\,\eta_0} \left(1-R^+\right)$$

$$+ \left(R^+-R^-\right) \frac{\left[\left(\left(R_0+g\right)\sin\theta - \frac{\partial g}{\partial\theta}\cos\theta\right)\sin\left(\phi_i-\phi\right) + \frac{\partial g}{\partial\phi}\frac{\cos\left(\phi_i-\phi\right)}{\sin\theta}\right]^2 \left[\left(R_0+g\right)\sin\theta\cos\left(\phi_i-\phi\right) - \frac{\partial g}{\partial\theta}\cos\theta\cos\left(\phi_i-\phi\right) - \frac{\partial g}{\partial\phi}\frac{\sin\left(\phi_i-\phi\right)}{\sin\theta}\right] E^i}{\eta_0\sqrt{\left(R_0+g\right)^2 + \left(\frac{\partial g}{\partial\theta}\right)^2 + \left(\frac{1}{\sin\theta}\frac{\partial g}{\partial\phi}\right)^2} \left[\left[\left(R_0+g\right)\cos\theta + \frac{\partial g}{\partial\theta}\sin\theta\right]^2 + \left[\left(\left(R_0+g\right)\sin\theta - \frac{\partial g}{\partial\theta}\cos\theta\right)\sin\left(\phi_i-\phi\right) + \frac{\partial g}{\partial\phi}\frac{\cos\left(\phi_i-\phi\right)}{\sin\theta}\right]^2\right]}$$

(222c)

$$M_{sx} = \frac{-\left[(R_0+g)\sin\theta\sin\phi - \frac{\partial g}{\partial\theta}\cos\theta\sin\phi - \frac{\partial g}{\partial\phi}\frac{\cos\phi}{\sin\theta}\right]E^i}{\sqrt{(R_0+g)^2 + \left(\frac{\partial g}{\partial\theta}\right)^2 + \left(\frac{1}{\sin\theta}\frac{\partial g}{\partial\phi}\right)^2}}\ (1-R^+)$$

$$+ (R^+-R^-)\left\{\frac{\left[\left[(R_0+g)\sin\theta\cos(\phi_i-\phi) - \frac{\partial g}{\partial\theta}\cos\theta\cos(\phi_i-\phi) - \frac{\partial g}{\partial\phi}\frac{\sin(\phi_i-\phi)}{\sin\theta}\right]\left[(R_0+g)\sin\theta\cos\phi - \frac{\partial g}{\partial\theta}\cos\theta\cos\phi + \frac{\partial g}{\partial\phi}\frac{\sin\phi}{\sin\theta}\right] - \cos\phi_i\left[(R_0+g)^2 + \left(\frac{\partial g}{\partial\theta}\right)^2 + \left(\frac{1}{\sin\theta}\frac{\partial g}{\partial\phi}\right)^2\right]\right]}{\sqrt{(R_0+g)^2 + \left(\frac{\partial g}{\partial\theta}\right)^2 + \left(\frac{1}{\sin\theta}\frac{\partial g}{\partial\phi}\right)^2}\left[\left[(R_0+g)\cos\theta + \frac{\partial g}{\partial\theta}\sin\theta\right]^2 + \left[(R_0+g)\sin\theta\sin(\phi_i-\phi) - \frac{\partial g}{\partial\theta}\cos\theta\sin(\phi_i-\phi) + \frac{\partial g}{\partial\phi}\frac{\cos(\phi_i-\phi)}{\sin\theta}\right]^2\right]}\right.$$

$$\left.\cdot\ \left[(R_0+g)\sin\theta\sin(\phi_i-\phi) - \frac{\partial g}{\partial\theta}\cos\theta\sin(\phi_i-\phi) + \frac{\partial g}{\partial\phi}\frac{\cos(\phi_i-\phi)}{\sin\theta}\right]E^i\right\} \qquad (222d)$$

$$M_{sy} = \frac{\left[(R_0+g)\sin\theta\cos\phi - \frac{\partial g}{\partial\theta}\cos\theta\cos\phi + \frac{\partial g}{\partial\phi}\frac{\sin\phi}{\sin\theta}\right]E^i}{\sqrt{(R_0+g)^2 + \left(\frac{\partial g}{\partial\theta}\right)^2 + \left(\frac{1}{\sin\theta}\frac{\partial g}{\partial\phi}\right)^2}}\ (1+R^+)$$

$$+ (R^+-R^-)\left\{\frac{\left[\left[(R_0+g)\sin\theta\cos(\phi_i-\phi) - \frac{\partial g}{\partial\theta}\cos\theta\cos(\phi_i-\phi) - \frac{\partial g}{\partial\phi}\frac{\sin(\phi_i-\phi)}{\sin\theta}\right]\left[(R_0+g)\sin\theta\sin\phi - \frac{\partial g}{\partial\theta}\cos\theta\sin\phi - \frac{\partial g}{\partial\phi}\frac{\cos\phi}{\sin\theta}\right] - \sin\phi_i\left[(R_0+g)^2 + \left(\frac{\partial g}{\partial\theta}\right)^2 + \left(\frac{1}{\sin}\frac{\partial g}{\partial\phi}\right)^2\right]\right]}{\sqrt{(R_0+g)^2 + \left(\frac{\partial g}{\partial\theta}\right)^2 + \left(\frac{1}{\sin\theta}\frac{\partial g}{\partial\phi}\right)^2}\left[\left[(R_0+g)\cos\theta + \frac{\partial g}{\partial\theta}\sin\theta\right]^2 + \left[(R_0+g)\sin\theta\sin(\phi_i-\phi) - \frac{\partial g}{\partial\theta}\cos\theta\sin(\phi_i-\phi) + \frac{\partial g}{\partial\phi}\frac{\cos(\phi_i-\phi)}{\sin\theta}\right]^2\right]}\right.$$

$$\left.\left[(R_0+g)\sin\theta\sin(\phi_i-\phi) - \frac{\partial g}{\partial\theta}\cos\theta\sin(\phi_i-\phi) + \frac{\partial g}{\partial\phi}\frac{\cos(\phi_i-\phi)}{\sin\theta}\right]E^i\right\} \qquad (222e)$$

$$M_{sz} = \frac{(R^+-R^-)\left[(R_0+g)\sin\theta\cos(\phi_i-\phi) - \frac{\partial g}{\partial\theta}\cos\theta\cos(\phi_i-\phi) - \frac{\partial g}{\partial\phi}\frac{\sin(\phi_i-\phi)}{\sin\theta}\right]\left[(R_0+g)\cos\theta + \frac{\partial g}{\partial\theta}\sin\theta\right]\left[(R_0+g)\sin\theta\sin(\phi_i-\phi) - \frac{\partial g}{\partial\theta}\cos\theta\sin(\phi_i-\phi) + \frac{\partial g}{\partial\phi}\frac{\cos(\phi_i-\phi)}{\sin\theta}\right]E^i}{\sqrt{(R_0+g)^2 + \left(\frac{\partial g}{\partial\theta}\right)^2 + \left(\frac{1}{\sin\theta}\frac{\partial g}{\partial\phi}\right)^2}\left[\left[(R_0+g)\cos\theta + \frac{\partial g}{\partial\theta}\sin\theta\right]^2 + \left[(R_0+g)\sin\theta\sin(\phi_i-\phi) - \frac{\partial g}{\partial\theta}\cos\theta\sin(\phi_i-\phi) + \frac{\partial g}{\partial\phi}\frac{\cos(\phi_i-\phi)}{\sin\theta}\right]^2\right]} \qquad (222f)$$

The unit vector $\bar{r}_1$ that appears in the integrals is given by

$$\bar{r}_1 = \bar{u}_x\, r_{1x} + \bar{u}_y\, r_{1y} + \bar{u}_z\, r_{1z} \tag{223}$$

where

$$r_{1x} = \frac{1}{r}\left[r_s \sin\theta_s \cos\phi_s - \left(R_0+g\right)\sin\theta\cos\phi\right] \tag{224a}$$

$$r_{1y} = \frac{1}{r}\left[r_s \sin\theta_s \sin\phi_s - \left(R_0+g\right)\sin\theta\sin\phi\right] \tag{224b}$$

$$r_{1z} = \frac{1}{r}\left[r_s \cos\theta_s - \left(R_0+g\right)\cos\theta\right] \tag{224c}$$

$$r = \sqrt{r_s^2 + \left(R_0+g\right)^2 - 2r_s\left(R_0+g\right)\left[\sin\theta_s \sin\theta\cos\left(\phi_s-\phi\right) + \cos\theta_s\cos\theta\right]}$$

The components of the scattered electric field intensity when the incident field intensity is z-directed are then given by

$$E_x = -\frac{j}{4\pi\omega\epsilon_0}\int\left[k^2 J_{sx} - k^2\left(J_{sx}r_{1x} + J_{sy}r_{1y} + J_{sz}r_{1z}\right) r_{1x} + k\omega\epsilon_0\left(M_{sy}r_{1z} - M_{sz}r_{1y}\right)\right]\frac{\exp(-jkr)}{r}\, dS \tag{225a}$$

$$E_y = -\frac{j}{4\pi\omega\epsilon_0}\int\left[k^2 J_{sy} - k^2\left(J_{sx}r_{1x} + J_{sy}r_{1y} + J_{sz}r_{1z}\right) r_{1y} + k\omega\epsilon_0\left(M_{sz}r_{1x} - M_{sx}r_{1z}\right)\right]\frac{\exp(-jkr)}{r}\, dS \tag{225b}$$

$$E_z = -\frac{j}{4\pi\omega\epsilon_0}\int\left[k^2 J_{sz} - k^2\left(J_{sx}r_{1x} + J_{sy}r_{1y} + J_{sz}r_{1z}\right) r_{1z} + k\omega\epsilon_0\left(M_{sx}r_{1y} - M_{sy}r_{1x}\right)\right]\frac{\exp(-jkr)}{r}\, dS \tag{225c}$$

The integrals are extremely complicated for arbitrary scatterer conductivity, permittivity, or permeability. One limiting case, in which the surface is perfectly conducting, results in a great simplification. Then $R^+ = R^- = -1$ so that the surface currents become

$$J_{sx} \approx \frac{-2\left[\left(R_0+g\right)\cos\theta + \frac{\partial g}{\partial \theta}\sin\theta\right]\cos\phi_i\, E^i}{\eta_0\, R} \tag{226a}$$

$$J_{sy} \approx \frac{-2\left[\left(R_0+g\right)\cos\theta + \frac{\partial g}{\partial \theta}\sin\theta\right]\sin\phi_i\, E^i}{\eta_0\, R} \tag{226b}$$

$$J_{sz} \approx \frac{-2\left[\left(R_0+g\right)\sin\theta\cos\left(\phi_i-\phi\right) - \frac{\partial g}{\partial \theta}\cos\theta\cos\left(\phi_i-\phi\right) - \frac{\partial g}{\partial \phi}\frac{\sin\left(\phi_i-\phi\right)}{\sin\theta}\right]}{\eta_0\, R}\, E^i \tag{226c}$$

$$M_{sx} = 0 \tag{226d}$$

$$M_{sy} = 0 \tag{226e}$$

$$M_{sz} = 0 \tag{226f}$$

The element of area on the surface, dS, is given by

$$dS = \left(R_0+g\right) R \sin\theta\, d\theta\, d\phi \tag{227}$$

If it is further assumed that the receiver height above the mean surface is much greater than σ_g, then the following approximations may be made;

$$r_{1x} \approx \frac{1}{r}\left(r_s \sin\theta_s \cos\phi_s - R_0 \sin\theta\cos\phi\right) \tag{228a}$$

$$r_{1y} \approx \frac{1}{r}\left(r_s \sin\theta_s \sin\phi_s - R_0 \sin\theta \sin\phi\right) \tag{228b}$$

$$r_{1z} \approx \frac{1}{r}\left(r_s \cos\theta_s - R_0 \cos\theta\right) \tag{228c}$$

$$r \approx \sqrt{r_s^2 + R_0^2 - 2r_s R_0\left(\sin\theta_s \sin\theta\cos\left(\phi_s-\phi\right) + \cos\theta_s\cos\theta\right)} \tag{228d}$$

When these expressions are inserted into the integrals for E_x, E_y, E_z, the following expressions result;

$$E_x = -\frac{j}{4\pi\omega\epsilon_0}\iint\left\{-\frac{2k^2}{\eta_0}\left[\cos\theta - \frac{1}{R_0}\frac{\partial g}{\partial\theta}\sin\theta\right]\cos\phi_i + \frac{k^2 2}{\eta_0 r^2}\left(r_s\sin\theta_s\cos\phi_s - R_0\sin\theta\cos\phi\right)\left(\left[\cos\theta + \frac{1}{R_0}\frac{\partial g}{\partial\theta}\sin\theta\right]\left\{\cos\phi_i\left[r_s\sin\theta_s\cos\phi_s - R_0\sin\theta\cos\phi\right]\right.\right.\right.$$

$$\left.\left.\left. + \sin\phi_i\left[r_s\sin\theta_s\sin\phi_s - R_0\sin\theta\sin\phi\right]\right\} - \left[\sin\theta\cos\left(\phi_i-\phi\right) - \frac{1}{R_0}\frac{\partial g}{\partial\theta}\cos\theta\cos\left(\phi_i-\phi\right) - \frac{1}{R_0\sin\theta}\frac{\partial g}{\partial\phi}\sin\left(\phi_i-\phi\right)\right]\left[r_s\cos\theta_s - R_0\cos\theta\right]\right)\right\}\frac{\exp(-jkr)}{r}E^i R_0^2\sin\theta d\theta d\phi$$

$$E_y = -\frac{j}{4\pi\omega\epsilon_0}\iint\left\{-\frac{2k^2}{\eta_0}\left[\cos\theta + \frac{1}{R_0}\frac{\partial g}{\partial\theta}\sin\theta\right]\sin\phi_i - \frac{k^2 2}{\eta_0 r^2}\left(r_s\sin\theta_s\sin\phi_s - R_0\sin\theta\sin\phi\right)\left(\left[\cos\theta + \frac{1}{R_0}\frac{\partial g}{\partial\theta}\sin\theta\right]\left\{\cos\phi_i\left[r_s\sin\theta_s\cos\phi_s - R_0\sin\theta\cos\phi\right]\right.\right.\right. \quad (229a)$$

$$\left.\left.\left. + \sin\phi_i\left[r_s\sin\theta_s\sin\phi_s - R_0\sin\theta\sin\phi\right]\right\} + \left[\sin\theta\cos\left(\phi_i-\phi\right) - \frac{1}{R_0}\frac{\partial g}{\partial\theta}\cos\theta\cos\left(\phi_i-\phi\right) - \frac{1}{R_0\sin\theta}\frac{\partial g}{\partial\phi}\sin\left(\phi_i-\phi\right)\right]\left[r_s\cos\theta_s - R_0\cos\theta\right]\right)\right\}\frac{\exp(-jkr)}{r}E^i R_0^2\sin\theta d\theta d\phi$$

$$E_z = -\frac{j}{4\pi\omega\epsilon_0}\iint\left\{-\frac{2k^2}{\eta_0}\left[\sin\theta\cos\left(\phi_i-\phi\right) - \frac{1}{R_0}\frac{\partial g}{\partial\theta}\cos\theta\cos\left(\phi_i-\phi\right) - \frac{1}{R_0\sin\theta}\frac{\partial g}{\partial\phi}\sin\left(\phi_i-\phi\right)\right] + \frac{k^2 2}{\eta_0 r^2}\left(r_s\cos\theta_s - R_0\cos\theta\right)\left(\left[\cos\theta + \frac{1}{R_0}\frac{\partial g}{\partial\theta}\sin\theta\right]\left\{\cos\phi_i\left[r_s\sin\theta_s\cos\phi_s - R_0\sin\theta\cos\phi\right]\right.\right.\right. \quad (229b)$$

$$\left.\left.\left. + \sin\phi_i\left[r_s\sin\theta_s\sin\phi_s - R_0\sin\theta\sin\phi\right]\right\} + \left[\sin\theta\cos\left(\phi_i-\phi\right) - \frac{1}{R_0}\frac{\partial g}{\partial\theta}\cos\theta\cos\left(\phi_i-\phi\right) - \frac{1}{R_0\sin\theta}\frac{\partial g}{\partial\phi}\sin\left(\phi_i-\phi\right)\right]\left[r_s\cos\theta_s - R_0\cos\theta\right]\right)\right\}\frac{\exp(-jkr)}{r}E^i P_0^2\sin\theta d\theta d\phi$$

where the integration is over the illuminated portion of the surface (229c)

If $r_s - R_0$ is sufficiently large, i. e., if the point r_s is sufficiently elevated above the surface, and if the frequency is not too great, then in the exponential terms r may be approximated by

$$r \approx R_1 - g \cos \psi_1 \tag{230}$$

where

$$R_1 \equiv \sqrt{R_0^2 + r_s^2 - 2 R_0 r_s \left[\sin\theta \sin\theta_s \cos\left(\varphi - \varphi_s\right) + \cos\theta \cos\theta_s\right]} \tag{231a}$$

$$\cos \psi_1 \equiv \frac{r_s\left[\sin\theta_s \sin\theta \cos\left(\phi - \phi_s\right) + \cos\theta\cos\theta_s\right] - R_0}{R_1} \tag{231b}$$

In the $1/r$ terms, r may be approximated by

$$\frac{1}{r} \approx \frac{1}{R_1} \tag{232}$$

In a similar manner, r_2 in the exponential terms may be approximated by

$$R_2 \approx R_2 - g \cos \psi_2 \tag{233}$$

where

$$R_2 \equiv \sqrt{r_i^2 + R_0^2 - 2 r_i R_0 \left[\sin\theta_i \sin\theta \cos\left(\phi_i - \phi\right) + \cos\theta_i \cos\theta\right]} \tag{234a}$$

$$\cos \psi_2 \equiv \frac{r_i\left[\sin\theta_i \sin\theta \cos\left(\phi_i - \phi\right) + \cos\theta_i\cos\theta\right] - R_0}{R_2} \tag{234b}$$

With these last approximations, the incident field may be written in the form

$$E^i = \frac{E^0\left(r_i - R_0\right)}{R_2} \exp\left(-jkR_2\right) \exp\left(jkg \cos\psi_2\right) \tag{235}$$

where E^0 is the value of the incident field at a point on the mean surface directly below the source. The term $\frac{E^i}{r} \exp(-jkr)$ is now given by

$$\frac{E^i}{r} \exp(-jkr) \approx \frac{E^0\left(r_i - R_0\right)}{R_1 R_2} \exp\left[-jk\left(R_1 + R_2\right)\right] \exp\left[jkg\left(\cos\psi_1 + \cos\psi_2\right)\right] \tag{236}$$

The terms in the integrals that include the derivatives of g can be replaced in a manner similar to that used by Staras[31] so that they appear as derivatives of the exponential term, $(\exp\ jkg[\cos\psi_1 + \cos\psi_2])$. This artifice eliminates the need for the joint probability density function of g and its derivatives when the autocorrelation and cross-correlation functions of the scattered field components are being evaluated. Only the joint probability density function of the values of g at two separate points on the surface is required. The terms containing derivatives of g can be rewritten as follows.

$$\frac{1}{R_0}\frac{\partial g}{\partial\theta}\exp\left(jk[\cos\psi_1+\cos\psi_2]\right)=\frac{1}{R_0[\cos\psi_1+\cos\psi_2]}\left[g\left(\sin\psi_1\frac{\partial\psi_1}{\partial\theta}+\sin\psi_2\frac{\partial\psi_2}{\partial\theta}\right)+\frac{1}{jk}\frac{\partial}{\partial\theta}\right]\exp\left(jkg[\cos\psi_1+\cos\psi_2]\right) \tag{237a}$$

$$\frac{1}{R_0\sin\theta}\frac{\partial g}{\partial\phi}\exp\left(jkg[\cos\psi_1+\cos\psi_2]\right)=\frac{1}{[\cos\psi_1+\cos\psi_2]R_0\sin\theta}\left[g\left(\sin\psi_1\frac{\partial\psi_1}{\partial\phi}+\sin\psi_2\frac{\partial\psi_2}{\partial\phi}\right)+\frac{1}{jk}\frac{\partial}{\partial\phi}\right]\exp\left(jkg[\cos\psi_1+\cos\psi_2]\right) \tag{237b}$$

All the components are now available to evaluate the expectations given in equation (193).

The computation of the expectations in equation (193) results in terms of the form (Appendix I).

$$E\left[\exp\left(jk[ga-g'a']\right)\right]=\exp\left(-\frac{1}{2}k^2\sigma_g^2\left[a^2+a'^2-2aa'\rho\right]\right) \tag{238a}$$

$$E\left[g\exp\left(jk[ga-g'a']\right)\right]=jk\sigma_g^2\left(a-a'\rho\right)\exp\left(-\frac{1}{2}k^2\sigma_g^2\left[a^2+a'^2-2aa'\rho\right]\right) \tag{238b}$$

$$E\left[g'\exp\left(jk[ga-g'a']\right)\right]=-jk\sigma_g^2\left(a'-a\rho\right)\exp\left(-\frac{1}{2}k^2\sigma_g^2\left[a^2+a'^2-2aa'\rho\right]\right) \tag{238c}$$

$$E\left[g\,g'\exp\left(jk\left[ga-g'\,a'\right]\right)\right] = \sigma_g^2\left[\rho - k^2\sigma_g^2\left(\left[a'^2 + a^2 - a\,a'\right]\rho - a\,a'\right)\right]$$
$$\exp\left(-\frac{1}{2}k^2\sigma_g^2\left[a^2 + a'^2 - 2\,a\,a'\,\rho\right]\right) \qquad (238d)$$

where

$$a \equiv \cos\psi_1 + \cos\psi_2$$

$$a' \equiv \cos\psi'_1 + \cos\psi'_2$$

The primes denote the values of the various quantities at θ, ϕ, θ_{i2}, ϕ_{i2}, θ_{s2}, ϕ_{s2} while the absence of a prime denotes their values at θ, ϕ, θ_{i1}, ϕ_{i1}, θ_{s1}, ϕ_{s1}.

If $k^2\sigma_g^2$ is large, then the exponential term is very small except when $a \approx a'$ and $\rho \approx 1$. This condition corresponds to

$$\theta \approx \theta' \qquad (239a)$$

$$\phi \approx \phi' \qquad (239b)$$

$$\theta_{s1} \approx \theta_{s2} \qquad (239c)$$

$$\phi_{s1} \approx \phi_{s2} \qquad (239d)$$

$$\theta_{i1} \approx \theta_{i2} \qquad (239e)$$

$$\phi_{i1} \approx \phi_{i2} \qquad (239f)$$

When these expectations are substituted in equation (192) and integrated over θ, ϕ, θ', ϕ', they result in the desired correlation functions from which the spectrum can be computed. The major variations in the integrands will occur in the exponential terms. All other terms remain nearly constant over the ranges of integration in which the exponentials are significant. Therefore, the integrals of equation (192) will contain terms of the form

$$\exp\left(-\frac{1}{2}k^2\sigma_g^2\left[a^2+a'^2-2aa'\rho\right]\right)\ \exp\left(-jk\left[R_1 + R_2 - R'_1 - R'_2\right]\right) \qquad (240)$$

To perform the integration over θ' and ϕ', the terms a', R_1', and R_2' are expanded in power series about their values at θ, ϕ as follows.

$$a' = a'_0 + a'_\theta \Delta\theta + a'_\phi \Delta\phi + \frac{1}{2} a'_{\theta\theta} (\Delta\theta)^2 + \frac{1}{2} a'_{\phi\phi} (\Delta\phi)^2 + a'_{\theta\phi}\Delta\theta\Delta\phi + \ldots \tag{241a}$$

$$\begin{aligned} -R'_1 - R'_2 = &-\left(R'_{10} + R'_{20}\right) - \left(R'_1 + R'_2\right)_\theta \Delta\theta - \left(R'_1 + R'_2\right)_\phi \Delta\phi \\ &- \frac{1}{2}\left(R'_1 + R'_2\right)_{\theta\theta} (\Delta\theta)^2 - \frac{1}{2}\left(R'_1 + R'_2\right)_{\phi\phi} (\Delta\phi)^2 \\ &- \left(R'_1 + R'_2\right)_{\theta\phi} \Delta\theta\Delta\phi + \ldots \end{aligned} \tag{241b}$$

where

$$\Delta\theta \equiv \theta' - \theta \tag{242a}$$

$$\Delta\phi \equiv \phi' - \phi \tag{242b}$$

$$a'_0 \equiv a' \Big|_{\substack{\theta'=\theta \\ \phi'=\phi}} \tag{242c}$$

$$a'_\theta \equiv \frac{\partial a'}{\partial \theta'} \Big|_{\substack{\theta'=\theta \\ \phi'=\phi}} \tag{242d}$$

etc.

In addition, the correlation coefficient for the surface is approximated by the first two terms of its series expansion in ℓ^2/L^2 and takes on the form

$$\rho \approx 1 - \frac{\ell^2}{L^2} \approx 1 - \frac{R_0^2}{L^2} \left[(\Delta\theta)^2 + \sin^2\theta \ (\Delta\phi)^2\right] \tag{243}$$

In terms of these series expansions, the exponential term takes on the following form.

$$\exp\left(-\tfrac{1}{2}k^2\sigma_g^2\left[a-a_0'\right]^2\right)\ \exp\left(-jk\left[R_1+R_2-R_{10}'-R_{20}'\right]\right)$$

$$\cdot\exp\left[\left\{-\tfrac{1}{2}k^2\sigma_g^2\left[2aa_\theta'\frac{R_0^2}{L^2}+\left(a_\theta'\right)^2-\left(a-a_0'\right)a_{\theta\theta}'\right]+j\tfrac{1}{2}k\left(R_1'+R_2'\right)_{\theta\theta}\right\}(\Delta\theta)^2+\left\{-\tfrac{1}{2}k^2\sigma_g^2\left[2aa_0'\frac{R_0^2}{L^2}\sin^2\theta+\left(a_\phi'\right)^2-\left(a-a_0'\right)a_{\phi\phi}'\right]+j\tfrac{1}{2}k\left(R_1'+R_2'\right)_{\phi\phi}\right\}(\Delta\phi)^2\right.\quad(244)$$

$$+\left\{-\tfrac{1}{2}k^2\sigma_g^2\left[-2\left(a-a_0'\right)a_\theta'+2\left(a_\theta'a_\phi'-\left(a-a_0'\right)a_{\theta\phi}'\right)(\Delta\phi)\right]+jk\left[\left(R_1'+R_2'\right)_\theta+\left(R_1'+R_2'\right)_{\theta\phi}(\Delta\phi)\right]\right\}(\Delta\theta)$$

$$\left.+\left\{-\tfrac{1}{2}k^2\sigma_g^2\left[-2\left(a-a_0'\right)a_\phi'\right]+jk\left(R_1'+R_2'\right)_\phi\right\}\Delta\phi\right]$$

$$a=\frac{r_{s1}\sin\theta\cos\left(\phi_{s1}-\phi\right)-R_0}{\sqrt{R_0^2+r_{s1}^2-2R_0r_{s1}\sin\theta\cos\left(\phi_{s1}-\phi\right)}}+\frac{r_{i1}\sin\theta\cos\left(\phi_{i1}-\phi\right)-R_0}{\sqrt{R_0^2+r_{i1}^2-2R_0r_{i1}\sin\theta\cos\left(\phi_{i1}-\phi\right)}}\quad(245a)$$

$$a_0'=\frac{r_{s2}\sin\theta\cos\left(\phi_{s2}-\phi\right)-R_0}{\sqrt{R_0^2+r_{s2}^2-2R_0r_{s2}\sin\theta\cos\left(\phi_{s2}-\phi\right)}}+\frac{r_{i2}\sin\theta\cos\left(\phi_{i2}-\phi\right)-R_0}{\sqrt{R_0^2+r_{i2}^2-2R_0r_{i2}\sin\theta\cos\left(\phi_{i2}-\phi\right)}}\quad(245b)$$

$$R_1=\sqrt{R_0^2+r_{s1}^2-2R_0r_{s1}\sin\theta\cos\left(\phi_{s1}-\phi\right)}\quad(245c)$$

$$R_2=\sqrt{R_0^2+r_{i1}^2-2R_0r_{i1}\sin\theta\cos\left(\phi_{i1}-\phi\right)}\quad(245d)$$

$$R_{10}'=\sqrt{R_0^2+r_{s2}^2-2R_0r_{s2}\sin\theta\cos\left(\phi_{s2}-\phi\right)}\quad(245e)$$

$$R_{20}'=\sqrt{R_0^2+r_{i2}^2-2R_0r_{i2}\sin\theta\cos\left(\phi_{i2}-\phi\right)}\quad(245f)$$

$$\left(R_1'+R_2'\right)_\theta=-\left[\frac{R_0r_{s2}\cos\theta\cos\left(\phi_{s2}-\phi\right)}{R_{10}'}+\frac{R_0r_{i2}\cos\theta\cos\left(\phi_{i2}-\phi\right)}{R_{20}'}\right]\quad(245g)$$

$$\left(R_1'+R_2'\right)_\phi=-\left[\frac{R_0r_{s2}\sin\theta\sin\left(\phi_{s2}-\phi\right)}{R_{10}'}+\frac{R_0r_{i2}\sin\theta\sin\left(\phi_{i2}-\phi\right)}{R_{20}'}\right]\quad(245h)$$

$$(R_1' + R_2')_{\theta\theta} = \left[\frac{(R_{10}')^2 \sin\theta - R_0 r_{s2}\cos^2\theta\cos(\phi_{s2}-\phi)}{(R_{10}')^3}\right] R_0 r_{s2}\cos(\phi_{s2}-\phi) \tag{245i}$$

$$+ \left[\frac{(R_{20}')^2 \sin\theta - R_0 r_{i2}\cos^2\theta\cos(\phi_{i2}-\phi)}{(R_{20}')^3}\right] R_0 r_{i2}\cos(\phi_{i2}-\phi)$$

$$(R_1' + R_2')_{\phi\phi} = \left[\frac{(R_{10}')^2\cos(\phi_{s2}-\phi) - R_0 r_{s2}\sin\theta\sin^2(\phi_{s2}-\phi)}{(R_{10}')^3}\right] R_0 r_{s2}\sin\theta \tag{245j}$$

$$+ \left[\frac{(R_{20}')^2\cos(\phi_{i2}-\phi) - R_0 r_{i2}\sin\theta\sin^2(\phi_{i2}-\phi)}{(R_{20}')^3}\right] R_0 r_{i2}\sin\theta$$

$$(R_1' + R_2')_{\theta\phi} = -\left[\frac{(R_{10}')^2 + R_0 r_{s2}\sin\theta\cos(\phi_{s2}-\phi)}{(R_{10}')^3}\right]\cos\theta\sin(\phi_{s2}-\phi) R_0 r_{s2} \tag{245k}$$

$$\left[\frac{(R_{20}')^2 + R_0 r_{s2}\sin\theta\cos(\phi_{i2}-\phi)}{(R_{20}')^3}\right]\cos\theta\sin(\phi_{i2}-\phi) R_0 r_{i2}$$

$$a_\theta' = \frac{\left[(R_{10}')^2 + R_0\left[r_{s2}\sin\theta\cos(\phi_{s2}-\phi) - R_0\right]\right] r_{s2}\cos\theta\cos(\phi_{s2}-\phi)}{(R_{10}')^3} + \frac{\left[(R_{20}')^2 + R_0\left[r_{i2}\sin\theta\cos(\phi_{i2}-\phi) - R_0\right]\right] r_{i2}\cos\theta\cos(\phi_{i2}-\phi)}{(R_{20}')^3} \tag{245l}$$

$$a_\phi' = \frac{\left[(R_{10}')^2 + R_0\left[r_{s2}\sin\theta\cos(\phi_{s2}-\phi) - R_0\right]\right] r_{s2}\sin\theta\sin(\phi_{s2}-\phi)}{(R_{10}')^3} + \frac{\left[(R_{20}')^2 + R_0\left[r_{i2}\sin\theta\cos(\phi_{i2}-\phi) - R_0\right]\right] r_{i2}\sin\theta\sin(\phi_{i2}-\phi)}{(R_{20}')^3} \tag{245m}$$

$$a_{\theta\theta}' = \frac{\left[(R_{10}')^2\left\{\left[R_0^2 - (R_{10}')^2\right]\sin\theta - R_0 r_{s2}\cos(\phi_{s2}-\phi)\right\} + 3R_0 r_{s2}\cos^2\theta\cos(\phi_{s2}-\phi)\left\{(R_{10}')^2 - R_0^2 + R_0 r_{s2}\sin\theta\cos(\phi_{s2}-\phi)\right\}\right] r_{s2}\cos(\phi_{s2}-\phi)}{(R_{10}')^5} \tag{245n}$$

$$+ \frac{\left[(R_{20}')^2\left\{\left[R_0^2 - (R_{20}')^2\right]\sin\theta - R_0 r_{i2}\cos(\phi_{i2}-\phi)\right\} + 3R_0 r_{i2}\cos^2\theta\cos(\phi_{i2}-\phi)\left\{(R_{20}')^2 - R_0^2 + R_0 r_{i2}\sin\theta\cos(\phi_{i2}-\phi)\right\}\right] r_{i2}\cos(\phi_{i2}-\phi)}{(R_{20}')^5}$$

$$a'_{\phi\phi} = \frac{\left[-(R'_{10})^2\left\{\left[(R'_{10})^2 - R_0^2\right]\cos(\phi_{s2}-\phi) + R_0 r_{s2}\sin\theta\right\} + 3R_0 r_{s2}\sin\theta\sin^2(\phi_{s2}-\phi)\left\{(R'_{10})^2 - R_0^2 + R_0 r_{s2}\sin\theta\cos(\phi_{s2}-\phi)\right\}\right] r_{s2}\sin\theta}{(R'_{10})^5}$$

$$+\frac{\left[-(R'_{20})^2\left\{\left[(R'_{20})^2 - R_0^2\right]\cos(\phi_{i2}-\phi) + R_0 r_{i2}\sin\theta\right\} + 3R_0 r_{i2}\sin\theta\sin^2(\phi_{i2}-\phi)\left\{(R'_{20})^2 - R_0^2 + R_0 r_{i2}\sin\theta\cos(\phi_{i2}-\phi)\right\}\right] r_{i2}\sin\theta}{(R'_{20})^5} \tag{245o}$$

At this point it is desirable to examine the relative magnitudes of the various terms to see what additional simplifications can be made before the integration is performed. The examination was performed for the following assumed values of parameters.

frequency = 6 GHz

σ = 0.01 mile

L = 20σ = 0.2 mile

R_0 = 2100 miles

It was also assumed that angles of incidence and reflection are less than 60° to the normal of the average surface. Under these assumptions the magnitude of the last exponential term is controlled by terms containing R_0^2/L^2 so that the magnitude is less than 0.001 within a region given by

$$(\Delta\theta)^2 + \sin^2\theta\,(\Delta\phi)^2 < 6.1 \times 10^{-14}$$

thus, $\Delta\theta$ and $\sin\theta\Delta\phi$ lie inside a circle of radius 2.47×10^{-7} radian. If the magnitudes of other terms are examined for $\Delta\theta$ and $\Delta\phi$ within the prescribed region and for $r_i \sim 12,000$ meter, $r_s \sim 2110$ miles, and for angles of incidence and reflection near 45°, it is found that $k(R'_1 + R'_2)_{\theta\theta}(\Delta\theta)^2$ and $k(R'_1 + R'_2)_{\phi\phi}(\Delta\phi)^2$ are negligible. For r_2 greater than 2110 miles, the quadratic phase terms are even smaller so that unless r_s is very close to the surface, i.e. much less than 10 miles, they may be neglected. The cross term $k(R'_1 + R'_2)_{\theta\phi}\,\Delta\theta\Delta\phi$ is also negligible. Calculation of a'_{ϕ}, $a'_{\phi\phi}$, a'_{θ}, and $a'_{\theta\theta}$ about the specular point indicates that they are also negligible compared with the terms containing R_0^2/L^2 and may be neglected. The integral then simplifies greatly to

$$\exp\left(-\tfrac{1}{2}k^2\sigma_g^2\left[s - a_0'\right]^2\right)\exp\left(-jk\left[R_1 + R_2 - R_{10}' - R_{20}'\right]\right)$$
$$\cdot\exp\left(-\tfrac{1}{2}k^2\sigma_g^2\left[2aa_0'\frac{R_0^2}{L^2}\right]\left[(\Delta\theta)^2 + \sin^2\theta\,(\Delta\phi)^2\right] + jk\,(R_1' + R_2')_{\theta}\,\Delta\theta + jk\,(R_1' + R_2')_{\phi}\,\Delta\phi\right) \tag{246}$$

As stated previously, the other terms not contained in the exponential vary slowly over the region for which the exponentials are significant and are, therefore, considered as constants at their values for $\Delta\theta$ and $\Delta\phi = 0$ during the integration. When the integration over $\Delta\theta$ and $\Delta\phi$ for the exponential term is carried out, there results.

$$1 \sim \frac{\pi}{k^2 \sigma_w^2 a a_0 \left(\frac{R_0}{L}\right)^2 \sin\theta} \exp\left(-\frac{1}{2} k^2 \sigma_w^2 \left[a - a_0\right]^2 - \frac{L^2}{4 R_0^2 \sigma_w^2 a a_0} \left[\left(R_1' + R_2'\right)_\theta^2 + \frac{\left(R_1' + R_2'\right)_\phi^2}{\sin^2\theta}\right]\right) \qquad (247)$$

$$\cdot \exp\left(-jk\left[R_1 + R_2 - R_{10}' - R_{20}'\right]\right)$$

Performance of the remaining integrations over θ and ϕ requires some more detailed study of the exponential as a function of $\theta, \phi, \phi_{i1}, \phi_{s1}, \phi_{i2}, \phi_{s2}$. This study has not been completed, but perhaps the conditions will allow application of the methods of steepest descent to accomplish the evaluation.

Once the integrations over θ and ϕ have been carried out, the expressions that result are the various correlation functions. Unfortunately, the study of the spectrum has not been completed during this report period. It would be of interest to complete the work since it would allow a comparison between the scalar treatment of scattering by a rough planar surface with the results of the present vector treatment of scattering by a rough sphere.

6.0 Use of Millimeter Waves to Overcome Blackout

A critical portion of a Mars probe mission is that during which the landing capsule is entering the planetary atmosphere at high velocity. During this period the shock waves will cause the atmosphere to become ionized, as illustrated by the sketch of an entry vehicle shown in figure 20; the ionization causes severe effects on the propagation of radio waves in the vicinity of the probe. These effects result primarily from interaction of the electric field with the free electrons in the ionized sheath. The major effects on propagation that occur may be expressed in terms of a modified permittivity of the ionized medium or plasma. Since this permittivity is non-uniform and lossy, the propagation phenomena that occur are extremely complicated and very difficult to describe analytically. Their overall effect on communication systems is generally a reduction in signal level resulting from detuning of antenna elements, distortion of their radiation patterns, dephasing of elements in an array, and attenuation of signals because of dissipation within the plasma. Further, if the plasma is in the vicinity of a receiving antenna, there will be additional noise contributed by the plasma.

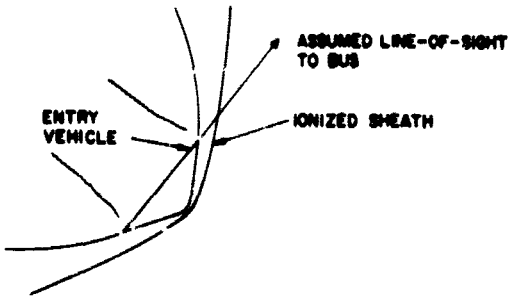

Figure 20. Illustration of plasma sheath about entry vehicle.

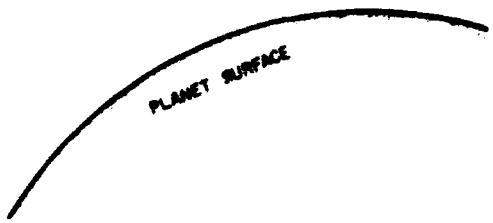

An extensive literature already exists on the subject of interaction of antennas with plasmas and the propagation of electromagnetic waves through plasmas.[35, 36, 37, 38] The antenna plasma interaction studies are usually quite specialized and it is difficult to generalize results. The propagation studies are essentially restricted to propagation through media that vary only in one dimension, an idealization that is seldom approached in practical situations. Consequently, only estimates can be made of the magnitudes of effects to be expected as far as total signal level variations are concerned and as far as increased noise levels are concerned. More detailed discussion of the plasma-electromagnetic wave interaction is contained in Appendix J.

Since all but relatively simple plasma-antenna configurations are extremely difficult to analyze, a simple model was assumed in this study. The model assumed is a plane wave propagating through a plasma that varies only in one direction. This assumption may not be as impractical as it might first appear since for electrically large arrays phased to form a beam in a particular direction, the field in the vicinity of the aperture is nearly plane except very close to the individual radiating elements.

Signal attenuation calculations were performed for four different entry profiles for a Mars VM-7 atmosphere.[28] The lander model employed in the calculations is illustrated in figure 21. The calculations were done for an antenna that looks sideways through the sheath. The entry trajectories were calculated using the Hughes Planetary Glide program which solves stepwise the equations of motion for a point mass vehicle entering the atmosphere.[39]

The entry profiles are shown in figure 22. The ratio of weight to drag, W/C_DA, has been selected as 3 for these profiles. The angle α in these figures is the entry angle relative to a horizontal line. Attenuation was computed with the aid of a machine solution of the equation

$$\frac{d^2 E}{dz^2} + k^2 \epsilon(z) E = 0 \qquad (248)$$

which assumes that the waves are normally incident on the sheath. Calculations were performed for radiation at 1, 10, and 94 GHz, and curves were plotted of attenuation versus time measured from the 500,000 foot altitude for the four entry profiles considered. A VHF or UHF frequency was not included because extremely severe blackout was expected in nearly all VHF and UHF cases and therefore the data would be of little comparative value. The attentuation curves are shown in figure 23. It is evident that even the microwave frequencies suffer severe blackout for all cases considered and that the 94 GHz suffers severe blackout for two of the profiles. However, the two remaining profiles show that no signal degradation occurs at 94 GHz. Although the calculations are not to be considered conclusive, they do indicate that millimeter-wave systems may overcome the entry blackout problem provided that they may be satisfactorily implemented from the point of view of power, weight, and complexity. These aspects are considered in the next section.

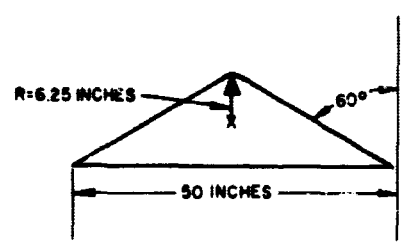

Figure 21. Assumed shape of entry vehicle.

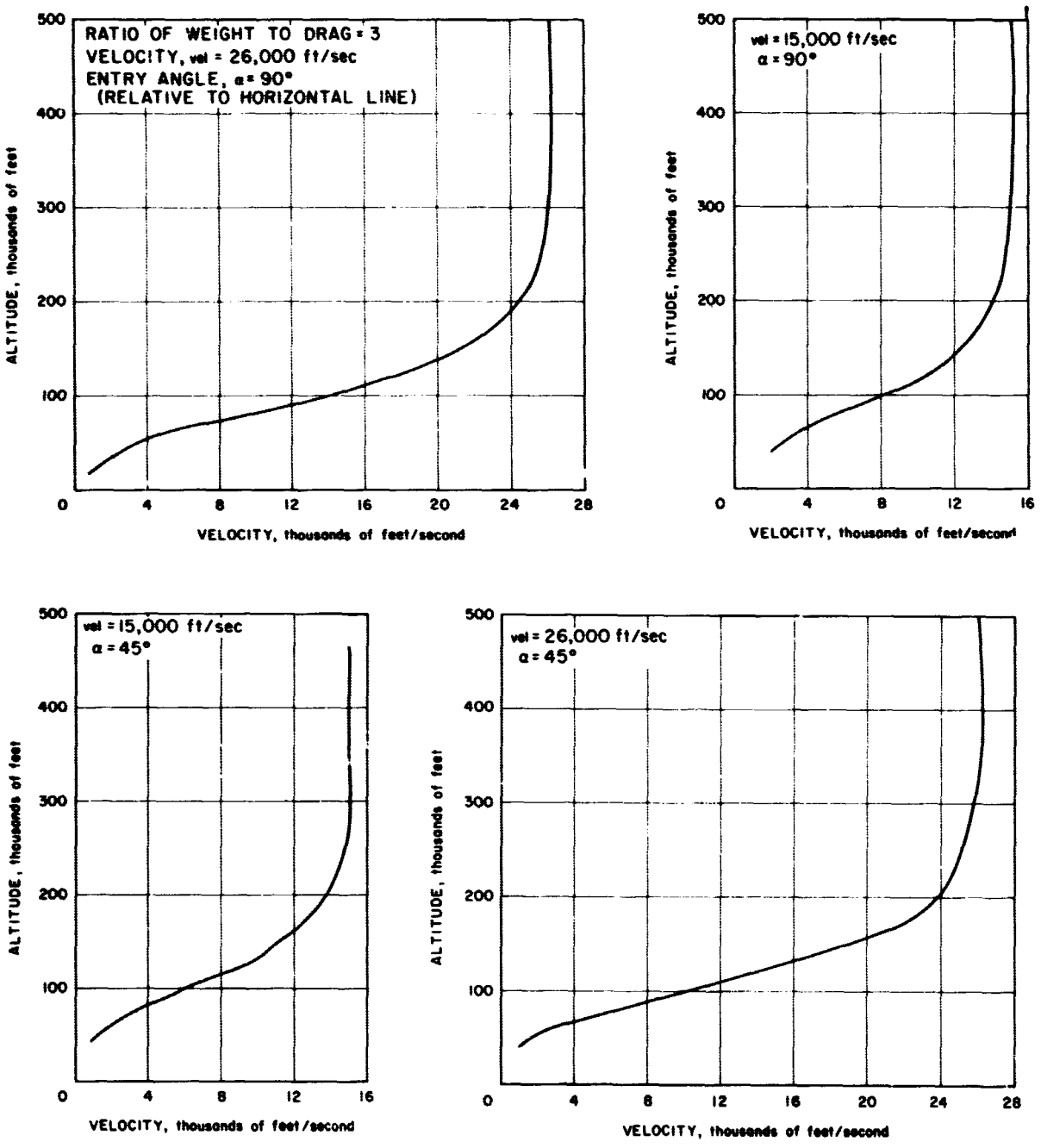

Figure 22. Typical entry profiles for non-survivable probe.

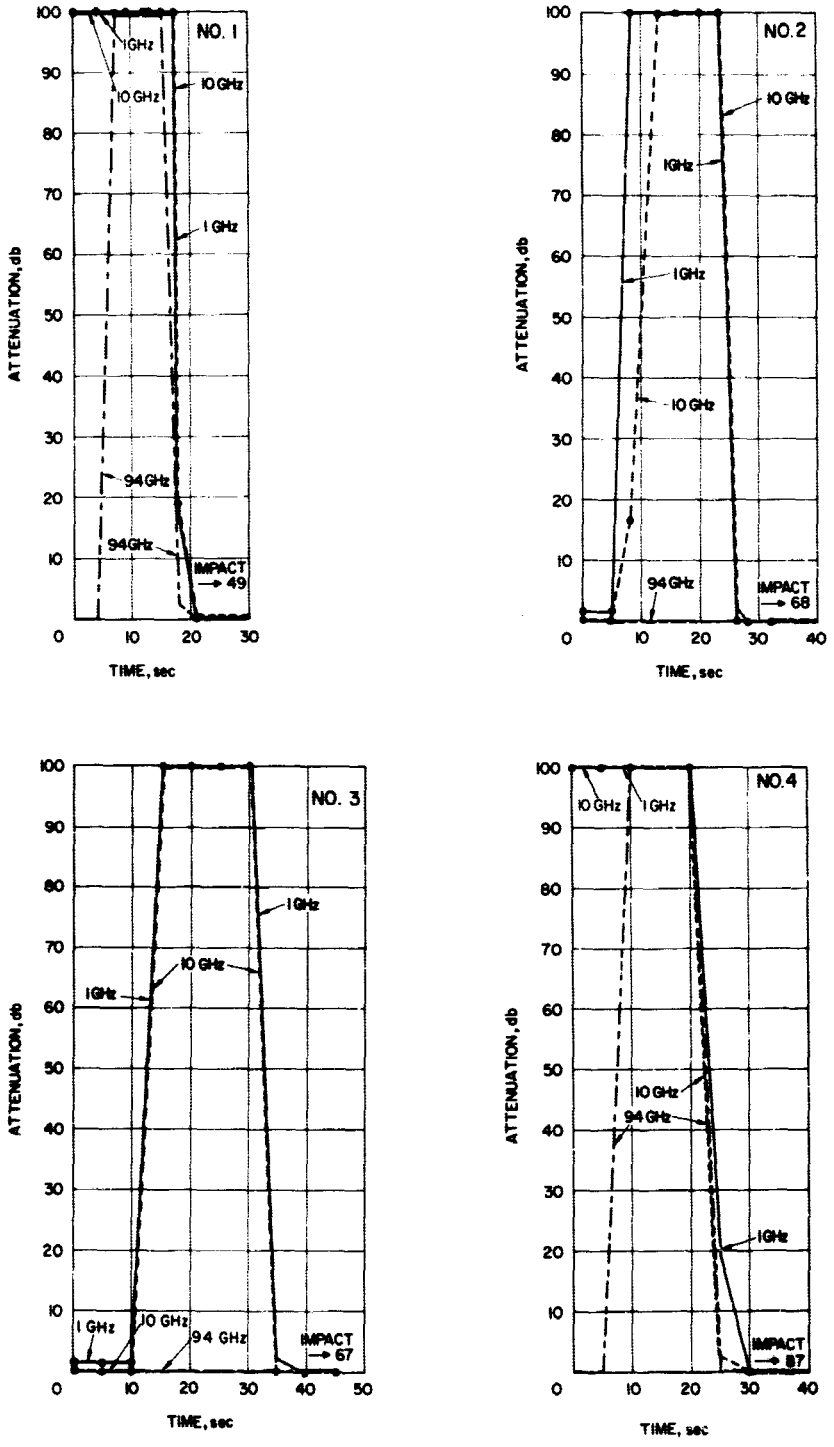

Figure 23. Attenuation versus time for entry profiles.

7.0 Evaluation of Systems at Different Frequencies

There are many evaluations of self-steering arrays that can be made. The standards of evaluation will differ depending on the quality criterion that is important in any application. For example, in the Final Report – Part I, a system that used phase inversion by mixing was considered. The assumptions made were that the total radiated power was fixed and that the number of elements was limited only by the available aperture and by the spacing required to suppress grating lobes for a specific region of coverage. The signal-to-noise ratio of the received signal was the quantity of interest. The primary power requirements and system weight were not considered.

In this section, a different criterion is applied. It is assumed that the available power is limited and the effective radiated power (ERP) and weight are estimated for several self-steering systems. Two frequencies, 8 GHz and 94 GHz, are selected; the higher frequency was selected because the calculations of blackout reported in the previous section indicate that 94 GHz may not be blacked-out during planetary entry. It is emphasized that, while the numerical values of ERP and weights are only estimated, the estimates are based on knowledge obtained from past experience in building space electronics and on experience in the development of millimeter-wave sources.

The systems considered are shown in figure 24. Each system has a single doppler tracking loop in addition to the self-steering circuitry. The estimated weights and required powers for the various circuits are presented in Table II. It is assumed that at 8 GHz 80 mw can be obtained from each high-level mixer with an input of 470 mw. It is assumed that at 94 GHz 5 mw can be obtained from each high-level mixer with an input of 50 mw. The transmitter at 8 GHz is assumed to be a solid-state source with a weight of 0.13 pound per watt. The power supplies for the 8-GHz system were assumed to weigh about 0.61 ounce per watt of d-c output power. At 94 GHz backward-wave oscillators are assumed to supply the first local oscillator and transmitter powers. Their weights are considerably higher than solid-state sources and, for the systems assumed, are estimated at about 10 pounds each. Their power supply weights are estimated at a total of 10 pounds. At each frequency, an additional 30 percent is added to the weight to account for housings, etc. The available raw power was assumed to be 52 watts in all cases, and power supplies were assumed to be 65 percent efficient. The 52-watt figure was selected because it will provide about 10 watts of transmitted power at 300 MHz, a frequency considered for the lander orbiter link.[1] If more prime power was available, additional elements could be used in each array. The effective radiated power increases as the square of the number of elements if the power radiated per element is kept fixed. For these systems this relationship would exist since the power per element is limited by the capabilities of the output high-level mixers. However, the weight of the system rapidly increases as a function of the number of elements so that, if weight is a limitation, increasing the power beyond a certain limit may not be practical.

The effective radiated powers and estimated weights are illustrated in Table III. It is apparent that for the power constraint employed, the effective radiated powers are quite small.

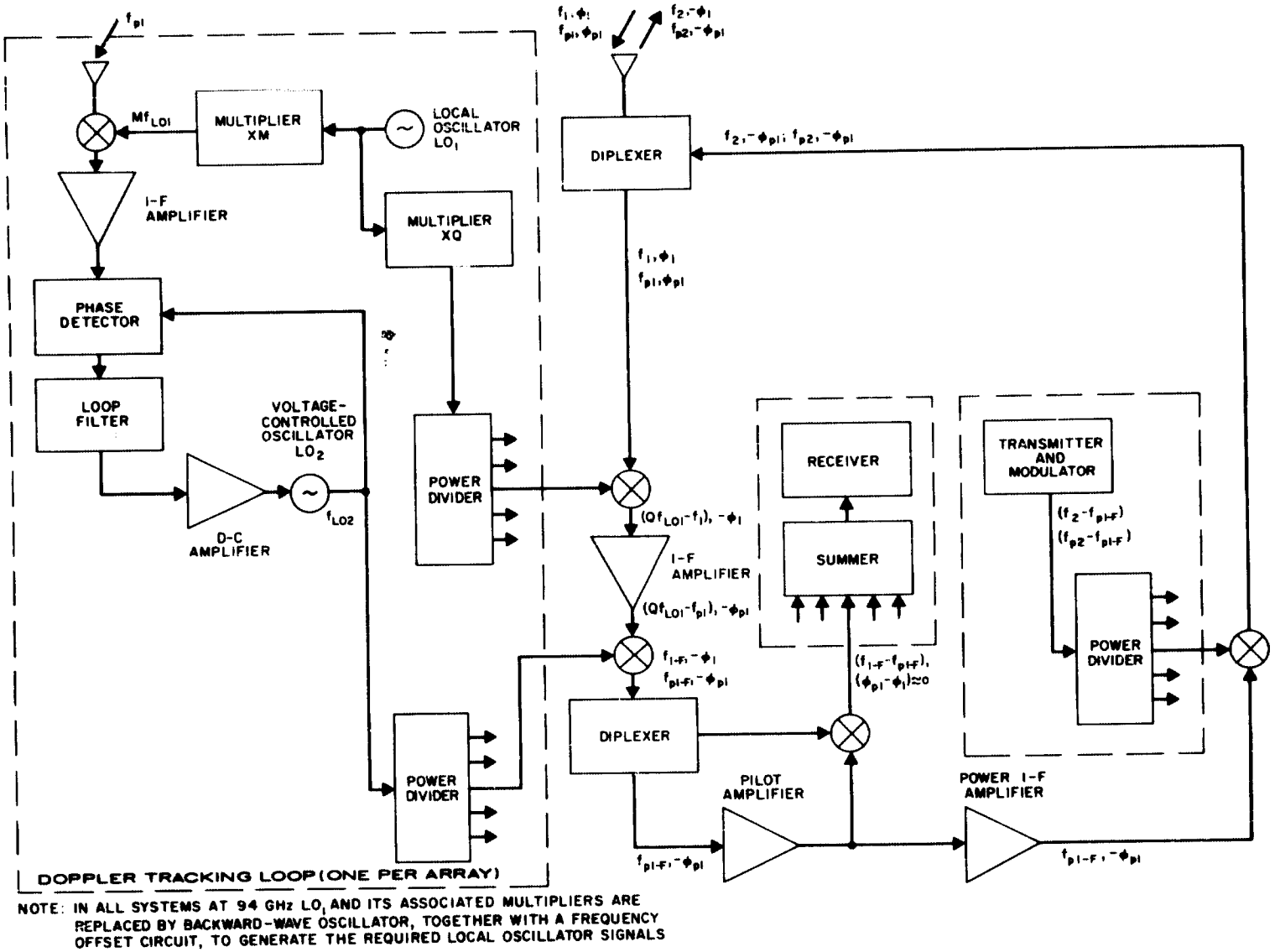

(a) ORBITER ANTENNA NO. 1

Figure 24. Possible self-steering array configurations.

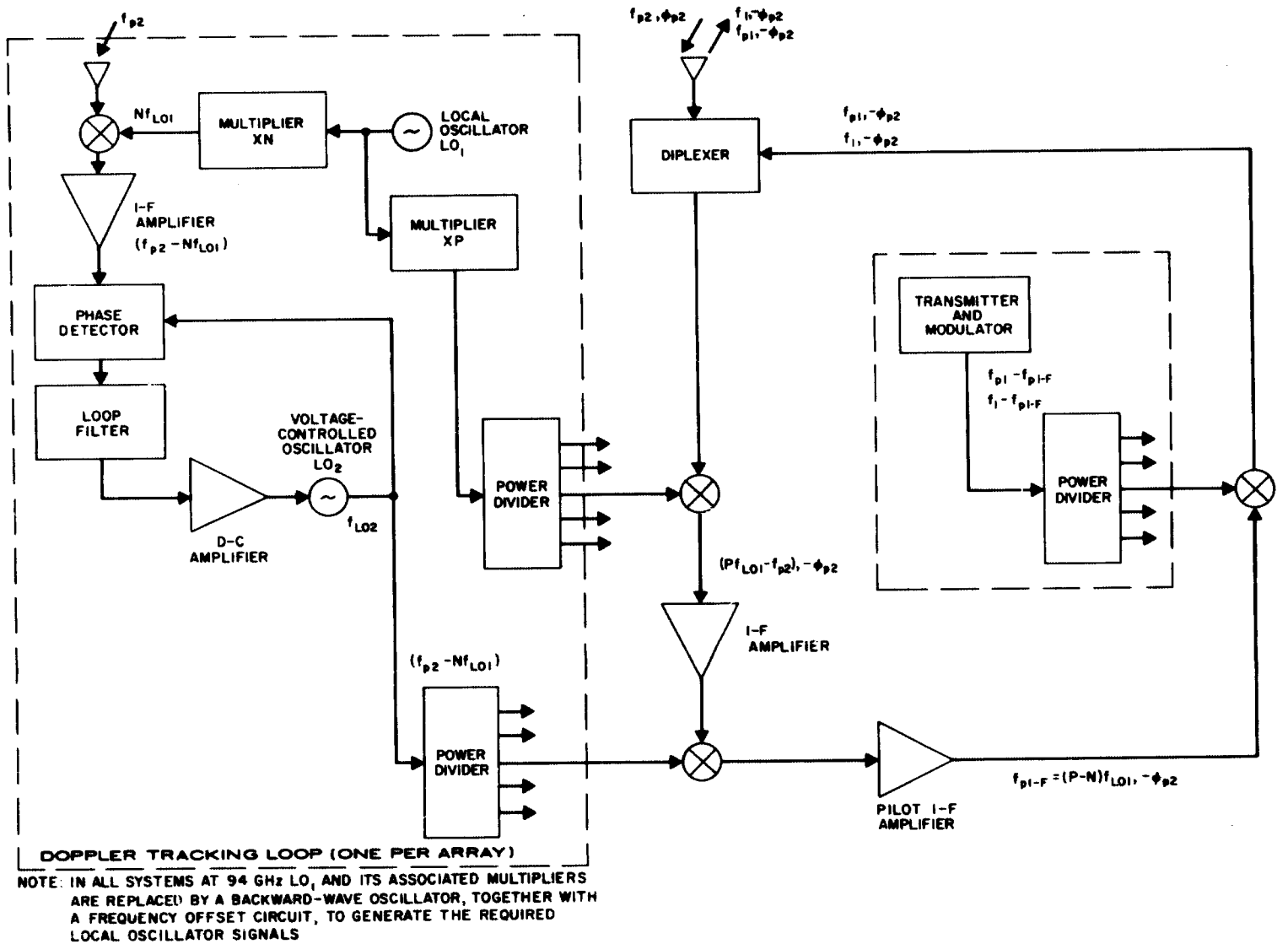

(b) LANDER ANTENNA NO. 1

Figure 24. – Continued.

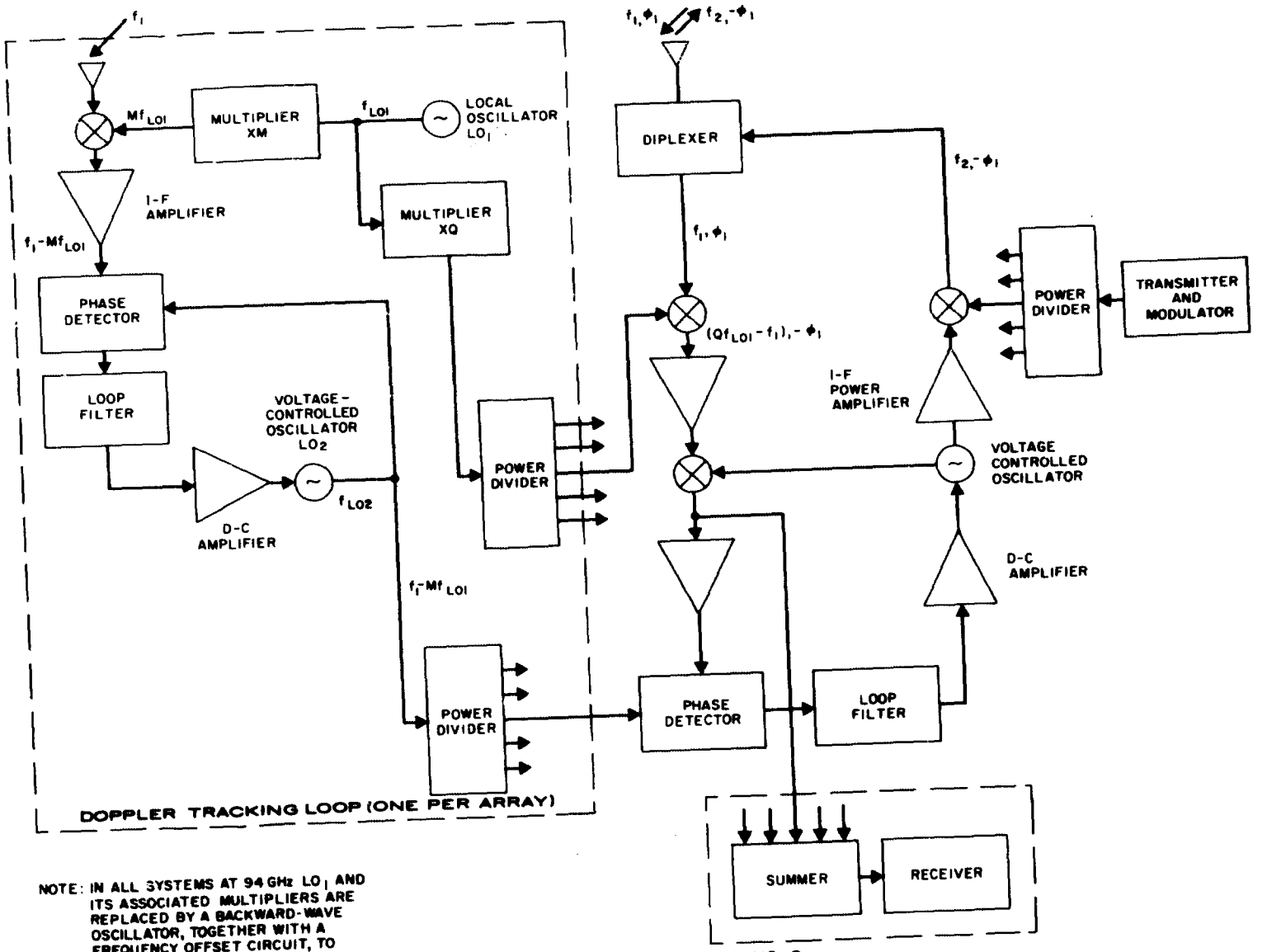

(c) ORBITER ANTENNA NO. 2

Figure 24. – Continued.

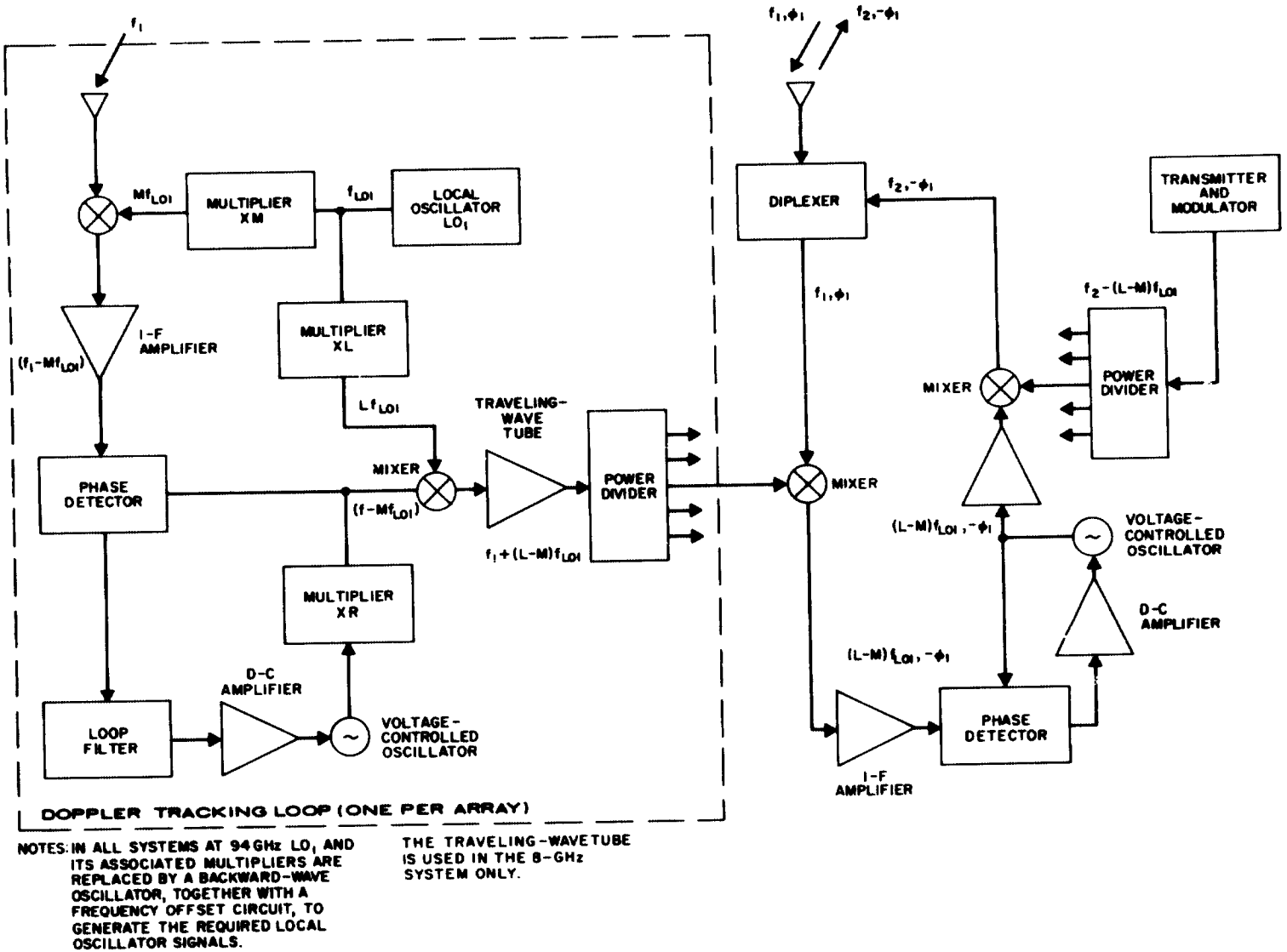

NOTES: IN ALL SYSTEMS AT 94 GHz LO_1 AND ITS ASSOCIATED MULTIPLIERS ARE REPLACED BY A BACKWARD-WAVE OSCILLATOR, TOGETHER WITH A FREQUENCY OFFSET CIRCUIT, TO GENERATE THE REQUIRED LOCAL OSCILLATOR SIGNALS.

THE TRAVELING-WAVE TUBE IS USED IN THE 8-GHz SYSTEM ONLY.

(d) LANDER ANTENNA NO. 2

Figure 24. – Concluded.

Another aspect of interest is the noise figure of the systems. It is estimated that noise figures of 6 to 8 db can be realized at 8 GHz, and at 94 GHz, noise figures of 16 db might be expected.

TABLE II. ESTIMATED WEIGHTS AND POWER REQUIREMENTS OF SELF-STEERING ARRAYS

a) ORBITER ANTENNA NO. 1 (FIGURE 24a)

Components	Quantity	8 GHz		94 GHz	
		Weight, ounces	Power required, mW per element	Weight, ounces	Power required, mW per element
Microwave					
Antenna element	K + 1	1.5 each		0.2 each	
Diplexer	K	2.0 each		4.0 each	
Low noise mixer	K + 1	1.0 each		3.0 each	
High-level mixer	K	1.5 each		4.0 each	
Power divider	2	1.0 each		1.0 each	
Times-M multiplier	1	1.9 each		–	
Times-Q multiplier	1	1.9 each		–	
Local oscillator	1	6.4 each	30	160 each	5
Transmitter	1	1.6 per watt	1400	160 each	250
Intermediate frequency (for both r-f frequencies)					
I-f preamplifiers	K	1.0 each	110		
Second mixer	K	0.5 each			
I-f divider-summer	2	0.5 each			
Local oscillator	1	0.1 each	10		
Crystal diplexer	K	1.0 each			
Pilot amplifier	K	2.0 each	190		
Third mixer	K	0.5 each			
I-f power amplifier	K	1.5 each	300		
I-f high-gain amplifier	1	3.0 each			
Loop filter	1	0.19 each	320/K		
Phase detector	1	0.51 each			
Receiver	1	6.4 each	640/K		
D-c amplifier	1	0.51 each	102/K		
Power supply (65 percent efficient)	1	0.61 per watt	18,200/K		

TABLE II. ESTIMATED WEIGHTS AND POWER REQUIREMENTS OF SELF-STEERING ARRAYS – CONTINUED

b) LANDER ANTENNA NO. 1 (FIGURE 24b)

Components	Quantity	8 GHz		94 GHz	
		Weight, ounces	Power required, mW per element	Weight, ounces	Power required, mW per element
Microwave					
Antenna element	K + 1	1.5 each		0.2 each	
Diplexer	K	2.0 each		4.0 each	
Low-noise mixer	K + 1	1.0 each		3.0 each	
High-level mixer	K	1.5 each		4.0 each	
Power divider	2	1.0 each		1.0 each	
Times-N multiplier	1	1.9 each		–	
Times-R multiplier	1	1.9 each		–	
Local oscillator	1	6.4 each	30	160 each	5
Transmitter	1	1.6 per watt	1400	160 each	250
Intermediate frequency (for both r-f frequencies)					
I-f amplifier	K + 1	3.0 each	300		
Second mixer	K	0.5 each			
I-f power divider	1	0.25 each			
Pilot amplifier	K	1.5 each	300		
Loop filter	1	0.19 each			
Phase detector	1	0.64 each			
Local oscillator	1	0.1 each	10		
D-c amplifier	1	0.51 each	102/K		
Power supply (65 percent efficient)	1	0.61 per watt	18,200/K		

TABLE II. ESTIMATED WEIGHTS AND POWER REQUIREMENTS OF SELF-STEERING ARRAYS – CONTINUED

c) ORBITER ANTENNA NO. 2. (FIGURE 24c)

Components	Quantity	8 GHz		94 GHz	
		Weight, ounces	Power required, mW per element	Weight, ounces	Power required, mW per element
Microwave					
Antenna element	K + 1	1.5 each		0.2 each	
Diplexer	K	2.0 each		4.0 each	
Low-noise mixer	K + 1	1.0 each		3.0 each	
Power divider	2	1.0 each		1.0 each	
High-level mixer	K	1.5 each		4.0 each	
Times-N multiplier	1	1.92 each		–	
Times-Q multiplier	1	1.92 each		–	
Local oscillator	1	6.4 each	30	160 each	5
Transmitter	1	1.6 per watt	1400	160 each	250
Intermediate frequency (for both r-f frequencies)					
I-f preamplifier	K	1.0 each	110		
Second mixer	K	0.5 each			
I-f amplifier	K	2.0 each	190		
Phase detector	K + 1	0.5 each			
Loop filter	K + 1	0.2 each			
Voltage-controlled oscillator	K	1.0 each	200		
I-f power divider	2	0.5 each			
D-c amplifier	K + 1	0.5 each	100		
I-f power amplifier	K	1.5 each	300		
Receiver	1	6.4 each	640/K		
High-gain i-f amplifier	1	3.0 each	320/K		
Voltage-controlled oscillator 2	1	0.2 each	20		
Power supply (65 percent efficient)	1	0.61 per watt	18,200/K		

TABLE II. ESTIMATED WEIGHTS AND POWER REQUIREMENTS OF SELF-STEERING ARRAYS – CONCLUDED

d) LANDER ANTENNA NO. 2 (FIGURE 24d)

Components	Quantity	8 GHz		94 GHz	
		Weight, ounces	Power required, mW per element	Weight, ounces	Power required, mW per element
Microwave					
Antenna element	K + 1	1.5 each		0.2 each	
Diplexer	K	2.0 each		4.0 each	
Low-loss mixer	K + 1	1.0 each		3.0 each	
High-level mixer	K	1.0 each		1.0 each	
Power divider	2	1.5 each		4.0 each	
Times-M multiplier	1	1.92 each			
Times-Q multiplier	1	1.92 each			
Local oscillator	1	6.4 each	12	160 each	5
Transmitter	1	1.6 per watt	1400	160 each	250
Traveling-wave tube	1	0.19 per element	40		
Intermediate frequency (for both r-f frequencies)					
I-f amplifier	K + 1	3.0 each	300		
Phase detectors	K + 1	0.5 each			
Loop filters	K + 1	0.2 each			
D-c amplifier	K + 1	0.5 each	100		
Voltage-controlled oscillator	K	1.0 each	200		
Voltage-controlled local oscillator 2	1	0.15 per element	15		
I-f power amplifier	K	1.5 each	300		
Power supplies (65 percent efficient)	1	0.61 per watt	18,200/K		

TABLE III. SUMMARY OF CHARACTERISTICS OF REPRESENTATIVE SELF-STEERING SYSTEMS FOR FIXED PRIME POWER

Characteristic	8 GHz	94 GHz
Orbiter Antenna No. 1		
Raw power, watts	52	52
Number of elements, K	16	38
Effective radiated power, watts	20.5 g_e*	7.20 g_e*
Weight, pounds	22.4	100
Lander Antenna No. 1		
Raw power, watts	52	52
Number of elements, K	16	39
Effective radiated power, watts	20.5 g_e*	7.6 g_e*
Weight, pounds	19.4	100
Orbiter Antenna No. 2		
Raw power, watts	52	52
Number of elements, K	14	28
Effective radiated power, watts	15.7 g_e	3.9 g_e
Weight, pounds	21	86
Lander Antenna No. 2		
Raw power, watts	52	52
Number of elements, K	14	29
Effective radiated power, watts	15.7 g_e	4.2 g_e
Weight, pounds	19	84

*g_e is the element gain.

CONCLUSION

Analysis of Results

During the course of this study, the applicability of self-steering arrays to planetary probe missions has been considered. A consideration of possible mission requirements indicated that self-steering arrays that use phase inversion by mixing may be applicable to the lander-bus communication link because of the relatively short distance involved. Phase-locked loops with their extremely narrow noise bandwidths will probably be required for the bus-earth link because of the large transmission distances and corresponding low signal levels. Effort has been concentrated on determining the performance capabilities of both types of self-steering arrays when they are used with various digital modulation schemes. To make the desired assessment, a number of different problems were analyzed. The results are summarized in this section.

As one problem of interest, the effects of the communications environment on the successful operation of each phase-locked loop of an adaptive array must be determined. In this report, the criteria for successful loop operation, acquisition, and loss-of-lock probabilities are calculated for a multipath environment. The model for the environment consists of two signal paths, the direct or primary earth-bus path and the secondary earth-planet-bus path. In the most general model, additive gaussian noise is also included.

The results for slow-fading multipath signals consist of simple acquisition and loss-of-lock limits for the noiseless deterministic case in which only the interaction between the two signal paths is significant enough to affect the loop operation. For the dual-path plus random perturbations case (without additive receiver noise), loss-of-lock probabilities are calculated, and elementary error functions of the loop parameters result. Finally, complex integrals are evolved for the general case in which dual-path, random fluctuation, and additive noise effects are all included.

For the analysis of fast-fading multipath signals, Rician fading processes with flat spectra were assumed. The result was just an equivalent rise in additive white noise level. Consequently, early results on this program are directly applicable with an appropriate scale change in the signal-to-noise ratio. It is interesting to contrast this result with the results of the slow-fading analyses. For fast fading, both the amplitude noise and the phase noise contribute to a lowering of the loop signal-to-noise ratio. However, for slow fading, the phase noise component of the fading signal may be tracked by the loop so that only the amplitude noise affects the resultant density functions of the phase errors.

The density functions derived for slow and fast fading are density functions of phase errors in a single phase-locked loop. In an antenna array, the signal to be demodulated consists of a sum of the outputs of many independent phase-locked loops. The density function of this sum approaches gaussian for a multi-element array. But, as can be seen from the calculations presented here, the density function of an array of a few elements differs significantly from gaussian at large phase angles. The result is a larger error probability in demodulation than that calculated with a gaussian density function and the same variance.

For intermediate fading rates, an expression is derived for the probability density function of the phase error of a first-order, phase-locked loop which is tracking a fading signal embedded in noise. The resulting expression is in terms of the average input signal amplitude, the fluctuating power spectrum of the signal amplitude, and the additive noise spectrum. For zero fluctuating power, the phase error density function reduces to the well-known non-fading result.

In subsequent sections, the demodulation of the set of signals obtained after independent processing at each antenna element is treated. The fact that the processing is effected by a phase-locked loop is of no consequence in these analyses, although the noise levels and phase variances are numerically determined by the specific processor utilized. The only inherent assumption is that of a large number of antenna elements. If few antenna elements are used, the phase probability density function derived in the sections on convergence to gaussian statistics must be used in place of the gaussian function. However, the results would qualitatively be the same as those derived here.

The error probabilities are calculated for detection in a multipath environment (including time delay anomalies). The modulation systems considered were coherent phase, frequency, and amplitude shift keys and incoherent frequency and amplitude shift keys. The effects of the time-delay anomalies are presented in graphic form. In the calculations doppler shifts were assumed to be identical for all multipath rays. The effect of the doppler shift anomalies on the results was considered separately. It was found that these anomalies actually improve demodulation accuracy, provided that the doppler shift of the primary signal is known.

Some time was devoted to a study of the manner in which the outputs of the phase-locked loops (which are independently associated with each element of the retrodirective array) are optimally added so that the modulation distortion is minimized. The required weighting coefficients were derived and defined.

An analysis was performed that leads to estimates of error probabilities in the detection of digitally modulated signals received by a system that uses phase inversion by mixing. Expressions were derived for the outputs of correlation detectors and can be used to calculate error probabilities for digitally coded signals.

Several studies are concerned with the problem of determining the spectrum of the fields scattered by a large rough spherical scatter when a spherical monochromatic wave is incident on it. The treatment employed a vector approach rather than a scalar approach and differs from other approaches in that it takes the curvature of the scatterer into account. The problem was carried to the point at which the correlation functions of the three components of the scattered electric field intensity were obtained as double integrals over the scatterer coordinates. Evaluation of the final integrations remains to be carried out.

The effects of entry-induced plasmas on propagation of radio waves to or from an entry probe were considered. An analysis was made of attenuation versus time for four entry profiles of a non-survivable probe. The analysis indicates that at 94 GHz there may be no blackout. From this result it would appear that millimeter waves may be useful in entry-vehicle communication systems to overcome the entry blackout problem.

Four self-steering systems were devised to obtain an estimate of the effective radiated power, the weight, and the noise performance of microwave and millimeter-wave self-steering arrays. A fixed, available prime power of 52 watts was assumed as a constraint. Although the effective radiated powers for this constraint were relatively small, the availability of increased prime power and increased component efficiencies will increase the effective radiated power even more rapidly. This conclusion follows from the fact that more available prime power or higher efficiencies permit the use of more radiating elements and, consequently, provide greater array gain. For example, a tenfold increase in the available prime power would allow approximately a tenfold increase in the number of elements, thereby resulting in an increase of effective radiated power by a factor of one hundred. Improvements in system noise figures will further improve overall performance by increasing signal-to-noise ratios for a fixed available power or by allowing reduced effective radiated power for a given signal-to-noise ratio.

Recommendations

The studies that were performed during the course of this program have resulted in considerable new data concerning the effects of noise and simple multipath signals on the operation of self-steering arrays. Phase errors in phase-locked loops were computed, and probabilities of error in detection of various digitally modulated signals were determined when detected by self-steering systems. A vector analysis of the nature of radio signals scattered by rough spherical surfaces was partially completed to obtain improved estimates as to the spectrum of the scattered signal.

An analysis of blackout during entry into a Martian atmosphere has supported the belief that use of millimeter waves can alleviate the entry blackout problem, and a study of power and weights of several specific systems indicates that self-steering arrays are feasible for planetary entry communication systems.

As a result of the study, many of the tools necessary for the evaluation of the application of self-steering arrays to specific missions are available. At this juncture, it is recommended that these results be incorporated into some specific mission analyses to permit an overall assessment of the applicability of the systems. It is also recommended that further study be made of the spectra of scattered signals in the presence of moving sources and receivers.

Finally, additional upper microwave and millimeter-wave components should be further developed to improve the predicted capabilities of self-steering antennas in these frequency ranges.

Antenna Department, Aerospace Group
Hughes Aircraft Company
Culver City, California, 25 March 1968.

APPENDIX A

PROBABILITY DENSITY FUNCTION OF STEADY-STATE PHASE ERRORS IN PHASE-LOCKED LOOPS

For the problem under consideration, the differential equation of the phase-locked loop is, from equation (8),

$$\frac{d\phi}{dt} = (\delta\ddot{\theta})\, t + (\delta\dot{\theta}) - C_0 K_1 K_2 \left[\alpha \tilde{A} \sin \phi\,(t) + n'(t)\right]$$

$$- C_1 K_1 K_2 \int_0^t \left[\alpha \tilde{A} \sin \phi\,(u) + n'(u)\right] du \qquad \text{(A1)}$$

For the method of analysis employed, $\phi(t)$ is written

$$\phi(t) = C_1 \epsilon(t) + C_0 \frac{d\epsilon(t)}{dt} \qquad \text{(A2)}$$

On substitution of equation (A2) into (A1), there results the following equation:

$$C_0 \frac{d^2\epsilon}{dt^2} + C_0 K_1 K_2 \left[\alpha \tilde{A} \sin\left(C_1\epsilon + C_0 \frac{d\epsilon}{dt}\right) + n'(t)\right]$$

$$= - C_1 \frac{d\epsilon}{dt} + (\delta\ddot{\theta})\, t + (\delta\dot{\theta})$$

$$- C_1 K_1 K_2 \int_0^t \left[\alpha \tilde{A} \sin\left(C_1\epsilon + C_0 \frac{d\epsilon}{du}\right) + n'(u)\right] du \qquad \text{(A3)}$$

If the left-hand side of this equation is denoted by $\Omega_L(t)$ and the right-hand side by $\Omega_R(t)$, then the expression may be written that

$$\frac{d}{dt}\Omega_R(t) = -\frac{C_1}{C_0}\Omega_R + (\delta\ddot{\tilde{\theta}}) \tag{A4}$$

This equation has a solution of the form

$$\Omega_R(t) = \frac{C_0}{C_1}(\delta\ddot{\tilde{\theta}}) + D\exp\left[-\frac{C_1}{C_0}t\right] \tag{A5}$$

where D is determined from initial conditions. Since the steady-state solution is of interest, the solution approaches the first term of equation (A5) as $t \to \infty$. Consequently, as $t \to \infty$, the quantity Ω_L satisfies

$$C_0\frac{d^2\epsilon}{dt^2} + C_0 K_1 K_2\left[\alpha\tilde{A}\sin\left(C_1\epsilon + C_0\frac{d\epsilon}{dt}\right) + n'(t)\right] = \frac{C_0}{C_1}(\delta\ddot{\tilde{\theta}}) \tag{A6}$$

On using the definitions $y_0 \equiv \epsilon$ and $y_1 \equiv \frac{d\epsilon}{dt}$, the system equations become

$$\frac{dy_1}{dt} + K_1 K_0 \alpha\tilde{A}\sin(C_1 y_0 + C_0 y_1) = -K_1 K_2 n'(t) + \frac{1}{C_1}(\delta\dot{\tilde{\theta}}) \tag{A7a}$$

$$\frac{dy_0}{dt} = y_1 \tag{A7b}$$

Viterbi[24] has shown that insofar as the loop is concerned, $n'(t)$ looks like white noise. Consequently, $\underset{\sim}{y} \equiv [y_0, y_1]$ forms a vector Markov process. The probability density function of this vector satisfies the two-dimensional Fokker-Planck equation.[24]

$$\frac{\partial p(\underline{y}, t)}{\partial t} = -\frac{\partial}{\partial y_0}[A_0(\underline{y})\, p(\underline{y}, t)] - \frac{\partial}{\partial y_1}[A_1(\underline{y}),\, p(\underline{y}, t)]$$

$$+ \frac{1}{2}\frac{\partial^2}{\partial y_0^2}[A_{00}(\underline{y})\, p(\underline{y}, t)]$$

$$+ \frac{1}{2}\frac{\partial^2}{\partial y_0\, \partial y_1}[A_{01}(\underline{y})\, p(\underline{y}, t)]$$

$$+ \frac{1}{2}\frac{\partial^2}{\partial y_1\, \partial y_0}[A_{10}(\underline{y})\, p(\underline{y}, t)]$$

$$+ \frac{1}{2}\frac{\partial^2}{\partial y_1^2}[A_{11}(\underline{y})\, p(\underline{y}, t)] \qquad \text{(A8a)}$$

in which[†]

$$\begin{cases} A_k(\underline{y}) \equiv \lim\limits_{\Delta t \to 0} \dfrac{E(\Delta y_k \mid \underline{y})}{\Delta t} \\ A_{k\ell}(\underline{y}) \equiv \lim\limits_{\Delta t \to 0} \dfrac{E(\Delta y_k\, \Delta y_\ell \mid \underline{y})}{\Delta t} \end{cases} \qquad \text{(A8b)}$$

From equations (A7), the increments in the y_i are

$$\Delta y_0 = y_1(t)\, \Delta t$$

$$\Delta y_1 = -\left[K_1 K_2 \alpha \tilde{A} \sin(C_1 y_0 + C_0 y_1) - \frac{1}{C_1}(\delta\ddot{\tilde{\theta}})\right] \Delta t$$

$$- K_1 K_2 \int_t^{t+\Delta t} n'(u)\, du$$

[†](For notational convenience, the expression "given $\delta\tilde{\theta}$, $\delta\dot{\tilde{\theta}}$, $\delta\ddot{\tilde{\theta}}$" is not written explicitly, although it is implied.)

so that the A_k and $A_{k\ell}$ are given by

$$A_0 (\underset{\sim}{y}) = E (y_1 \mid \underset{\sim}{y}) = y_1$$

$$A_1 (\underset{\sim}{y}) = E \left(- \left[K_1 K_2 \alpha \tilde{A} \sin (C_1 y_0 + C_0 y_1) - \frac{1}{C_1} (\delta \ddot{\tilde{\theta}}) \right] \Big| \underset{\sim}{y} \right)$$

$$= - \left[K_1 K_2 \alpha \tilde{A} \sin (C_1 y_0 + C_0 y_1) - \frac{1}{C_1} (\delta \ddot{\tilde{\theta}}) \right]$$

$$A_{00} = A_{10} = A_{01} = 0$$

$$A_{11} (\underset{\sim}{y}) = \lim_{\Delta t \to 0} \frac{E \left\{ (K_1 K_2)^2 \left(\int_t^{t+\Delta t} n' (u)\, du \right)^2 \right\}}{\Delta t} = (K_1 K_2) \frac{N_0}{2}$$

On using these values, the Fokker-Planck equation becomes

$$\frac{\partial p}{\partial t} = - y_1 \frac{\partial p}{\partial y_o} + \frac{\partial}{\partial y_1} \left[K_1 K_2 \alpha \tilde{A} \sin (C_1 y_0 + C_0 y_1)\, p - \frac{1}{C_1} \delta \ddot{\tilde{\theta}}\, p \right]$$

$$\left(\frac{K_1 K_2}{2} \right)^2 N_0 \frac{\partial^2 p}{\partial y_1^2} \tag{A9}$$

with $p (\underset{\sim}{y}, t)$ satisfying the initial condition

$$p (\underset{\sim}{y}, 0) = \delta \left(y_0 - y_0 (0) \right) \delta \left(y_1 - y_1 (0) \right) \tag{A10}$$

From equation (A2) and the definitions of y_0 and y_1, the probability density function of ϕ may then be found from

$$p (\phi, t) = \frac{C_0}{C_1} \int_{-\infty}^{\infty} p \left(\frac{\phi - C_0 y_1}{C_1}, y_1, t \right) dy_1$$

Since the calculations are for the steady-state solution,

$$P (y_0, y_1) = \lim_{t \to \infty} p (y_0, y_1, t)$$

and

$$\lim_{t\to\infty} \frac{\partial\, p\,(\phi,\, t)}{\partial t} = 0 = \lim_{t\to\infty} \frac{\partial\, p\,(y_0\, y_1,\, t)}{\partial t}$$

The steady-state equivalent of equation (A9) is

$$0 = -\,y_1\, \frac{\partial p(y_0,\, y_1)}{\partial\, y_0} + K_1\, K_2\, \alpha\, \tilde{A}\, \frac{\partial}{\partial\, y_1} \left[\sin\,(C_1\, y_0 + C_0\, y_1)\, p\,(y_0,\, y_1)\right]$$

$$-\,\frac{1}{C_1}\,(\delta\ddot{\theta})\, \frac{\partial\, p\,(y_0,\, y_1)}{\partial\, y_1} + \left(\frac{K_1\, K_2\, \sqrt{N_0}}{2}\right)^2 \frac{\partial^2\, p\,(y_0,\, y_1)}{\partial y_1^{\,2}}$$

Using the relation between ϕ and y_1 and y_2 and the substitution $z = C_1\, y_0$ results in

$$y_0 = z/C_1, \qquad y_1 = \frac{\phi - z}{C_0}$$

Then,

$$0 = -\left(\frac{\phi - z}{C_0}\right) C_1\, \frac{\partial}{\partial z}\, p\left(\frac{z}{C_1}, \frac{\phi - z}{C_0}\right) + C_0 K_1\, K_2\, \alpha\, \tilde{A}\, \frac{\partial}{\partial \phi} \left[\sin \phi\; p\left(\frac{z}{C_1}, \frac{\phi - z}{C_0}\right)\right]$$

$$-\,\frac{1}{C_1}\,(\delta\ddot{\theta})\, C_0\, \frac{\partial}{\partial \phi}\, p\left(\frac{z}{C_1}, \frac{\phi - z}{C_0}\right) + \left(\frac{K_1\, K_2\, \sqrt{N_0}}{2}\right)^2 C_0\, \frac{\partial^2}{\partial \phi^2}\, p\left(\frac{z}{C_1}, \frac{\phi - z}{C_0}\right)$$

Transforming to $p\,(\phi,\, z)$ by

$$p\,(z,\, \phi) = p\left(\frac{z}{C_1}, \frac{\phi - z}{C_0}\right) |J|$$

this expression becomes

$$\frac{C_1}{C_0^2}(\phi - z)\left(\frac{\partial}{\partial\phi} + \frac{\partial}{\partial z}\right) p(\phi, z) = K_1 K_2 \alpha \tilde{A} \frac{\partial}{\partial\phi}(\sin\phi)\, p(\phi, z)$$

$$- \frac{1}{C_1}(\delta\ddot{\theta}) \frac{\partial}{\partial\phi} p(\phi, z)$$

$$+ \left(\frac{K_1 K_2 \sqrt{N_0}}{2}\right)^2 \frac{\partial^2}{\partial\phi^2} p(\phi, z) \qquad \text{(A11)}$$

In terms of the probability density function of the steady-state phase error,

$$p(\phi) = \int_{-\infty}^{\infty} p(\phi, z)\, dz$$

and equation (A11) reduces to an ordinary differential equation by integration:

$$\frac{C_1}{C_0^2}\phi \frac{d}{d\phi} p(\phi) - \frac{C_1}{C_0^2}\int_{-\infty}^{\infty} z \frac{\partial}{\partial\phi} p(\phi, z)\, dz + \frac{C_1}{C_0^2}\phi \int_{-\infty}^{\infty} \frac{\partial}{\partial z} p(\phi, z)\, dz$$

$$- \frac{C_1}{C_0^2}\int_{-\infty}^{\infty} z \frac{\partial}{\partial z} p(\phi, z)\, dz = K_1 K_2 \alpha \tilde{A} \frac{d}{d\phi}[\sin\phi\, p(\phi)]$$

$$- \frac{1}{C_1}(\delta\ddot{\theta}) \frac{d}{d\phi} p(\phi) + \left(\frac{K_1 K_2 \sqrt{N_0}}{2}\right)^2 \frac{d^2 p(\phi)}{d\phi^2}$$

or

$$\frac{C_1}{C_0^2}\left\{\phi\frac{d}{d\phi}p(\phi) - \frac{d}{d\phi}\int_{-\infty}^{\infty} z\,p(\phi, z)\,dz + \phi\int_{-\infty}^{\infty}\frac{\partial}{\partial z}p(\phi, z)\,dz\right.$$

$$\left. - \int_{-\infty}^{\infty} z\frac{\partial}{\partial z}p(\phi, z)\,dz\right\} = K_1 K_2\,\alpha\,\tilde{A}\frac{d}{d\phi}[\sin\phi\,p(\phi)]$$

$$- \frac{1}{C_1}(\delta\ddot{\theta})\frac{d}{d\phi}p(\phi) + \left(\frac{K_1 K_2\sqrt{N_0}}{2}\right)^2\frac{d^2 p(\phi)}{d\phi^2}$$

But

$$\int_{-\infty}^{\infty}\frac{\partial}{\partial z}p(\phi, z)\,dz = p(\phi, +\infty) - p(\phi, -\infty) = 0$$

Let

$$u = z \quad \text{and} \quad dv = \frac{\partial}{\partial z}p(\phi, z)\,dz;$$

then

$$\int_{-\infty}^{\infty} z\frac{\partial}{\partial z}p(\phi, z)\,dz = uv - \int v\,du = z\,p(\phi, z)\Big|_{-\infty}^{\infty} - \int_{-\infty}^{\infty} p(\phi, z)\,dz$$

But

$$\int_{-\infty}^{\infty} p(z)\,dz = 1$$

by definition of a probability density function so that p (z) must vanish faster than $1/z$ as $z \to \pm\infty$. Therefore,

$$\int_{-\infty}^{\infty} z\frac{\partial}{\partial z}p(\phi, z)\,dz = \frac{z}{z^{1+\epsilon}}\Big|_{-\infty}^{\infty} - p(\phi) = -p(\phi)$$

The equation becomes

$$\frac{C_1}{C_0^2}\left\{\frac{d}{d\phi}[\phi p(\phi)] - \frac{d}{d\phi}\int_{-\infty}^{\infty} z\, p(\phi, z)\, dz\right\} = K_1 K_2 a \tilde{A} \frac{d}{d\phi}[\sin\phi\, p(\phi)]$$

$$- \frac{1}{C_1}\delta\ddot{\theta}\frac{d}{d\phi}p(\phi) + \left(\frac{K_1 K_2\sqrt{N_0}}{2}\right)^2 \frac{d^2 p(\phi)}{d\phi^2}$$

But

$$\int_{-\infty}^{\infty} z p(\phi, z)\, dz = p(\phi)\int_{-\infty}^{\infty} z\, p(z|\phi)\, dz = p(\phi) E(z|\phi)$$

so that the differential equation becomes

$$0 = \frac{d}{d\phi}\left\{\left[K_1 K_2 a \tilde{A} \sin\phi - \frac{\delta\ddot{\theta}}{C_1} - \frac{C_1}{C_0^2}\phi + \frac{C_1}{C_0^2} E(z|\phi)\right] p(\phi) + \left(\frac{K_1 K_2\sqrt{N_0}}{2}\right)^2 \frac{dp(\phi)}{d\phi}\right\}$$

$$0 = \frac{d}{d\phi}\left\{\left[\frac{4 a \tilde{A}}{K_1 K_2 N_0}\sin\phi - \frac{4\delta\ddot{\theta}}{C_1 (K_1 K_2)^2 N_0} - \frac{4 C_1}{C_0^2 (K_1 K_2)^2 N_0}\phi + \frac{4 C_1}{C_0^2 (K_1 K_2)^2 N_0} E(z|\phi)\right] p(\phi) + \frac{dp(\phi)}{d\phi}\right\} \qquad \text{(A12)}$$

From the definition of z and ϕ in terms of y_0 and y_1 it may be seen that

$$E(z|\phi) = E\left([\phi - C_0 y_1]|\phi\right) = \phi - C_0 E(y_1|\phi)$$

Equation (A12) then becomes

$$0 = \frac{d}{d\phi}\left\{\left[\frac{4\tilde{A}}{K_1 K_2 N_0}\left(\sin\phi - \frac{\delta\ddot{\theta}}{C_1 a \tilde{A} K_1 K_2}\right) - \frac{4 C_1}{C_0 (K_1 K_2)^2 N_0} E(y_1|\phi)\right] p(\phi) + \frac{dp(\phi)}{d\phi}\right\} \qquad \text{(A13)}$$

For small $C_1 \neq 0$ ($C_1 \ll C_0 \alpha \tilde{A} K_1 K_2$), equation (A13) may be written as

$$0 = \frac{d}{d\phi}\left[\frac{4\alpha\tilde{A}}{K_1K_2N_0}\left(\sin\phi - \frac{\delta\ddot{\tilde{\theta}}}{C_1\alpha\tilde{A}K_1K_2}\right)p(\phi) + \frac{dp(\phi)}{d\phi}\right]$$

By integration, a first-order linear differential equation results in the solution

$$p(\phi \mid \delta\ddot{\tilde{\theta}}) \approx C \exp\left\{\frac{4\alpha\tilde{A}}{K_1K_2N_0}\left(\cos\phi + \frac{\delta\ddot{\tilde{\theta}}}{C_1\alpha\tilde{A}K_1K_2}\phi\right)\right\}$$

$$\left[1 + D\int_{-\pi}^{\phi} \exp\left\{-\frac{4\alpha\tilde{A}}{K_1K_2N_0}\left(\cos x + \frac{\delta\ddot{\tilde{\theta}}}{C_1\alpha\tilde{A}K_1K_2}x\right)\right\}dx\right] \quad -\pi \leq \phi < \pi \tag{A14}$$

where

$$D = \frac{\exp\left[-2\left(\frac{4\delta\ddot{\tilde{\theta}}}{C_1(K_1K_2)^2N_0}\right)\right] - 1}{\int_{-\pi}^{\pi} \exp\left\{\frac{4\alpha\tilde{A}}{K_1K_2N_0}\left(\cos x + \frac{\delta\ddot{\tilde{\theta}}}{C_1\alpha\tilde{A}K_1K_2}x\right)\right\}dx}$$

and C is chosen so that

$$\int_{-\pi}^{\pi} p\left(\phi \mid \delta\ddot{\tilde{\theta}}\right) d\phi = 1$$

The general characteristics of $p(\phi \mid \delta\ddot{\tilde{\theta}})$ may be seen from a few approximations to equation (A14) for small $\delta\ddot{\tilde{\theta}}$. If $\delta\ddot{\tilde{\theta}} \ll C_1 AK_1K_2$, then $D \approx 0$ and

$$p(\phi \mid \delta\ddot{\tilde{\theta}}) \sim C \exp\left\{\frac{4\alpha\tilde{A}}{K_1K_2N_0}\left(\cos\phi + \frac{\delta\ddot{\tilde{\theta}}}{C_1\alpha\tilde{A}K_1K_2}\phi\right)\right\}$$

The mean phase error is approximately the same as the most likely error; that is, the value of ϕ which maximizes

$$\left\{\cos\phi + \frac{\delta\ddot{\tilde{\theta}}}{C_1\alpha\tilde{A}K_1K_2}\phi\right\}$$

This value is determined from the following equation.

$$0 = \frac{d}{d\phi}\left\{\cos\phi + \frac{\delta\ddot{\tilde{\theta}}}{C_1 \alpha \tilde{A} K_1 K_2}\phi\right\} = -\sin\phi + \frac{\delta\ddot{\tilde{\theta}}}{C_1 \alpha \tilde{A} K_1 K_2}$$

Consequently,

$$E(\phi|\delta\ddot{\tilde{\theta}}) \approx \sin^{-1}\frac{\delta\ddot{\tilde{\theta}}}{C_1 \alpha \tilde{A} K_1 K_2} \tag{A15}$$

The variance of phase errors is approximated through a linear analysis assuming a high signal-to-noise ratio (SNR).[40] The result is

$$\sigma_\phi^2 \approx \frac{N_0 B_1}{(\alpha\tilde{A})^2} = \frac{N_0}{(2\alpha\tilde{A})^2}\left(\alpha\tilde{A}\, C_0 K_1 K_2 + C_1/C_0\right) \tag{A16}$$

The above approximate analysis shows that the effect of $\delta\ddot{\tilde{\theta}}$ is to shift the mean error from zero and to introduce asymmetry into the probability density function, while the effect of the second-order part of the loop (represented by C_1) is to decrease this shift while increasing error variance.

With a high SNR assumption, an approximate solution to equation (A13) can be found without the assumption of a small second-order part (C_1) of the loop. This result is possible through a linear approximation to $\sin\phi$, which arises in the evaluation of $E(y, |\phi)$. Specifically, the discussion will utilize equation (A13) which has a term with $E(y, |\phi)$. When C_1 is small, this term is small. But with a general C_1 this term cannot be ignored; some estimate of $E(y, |\phi)$ must be provided. The parametric definition of ϕ can be recalled:

$$\phi(t) = C_1\epsilon(t) + C_0\frac{d\epsilon(t)}{dt}$$

$$y_0(t) = \epsilon(t)$$

$$y_1(t) = \frac{d\epsilon(t)}{dt}$$

And from equation (A9), it may be recalled that

$$\frac{dy_1(t)}{dt} = -K_1K_2\alpha\tilde{A}\sin(C_1y_0 + C_0y_1) - K_1K_2n'(t) + \frac{1}{C_1}(\delta\ddot{\tilde{\theta}})$$

$$= -K_1K_2\alpha\tilde{A}\sin(\phi(t)) - K_1K_2n'(t) + \frac{1}{C_1}(\delta\ddot{\tilde{\theta}})$$

Integrating yields

$$y_1(\infty) - y_1(t) = -K_1K_2\alpha\tilde{A}\int_t^\infty \left[\sin\phi(u) - \frac{\delta\ddot{\theta}}{C_1K_1K_2\alpha A}\right] du$$

$$-K_1K_2\int_t^\infty n'(u)du$$

Taking expectations and recalling that n' (t) is a zero mean process results in

$$E\left[y_1(\infty)\,|\,\phi(\infty)\right] - E\left[y_1(t)|\phi(t)\right] = -K_1K_2\alpha\tilde{A}\int_t^\infty \left\{E\left[\sin\phi\ (u)\right] - \frac{\delta\ddot{\theta}}{C_1K_1K_2\alpha\tilde{A}}\right\}du$$

But $\phi(\infty) = C_1y_0(\infty) + C_0y_1(\infty)$, so that since $\phi(\infty)$ is a finite constant (if a solution exists), then $y_0(\infty)$ and $y_1(\infty)$ must be finite constants also (since C_0, C_1 are arbitrary). But

$$y_1(t) = \frac{d}{dt}\,y_0(t)$$

so that for $y_0(\infty)\left(=\lim_{t\to\infty} y_0(t)\right)$ to exist, $y_1(\infty)\left(=\lim_{t\to\infty} y_1(t)\right)$ must vanish.

Hence $E\left[y_1(\infty)\,|\,\phi(\infty)\right] = 0$, and there is

$$E\left[y_1(t)\,|\,\phi(t)\right] = K_1K_2\alpha\tilde{A}\int_t^\infty \left\{E\left[\sin\phi(u)\,|\,\phi(t)\right] - \frac{\delta\ddot{\theta}}{C_1K_1K_2\alpha\tilde{A}}\right\}du$$

Then equation (A13) becomes, still without any approximations,

$$0 = \frac{d}{d\phi}\left\{\frac{4\alpha\tilde{A}}{K_1K_2N_o}\left[\left(\sin\phi(t) - \frac{\delta\ddot{\theta}}{C_1\alpha\tilde{A}K_1K_2}\right) - \frac{C_1}{C_0}\int_t^\infty \left\{E\left[\sin\phi(u)\,|\,\phi(t)\right] - \frac{\delta\ddot{\theta}}{C_1K_1K_2\alpha\tilde{A}}\right\}du\right]p(\phi) + \frac{dp(\phi)}{d\phi}\right\} \tag{A17}$$

The high SNR approximation that is necessary for a convenient analytical form can be demonstrated next. In the case of high SNR, the random fluctuations of $\phi(t)$ about its mean are small so that

$$E[\sin \phi(u) | \phi(t)] - \delta\ddot{\tilde{\theta}} \Big/ \left(C_1 K_1 K_2 \alpha \tilde{A}\right)$$

may be linearized. In fact, because of a linearization,

$$\sin \phi(t) - \frac{\delta \ddot{\tilde{\theta}}}{C_1 K_1 K_2 \alpha \tilde{A}}$$

is gaussian with zero mean (at high SNR); this gaussian approximation is used to evaluate $E(y_1|\phi)$ only – it is not used in the other more significant terms in equation (A17). Let

$$y_2(u) = \sin \phi(u) - \frac{\delta \ddot{\tilde{\theta}}}{C_1 K_1 K_2 \alpha \tilde{A}}$$

$$y_1(t) = \phi(t)$$

$y_2(u)$ is approximately gaussian with zero mean and $1/\alpha$ variance, as is $y_1(t)$. But

$$p\left[y_2 \middle| y_1\right] = \frac{\sqrt{\alpha}}{\sqrt{2\pi}\sqrt{1-\rho^2}} \exp - \left\{\frac{\alpha (y_2 - \rho y_1)^2}{2(1-\rho^2)}\right\}$$

where $\rho(u-t)$ is the normalized covariance function. Then defining normalized variables $z_2 = \sqrt{\alpha}\, y_2$ and $z_1 = \sqrt{\alpha}\, y_1$,

$$E\left[z_2 | z_1\right] = \int_{-\infty}^{\infty} z_2\, p(z_2 | z_1)\, dz_2$$

$$= \int_{-\infty}^{\infty} \frac{z_2}{\sqrt{2\pi}\sqrt{1-\rho^2}} \exp\left\{-\frac{(z_2 - \rho z_1)}{2(1-\rho^2)}\right\} dz_2$$

$$= \frac{\sqrt{1-\rho}}{\sqrt{2\pi}} \int_{-\infty}^{\infty} \exp\left[\frac{-(z_2 - \rho z_1)^2}{2(1-\rho^2)}\right] \left\{\frac{-(z_2 - \rho z_1)}{(1-\rho^2)}\right\} dz_2$$

$$+ \frac{1}{\sqrt{2\pi}\sqrt{1-\rho^2}} \int_{-\infty}^{\infty} \rho z_1 \exp\left[-\frac{(z_2 - \rho z_1)^2}{2(1-\rho^2)}\right] dz_2$$

The first term is just of the form

$$-\frac{\sqrt{1-\rho^2}}{\sqrt{2\pi}} \int_{-\infty}^{\infty} \exp\left[-a^2\right] a\, da = 0 \text{ (by odd symmetry)}$$

Then

$$E(z_2 | z_1) = \rho z_1 \int_{-\infty}^{\infty} \frac{\exp\left[-\frac{(z_2 - \rho z_1)^2}{2(1-\rho^2)}\right]}{\sqrt{2\pi}\sqrt{1-\rho^2}}\, dz_2$$

$$= \rho z_1 \int_{-\infty}^{\infty} \frac{1}{\sqrt{\pi}} \exp\left[-x^2\right] dx$$

$$E(z_2 | z_1) = \rho z_1$$

Therefore,

$$\int_{\tau=0}^{\infty}\left[\left\{E \sin \phi(t+\tau)\,\middle|\,\phi(t)\right\} - \frac{\delta\ddot{\theta}}{C_1K_1K_2\alpha\tilde{A}}\right]d\tau \cong \left[\int_{\tau=0}^{\infty}\rho_\phi(\tau)\,dt\right]\phi(t)$$

$$\cong \left[\int_0^{\infty}\rho_\phi(\tau)\,dt\right]\sin\phi(t)$$

By the Wiener-Khintchine theorem,

$$\int_0^{\infty}\rho_\phi(\tau)\,d\tau = \frac{1}{2\sigma_{y_2}^2}\int_{-\infty}^{\infty}R_\phi(\tau)\,d\tau = \frac{S_\phi(0)}{2\sigma_\phi^2}$$

where the phase spectral density is

$$S_\phi(\omega) = \left|\frac{K_1K_2F(i\omega)/i\omega}{1+\alpha\tilde{A}K_1K_2F(i\omega)/i\omega}\right|^2 S_n(\omega)$$

$$= \frac{N_0}{2(\alpha\tilde{A})^2}\left|H(i\omega)\right|^2$$

Where $S_n(\omega) = N_0/2$ is the one-sided white noise spectral density and $H(i\omega)$ is the closed-loop transfer function of the phase-locked loop. For the second-order loop being discussed,

$$F(s) = \frac{C_0s + C_1}{s}$$

The closed-loop transfer function is

$$H(s) = \frac{\alpha\tilde{A}K_1K_2(C_0s + C_1)}{s^2+\alpha\tilde{A}K_1K_2(C_0s+C_1)}$$

$$H(0) = \frac{\alpha\tilde{A}K_1K_2C_1}{\alpha\tilde{A}K_1K_2C_1} = 1$$

Therefore,

$$S_\phi(0) = N_0/2(\alpha\tilde{A})^2$$

The phase variance is

$$\sigma_\phi^2 = \lim_{T\to\infty} \frac{1}{2T} \int_{-T}^{T} |\phi(t)|^2 \, dt = \frac{1}{2\pi} \int_{-\infty}^{\infty} S_\phi(\omega) \, d\omega$$

$$= \frac{1}{2\pi} \frac{N_0'(K_1K_2C_0)^2}{2} \int_{-\infty}^{\infty} \left| \frac{\left(i\omega + \frac{C_1}{C_0}\right)}{\left[-\omega^2 + (AK_1K_2C_0)\, i\omega + (\alpha\tilde{A}K_1K_2C_0)\frac{C_1}{C_0}\right]} \right|^2 d\omega$$

$$\sigma_\phi^2 = \frac{N_0'}{4(\alpha\tilde{A})^2} \left(\alpha\tilde{A}K_1K_2C_0 + \frac{C_1}{C_0}\right)$$

Then

$$\int_0^\infty \left\{ E\left\{\sin\phi(t+\tau) \middle| \phi(t)\right\} - \frac{\delta\ddot{\theta}}{C_1K_1K_2\alpha\tilde{A}} \right\} d\tau \cong \frac{\sin\phi(t)}{\alpha\tilde{A}K_1K_2C_0 + C_1/C_0} \qquad \text{(A18)}$$

which is valid only for high SNR and small $\delta\ddot{\theta}$.

Finally, equation (A17) may now be rewritten as

$$0 = \frac{d}{d\phi}\left\{ \frac{4\alpha\tilde{A}}{K_1K_2N_0} \left[(\sin\phi)\left(1 - \frac{1}{\alpha\tilde{A}K_1K_2C_0{}^2/C_1 + 1}\right) - \frac{\delta\dddot{\theta}}{C_1\alpha\tilde{A}K_1K_2} \right] p(\phi) + \frac{dp(\phi)}{d\phi} \right\}$$

$$= \frac{d}{d\phi}\left\{ \frac{4\alpha\tilde{A}}{K_1K_2N_0} \left(\frac{\alpha\tilde{A}K_1K_2C_0{}^2/C_1}{\alpha\tilde{A}K_1K_2C_0{}^2K_1 + 1} \sin\phi - \frac{\delta\dddot{\theta}}{C_1\alpha\tilde{A}K_1K_2} \right) p(\phi) + \frac{dp(\phi)}{d\phi} \right\}$$

With the boundary conditions

$$p(\pi) = p(-\pi)$$

$$\int_{-\pi}^{\pi} p(\phi)\, d\phi = 1$$

the rewritten equation gives the solution for high SNR:

$$p(\phi \mid \delta\ddot{\theta}) = C \exp\left\{\frac{4(\alpha\tilde{A})^2/N_0}{\alpha\tilde{A}K_1K_2 + \frac{C_1}{C_0^2}}(\cos\phi) + \frac{(4\delta\ddot{\theta})\phi}{C_1N_0(K_1K_2)^2}\right\}$$

$$\cdot\left[1 + D\int_{-\pi}^{\phi}\exp\left\{-\frac{4(\alpha\tilde{A})^2\cos x}{\left(\alpha\tilde{A}K_1K_2 + C_1/C_0^2\right)N_0} - \frac{4\delta\ddot{\theta}\, x}{C_1N_0(K_1K_2)^2}\right\}dx\right] \quad -\pi \le \phi < \pi \qquad \text{(A19)}$$

where

$$\begin{cases} D = \dfrac{\exp\left(-2\pi\, 4\delta\ddot{\theta}/C_1N_0(K_1K_2)^2\right) - 1}{\int_{-\pi}^{\pi}\exp\left\{-\dfrac{4(\alpha\tilde{A})^2\cos x}{N_0(\alpha\tilde{A}K_1K_2 + C_1/C_0^2)} - \dfrac{4\delta\ddot{\theta}\, x}{C_1N_0(K_1K_2)^2}\right\}dx} \\ C = 1\Big/\int_{-\pi}^{\pi}\dfrac{p(\phi)}{C}\,d\phi \end{cases}$$

APPENDIX B

PROBABILITY DENSITY FUNCTIONS OF PHASE ERRORS IN MULTI-ELEMENT ARRAYS

For independent phase-locked loops, the characteristic function of the sum of the phases is the same as the product of the characteristic functions of the components, i.e.,

$$M(jv) = \prod_{i=1}^{N} M_{\varphi_i}(jv) \tag{B1}$$

Consequently, the density function $\left(p(\gamma) = \mathfrak{F}[M_\gamma(jv)]\right)$ of the sum is an (N-1) dimensional convolution of the density functions of the components.

(1) For N = 2, this procedure yields

$$p_{2\gamma}(x) = \int_{-\infty}^{\infty} p_{\varphi_1}(x - \varphi_2) p_{\varphi_2}(\varphi_2)\, d\varphi_2 \tag{B2}$$

But

$$p_\varphi(\varphi) = C \exp[a \cos\varphi]\,[U(\varphi + \pi) - U(\varphi - \pi)]$$

where U(x) is the unit step function, so that

$$p_{2\gamma}(x) = C^2 \int_{-\infty}^{\infty} \exp\left[a\cos(x-\varphi_2)\right] \exp\left[a\cos\varphi_2\right] \left[U(x-\varphi_2+\pi) - U(x-\varphi_2-\pi)\right] \cdot \left[U(\varphi_2+\pi) - U(\varphi_2-\pi)\right] d\varphi_2$$

$$= C^2 \int_{-\pi}^{\pi} \exp\left\{a\left[\cos(x-\varphi_2) + \cos\varphi_2\right]\right\} \left[U(x-\varphi_2+\pi) - U(x-\varphi_2-\pi)\right] d\varphi_2$$

$$= C^2 \int_{-\pi}^{\pi} \exp\left[2a\cos\frac{x}{2}\cos\left(\varphi_2 - \frac{x}{2}\right)\right] \left[U(x-\varphi_2+\pi) - U(x-\varphi_2-\pi)\right] d\varphi_2$$

The substitution is made that $\varphi = \varphi_2 - x/2$. Then

$$p_{2\gamma}(x) = \begin{cases} C^2 \displaystyle\int_{-\pi-x/2}^{x+\pi-x/2} \exp\left[2a\cos\frac{x}{2}\cos\varphi\right] d\varphi & -2\pi \le x \le 0 \\ C^2 \displaystyle\int_{x-\pi-x/2}^{\pi-x/2} \exp\left[2a\cos\frac{x}{2}\cos\varphi\right] d\varphi & 2\pi \ge x \ge 0 \end{cases}$$

$$p_{2\gamma}(x) = \left\{ \begin{array}{ll} C^2 \int_{-(\pi+x/2)}^{(\pi+x/2)} \exp\left[2a \cos\frac{x}{2}\cos\varphi\right] d\varphi & x \le 0 \\ C^2 \int_{-(\pi-x/2)}^{(\pi-x/2)} \exp\left[2a \cos\frac{x}{2}\cos\varphi\right] d\varphi & x \ge 0 \end{array} \right\} \quad |x| < 2\pi$$

$$p_{2\gamma}(x) = C^2 \int_{-(\pi-|x/2|)}^{(\pi-|x/2|)} \exp\left[2a \cos\frac{x}{2}\cos\varphi\right] d\varphi \qquad |x| < 2\pi$$

$$p_{2\gamma}(2\gamma) = C^2 \int_{-(\pi-|\gamma|)}^{(\pi-|\gamma|)} \exp\left[2a \cos\gamma \cos\varphi\right] d\varphi \qquad |\gamma| < \pi$$

$$p_{\gamma}(\gamma) = 2p_{2\gamma}(2\gamma) = \frac{1}{\pi^2 I_0^2(a)} \int_0^{\pi-|\gamma|} \exp[2a \cos\gamma \cos\varphi]\, d\varphi \qquad |\gamma| < \pi \quad \text{(B3)}$$

which is equation (21).

(2) For N = 3, $\xi \neq \frac{1}{3}(\varphi_1 + \varphi_2 + \varphi_3)$. In general

$$\tan\xi = \frac{\sin\varphi_1 + \sin\varphi_2 + \sin\varphi_3}{\cos\varphi_1 + \cos\varphi_2 + \cos\varphi_4}$$

However, for small σ_φ,

$$\xi \approx \frac{\sin\varphi_1 + \sin\varphi_2 + \sin\varphi_3}{\cos\varphi_1 + \cos\varphi_2 + \cos\varphi_3} \approx (\varphi_1 + \varphi_2 + \varphi_3)/3$$

$$M_{3\xi}(jv) = E\left\{\exp[jv\xi]\right\} = M_{\varphi}(jv)\, M_{\varphi_2}(jv)\, M_{\varphi_3}(jv) \quad \text{(B4)}$$

$$= \left[\int_{-\pi}^{\pi} d\varphi_1 p(\varphi_1)\exp\left(jv\varphi_1\right)\right]\left[\int_{-\pi}^{\pi} d\varphi_2 p(\varphi_2)\exp\left(jv\varphi_2\right)\right]\left[\int_{-\pi}^{\pi} d\varphi_3 p(\varphi_3)\exp\left(jv\varphi_3\right)\right]$$

$$= \int_{-\pi}^{\pi} d\varphi_1 p(\varphi_1) \int_{-\pi}^{\pi} d\varphi_2 p(\varphi_2) \int_{-\pi}^{\pi} d\varphi_3 p(\varphi_3)\exp\left[jv(\varphi_1+\varphi_2+\varphi_3)\right]$$

$$p_{3\xi}(x) = \int_{-\infty}^{\infty} dv \exp[jvx] \int_{-\pi}^{\pi} d\varphi_1 p(\varphi_1) \int_{-\pi}^{\pi} d\varphi_2 p(\varphi_2) \int_{-\pi}^{\pi} d\varphi_3 p(\varphi_3) \exp\left[jv\left(\varphi_1+\varphi_2+\varphi_3\right)\right]$$

$$= \int_{-\pi}^{\pi} d\varphi_1 p(\varphi_1) \int_{-\pi}^{\pi} d\varphi_2 p(\varphi_2) \int_{-\pi}^{\pi} d\varphi_3 p(\varphi_3) \int_{-\infty}^{\infty} dv \exp\left\{-jv\left[x-\left(\varphi_1+\varphi_2+\varphi_3\right)\right]\right\}$$

$$= \int_{-\pi}^{\pi} d\varphi_2 p(\varphi_2) \int_{-\pi}^{\pi} d\varphi_3 p(\varphi_3) p\left(x-\varphi_2-\varphi_3\right)\left[U\left(x-\varphi_2-\varphi_3+\pi\right) - U\left(x-\varphi_2-\varphi_3-\pi\right)\right]$$

$$= \int_{-\pi}^{\pi} d\varphi_2 p(\varphi_2) \int_{-\infty}^{\infty} d\varphi_3 p(\varphi_3) p\left(x-\varphi_2-\varphi_3\right)\left[U(\varphi_3+\pi) - U(\varphi_3-\pi)\right]$$
$$\cdot\left[U\left(x-\varphi_2-\varphi_3+\pi\right) - U\left(x-\varphi_2-\varphi_3-\pi\right)\right]$$

$$= \int_{-\pi}^{\pi} d\varphi_2 p(\varphi_2) \cdot \begin{cases} 0 & \begin{cases} x+2\pi<\varphi_2<\infty \\ -\infty<\varphi_2<x-2\pi \end{cases} \\ \int_{x-\varphi_2-\pi}^{\pi} d\varphi_3 p(\varphi_3) p\left(x-\varphi_2-\varphi_3\right) & \text{for} \quad x-2\pi<\varphi_2<x \\ \int_{-\pi}^{x-\varphi_2+\pi} d\varphi_3 p(\varphi_3) p\left(x-\varphi_2-\varphi_3\right) & \text{for} \quad x<\varphi_2<x+2\pi \end{cases}$$

$$= \int_{x-2\pi}^{\pi} d\varphi_2 p(\varphi_2) \int_{x-\varphi_2-\pi}^{\pi} d\varphi_3 p(\varphi_3) p\left(x-\varphi_2-\varphi_3\right) \qquad \text{for} \quad \pi<x<3\pi$$

$$= \int_{-\pi}^{x} d\varphi_2 p(\varphi_2) \int_{x-\varphi_2-\pi}^{\pi} d\varphi_3 p(\varphi_3) p\left(x-\varphi_2-\varphi_3\right) \qquad \text{for} \quad -\pi<x<\pi$$
$$+ \int_{x}^{\pi} d\varphi_2 p(\varphi_2) \int_{\pi}^{x-\varphi_2+\pi} d\varphi_3 p(\varphi_3) p\left(x-\varphi_2-\varphi_3\right)$$

and

$$p_{3\xi}(x) = \int_{-\pi}^{x+2\pi} d\varphi_2\, p(\varphi_2) \int_{-\pi}^{x-\varphi_2+\pi} d\varphi_3\, p(\varphi_3)\, p(x-\varphi_2-\varphi_3) \qquad \text{for} \quad -3\pi<x<-\pi$$

But $p(\varphi) = p(-\varphi)$ so that

$$p_{3\xi}(x) = \int_{-\pi}^{-|x|+2\pi} d\varphi_2\, p(\varphi_2) \int_{-\pi}^{-|x|-\varphi_2+\pi} d\varphi_3\, p(\varphi_3)\, p(|x|+\varphi_2+\varphi_3) \qquad \text{for} \quad \pi<x<3\pi$$

$$= \int_{-\pi}^{x} d\varphi_2\, p(\varphi_2) \int_{x-\varphi_2-\pi}^{\pi} d\varphi_3\, p(\varphi_3)\, p(x-\varphi_2-\varphi_3)$$

$$+ \int_{-\pi}^{-x} d\varphi_2\, p(\varphi_2) \int_{-x-\varphi_2-\pi}^{\pi} d\varphi 3\, p(\varphi_3)\, p(x+\varphi_2+\varphi_3) \qquad \text{for} \quad |x|<\pi$$

$$\left[\text{where} \quad p(x+\varphi_2+\varphi_3) = p(-x-\varphi_2-\varphi_3)\right]$$

$$= \int_{-\pi}^{-|x|+2\pi} d\varphi_2\, p(\varphi_2) \int_{-\pi}^{-|x|-\varphi_2+\pi} d\varphi_3\, p(\varphi_3)\, p(-|x|-\varphi_2-\varphi_3) \qquad \text{for} \quad -3\pi<x<-\pi$$

$$\left[\text{where} \quad p(-|x|-\varphi_2-\varphi_3) = p(|x|+\varphi_2+\varphi_3)\right]$$

$$= \int_{-\pi}^{-|x|+2\pi} d\varphi_2\, p(\varphi_2) \int_{-\pi}^{-|x|-\varphi_2+\pi} d\varphi_3\, p(\varphi_3)\, p(|x|+\varphi_2+\varphi_3) \qquad \text{for} \quad \pi<|x|<3\pi$$

$$= \int_{-\pi}^{|x|} d\varphi_2\, p(\varphi_2) \int_{|x|-\varphi_2-\pi}^{\pi} d\varphi_3 p(\varphi_3)\, p(|x|-\varphi_2-\varphi_3)$$

$$+ \int_{-\pi}^{-|x|} d\varphi_2\, p(\varphi_2) \int_{-|x|-\varphi_2-\pi}^{\pi} d\varphi_3\, p(\varphi_3)\, p(-|x|-\varphi_2-\varphi_3) \qquad \text{for} \quad |x|<\pi$$

$$p_{3\gamma}(x) = \int_{|x|-2\pi}^{\pi} d\varphi_2\, p(\varphi_2) \int_{|x|-\varphi_2-\pi}^{\pi} d\varphi_3\, p(\varphi_3)\, p\left(|x| - \varphi_2 - \varphi_3\right) \quad \text{for} \quad \pi<|x|<3\pi$$

$$= \int_{-|x|}^{\pi} d\varphi_2\, p(\varphi_2) \int_{|x|+\varphi_2-\pi}^{\pi} d\varphi_3\, p(\varphi_3)\, p\left(|x| + \varphi_2 - \varphi_3\right)$$

$$+ \int_{|x|}^{\pi} d\varphi_2\, p(\varphi_2) \int_{-|x|+\varphi_2-\pi}^{\pi} d\varphi_3\, p(\varphi_3)\, p\left(-|x| + \varphi_2 - \varphi_3\right) \quad \text{for} \quad |x|<\pi$$

Therefore,

$$p_{\gamma}(\gamma) = 3 \int_{|3\gamma|-2\pi}^{\pi} d\varphi_3\, p(\varphi_3) \int_{|3\gamma|-\varphi_3-\pi}^{\pi} d\varphi_2\, p(\varphi_2)\, p\left(|3\gamma| - \varphi_3 - \varphi_2\right) \quad \text{for} \quad \frac{\pi}{3}<|\gamma|<\pi$$

$$= 3 \int_{-|3\gamma|}^{\pi} d\varphi_3 p(\varphi_3) \int_{|3\gamma|+\varphi_3-\pi}^{\pi} d\varphi_2 p(\varphi_2)\, p\left(|3\gamma| + \varphi_3 - \varphi_2\right)$$

$$+ 3 \int_{|3\gamma|}^{\pi} d\varphi_3 p(\varphi_3) \int_{-|3\gamma|+\varphi_3-\pi}^{\pi} d\varphi_2 p(\varphi_2) p\left(-|3\gamma| + \varphi_3 - \varphi_2\right) \quad \text{for} \quad |\gamma|<\frac{\pi}{3}$$

$$p_\gamma(\gamma) = \frac{3}{\left[2\pi I_0(a)\right]^3} \int_{|3\gamma|-2\pi}^{\pi} dx \exp[a\cos x] \int_{|3\gamma|-x-\pi}^{\pi} dy \exp[a\cos y] \cdot \exp\left[a\cos\left(|3\gamma| - x - y\right)\right]$$

$$\text{for } \frac{\pi}{3} < |\gamma| < \pi \tag{B5}$$

$$= \frac{3}{\left[2\pi I_0(a)\right]^3} \left\{ \int_{-|3\gamma|}^{\pi} dx \exp[a\cos x] \int_{|3\gamma|+x-\pi}^{\pi} dy \exp[a\cos y] \cdot \exp\left[a\cos\left(|3\gamma| + x - y\right)\right] \right.$$

$$\left. + \int_{|3\gamma|}^{\pi} dx \exp[a\cos x] \int_{-|3\gamma|+x-\pi}^{\pi} dy \exp[a\cos y] \cdot \exp\left[a\cos\left(|3\gamma| + x - y\right)\right] \right\}$$

$$\text{for } |\gamma| < \frac{\pi}{3}$$

which is equation (136).

APPENDIX C

AVERAGE ERROR PROBABILITIES OF COHERENT PHASE SHIFT KEY MODULATION IN A MULTIPATH ENVIRONMENT

For coherent phase shift key (PSK) demodulation, ϕ_{1k} and ϕ_{2k} independent of k are

$$\phi_1(t) = \sqrt{\frac{2}{T}} \cos(\omega t - \theta)$$
$$\phi_2(t) = \sqrt{\frac{2}{T}} \sin(\omega t - \theta) \tag{C1}$$

The signal energies and frequencies are similarly independent of coding subscripts so that

$$E_p = E_s = E$$
$$\omega_p = \omega_s = \omega \tag{C2}$$

Then the correlator outputs become [from equation (60)]

$$x = a_{1ps} \cos\theta + b_{1ps} \sin\theta + n_1$$
$$y = a_{2ps} \cos\theta + b_{2ps} \sin\theta + n_2 \tag{C3}$$

where

$$a_{1ps} = \sqrt{E} \cos\phi_p + \Omega\sqrt{E} \cos(\phi_s + \omega\tau)$$
$$a_{2ps} = -\sqrt{E} \sin\phi_p - \Omega\sqrt{E} \sin(\phi_s + \omega\tau)$$
$$b_{1ps} = \sqrt{E} \sin\phi_p + \Omega\sqrt{E} \sin(\phi_s + \omega\tau)$$
$$b_{2ps} = \sqrt{E} \cos\phi_p + \Omega\sqrt{E} \cos(\phi_s + \omega\tau)$$

and the phase code is $\phi_i = \frac{2\pi i}{m}$. (C4)

The noise terms n_1, n_2 are independent gaussian variables of variance variance N_0

$$p(x, y \mid p, s, \theta, \tau) = \frac{1}{2\pi N_0} \exp \left\{ - \frac{1}{2N_0} \left[\left(x - a_{1ps} \cos\theta - b_{1ps} \sin\theta \right)^2 + \left(y - a_{2ps} \cos\theta - b_{2ps} \sin\theta \right)^2 \right] \right\}$$

$$= \frac{1}{2\pi N_0} \exp \left\{ - \frac{1}{2} \left[\left(\frac{x}{\sqrt{N_0}} - \sqrt{\frac{E}{N_0}} \left[\cos\left(\theta - \frac{2\pi p}{m} \right) + \Omega \cos\left(\theta - \frac{2\pi s}{m} - \omega\tau \right) \right] \right)^2 + \left(\frac{y}{\sqrt{N_0}} - \sqrt{\frac{E}{N_0}} \left[\sin\left(\theta - \frac{2\pi p}{m} \right) + \Omega \sin\left(\theta - \frac{2\pi s}{m} - \omega\tau \right) \right] \right)^2 \right] \right\} \qquad (C5)$$

Average error probability is then

$$P_e = \int_0^\infty d\tau p(\tau) \int_0^\infty d\theta p(\theta) \frac{1}{m} \sum_{s=1}^{m} \frac{1}{m} \sum_{p=1}^{m} P_e(p, s, \theta, \tau) \qquad (C6)$$

But

$$P_e(p, s, \theta, \tau) = \Pr\left(x, y \notin R_p \mid p, s, \theta, \tau \right)$$

$$= 1 - \int_0^\infty dx \int_{x\tan\left(-\frac{2\pi p}{m} - \frac{\pi}{m} \right)}^{x\tan\left(-\frac{2\pi p}{m} + \frac{\pi}{m} \right)} dy \; p(x, y \mid p, s, \theta, \tau) \qquad (C7)$$

Then, by symmetry,

$$P_e(\theta, \tau) = 1 - \int_0^\infty dx \int_{x\tan\left(-\frac{2\pi p}{m} - \frac{\pi}{m} \right)}^{x\tan\left(-\frac{2\pi p}{m} + \frac{\pi}{m} \right)} dy \frac{1}{m} \sum_{s=1}^{m} p(x, y \mid p, s, \theta, \tau) \qquad (C8)$$

For perfect coherence ($\theta = 0$) and binary coding ($m = 2$), this expression yields

$$P_e(\tau) = 1 - \int_0^{\infty} dx \int_{x\tan\left(-\frac{\pi}{2}\right)}^{x\tan\left(+\frac{\pi}{2}\right)} dy \, \frac{1}{2} \sum_{s=1}^{2} p(x, y \mid 0, s, 0, \tau) \tag{C9}$$

where

$$p(x, y \mid 0, s, 0, \tau) = \frac{1}{2\pi N_0} \exp\left[-\frac{1}{2}\left\{\left[\frac{x}{\sqrt{N_0}} - \sqrt{\frac{E}{N_0}}\left(1 + \Omega\cos\left[\omega\tau + \pi s\right]\right)\right]^2 + \left[\frac{y}{\sqrt{N_0}} + \sqrt{\frac{E}{N_0}}\,\Omega\sin\left(\omega\tau + \pi s\right)\right]^2\right\}\right] \tag{C10}$$

Therefore,

$$P_e(\tau) = 1 - \int_0^{\infty} dx \frac{1}{2} \sum_{s=1}^{2} \int_{-\infty}^{\infty} dy \, \frac{\exp\left[-\frac{1}{2}\left(\frac{x}{\sqrt{N_0}} - \sqrt{\frac{E}{N_0}}\left[1+\Omega\cos(\omega\tau+\pi s)\right]\right)^2\right]}{\sqrt{2\pi N_0}} \cdot \frac{\exp\left[-\frac{1}{2}\left(\frac{y}{\sqrt{N_0}} + \sqrt{\frac{E}{N_0}}\,\Omega\sin(\omega\tau+\pi s)\right)^2\right]}{\sqrt{2\,N_0}}$$

$$= 1 - \frac{1}{2} \sum_{s=1}^{2} \int_0^{\infty} dx \, \frac{\exp - \frac{1}{2}\left[x - \sqrt{\frac{E}{N_0}}\left(1+\Omega\cos\left[\omega\tau+\pi s\right]\right)^2\right]}{\sqrt{2\pi}}$$

$$= 1 - \frac{1}{2} \sum_{s=1}^{2} \left\{1 - \Phi\left[-\sqrt{\frac{E}{N_0}}\left(1+\Omega\cos\left[\omega\tau+\pi s\right]\right)\right]\right\}$$

$$= \frac{1}{2}\Phi\left[-\sqrt{\frac{E}{N_0}}\left(1-\Omega\left|\cos\omega\tau\right|\right)\right] + \frac{1}{2}\Phi\left[-\sqrt{\frac{E}{N_0}}\left(1+\Omega\left|\cos\omega\tau\right|\right)\right] \tag{C11}$$

APPENDIX D

AVERAGE ERROR PROBABILITIES OF DIFFERENTIALLY COHERENT PHASE SHIFT KEY MODULATION IN A MULTIPATH ENVIRONMENT

The operation of differentially coherent phase shift key (DPSK) demodulators is the same as that of PSK demodulators with the exception that the decoding is achieved by the detection of phase differences rather than absolute phase.

The present correlator outputs are then

$$x_1 = \sqrt{E}\cos\left(\frac{2\pi p}{m} + \phi_p + \theta\right) + \Omega\sqrt{E}\cos\left(\frac{2\pi s}{m} + \phi_s + \omega\tau + \theta\right) + n_{11}$$

$$y_1 = \sqrt{E}\sin\left(\frac{2\pi p}{m} + \phi_p + \theta\right) - \Omega\sqrt{E}\sin\left(\frac{2\pi s}{m} + \phi_s + \omega\tau + \theta\right) + n_{12} \qquad \text{(D1)}$$

and the preceding correlator outputs are

$$x_2 = \sqrt{E}\cos\left(\phi_p + \theta\right) + \Omega\sqrt{E}\cos\left(\phi_s + \omega\tau + \theta\right) + n_{21}$$

$$y_2 = -\sqrt{E}\sin\left(\phi_p + \theta\right) - \Omega\sqrt{E}\sin\left(\phi_s + \omega\tau + \theta\right) + n_{22} \qquad \text{(D2)}$$

The demodulator then calculates the phase difference between x_1, y_1 and x_2, y_2. The difference is used as a basis for the decoding decision according to its closeness to the phase $2\pi i/m$.

For $\Omega = 0$, the phase difference, η, is just $2\pi p/m$ perturbed by the phasor transformation of the gaussian noises n_{11}, n_{12}, n_{21}, n_{22}.

This noise perturbation must be more than π/m (in phase magnitude) for an error to arise. The error probability is given by

$$P_e(\tau) = \frac{1}{m} \sum_{s=1}^{m} \int_{\pi/m}^{\pi} d\eta \, p(\eta \,|\, s, \tau) \tag{D3}$$

The probability density function, $p(\eta \,|\, s, \tau)$, has been derived for $\Omega = 0$ by Fleck and Trabka;[41]

$$p(\eta \,|\, \Omega = 0) = \frac{1}{\pi} \int_{\phi=0}^{\pi/2} \sin\phi \left[1 + \frac{E}{2N_0}(1 + \cos\eta \sin\phi)\right] \exp\left[-\frac{E}{2N_0}(1 - \cos\eta \sin\phi)\right] d\phi \qquad \eta > 0 \tag{D4}$$

This expression must be modified in accordance with the phase distortions introduced by the Ω-dependent terms in equations (D1) and (D2).

APPENDIX E

AVERAGE ERROR PROBABILITIES OF COHERENT FREQUENCY SHIFT KEY MODULATION IN A MULTIPATH ENVIRONMENT

For coherent frequency shift key (FSK) detection, only ϕ_{1k} is used for the correlator. The correlator outputs are then

$$x_k = \int_0^T s(t)\,\phi_{1k}(t)\,dt = \frac{2\sqrt{E}}{T}\int_0^T \cos\left(\omega_p t\right)\cos\left(\omega_k t - \theta_k\right)dt$$

$$+ \Omega\,\frac{2\sqrt{E}}{T}\int_0^T \cos\left[\omega_s(t+\tau)\right]\cos\left(\omega_k t - \theta_k\right)dt + n_k \quad . \qquad \text{(E1a)}$$

$$= \sqrt{E}\,a_{pk} + \Omega\sqrt{E}\,b_{sk} + n_k$$

where

$$a_{pk} = \frac{2}{T}\int_0^T \cos\omega_p t\cos\left(\omega_k t - \theta_k\right)dt = \begin{cases}\cos\theta_p\ , & k = p\\ 0\ , & k \neq p\end{cases} \qquad \text{(E1b)}$$

$$b_{sk} = \frac{2}{T}\int_0^T \cos\omega_s(t+\tau)\cos\left(\omega_k t - \theta_k\right)dt = \begin{cases}\cos\left(\theta_s + \omega_s\tau\right), & k = s\\ 0\ , & k \neq s\end{cases}$$

Since $n_1, n_2, \ldots, n_m$ are independent gaussian variables, the joint probability density function of correlator outputs, conditional on p and s, is

$$p\left(x_1, x_2, \ldots, x_m \mid p, s, \theta_p, \theta_s, \tau\right) = \frac{1}{\left(2\pi N_0\right)^{m/2}}$$

$$\prod_{k=1}^{m} \exp\left\{ - \frac{\left[x_k - \sqrt{E}\left(a_{pk} + \Omega b_{sk}\right)\right]^2}{2N_0} \right\} \tag{E2}$$

The error probability conditioned on p and s is then

$$P_e\left(p \neq s, \theta_p, \theta_s, \tau\right) = 1 - \frac{1}{\left(2\pi N_0\right)^{m/2}}$$

$$\cdot \int_{-\infty}^{\infty} dx_p \exp\left\{ - \frac{1}{2N_0}\left[x_p - \sqrt{E}\left(a_{pp} + \Omega b_{sp}\right)\right]^2 \right\}$$

$$\cdot \int_{-\infty}^{x_p} dx_p \exp\left\{ - \frac{1}{2N_0}\left[x_s - \sqrt{E}\left(a_{ps} + \Omega b_{ss}\right)\right]^2 \right\} \tag{E3}$$

$$\left[\int_{-\infty}^{x_p} \exp\left\{ - \frac{x_k^2}{2N_0} \right\} dx_s \right]^{m-2}$$

$$P_e\left(p = s, \theta_p, \theta_s, \tau\right) = 1 - \frac{1}{\left(2\pi N_0\right)^{m/2}}$$

$$\cdot \int_{-\infty}^{\infty} dx_p \exp\left\{ - \frac{1}{2N_0} \left[x_p - \sqrt{E}\left(a_{pp} + \Omega b_{sp}\right)\right]^2 \right\} \qquad \text{(E4)}$$

$$\cdot \left[\int_{-\infty}^{x_p} \exp\left\{- \frac{x_k^2}{2N_0}\right\} dx_p\right]^{m-1}$$

$$\text{But } P_e\left(\left|\theta_i\right|, \tau\right) = \frac{1}{m^2} \sum_{p=1}^{m} \sum_{s=1}^{m} P_e\left(p, s, \theta_p, \theta_s, \tau\right)$$

$$= \frac{1}{m^2} \sum_{p=1}^{m} P_e\left(p = s, \theta_p, \theta_s, \tau\right) \qquad \text{(E5)}$$

$$+ \frac{1}{m^2} \underbrace{\sum_{p=1}^{m} \sum_{s=1}^{m}}_{p \neq s} P_e\left(p \neq s, \theta_p, \theta_s, \tau\right)$$

And by symmetry

$$P_e\left(\left|\theta_i\right|,\tau\right)=\frac{\frac{1}{m}\sum_{p=1}^{m}P_c\left(p=s,\theta_p,\theta_s,\tau\right)}{m}+\frac{1}{m}\underbrace{\sum_{p=1}^{m}\sum_{s=1}^{m}}_{s\neq p}P_e\left(p,s,\theta_p,\theta_s,\tau\right)$$

$$=\frac{\frac{1}{m}\sum_{p=1}^{m}}{m}\left\{1-\frac{1}{\left(2\pi N_0\right)}m/2\int_{-\infty}^{\infty}dx\exp\left\{-\frac{1}{2N_0}\left[x\right.\right.\right.$$

$$\left.\left.\left.-\sqrt{E}\left(\cos\theta_p+\Omega\cos\left(\theta_p+\omega_p\tau\right)\right]\right]^2\right\}$$

$$\cdot\left[\int_{-\infty}^{x}\exp\left(\frac{-y^2}{2N_0}\right)dy\right]^{m-1}\Bigg\}$$

$$+\frac{1}{m^2}\sum_{\substack{p=1\\p\neq s}}^{m}\sum_{s=1}^{m}\left\{1-\frac{1}{\left(2\pi N_0\right)}m/2\right.$$

$$\cdot\int_{-\infty}^{\infty}dx\exp\left\{-\frac{1}{2N_0}\left[x-\sqrt{E}\cos\theta_p\right]^2\right\}$$

$$\cdot\int_{-\infty}^{x}dy\exp\left\{-\frac{1}{2N_0}\left[y-\sqrt{E}\,\Omega\cos\left(\theta_s+\omega_s\tau\right)\right]^2\right\}$$

$$\left.\cdot\left[\int_{-\infty}^{x}\exp\left(-\frac{z^2}{2N_0}\right)dz\right]^{m-2}\right\}\qquad\text{(E6)}$$

$$\text{Then } P_e(\tau) = \int_{-\infty}^{\infty} \cdots \int_{-\infty}^{\infty} d\theta_1 \prod_{s=2}^{m} d\theta_3 \, p(\theta_1) \, p(\theta_s) \, P_e(\theta_1, \theta_s, \tau) \qquad \text{(E7)}$$

For perfect coherence ($|\theta_i| \equiv 0$) and binary coding (m = 2), this expression yields

$$P_e(\tau) = \frac{1}{4} \sum_{p=1}^{2} \left[1 - \frac{1}{2\pi N_0} \int_{-\infty}^{\infty} dx \left\{ - \frac{1}{2N_0} \left[x - \sqrt{E} \left(1 + \Omega \cos \omega_p \tau \right) \right]^2 \right\} \right.$$

$$\left. \cdot \int_{-\infty}^{x} \exp \left[-y^2 / 2N_0 \right] dy \right]$$

$$+ \frac{1}{4} \sum_{\substack{p=1 \\ p \neq s}}^{2} \sum_{s=1}^{2} \left[1 - \frac{1}{2\pi N_0} \int_{-\infty}^{\infty} dx \exp \left[- \frac{(x - \sqrt{E})^2}{2N_0} \right] \right.$$

$$\left. \cdot \int_{-\infty}^{x} \exp - \frac{1}{2N_0} \left[y - \sqrt{E} \, \Omega \cos \omega_s \tau \right]^2 dy \right]$$

$$= 1 - \frac{1}{4} \int_{-\infty}^{\infty} \frac{dx}{\sqrt{2\pi}} \exp - \frac{1}{2} \left[x - \sqrt{\frac{E}{N_0}} \left(1 + \Omega \cos \omega_1 \tau \right) \right]^2$$

$$\cdot \int_{-\infty}^{x} \exp \left[-y^2 / 2 \right] \frac{dy}{\sqrt{2\pi}}$$

$$- \frac{1}{4} \int_{-\infty}^{\infty} \frac{dx}{\sqrt{2\pi}} \exp - \frac{1}{2} \left[x - \sqrt{\frac{E}{N_0}} \left(1 + \Omega \cos \omega_2 \tau \right) \right]^2$$

$$\int_{-\infty}^{x} \exp \left[- y^2/2 \right] \frac{dy}{\sqrt{2\pi}}$$

$$- \frac{1}{4} \int_{-\infty}^{\infty} \frac{dx}{\sqrt{2\pi}} \exp - \frac{\left(x - \sqrt{\frac{E}{N_0}} \right)^2}{2}$$

$$\cdot \int_{-\infty}^{x} \exp - \frac{\left(y - \sqrt{\frac{E}{N_0}} \Omega \cos \omega_1 \tau \right)^2}{2} \frac{dy}{\sqrt{2\pi}}$$

$$- \frac{1}{4} \int_{-\infty}^{\infty} \frac{dx}{\sqrt{2\pi}} \exp - \frac{\left(x - \sqrt{\frac{E}{N_0}} \right)^2}{2}$$

$$\cdot \int_{-\infty}^{x} \exp - \frac{\left(y - \sqrt{\frac{E}{N_0}} \Omega \cos \omega_2 \tau \right)^2}{2} \frac{dy}{\sqrt{2\pi}}$$

$$= 1 - \frac{1}{4}\int_{-\infty}^{\infty}\frac{dx}{\sqrt{2\pi}}\exp\left[-x^2/2\right]\int_{-\infty}^{x+\sqrt{\frac{E}{N_0}}\left(1+\Omega\cos\omega_1\tau\right)}\frac{dy}{\sqrt{2\pi}}\exp\left[-y^2/2\right]$$

$$- \frac{1}{4}\int_{-\infty}^{\infty}\frac{dx}{\sqrt{2\pi}}\exp\left[-x^2/2\right]\int_{-\infty}^{x+\sqrt{\frac{E}{N_0}}\left(1+\Omega\cos\omega_2\tau\right)}\frac{dy}{\sqrt{2\pi}}\exp\left[-y^2/2\right]$$

$$- \frac{1}{4}\int_{-\infty}^{\infty}\frac{dx}{\sqrt{2\pi}}\exp\left[-x^2/2\right]\int_{-\infty}^{x+\sqrt{\frac{E}{N_0}}\left(1-\Omega\cos\omega_1\tau\right)}\frac{dy}{\sqrt{2\pi}}\exp\left[-y^2/2\right]$$

$$- \frac{1}{4}\int_{-\infty}^{\infty}\frac{dx}{\sqrt{2\pi}}\exp\left[-x^2/2\right]\int_{-\infty}^{x+\sqrt{\frac{E}{N_0}}\left(1-\Omega\cos\omega_2\tau\right)}\frac{dy}{\sqrt{2\pi}}\exp\left[-y^2/2\right]$$

$$= 1 - \frac{1}{4}\sum_{k=1}^{2}\sum_{\ell=1}^{2}\int_{-\infty}^{\infty}\frac{\exp\left[-x^2/2\right]}{\sqrt{2\pi}}\Phi\left[x+\sqrt{\frac{E}{N_o}}\left(1+(-1)^k\cos\omega_\ell\tau\right)\right]dx \tag{E8}$$

These integrals are of the form

$$\int_{-\infty}^{\infty}\frac{dx}{\sqrt{2\pi}}\exp\left[-x^2/2\right]\int_{-\infty}^{x+K}\frac{dy}{\sqrt{2\pi}}\exp\left[-y^2/2\right] \tag{E9}$$

which can be simplified by a change of variable, a reversal of order of integration, and the completion of squares in the exponents:

$$\int_{-\infty}^{\infty}\frac{dx}{\sqrt{2\pi}}\exp\left[-x^2/2\right]\int_{-\infty}^{x+K}\frac{dy}{\sqrt{2\pi}}\exp\left[-\hat{y}^2/2\right] = \Phi\left(K\sqrt{2}\right) \tag{E10}$$

Therefore,

$$P_e(\tau) = 1 - \frac{1}{4} \sum_{k=1}^{2} \sum_{\ell=1}^{2} \Phi \left\{ \sqrt{\frac{E}{2N_0}} \left[1 + (-1)^k \cos\omega_\ell \tau \right] \right\}$$

$$= \frac{1}{2} \sum_{\ell=1}^{2} \left\{ \frac{1}{2} \Phi \left[-\sqrt{\frac{E}{2N_0}} \left(1 - \Omega \left| \cos\omega_\ell \tau \right| \right) \right] \right.$$

$$\left. + \frac{1}{2} \Phi \left[-\sqrt{\frac{E}{2N_0}} \left(1 + \Omega \left| \cos\omega_\ell \tau \right| \right) \right] \right\} \qquad \text{(E11)}$$

APPENDIX F

AVERAGE ERROR PROBABILITIES OF INCOHERENT FREQUENCY SHIFT KEY MODULATION IN A MULTIPATH ENVIRONMENT

The correlator outputs for incoherent frequency shift key (FSK) detectors are

$$x_k = \int_0^T s(t)\,\phi_{1k}(t)\,dt = \sqrt{E}\,a_{1pk} + \Omega\sqrt{E}\,b_{1sk} + n_{1k}$$

$$y_k = \int_0^T s(t)\,\phi_{2k}(t)\,dt = \sqrt{E}\,a_{2pk} + \Omega\sqrt{E}\,b_{2sk} + n_{2k} \qquad \text{(F1a)}$$

where

$$a_{1pk} = \frac{2}{T}\int_0^T \cos\omega_p t \cos\left(\omega_k t - \theta_k\right)dt = \begin{cases} \cos\theta_p, & k = p \\ 0, & k \neq p \end{cases}$$

$$a_{2pk} = \frac{2}{T}\int_0^T \sin\omega_p t \cos\left(\omega_k t - \theta_k\right)dt = \begin{cases} -\sin\theta_p, & k = p \\ 0, & k \neq p \end{cases}$$

$$b_{1sk} = \frac{2}{T}\int_0^T \cos\omega_s(t+\tau)\cos\left(\omega_k t - \theta_k\right)dt \qquad \text{(F1b)}$$

$$= \begin{cases} \cos\left(\theta_s + \omega_s\tau\right), & k = s \\ 0, & k \neq s \end{cases}$$

$$b_{2sk} = \frac{2}{T}\int_0^T \sin\omega_s(t+\tau)\cos\left(\omega_k t - \theta_k\right)dt$$

$$= \begin{cases} -\sin\left(\theta_s + \omega_s\tau\right), & k = s \\ 0, & k \neq s \end{cases}$$

Since $|n_{1k}, n_{2k}|$ is a set of mutually independent gaussian random variables with means zero and variances N_0, the random variable

$$\nu_k = \frac{|z_k|}{\sqrt{N_0}} = \frac{\sqrt{x_k^2 + y_k^2}}{\sqrt{N_0}} \tag{F2}$$

is Rician distributed:

$$p\left(\nu_k | s, p\right) = \nu_k I_0 \left[\nu_k \sqrt{\frac{E}{N_0} C_{psk}^2}\right] \exp\left[-\frac{1}{2}\left(\nu_k^2 + \frac{E}{N_0} C_{psk}^2\right)\right]$$

where

$$C_{psk}^2 = \left(a_{1pk} + \Omega b_{1sk}\right)^2 + \left(a_{2pk} + \Omega b_{2sk}\right)^2 \tag{F3}$$

$$1 - P_e\left(s, p, \tau, |\theta_k|\right) = Pr\left(\nu_p > \nu_k, \quad k \neq p\right)$$

$$= \int_0^\infty d\nu_p p\left(\nu_p\right) \prod_{\substack{k=1 \\ k \neq p}}^{m} \int_0^{\nu_p} d\nu_k \, p\left(\nu_k\right)$$

$$P_e\left(\tau, |\theta_k|\right) = 1 - \frac{1}{m} \sum_{s=1}^{m} \frac{1}{m} \sum_{p=1}^{m} \int_0^\infty d\nu_p p\left(\nu_p\right) \prod_{\substack{k=1 \\ k \neq p}}^{m} \int_0^{\nu_p} d\nu_k \, p\left(\nu_k\right) \tag{F4}$$

Then given the probability density function of phase-locked-loop phase outputs,

$$P_e(\tau) = \int_{-\infty}^{\infty} \cdots \int_{-\infty}^{\infty} d\theta_1 d\theta_2 \cdots d\theta_m p\left(\theta_1\right) p\left(\theta_2\right) \cdots p\left(\theta_m\right) P_e\left(\tau, |\theta_k|\right) \tag{F5}$$

Then specific values for C_{psk}^2 are

$$C_{sss}^2 = C_{ppp}^2 = \left[\cos\theta_p + \Omega \cos\left(\theta_p + \omega_p \tau\right)\right]^2 + \left[-\sin\theta_p - \Omega \sin\left(\theta_p + \omega_p \tau\right)\right]^2$$

$$= \left(1 + \Omega^2 + 2\Omega \cos\omega_p \tau\right)$$

$$C^2_{psp} = \left(\cos \theta_p \right)^2 + \left(-\sin \theta_p \right)^2$$

$$= 1 \quad , \qquad s \neq p$$

$$C^2_{pss} = \left[\Omega \cos \left(\theta_s + \omega_s \tau \right) \right]^2 + \left[-\Omega \sin \left(\theta_s + \omega_s \tau \right) \right]^2$$

$$= \Omega^2 \quad , \qquad s \neq p$$

$$C^2_{psk} = 0 \quad , \qquad k \neq s, \; k \neq p$$

APPENDIX G

AVERAGE ERROR PROBABILITIES OF COHERENT AMPLITUDE SHIFT KEY MODULATION IN A MULTIPATH ENVIRONMENT

For coherent amplitude shift key (ASK) detection, only the function $\phi_1(t) = \sqrt{\frac{2}{T}} \cos(\omega t - \theta)$ is used for correlation. The correlator outputs, then, are

$$\begin{aligned} x &= \int_0^T s(t)\phi_1(t)dt \\ &= \sqrt{E_p}\cos\theta + \Omega\sqrt{E_s}\cos(\theta+\omega\tau) + n \end{aligned} \tag{G1}$$

Since n is gaussian,

$$p(x|p,s,\theta,\tau) = \frac{1}{\sqrt{2\pi N_0}} \exp -\left[\frac{1}{2N_0}\left(x - \sqrt{E_p}\cos\theta - \Omega\sqrt{E_s}\cos(\theta+\omega\tau)\right)^2\right] \tag{G2}$$

Therefore, the conditional error probability is

$$P_e(p,s,\theta,\tau) = Pr\left(x \notin R_p | p,s,\theta,\tau\right)$$

The decision regions are based on the amplitude coding levels that are described by

$$E_1 \doteq 0$$

$$\sqrt{E_{k+1}} - \sqrt{E_k} = \Delta$$

$$\sqrt{E_k} = (k-1)\Delta$$

or therefore

$$\begin{aligned} P_e(1,s,\theta,\tau) &= Pr\left(x \notin R_1 | 1,s,\theta,\tau\right) \\ &= \int_{\Delta/2}^{\infty} p(x|1,s,\theta,\tau)dx \end{aligned}$$

$$= \int_{\frac{\Delta}{2\sqrt{N_0}}}^{\infty} \frac{1}{\sqrt{2x}} \exp\left\{-\frac{1}{2}\left[x - \Omega\sqrt{\frac{E_s}{N_0}}\cos(\theta+\omega\tau)\right]^2\right\} dx$$

$$P_e(1, s, \theta, \tau) = 1 - \Phi\left\{\frac{\Delta}{2\sqrt{N_0}}\left[1 - 2\Omega(s-1)\cos(\theta+\omega\tau)\right]^2\right\} \qquad \text{(G3)}$$

$$P_e(m, s, \theta, \tau) = \Pr\left(x \notin R_m \mid m, s, \theta, \tau\right)$$

$$= \int_{-\infty}^{\sqrt{E_m} - \frac{\Delta}{2}} p(x \mid m, s, \theta, \tau)\, dx$$

$$= \int_{-\infty}^{\left(m - \frac{3}{2}\right)\frac{\Delta}{\sqrt{N_0}}} dx \frac{1}{\sqrt{2\pi}} \exp\left\{-\frac{1}{2}\left[x - \frac{(m-1)\Delta}{\sqrt{N_0}}\cos\theta - \Omega\frac{(s-1)\Delta}{\sqrt{N_0}}\cos(\theta+\omega\tau)\right]^2\right\}$$

$$= \Phi\left\{\frac{\Delta}{2\sqrt{N_0}}\left[2m-3-(2m-2)\cos\theta-\Omega(2s-2)\cos(\theta+\omega\tau)\right]^2\right\}$$

$$= \Phi\left\{\frac{\Delta}{2\sqrt{N_0}}\left[-1+2(m-1)(1-\cos\theta)-2\Omega(s-1)\cos(\theta+\omega\tau)\right]\right\}$$

$$P_e(m, s, \theta, \tau) = \Phi\left\{\frac{(m-1)\Delta}{\sqrt{N_0}}\left[1 - \frac{1}{2(m-1)} - \cos\theta - \Omega\left(\frac{s-1}{m-1}\right)\cos(\theta+\omega\tau)\right]\right\} \qquad \text{(G4)}$$

$$= \frac{1}{m^2}\sum_{s=1}^{m}\left[1-\Phi\left\{\frac{\Delta}{2\sqrt{N_0}}\left[1-2\Omega(s-1)\cos(\theta+\omega\tau)\right]\right\}\right]$$

$$+\frac{1}{m^2}\sum_{s=1}^{m}\Phi\left\{\frac{(m-1)\Delta}{\sqrt{N_0}}\left[1-\frac{1}{2(m-1)}-\cos\theta-\Omega\left(\frac{s-1}{m-1}\right)\cos(\theta+\omega\tau)\right]\right\}$$

$$+\frac{m-2}{m}-\frac{1}{m^2}\sum_{s=1}^{m}\sum_{p=2}^{m-1}\Phi\left\{\frac{(p-1)\Delta}{\sqrt{N_0}}\left[1+\frac{1}{2(p-1)}-\cos\theta-\Omega\left(\frac{s-1}{p-1}\right)\cos(\theta+\omega\tau)\right]\right\}$$

$$+\frac{1}{m^2}\sum_{s=1}^{m}\sum_{p=2}^{m=1}\Phi\left\{\frac{(p-1)\Delta}{\sqrt{N_0}}\left[1-\frac{1}{2(p-1)}-\cos\theta-\Omega\left(\frac{s-1}{p-1}\right)\cos(\theta+\omega\tau)\right]\right\}$$

Let $u = p-1$, $v = s-1$

$$P_e(\theta,\tau) = \frac{1}{m^2}\sum_{v=0}^{m-1}\Phi\left\{-\frac{\Delta}{2\sqrt{N_0}}\left[1-2\Omega v\cos(\theta+\omega\tau)\right]\right\}$$

$$+\frac{m-2}{m}-\frac{1}{m^2}\sum_{v=0}^{m-1}\sum_{u=1}^{m-2}\Phi\left\{\frac{u\Delta}{\sqrt{N_0}}\left[1+\frac{1}{2u}-\cos\theta-\Omega\frac{v}{u}\cos(\theta+\omega\tau)\right]\right\}$$

$$+\frac{1}{m^2}\sum_{v=0}^{m-1}\sum_{u=1}^{m-1}\Phi\left\{\frac{u\Delta}{\sqrt{N_0}}\left[1-\frac{1}{2u}-\cos\theta-\Omega\frac{v}{u}\cos(\theta+\omega\tau)\right]\right\}$$

Then, given the probability density function of phase-locked-loop phase errors,

$$P_e(\tau) = \int_{-\infty}^{\infty} d\theta\, p(\theta)\; P_e(\theta,\tau)$$

And for $p \neq 1, m$:

$$P_e(p,s,\theta,\tau) = Pr\left(x \notin R_p \mid p,s,\theta,\tau\right) = 1 - Pr\left(x \notin R_p \mid p,s,\theta,\tau\right)$$

$$= 1 - \int_{\sqrt{E_p} - \frac{\Delta}{2}}^{\sqrt{E_p} + \frac{\Delta}{2}} p\,(x \mid p,s,\theta,\tau)\,dx$$

$$= 1 - \int_{\left(p-\frac{3}{2}\right)\frac{\Delta}{\sqrt{N_0}}}^{\left(p-\frac{1}{2}\right)\frac{\Delta}{\sqrt{N_0}}} \frac{1}{\sqrt{2a}} \exp\left\{-\frac{1}{2}\left[x - \frac{(p-1)\Delta}{\sqrt{N_0}}\cos\theta - \Omega\frac{(s-1)\Delta}{\sqrt{N_0}}\cos(\theta+\omega\tau)\right]^2\right\} dx$$

$$P_e(p,s,\theta,\tau) = 1 - \left[\Phi\left\{\frac{(p-1)\,\Delta}{\sqrt{N_0}}\left[1 + \frac{1}{2(p-1)} - \cos\theta - \Omega\left(\frac{s-1}{p-1}\right)\cos(\theta+\omega\tau)\right]\right\}\right. \qquad \text{(G5)}$$

$$\left. - \Phi\left\{\frac{(p-1)\,\Delta}{\sqrt{N_0}}\left[1 - \frac{1}{2(p-1)} - \cos\theta - \Omega\left(\frac{s-1}{p-1}\right)\cos(\theta+\omega\tau)\right]\right\}\right]$$

Consequently, the average error probability, conditional on the parameters θ, τ is

$$P_e(\theta,\tau) = \frac{1}{m}\sum_{s=1}^{m} \frac{1}{m}\sum_{p=1}^{m} P_e(p,s,\theta,\tau)$$

APPENDIX H

AVERAGE ERROR PROBABILITIES OF INCOHERENT AMPLITUDE SHIFT KEY MODULATION IN A MULTIPATH ENVIRONMENT

For incoherent amplitude shift key (ASK) detection, the pertinent orthonormal functions are

$$\phi_1 = \sqrt{\frac{2}{T}} \cos(\omega t - \theta), \quad \phi_2 = \sqrt{\frac{2}{T}} \sin(\omega t - \theta).$$

The correlator outputs are

$$\begin{cases} x = \int_0^T s(t)\,\phi_1(t)dt = \sqrt{E_p}\cos\theta + \Omega\sqrt{E_s}\cos(\theta+\omega\tau) + n_1 \\ y = \int_0^T s(t)\,\phi_2(t)dt = -\sqrt{E_p}\sin\theta - \Omega\sqrt{E_s}\sin(\theta+\omega\tau) + n_2 \end{cases} \tag{H1}$$

The decision is based on

$$\nu = \frac{z}{\sqrt{N_0}} = \frac{\sqrt{x^2+y^2}}{\sqrt{N_0}}$$

Since n_1, n_2 are independent gaussian random variables, ν is Rician distributed.[2] In fact if x_{ps} and y_{ps} are defined as

$$\begin{cases} x_{ps} = \sqrt{E_p}\cos\theta + \Omega\sqrt{E_s}\cos(\theta+\omega\tau) \\ y_{ps} = -\sqrt{E_p}\sin\theta - \Omega\sqrt{E_s}\sin(\theta+\omega\tau) \end{cases} \tag{H2}$$

then

$$p(\nu|p, s, \theta, \tau) = \nu\ I_0\left(\frac{\nu\sqrt{x_{ps}^2 + y_{ps}^2}}{\sqrt{N_0}}\right)\exp\left[-\frac{1}{2}\left(\nu^2 + \frac{x_{ps}^2 + y_{ps}^2}{N_0}\right)\right] \quad \text{(H3)}$$

Recalling $\sqrt{E_k} = (k-1)\,\Delta$,

$$P_e(1, s, \theta, \tau) = 1 - \int_0^{\Delta/2\sqrt{N_0}} \nu\ I_0\left[\nu\Omega(s-1)\Delta/\sqrt{N_0}\right] \cdot \exp\left[-\frac{1}{2}\left(\nu^2 + \frac{\Omega^2(s-1)^2\Delta^2}{N_0}\right)\right] d\nu \quad \text{(H4)}$$

$$P_e(m, s, \theta, \tau) = 1 - \int^{\infty} \nu\ I_0\left\{\frac{\nu\,\Delta}{\sqrt{N_0}}\left[(m-1)^2 + \Omega^2(s-1)^2 + 2\Omega(m-1)(s-1)\cos\omega\tau\right]^{1/2}\right\} \cdot \exp\left\{-\frac{1}{2}\left[\nu^2 + \frac{\Delta^2}{N_0}\left((m-1)^2 + \Omega^2(s-1)^2 + 2\Omega(m-1)(s-1)\cos\omega\tau\right)\right]\right\} d\nu \quad \text{(H5)}$$

for $p \neq 1$, m

$$P_e(p, s, \theta, \tau) = 1 - \int_{(p-3/2)\frac{\Delta}{\sqrt{N_0}}}^{\left(p-\frac{1}{2}\right)\frac{\Delta}{\sqrt{N_0}}} \nu\ I_0\left\{\frac{\nu\,\Delta}{\sqrt{N_0}}\left[(p-1)^2 + \Omega^2(s-1)^2 + 2\Omega(p-1)(s-1)\cos\omega\tau\right]^{1/2}\right\} \cdot \exp\left\{-\frac{1}{2}\left[\nu^2 + \frac{\Delta^2}{N_0}\left((p-1)^2 + \Omega^2(s-1)^2 + 2\Omega(p-1)(s-1)\cos\omega\tau\right)\right]\right\} d\nu \quad \text{(H6)}$$

Then the mean error probability conditioned on θ, τ is

$$P_e(\theta,\tau) = \frac{1}{m}\sum_{v=0}^{m-1}\left\{\frac{1}{m}\int_{\Delta/2\sqrt{N_0}}^{\infty} \nu I_0\left[\frac{\nu\Omega v\Delta}{\sqrt{N_0}}\right]\exp\left[-\frac{1}{2}\left(\nu^2+\frac{\Omega^2v^2\Delta^2}{N_0}\right)\right]d\nu\right.$$

$$+\frac{1}{m}-\frac{1}{m}\int_{\left(m-\frac{3}{2}\right)\frac{\Delta}{\sqrt{N_0}}}^{\infty}\nu I_0\left[\frac{\nu\Delta}{\sqrt{N_0}}\left[(m-1)^2+\Omega^2v^2+2\Omega(m-1)v\cos\omega\tau\right]^{1/2}\right]$$

$$\left.\cdot\exp\left[-\frac{1}{2}\left[\nu^2+\frac{\Delta^2}{N_0}\left((m-1)^2+\Omega^2v^2+2\Omega(m-1)v\cos\omega\tau\right)\right]\right]d\nu\right\}$$

$$+\frac{1}{m}\sum_{u=1}^{m-2}\left\{1-\int_{\left(u-\frac{1}{2}\right)\frac{\Delta}{\sqrt{N_0}}}^{\left(u+\frac{1}{2}\right)\frac{\nu\Delta}{\sqrt{N_0}}}\nu I_0\left[\frac{\nu\Delta}{\sqrt{N_0}}\left[u^2+\Omega^2v^2+2\Omega uv\cos\omega\tau\right]^{1/2}\right]\right.$$

$$\left.\cdot\exp\left[-\frac{1}{2}\left[\nu^2+\frac{\Delta^2}{N_0}\left(u^2+\Omega^2v^2+2\Omega uv\cos\omega\tau\right)\right]\right]d\nu\right\}$$

$$=\frac{1}{m}\sum_{v=0}^{m-1}\left\{\frac{1}{m}\int_{\Delta/2\sqrt{N_0}}^{\infty}\nu I_0\left[\frac{\nu\Omega v\Delta}{\sqrt{N_0}}\right]\exp\left[-\frac{1}{2}\left(\nu^2+\frac{\Omega^2v^2\Delta^2}{N_0}\right)\right]d\nu\right.$$

$$+\frac{1}{m}-\frac{1}{m}\sum_{u=1}^{m-1}\int_{\left(u-\frac{1}{2}\right)\frac{\Delta}{\sqrt{N_0}}}^{\infty}\nu\, I_0\left\{\frac{\nu\Delta}{\sqrt{N_0}}\left[u^2+\Omega^2v^2+2\Omega uv\cos\omega\tau\right]^{1/2}\right\}$$

$$\cdot\exp\left\{-\frac{1}{2}\left[\nu^2+\frac{\Delta^2}{N_0}\left(u^2+\Omega^2v^2+2\Omega uv\cos\omega\tau\right)\right]\right\}d\nu \qquad \text{(H7)}$$

$$+\frac{m-2}{m}+\frac{1}{m}\sum_{u=1}^{m-2}\int_{\left(u+\frac{1}{2}\right)\frac{\Delta}{\sqrt{N_0}}}^{\infty}\nu\, I_0\left\{\frac{\nu\Delta}{\sqrt{N_0}}\left[u^2+\Omega^2v^2+2\Omega u\, v\cos\omega\tau\right]^{1/2}\right\}$$

$$\cdot\exp\left\{-\frac{1}{2}\left[\nu^2+\frac{\Delta^2}{N_0}\left(u^2+\Omega^2v^2+2\Omega u\, v\cos\omega\tau\right)\right]\right\}d\nu\Bigg\}$$

For binary coding this expression becomes

$$P_e(\tau)=\frac{1}{2}+\frac{1}{2}\sum_{v=0}^{1}\left\{\frac{1}{2}\int_{\Delta/2\sqrt{N_0}}^{\infty}\nu I_0\left(\frac{\nu\Omega v\Delta}{\sqrt{N_0}}\right)\right.$$

$$\cdot\exp\left[-\frac{1}{2}\left(\nu^2+\frac{\Omega^2v^2\Delta^2}{N_0}\right)\right]d\nu$$

$$-\frac{1}{2}\sum_{u=1}^{1}\int_{\left(u-\frac{1}{2}\right)\frac{\Delta}{\sqrt{N_0}}}^{\infty}\nu\, I_0\left(\frac{\nu\Delta}{\sqrt{N_0}}\left[u^2+\Omega^2v^2+2\Omega u\, v\cos\omega\tau\right]^{1/2}\right)\Bigg\}$$

$$\cdot\exp\left\{-\frac{1}{2}\left[\nu^2+\frac{\Delta^2}{N_0}\left(v^2+\Omega^2v^2+2\Omega uv\cos\omega\tau\right)\right]\right\}d\nu$$

$$= \frac{1}{2} + \frac{1}{4} \int_{\Delta/2\sqrt{N_0}}^{\infty} \nu \exp\left[-\nu^2/2\right] d\nu + \frac{1}{4} \int_{\Delta/2\sqrt{N_0}}^{\infty} \nu I_0 \left(\frac{\nu \Omega \Delta}{\sqrt{N_0}}\right)$$

$$\exp - \frac{1}{2}\left(\nu^2 + \frac{\Omega^2 \Delta^2}{N_0}\right) \, d\nu$$

$$- \frac{1}{4} \int_{\frac{\Delta}{2\sqrt{N_0}}}^{\infty} \nu \, I_0 \left[\frac{\nu \Delta}{\sqrt{N_0}}\right] \exp - \frac{1}{2}\left(\nu^2 + \frac{\Delta^2}{N_0}\right) d\nu$$

$$- \frac{1}{4} \int_{\frac{\Delta}{2\sqrt{N_0}}}^{\infty} \nu \, I_0 \left[\frac{\nu \Delta}{\sqrt{N_0}} \left(1 + \Omega^2 + 2\Omega \cos \omega \tau\right)^{1/2}\right]$$

$$\cdot \exp\left\{-\frac{1}{2}\left[\nu^2 + \frac{\Delta^2}{N_0}\left(1 + \Omega^2 + 2\Omega \cos \omega \tau\right)\right]\right\} d\nu \qquad \text{(H8)}$$

$$P_e(\tau) = \frac{1}{2} \int_{\Delta/2\sqrt{N_0}}^{\infty} \nu \exp\left(-\nu^2/2\right)\left[\frac{1}{2} + \frac{1}{2} I_0 \left(\frac{\nu \Delta \Omega}{\sqrt{N_0}}\right) \exp\left(-\frac{\Delta^2 \Omega^2}{2N_0}\right)\right] d\nu$$

$$+\frac{1}{2}\left[1-\int_{\Delta/2\sqrt{N_0}}^{\infty}\exp\left[-\frac{1}{2}\left(\nu^2+\frac{\Delta^2}{N_0}\right)\right]\left\{\frac{1}{2}\,I_0\left(\frac{\nu\Delta}{\sqrt{N_0}}\right)\right.\right.$$

$$\left.+\frac{1}{2}\,I_0\left(\frac{\nu\Delta}{\sqrt{N_0}}\sqrt{1+\Omega^2+2\Omega\cos\,\omega\,\tau}\right)\right.$$

$$\left.\left.\exp\left[\left(-\frac{\Delta^2}{2N_0}\right)\left(\Omega^2+2\,\Omega\cos\,\omega\,\tau\right)\right]\right\}\,d\nu\right] \qquad \text{(H9)}$$

APPENDIX I

EVALUATION OF EXPECTATIONS

In equations (238a-d), several expectations were given without proof. Their method of calculation is outlined here. The expectation of a function f(x, y) where x and y are stationary random processes is given by

$$E[f] = \int f(x, y)p(x, y)\, dx\, dy \tag{I1}$$

where p(x, y) is the joint probability density function of x and y and the integration is performed over all allowable values of x and y. In the cases of interest the random processes are g and g′. They are jointly gaussian with joint density function

$$p(g, g') = \frac{1}{2\pi\sigma_g^2(1-\rho^2)} \exp\left[-\frac{g^2 + g'^2 - 2\rho gg'}{2\sigma_g^2(1-\rho^2)}\right] \tag{I2}$$

where σ_g and ρ are defined in the body of the report. When this density function is used in equation (I1) and the integrals are evaluated, the expectations of equations (238a-d) result.

APPENDIX J

INTERACTION OF ELECTROMAGNETIC WAVE WITH PLASMAS

It is assumed that the plasma is electrically neutral and that the temperature is sufficiently low that the interaction of electromagnetic waves and acoustic waves may be neglected. It is also assumed that the interaction of electromagnetic waves with positive ions may be ignored. The equation of average motion of electrons can be written

$$-e\bar{\mathscr{E}} = m\frac{\partial \bar{v}}{\partial t} + m\nu\bar{v} \tag{J1}$$

where

e = magnitude of the electronic charge in coulombs

m = mass of electron in kilograms

$\bar{v}$ = the average electron velocity in meters per second

ν = the average collision frequency of the electrons in 1/sec

$\bar{\mathscr{E}}$ = the electric field intensity acting on the electron in volts per meter.

This equation reflects the further assumption that forces due to the interaction of electrons with the magnetic field are negligible.

Maxwell's equations for the electromagnetic fields are

$$-\nabla \times \bar{\mathscr{E}} = \mu_0 \frac{\partial \bar{\mathscr{H}}}{\partial t} \tag{J2a}$$

$$\nabla \times \bar{\mathscr{H}} = \epsilon_0 \frac{\partial \bar{\mathscr{E}}}{\partial t} + \bar{\mathscr{J}} \tag{J2b}$$

where

$\bar{\mathscr{H}}$ = the magnetic field intensity in amperes per meter

μ_0 = free space permeability in henrys/meter

ϵ_0 = free space permittivity in farads/meter

$\bar{\mathscr{J}}$ = electric current in amperes/sq meter

In the case of interest, $\bar{g}$ results from the motion of the electron and may be written as

$$\bar{g} = -Ne\bar{v} \tag{J3}$$

where N is the electron density in electrons/cu meter.

If it is assumed that all time varying quantities vary as exp (jωt), equations (J1), (J2), and (J3) may be rewritten

$$-e\bar{E} = m(\nu + j\omega)\bar{v} \tag{J4a}$$

$$-\nabla \times \bar{E} = j\omega\mu_0\bar{H} \tag{J4b}$$

$$\nabla \times \bar{H} = j\omega\epsilon_0\bar{E} + \bar{J} \tag{J4c}$$

$$\bar{J} = Ne\bar{v} \tag{J4d}$$

where the vectors are complex representations of the original time varying vectors. On combining (J4a) and (J4d) with equation (J4c), Maxwell's equations may be rewritten as

$$-\nabla \times \bar{E} = j\omega\mu_0\bar{H} \tag{J5a}$$

$$\nabla \times \bar{H} = j\omega\epsilon\bar{E} \tag{J5b}$$

where

$$\epsilon = \epsilon_0\left[\left(1 - \frac{\omega_p^2}{\nu^2 + \omega^2}\right) - j\frac{\nu}{\omega}\frac{\omega_p^2}{\nu^2 + \omega^2}\right] \tag{J5c}$$

and

$$\omega_p^2 \equiv \frac{Ne^2}{M\epsilon_0}$$

The term ϵ appears in equation (J5b) as a modified permittivity that depends on the electron density and the collision frequency and that consequently is a function of position when the plasma is inhomogeneous.

REFERENCES

1. Howard, J. E.: Study of Applications of Retrodirective and Self-adaptive Electromagnetic Wave Phase Controls to a Mars Probe. Fifth Quarterly (NAS 2-3297), Report No. P67-137, Antenna Department, Hughes Aircraft Co., 20 January to 30 April 1967.

2. Howard, J. E.: Study of Applications of Retrodirective and Self-adaptive Electromagnetic Wave Phase Controls to a Mars Probe. Sixth Quarterly (NAS 2-3297), Report No. P67-202, Antenna Department, Hughes Aircraft Co., 1 May to 31 July 1967.

3. Villeneuve, A. T.; Howard, J. E.; and Bershad, N. J.: Study of Applications of Retrodirective and Self-adaptive Electromagnetic Wave Phase Controls to a Mars Probe. Seventh Quarterly, Report No. P68-29 (NAS 2-3297), Antenna Department, Aerospace Group, Hughes Aircraft Co., Culver City, Calif., October 1967.

4. Villeneuve, A. T.; Ksienski, A. A.; and Young, G. O.: Study of Applications of Retrodirective and Self-adaptive Electromagnetic Wave Phase Controls to a Mars Probe. First Quarterly, Report No. P66-82 (NAS 2-3297), Antenna Department, Aerospace Group, Hughes Aircraft Co., March 1966.

5. Villeneuve, A. T.; Ksienski, A. A.; and Young, G. O.: Study of Applications of Retrodirective and Self-adaptive Electromagnetic Wave Phase Controls to a Mars Probe. Second Quarterly, Report No. P66-160 (NAS 2-3297), Antenna Department, Aerospace Group, Hughes Aircraft Co., May 1966.

6. Howard, J. E.; Villeneuve, A. T.; Young, G. O.; and Ksienski, A. A.: Study of Applications of Retrodirective and Self-adaptive Electromagnetic Wave Phase Controls to a Mars Probe. Third Quarterly, Report No. P66-230 (NAS 2-3297), Antenna Department, Aerospace Group, Hughes Aircraft Co., August 1966.

7. Villeneuve, A. T.; Ksienski, A. A.; Young, G. O.; and Howard, J. E.: Study of Applications of Retrodirective and Self-adaptive Electromagnetic Wave Phase Controls to a Mars Probe. Fourth Quarterly, Report No. P67-61 (NAS 2-3297), Antenna Department, Aerospace Group, Hughes Aircraft Co., October 1966.

8. Villeneuve, A. T.; Howard, J. E.; Young, G. O.; and Ksienski, A. A.: Study of Applications of Retrodirective and Self-adaptive Electromagnetic Wave Phase Controls to a Mars Probe. Final Report - Part I (NAS 2-3297), Report No. P67-153 (NASA CR-73119), Antenna Department, Aerospace Group, Hughes Aircraft Co., 8 November 1965 to 8 October 1966.

9. Gangi, A. F.: The Active Adaptive Antenna Array System. IEEE Trans. on AP, vol. AP-11, No. 4, July 1963, pp. 405-414.

10. Cutler, C. C.; Kompfner, R.; and Tillotson, L. C.: A Self-steering Array Repeater. Bell Syst. Tech. J., vol. 42, No. 8, August 1963, pp. 2013-2032.

11. Belfi, C. A.; et al.: A Satellite Data Transmission System. IEEE Trans. on AP, vol. AP-12, No. 2, March 1964, pp. 200-206.

12. Ghose, R. N.: Electronically Adaptive Antenna Systems. IEEE Trans. on AP, vol. AP-12, No. 2, March 1964, pp. 161-169.

13. Pon, C. Y.: Retrodirective Array Using the Heterodyne Technique. IEEE Trans. on AP, vol. AP-12, No. 2, March 1964, pp. 176-180.

14. Rutz-Phillipp, E. M.: Spherical Retrodirective Array. IEEE Trans. on AP, vol. AP-12, No. 2, March 1964, pp. 187-194.

15. Sichelstiel, B. A.; Waters, W. M.; and Wild, T. A.: Self-focusing Array Research Model. IEEE Trans. on AP, vol. AP-12, No. 2, March 1964, pp. 150-154.

16. Skolnik, M. I.; and King, D. D.: Self-phasing Array Antennas. IEEE Trans. on AP, vol. AP-12, No. 2, March 1964, pp. 142-149.

17. Svobda, D. E.: A Phase-locked Receiving Array for High-frequency Communications Use. IEEE Trans. on AP, vol. AP-12, March 1964, pp. 207-215.

18. Kummer, W. H.; and Villeneuve, A. T.: Spacecraft Antenna Systems. Interim Engineering Report, Report No. P65-35 (NAS 5-3545), Antenna Department, Aerospace Group, Hughes Aircraft Co., Jan. 1965.

19. Kummer, W. H.; and Birgenheier, R. A.: Spacecraft Antenna Systems. Final Engineering Report, Report No. P66-66 (NAS 5-3545), Antenna Department, Aerospace Group, Hughes Aircraft Co., Feb. 1966.

20. Gardner, F. M.: Phaselock Techniques, J. Wiley and Sons, 1966.

21. Robinson, L. M.: "TANLOCK: A Phase-lock Loop of Extended Tracking Capability," Proceedings of Convention on Military Electronics, 7-9 February, Los Angeles, California, 1962.

22. Balodis, M.: "Laboratory Comparison of Tan-Lock and Phase-Lock," Proceedings of National Telemetering Conference, paper 5-4, 1964.

23. Gardner, M. F., and J. L. Barnes. Transients in Linear Systems, vol. I, J. Wiley and Sons, 1942.

24. Viterbi, A. J.: Principles of Coherent Communication. McGraw-Hill Book Co., Inc., 1966.

25. Davenport, W. L.; and Root, W. R.: Introduction to Random Signals and Noise, chapter VIII. McGraw-Hill Book Co., Inc., 1958.

26. Middleton, D.: An Introduction to Statistical Communication Theory, chapter X. McGraw-Hill Book Co., Inc., 1960.

27. Tikhonov, V. I.: Fluctuation Action in the Simplest Parametric Systems, Automation and Remote Control, pp. 717-724, August 1958 (Russian translation).

28. Park, E. C.: Advanced Deep Space Communication Systems Study. Final Report (Contract NAS 12-81), pp. E-23 to E-41. Report No. P 67-15, Hughes Aircraft Co., 1967.

29. Morgan, S. P.: Interaction of Adaptive Antenna Arrays in an Arbitrary Environment. Bell Syst. Tech. J., vol 44, No. 1, pp. 23-47, 1965.

30. Kahn, L. R.: Ratio Squarer. Proc. IEEE, vol. 42, No. 11, pp. 1704, 1954.

31. Staras, H.: Selected Studies of VHF/UHF Communications for Planetary (Mars/Venus) Relay Links. Final Report (NAS 2-3772), Astro-Electronics Division, Radio Corp. of America, January 1967.

32. Beckman, P.; and Spizzichino, A.: Scattering of Electromagnetic Waves from a Rough Surface. Pergamon Press, 1963.

33. Kaufman, D. E.; and Lenhert, D. H.: The Scattering of Electromagnetic Waves from a Rough Surface of Arbitrary Dielectric Constant. Technical Report EE-TR-6 (NSR 17-004-003), Kansas St. Univ., Manhattan, May 1967.

34. Silver, S.: Microwave Antenna Theory and Design, p. 87, vol. 12, Radiation Laboratory Series, Mass. Inst. of Tech., McGraw-Hill Book Co., Inc., 1949.

35. Villeneuve, A. T.: Admittance of Waveguide Radiating into Plasma Environment. IEEE Trans. on AP. vol AP-13, No. 1. January 1965, pp 115-121.

36. Galejs, J.: Admittance of Waveguide Radiating into Stratified Plasma. IEEE Trans. on AP. vol AP-13, No. 1. January 1965, pp 64-70.

37. Heald, M. A.; and Wharton, C. B.: Plasma Diagnostics with Microwaves, John Wiley and Sons, Inc., New York, 1965.

38. Allis, W. P.; Buchsbaum, S. J.; and Bers, A.: Waves in Anisotropic Plasmas, M. I. T. Press, Cambridge, Mass., 1963.

39. Allen, J. H.; and Eggers, A. J.: A Study of the Motion and Aerodynamic Heating of Ballistic Missiles Entering the Earth's Atmosphere at High Supersonic Speeds. NACA Technical Report 1381, 1958.

40. Viterbi, A. J.: "Phase-lock-loop Systems," chapter 8, Space Communications, A. V. Balakrishnan, editor, McGraw-Hill Book Company, 1963.

41. Fleck, J. T.; and Trabka, E. A.: Error Probabilities of Multiple-state Differentially Coherent Phase Shift Keyed Systems in the Presence of White Gaussian Noise. Detect Memo No. 2A in Investigation of Digital Data Communications Systems, J. G. Lawton, ed. (Report No. VA-1420-S-1), Cornell Aeronautical Lab., Inc., 1961.